Indian J Chem
JULY 1990
CODEN:IJOCAP 29A(7) 613-722 (1990)
ISSN:0019-5103

सी.एफ.टी.आर.आई. क्षेत्रीय केन्द्र
C.F.T.R.I. REGIONAL CENTRE
294
डायरी नं:/DIARY NO.
दिनांक/DATE 16/7/90
लुधियाना/LUDHIANA-141 006

वैज्ञानिक तथा औद्योगिक अनुसंधान पुस्तकालय
SCIENTIFIC & RESEARCH LIBRARY
Accession No.
17 JUL 1990
16/7/90
सी.एफ.टी.आर.आई. क्षेत्रीय केन्द्र
REGIONAL CENTRE, LUDHIANA

Indian Journal of
CHEMISTRY

SECTION A

Inorganic, Bio-inorganic, Physical, Theoretical & Analytical Chemistry

Published by
PUBLICATIONS & INFORMATION DIRECTORATE, CSIR, NEW DELHI
in association with
THE INDIAN NATIONAL SCIENCE ACADEMY, NEW DELHI

NATIONAL UNION CATALOGUE OF SCIENTIFIC SERIALS IN INDIA

(NUCSSI)

1988

- Contains holdings data of more than 800 leading libraries of laboratories, universities & industries
- Presents information on 35,000 S & T serials
- Provides complete addresses of libraries
- Provides information on lending & reprographic facilities available
- Also, selected portions available on floppies
- Moderately priced Rs.1200/- in India, US $ 300/- abroad
- Limited copies available only. Rush your orders with DD in favour of Director, Insdoc to -

Deputy Head
Marketing & Customer Services Division
Indian National Scientific Documentation Centre
(INSDOC)
14, Satsang Vihar Marg, New Delhi-110 067
Telephone No. 660141,660143,660162 & 667043

DIRECTORY OF SCIENTIFIC RESEARCH INSTITUTIONS IN INDIA

- PRESENTS A COMPREHENSIVE LIST OF INSTITUTIONS IN INDIA ENGAGED IN FUNDAMENTAL & APPLIED RESEARCH IN S&T.
- PROVIDES COMPLETE POSTAL ADDRESS, TELEPHONE, TELEX NUMBERS ETC.
- PROVIDES DETAILS ON AREAS OF RESEARCH, IMPORTANT ACHIEVEMENTS, SPECIAL FACILITIES, PUBLICATIONS ETC.
- PRICE: Rs. 1200/- in India
  $ 600 Abroad
- DELIVERY : IMMEDIATELY.
- LIMITED COPIES AVAILABLE' PLACE ORDER IMMEDIATELY.

SEND ORDERS ALONGWITH DDs DRAWN IN FAVOUR OF DIRECTOR INSDOC TO -

Deputy Head
Marketing & Customer Services Division
Indian National Scientific Documentation Centre
(INSDOC)
14, Satsang Vihar Marg, New Delhi-110 067
Telephone No. 660141, 660143, 660162 & 667043

Indian Journal of Chemistry
Vol. 29A, July 1990, p. 721

ANNOUNCEMENTS

The 42nd Pittsburgh Conference & Exposition on Analytical Chemistry and Applied Spectroscopy

The 42nd Pittsburgh Conference & Exposition on Analytical Chemistry and Applied Spectroscopy will be held during March 4-8, 1991 at McCormick Place-on-the Lake, Chicago, Illinois, USA. Papers are invited for oral or poster presentation in the following areas: Atomic, vibrational and mass spectroscopy; liquid, gas and supercritical fluid chromatography; electrochemistry; thermal analysis etc., and application in biomedicine, forensic science, material characterisation etc.

Abstracts of the papers should be sent before 3 August 1990 to Mrs Alma Johnson, Program Secretary of the Conference. Further information may be obtained from Victor C. Zadnik, Exposition Chairman, Pittsburgh Conference, 300 Penn Center Blvd., Suite 332, Pittsburgh, PA 15235 USA.

Tenth National Symposium on Catalysis and Fourth Indo-Soviet Seminar on Catalysis

The Tenth National Symposium on Catalysis and the Fourth Indo-Soviet Seminar on Catalysis will be held on 18-20 December 1990 and 21 December 1990 respectively at the Indian Institute of Technology, Madras. All areas of catalysis will be covered and communications will be presented in the form of plenary lectures, contributed papers and poster presentations.

Further details may be obtained from Prof. C N Pillai, Convener Catalysis Symposium, Department of Chemistry, Indian Institute of Technology, Madras-600 036.

AUTHOR INDEX

Alias M O 624

Basumallick I N 647
Bhagat S D 652
Bhalla K C 639
Bhasin K K 710
Borkar A D 631

Chakraborty Utsabananda 647
Chakravortty V 713
Chaudhuri Ajit Kumar 697
Chauhan M S 693
Chauhan S 693

Das Sunanda 707
Dash Anadi C 670
Dash K C 713
Datta K K 613

Ghosh S K 656
Gowda B Thimme 680
Gowda N M N 661
Goyal R N 635
Gupta A R 639
Gupta Mool C 631
Gupta R K 618

Halesha R 661
Hazra D K 656

Jagannadham V 700

Khajuria Rajesh 710

Mahadevappa D S 676
Majmudar A A 639
Mohanty R K 647
Mishra Y K 618
Mukherjee A K 613
Mythily C K 676

Nandi Dipa 697
Natarajan C 666

Pal Prabir Kumar 697
Prasad R 618
Prusti Jayashree 670

Ramachandra P 680
Rangappa K S 676
Rao B Rajeshwar 652
Rao T R 716
Reddy G K N 661
Reddy K Venugopal 686
Reddy M Harilatha 686
Reddy P Rabindra 686

Sharadamani P R 700
Singh Genda 716
Singh Jai Deo 703
Singh S 713
Singh Sukhjinder 710
Srinivasan V 624
Srivastava Amit K 635
Srivastava M N 707
Srivastava S 703
Srivastava Sanjay Kumar 703
Srivastava T N 703
Sudhakar K 686
Syal V K 693

Tharmaraj P 666

Verma R D 710

वैज्ञानिक तथा अनुसंधान पुस्तकालय
SCIENTIFIC & RESEARCH LIBRARY
Accession No.....
17 JUL 1990
आई.एस.आर.आई. क्षेत्रीय केन्द्र
I. S. R. REGIONAL CENTRE, LUDHIANA

Indian Journal of Chemistry

Sect. A: Inorganic, Bio-inorganic, Physical, Theoretical & Analytical

VOL. 29A NUMBER 7 JULY 1990

CONTENTS

Some graph-theoretic studies on aniline and *p*-phenylenediamine-like systems in HMO formalism 613
A K Mukherjee* & K K Datta

Spectroscopic and molecular mechanics study of the conformational properties of methyl cyanoacetate and ethyl cyanoacetate 618
R Prasad*, Y K Mishra & R K Gupta

Adsorption and reactivity of thiophene on promoted molybdena and tungsta systems . 624
M O Alias & V Srinivasan*

Electrical and magnetic properties of poly(N-ethylaniline) 631
A D Borkar & Mool C Gupta*

Electrochemical oxidation of sulphamethoxazole at pyrolytic graphite electrode: An example of free radical dimerization 635
R N Goyal* & Amit K Srivastava

Complexation of hydrogen and alkali cations with 18 Crown6 in 25 and 50% (v/v) methanol-water mixtures 639
A A Majmudar, K C Bhalla & A R Gupta*

Volumetric and solvation behaviour of amino acids in some aqueous binaries: Part III-Glycine, DL-alanine and DL-α-aminobutyric acid in aqueous solutions of non-electrolytes at 298.15 K 647
I N Basumallick, R K Mohanty* & Utsabananda Chakraborty

Evaluation of solute-solvent interactions of some non-electrolytes with N-methylpyrrolidone by gas-liquid partition chromatography 652
B Rajeshwar Rao & S D Bhagat*

Conductometric determination of dissociation constants of picric acid in 2-methoxyethanol, 1,2-dimethoxyethane and their aqueous binary mixtures 656
S K Ghosh & D K Hazra*

Synthesis and NMR spectral studies of polynuclear complexes of rhodium(I) with bridging benzimidazole derivatives 661
R Halesha, N M N Gowda* & G K N Reddy

Synthesis and characterisation of copper(II), nickel(II), cobalt(II) and zinc(II) complexes of 3-(1-hydroxy-2-naphthyl)-5-(4-X-phenyl)pyrazolines 666
C Natarajan* & P Tharmaraj

Reactions in micellar solutions: Part 9—Kinetics of base hydrolysis of *cis*-(imidazole)-(salicylato)bis(ethylenediamine)cobalt(III) and ($\alpha\beta$S)-(sulphito)(tetraethylenepentamine)cobalt(III) in the presence of neutral, anionic and cationic surfactants in aqueous medium 670
Anadi C Dash* & Jayashree Prusti

Kinetics of oxidation of cinnamaldehyde by chloramine-T in perchloric acid and in alkaline medium catalysed by Os(VIII) 676
C K Mythily, K S Rangappa* & D S Mahadevappa

Kinetics and mechanism of oxidation of carbohydrazide by N,N-dichlorotoluene-*p*-sulphonamide in water-methanol medium 680
B Thimme Gowda* & P Ramachandra

A study of ternary metal-xanthosine complexes in solution—Thermodynamic aspects . 686
P Rabindra Reddy*, K Venugopal Reddy, M Harilatha Reddy & K Sudhakar

Notes

Solvation behaviour of some tetraalkylammonium ions in acetonitrile + dimethyl sulphoxide mixtures: Conductance and viscosity measurements at 25°C 693
V K Syal*, S Chauhan & M S Chauhan

Kinetics of nonaqueous polymerization of methyl methacrylate by manganic laurate-*n*-hexanethiol redox system in carbon tetrachloride 697
Dipa Nandi, Prabir Kumar Pal & Ajit Kumar Chaudhuri*

Kinetics and mechanism of oxidation of aromatic amines by N-bromoacetamide . . . 700
P R Sharadamani & V Jagannadham*

Synthesis and reactivity of diorganotellurium(IV) β-diketonates 703
T N Srivastava, Jai Deo Singh, Sanjay Kumar Srivastava* & S Srivastava

Mixed ligand complexes of copper(II), nickel(II), cobalt(II) and zinc(II) with nitrilotriacetic acid and iminodiacetic acid as primary ligands and 2-aminophenol as a secondary ligand 707
Sunanda Das & M N Srivastava*

Preparation and characterisation of diarylselenium(IV) trifluoroethoxides 710
Rajesh Khajuria, Sukhjinder Singh, K K Bhasin & R D Verma*

Dioxouranium(VI) complexes of tetradentate schiff base ligands 713
S Singh, V Chakravortty & K C Dash*

Synthesis and structural characterization of the lanthanide (III) complexes of 2-acetylpyridine isonicotinoyl hydrazone 716
T R Rao* & Genda Singh

Announcements 721

Erratum 722

Authors for correspondence are indicated by (*)

Indian Journal of Chemistry
Vol. 29A, July 1990, pp. 613-617

Some graph-theoretic studies on aniline and *p*-phenylenediamine-like systems in HMO formalism

A K Mukherjee* & K K Datta
Burdwan Raj College, Chemistry Department, Burdwan 713 104, India

Received 23 January 1989; revised 19 October 1989; accepted 21 November 1989

By studying the signs of the terms in the characteristic polynomials (CP) and their derivatives of the molecular graph, energy-level patterns and the upper and lower bounds to the smallest and largest positive eigenvalues have been determined for aniline- and *p*-phenylenediamine-like systems. The dependence of the HMO energies of the highest occupied molecular orbitals on the heteroatom Hückel parameters, represented by h and k, has been ascertained. The results are in agreement with the trends in the actually computed energy values compiled by Coulson and Streitwieser. The derived modes of dependence of the HOMO energy on h and k correctly predict the trends in electron donor properties of the systems under study with variation in electronegativities of the hetero atoms.

Graph theory (GT) has recently evoked much interest among theoretical chemists because it can lead to interesting results on molecular structure and chemical properties without involving long and tedious computations. For example, branching indices[1-7] derived from the molecular σ-bond topology have been used to predict physical and chemical properties of molecules in a kind of an information-theoretic approach. A good account of the use of GT in HMO formalism may be found in references 8 and 9. Very recently Mishra *et al.*[10] have calculated some important quantum chemical parameters of sulphur-nitrogen rings and stability of azacyclobutadienes using GT.

The application of Descarte's rule of signs to the characteristic polynomial (CP) of a molecular graph has been shown to yield results related to the energy of the highest occupied molecular orbital (HOMO)[11] and validity or nonvalidity of Hückel's $(4n+2)$ rule[12,13]. However, there are many other well-known theorems in polynomial algebra which have not been exploited much in the study of CP's. The aim of the present paper is to use one such theorem—the Budan-Fourier theorem[14]—for obtaining chemically interesting results related to the energy-level patterns and donor properties of aniline, phenol, *p*-phenylenediamine and *p*-quinol. Although a good number of methods[15-19] are available for constructing CP's, the process may be simplified by employing some recently developed[20,21] graph theoretical symmetry factorisation techniques; their use has been illustrated in the present paper.

Some graph-spectra features of the systems under study

Some chemically relevant graph-spectral features (F_1-F_6) of the conjugated molecules under study (Figs 1 and 2) are summarised below:

F_1 – For $0<h<1$ and $0<k<1$, aniline-like systems have exactly one eigenvalue in the ranges (0, 1) and (1,2) and exactly one positive eigenvalue above 2. The same is also true when $1<h\leqslant 2$ and $1\leqslant k\leqslant\sqrt{2}$.

F_2—With a given value of k, the eigenvalue of the highest occupied molecular orbital (HOMO) of an aniline-like system (G_1) should increase with increase in h; with a given $h>0$, the HOMO eigenvalue should decrease with increase in k.

F_3—If $h=1$, a *p*-phenylenediamine-like system (G_2) will have a doubly degenerate π-MO with eigenvalue = 1, whatever be the value of k.

F_4—For $2h=k^2$, G_2 has a non-bonding π-MO.

F_5—For $2h>k^2$, G_2 has five positive and three negative eigenvalues. When $2h<k^2$, G_2 has four positive and four negative eigenvalues.

F_6—When $2h>k^2$ and $1<h<5$, there is exactly one eigenvalue in the range (0,1) for systems having G_2-type graphs. For a fixed k, this eigenvalue increases with increase in h and for a fixed h, it decreases with increase in k.

Explanation of the above features

Case (a): aniline-like systems

The factorisation of aniline-like graphs according to schemes described in references 20 and 21

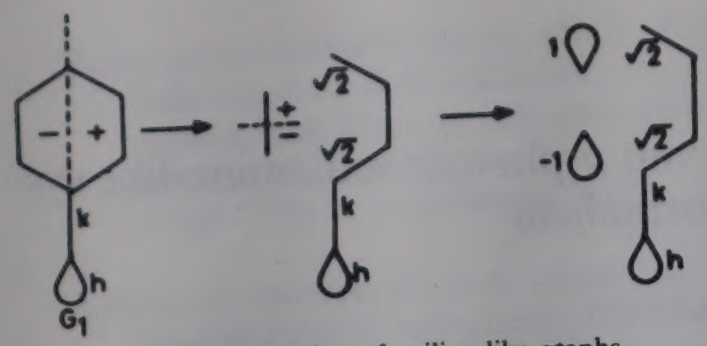

Fig. 1 – Factorisation of aniline-like graphs

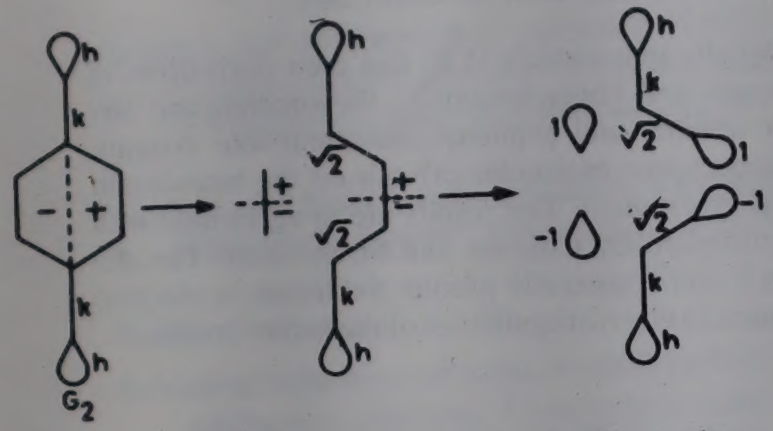

Fig. 2 – Factorisation of *p*-phenylenediamine-like graphs

is shown in Fig. 1. It shows that the CP of the aniline-like graph (G_1) has the form,

$$P(G_1; x) = (x^2 - 1)f(x) \quad \ldots (1)$$

where

$$f(x) = x^5 - hx^4 - (5 + k^2)x^3 + 5hx^2 + (4 + 3k^2)x - 4h \quad \ldots (2)$$

is the CP of the third factor graph in Fig. 1. Thus, ± 1 must be two zeros of $P(G_1; x)$ whatever be the values of h and k.

Eq. (2) gives $f(0) = -4h$, $f(1) = 2k^2$ and $f(2) = -2k^2$. Thus, according to Rolle's theorem[14], $f(x)$ should have zeros in the ranges (0,1) and (1,2) for $h > 0$. To ascertain the position of the HOMO of G_1, one must find the exact number of zeros of $f(x)$ in these ranges; we have done this by using Budan-Fourier theorem[14] which states that for a polynomial $P(x)$ of degree n, the zeros of which are real, the exact number of zeros in the range (a, b) is $N(a) - N(b)$ where $N(a)$ is the number of changes of sign in the sequence,

$$P(a), P^{(1)}(a), P^{(2)}(a), \ldots, P^{(n)}(a)$$

The superscripts on P indicate the orders of the derivatives of $P(x)$ with respect to x; $N(b)$ has a similar meaning.

The values of the zeroeth to fifth order derivatives of $f(x)$ at $x = 0$, 1 and 2 are shown in Table 1. From this table it is evident that for $0 < h < 1$ and $0 < k < 1$, $N(0) = 3$, $N(1) = 2$ and $N(2) = 1$. Thus, according to Budan-Fourier[14] theorem there is exactly one zero of $f(x)$ in the ranges (0,1)

Table 1 – Derivatives of f(x) at x = 0, 1 and 2

Order of derivative	Value of derivative at		
	x = 0	x = 1	x = 2
0	$-4h$	$2k^2$	$-2k^2$
1	$4 + 3k^2$	$-6 + 6h$	$24 - 12h - 9k^2$
2	$10h$	$-10 - 2h - 6k^2$	$100 - 38h - 12k^2$
3	$-6(5 + k^2)$	$30 - 24h - 6k^2$	$210 - 48h - 6k^2$
4	$-24h$	$120 - 24h$	$240 - 24h$
5	120	120	120

and (1,2) for the above mentioned values of h and k. When $1 < h \leqslant 2$, $N(0) = 3$ whatever be the value of k. For $x = 1$, signs of the aforesaid sequence of derivatives must have one of the following three patterns if $1 < h \leqslant 2$, whatever be the value of k:

+ + −	+	+ +
+ + −	−	+ +
+ + −	0	+ +

Sign Sequence 1.

The signs have been arranged row-wise. The blocked portion indicates that only the third order derivative may have different signs (or zero value) depending on k. Therefore, $N(1) = 2$. For $x = 2$, one obtains from Table 1 the following three sign-change patterns of the derivative sequence with $1 < h \leqslant 2$ and $1 \leqslant k \leqslant \sqrt{2}$:

−	+	+ + + +
−	−	+ + + +
−	0	+ + + +

Sign Sequence 2.

Here the first order derivative may have any sign depending on h and k as shown in the block. This gives $N(2) = 1$ and thus by Budan-Fourier theorem $f(x)$ has exactly one zero in the ranges (0,1) and (1,2) when $1 < h \leqslant 2$ and $1 \leqslant k \leqslant \sqrt{2}$.

Now, for $h > 0$, $f(x)$ has three changes of sign and so by Descarte's rule of signs $f(x)$ has three positive zeros (the adjacency matrix being hermitian, complex roots do not appear). Thus, one positive zero of $f(x)$ should be above 2. This explains the feature F_1.

If the positive eigenvalues x_i ($i = 1$ to 4) of G_1 are arranged as $x_1 < x_2 < x_3 < x_4$, the above analysis shows that $0 < x_1 < 1$, $x_2 = 1,1 < x_3 < 2$ and $x_4 > 2$, for $0 \leqslant h \leqslant 2$ and $1 \leqslant k \leqslant \sqrt{2}$. Recalling that x_i's are expressed in β unit (which is negative), we

Table 2 – Mode of variation of HOMO energy with h and k for aniline-like systems

Value of h	Value of k	HOMO energy (in β unit)
0	1	0
0.5	1	0.2767160
1.0	1	0.5042842
0.5	0.5	0.4091893
0.5	1.0	0.2767160
0.5	1.5	0.1824341

find that x_1 is the energy of the HOMO of an aniline-like system. In the following discussion we have determined the mode of variation of x_1 in an approximate manner (Table 2).

x_1 satisfies $f(x)=0$ and for $h>0$, $x_1 \neq 0$. When $0<h<1$ and $1 \leqslant k \leqslant \sqrt{2}$, we have already proved that $0<x_1<1$. So from Eq. (2), we can approximately write,

$$5hx_1^2+(4+3k^2)x_1-4h=0 \qquad \ldots 3(a)$$

which yields

$$x_1=[-(4+3k^2)+\sqrt{(4+3k^2)^2+80h^2}]/10h \qquad \ldots 3(b)$$

We get from 3(b)

$$\left(\frac{\partial x_1}{\partial k}\right)_k = \frac{(4+3k^2)[\sqrt{(4+3k^2)^2+80h^2}-(4+3k^2)]}{10h^2\sqrt{[(4+3k^2)^2+80h^2]}}$$

$$=(+)\text{ ve} \qquad \ldots 4(a)$$

and

$$\left(\frac{\partial x_1}{\partial k}\right)_h = \frac{3k}{5h}\left[\frac{4+3k^2}{\sqrt{[(4+3k^2)^2+80h^2]}}-1\right]=(-)\text{ ve}$$

$$\ldots 4(b)$$

This explains the feature F_2.

Case (b): p-phenylenediamine-like systems

The factorisation of such graphs (G_2) has been shown in Fig. 2. It shows that the CP for such a graph is given by,

$$P(G_2;x)=(x^2-1)\phi(x)\psi(x) \qquad \ldots (5)$$

where $$\phi(x)=x^3-(h+1)x^2-(k^2+2-h)x+(2h+k^2) \qquad \ldots (6)$$

and $$\psi(x)=x^3-(h-1)x^2-(k^2+2+h)x+(2h-k^2) \qquad \ldots (7)$$

When $h=1$, $\psi(1)=-2k^2$ and $\phi(1)=0$.

Table 3 – Derivatives of $\phi(x)$ at $x=0,1$ and 2

Order of derivative	Value of derivative at		
	$x=0$	$x=1$	$x=2$
0	$2h+k^2$	$2(h-1)$	$-k^2$
1	$-(k^2+2-h)$	$-(1+h+k^2)$	$6-3h-k^2$
2	$-2(h+1)$	$4-2h$	$10-2h$
3	6	6	6

Table 4 – Derivative of $\psi(x)$ at $x=0$ and 1

Order of derivative	Value of derivative at	
	$x=0$	$x=1$
0	$2h-k^2$	$-2k^2$
1	$-(k^2+2+h)$	$-3(h-1)-k^2$
2	$-2(h-1)$	$8-2h$
3	6	6

Thus, whatever be the value of k, 1 is a doubly degenerate eigenvalue of G_2-one value coming from the factor (x^2-1) and the other from the factor $\phi(x)$ of Eq. (5). This explains the feature F_3.

When $2h=k^2$, the factor $\psi(x)$ gives $x=0$ as one eigenvalue of G_2. This explains the feature F_4.

If $2h<k^2$, there are two changes of sign in both $\phi(x)$ and $\psi(x)$, irrespective of whether h is greater than, equal to or less than 1. Hence, including the eigenvalue +1 obtainable from the first factor in (5), G_2 should have five positive (and so three negative) eigenvalues. Again, if $2h<k^2$, $\phi(x)$ has two and $\psi(x)$ has one change of sign. Thus, G_2 has four positive (and so four negative) eigenvalues when $2h<k^2$. This explains the feature F_5.

The values of the zeroth to the third order derivatives of $\phi(x)$ and $\psi(x)$ are given in Tables 3 and 4 respectively. For $1<h<5$, one finds from these tables that for $x=0$ the signs of the sequence $\{\phi^{(i)}(0)\}$, $i=1$ to 3, will be like any one of the following rows.

+	+	−	+
+	−	−	+
+	0	−	+

Sign Sequence 3.

There is uncertainty in the sign of the first order derivative only, as shown in the block. In any case, $N(0)=2$. In the same way one can verify that $\{\phi^{(i)}(1)\}$ and $\{\phi^{(i)}(2)\}$ have the following sign-sequences (with $1<h<5$):

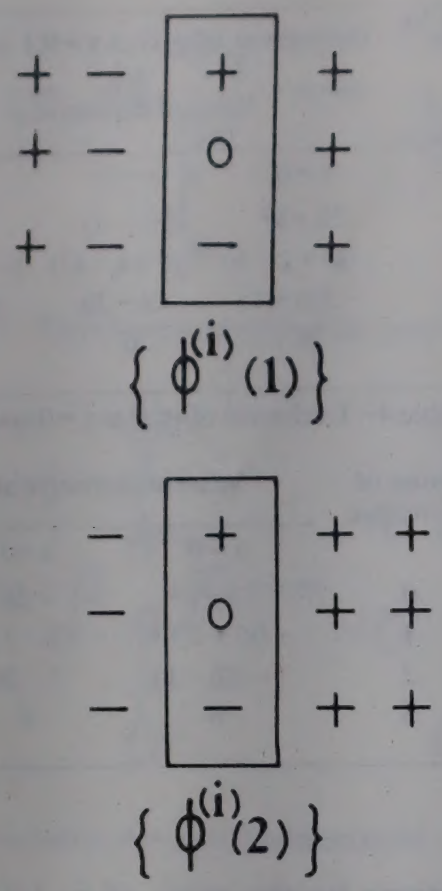

Sign Sequence 4.

Thus, N(1) = 2 and N(2) = 1. Hence, for $1 < h < 5$, there is no zero of $\phi(x)$ in (0,1) and exactly one zero in (1,2), whatever be the value of k.

Next we consider $\psi(x)$ under the condition $2h > k^2$ and $1 < h < 5$.... (A). The following sign-sequences can be obtained from Table 4.

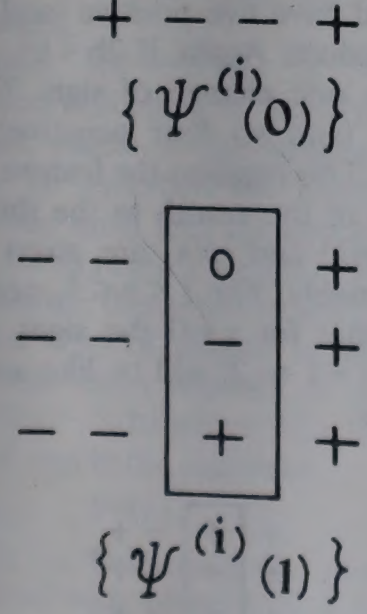

Sign Sequence 5.

Thus, N(0) = 2 and N(1) = 1 so that $\psi(x)$ has exactly one zero in (0,1) under the condition (A). And we have already proved that $\phi(x)$ has no zero in (0,1) under condition (A). Thus, $P(G_2; x)$ has only one zero in (0,1) when condition (A) is satisfied. Moreover, since it is a zero of the factor $\psi(x)$ we can approximately examine its mode of variation with h and k as follows:

Table 5 – Mode of variation of the eigenvalue x_j between 0 and 1 with change in h and k for the graph G_2 under the condition $2h > k^2$ and $1 < h < 5$

Value of h	Value of k	x_j
1	0.5	0.6074191
2	0.5	0.8577246
1	1.0	0.2541017
2	1.0	0.5719933
1	0.5	0.6074191
1	1.0	0.2541017
2	1.0	0.5719933
2	1.5	0.2714127

Neglecting x^3 from $\psi(x)$ and writing x_j for the root in (0,1), we have

$$(h-1)x_j^2 + (k^2+2+h)x_j - (2h-k^2) = 0 \qquad \ldots (8)$$

$$\left(\frac{\partial x_j}{\partial h}\right)_k = \frac{2 - x_j^2 - x_j}{2x_j(h-1) + k^2 + 2 + h} = (+)\text{ ve} \qquad \ldots 9(a)$$

and

$$\left(\frac{\partial x_j}{\partial k}\right)_h = -\frac{2k(x_j+1)}{2x_j(h-1) + k^2 + 2 + h} = (-)\text{ ve} \qquad \ldots 9(b)$$

This explains the feature F_6.

Discussion

That the highest occupied molecular orbital (HOMO) energy in β unit for most chemically interesting conjugated systems lies in the range (0,1) has been assumed by many workers[22] for estimating HOMO-LUMO separation graph-theoretically. We have proved this for aniline-like systems.

The mode of variation of the HOMO energy as described in the feature F_2 and proved in Eqs. 4(a) and 4(b) can be verified from Coulson's of π-electron calculations. For a ready reference we have shown some HOMO eigenvalues in Table 2, where the feature F_2 is obvious. Increase in h means increase in electronegativity of the heteroatom in G_1. With a fixed k, if electronegativity of the heteroatom increases, π-electrons from the ring are drawn towards the heteroatom which reduces the π-electron density in the ring. Thus, the energy of the HOMO should decrease with increase in h. Remembering that β is negative, we

get a qualitative explanation for the trend predicted by Eq. 4(a) and reflected in the first part of Table 2.

There are experimental evidences also for this trend. For example, the charge-transfer transition energies of complexes of tetracyanoethylene with aniline and N-methylaniline in $CHCl_3$ are 2.097 eV and 1.946 eV respectively[24] which show that N-methylaniline is the better donor. The inductive effect of $-CH_3$ reduces the h value of N-atom and thus makes the HOMO energy of N-methylaniline greater than that of aniline. With a given h, increase in k means increase in the resonance integral between the heteroatom andthe ring C-atom attached to it. Thus, with increase in k, more and more π-electrons are drawn towards the ring from the heteroatom which increases electron density in the ring and thus increases the HOMO energy. In β unit, therefore, the HOMO eigenvalue should decrease with increase in k at a fixed h. This is predicted by Eq. 4(b) and reflected in the second part of Table 2.

The results stated in the features F_{3-6} as regards the number of bonding, antibonding and non-bonding π-MO's for *p*-phenylenediamine-like systems can be verified from Coulson's compilation[23]. From Streitwieser's list[25] we find for oxygen atom, $h_O = 2$ and $k_{C-O} = 1$, which are applicable to *p*-quinol, and $h_O = 1$ and $k_{C=O} = 1$, which are applicable to *p*-benzoquinone. In both cases, $2h > k^2$, so that both these systems (with graph G_2) should have five bonding MOs. In *p*-benzoquinone there are 8 π-electrons, so that one bonding MO remains vacant which makes it a π-electron acceptor. Again, *p*-quinol has 10 π-electrons and all its bonding MOs are filled up; thus, it behaves as a π-donor. The existence of well-known charge-transfer complexes of the quinhydrone type[26,27] (in the solid state) is in agreement with these facts. For *p*-quinol and *p*-phenylenediamine, Streitwieser's list[25] also shows that the necessary heteroatom parameters satisfy condition (A). The physical reason for the variation of x_j (which is presumably the HOMO of *p*-quinol or *p*-phenylenediamine), as proved in Eqs 9(a) and 9(b), can be interpreted as done in the case of aniline above; such trends are shown in Table 5.

References

1 Wiener H, *J Am chem Soc*, 69 (1947) 17; 69 (1947) 2636; *J phys Chem*, 52 (1948) 425.
2 Hosoya H, *Bull chem Soc Japan*, 44 (1971) 2332.
3 Bonchev D & Trinajstić N, *J chem Phys*, 67 (1977) 1517.
4 Randic M, *J Am chem Soc*, 97 (1975) 6609.
5 Singh S, Mishra B K & Mishra R K, *Indian J Chem*, 27A (1988) 188.
6 Singh P P, *Indian J Chem*, 27A (1988) 469.
7 Rakshit S C, Banerjee M & Hazra B, *Indian J Chem*, 27A (1988) 183.
8 Gutman I & Polansky O E, *Mathematical concepts in organic chemistry* (Springer-Verlag, Berlin), 1986.
9 Graovac A, Gutman I & Trinajstić N, *Topological approach to the chemistry of conjugated molecules* (Springer-Verlag, Berlin), 1977.
10 Singh S, Mishra B K & Mishra R K, *Indian J Chem*, 27A (1988) 377; 677.
11 Gutman I, Trinajstić N & Živković T, *Tetrahedron*, 29 (1973) 3449.
12 Mukherjee A K, *Indian J Chem*, 25A (1986) 574.
13 Gutman I & Mukherjee A K, *Indian J Chem*, 27A (1988) 847.
14 Demidovich B P & Maron I A, *Computational mathematics* (Mir Publishers, Moscow), 1976, p. 176.
15 Sachs H, *Publ Math (Debrecen)*, 9 (1962) 270.
16 Hosoya H, *Theoret chim Acta*, 25 (1972) 215.
17 Aihara J, *J Am chem Soc*, 98 (1976) 6840.
18 Gutman I & Polansky O E, *Theoret chim Acta*, 60 (1981) 203 and references cited therein.
19 Balasubramanian K, *Theoret chim Acta*, 65 (1984) 49; *J comput Chem*, 3 (1984) 587.
20 (a) Mclelland B J, *J chem Soc, Faraday Trans II*, 78 (1982) 911.
(b) Dias J R in *Graph theory and topology in chemistry*, edited by R B King & D H Rouvray (Elsevier, Amstardam), 1987, p. 466.
21 Datta K K & Mukherjee A K, *Proc Indian Acad Sci, (Chem Sci)*, 101 (1989) 143.
22 Gutman I & Rouvray D H, *Chem Phys Lett*, 62 (1979) 384, and references cited therein.
23 Coulson C A & Streitwieser (Jr) A, *Dictionary of π-electron calculations* (Pergamon Press, Oxford), 1965.
24 Farrell P G & Newton J, *J phys Chem*, 69 (1965) 3506; *Tetrahedron Lett*, 45 (1966) 5517.
25 Streitwieser (Jr) A, *Molecular orbital theory for organic chemists* (John Wiley, New York) 1961, p. 135.
26 Michaelis L & Granick S, *J Am chem Soc*, 66 (1944) 1023.
27 Matsuda H, Osaki K & Natta I, *Bull chem Soc, Japan*, 31 (1958) 611.

Indian Journal of Chemistry
Vol. 29A, July 1990, pp. 618-623

Spectroscopic and molecular mechanics study of the conformational properties of methyl cyanoacetate and ethyl cyanoacetate

R Prasad*, Y K Mishra & R K Gupta†

Deparment of Chemistry, Devi Ahilya University, Vigyan Bhawan, Khandwa Road, Indore 452 001

Recevied 14 July 1988; revised 26 June 1989; accepted 11 September 1989

Infrared spectra of methyl cyanoacetate and ethyl cyanoacetate have been recorded in different solvents of varying polarity in the region 4000-600 cm^{-1} along with laser Raman spectra of the liquid samples of these compounds in the region 4000-50 cm^{-1}. Existence of conformers has been confirmed in both the molecules on the basis of splitting of some of the bands and CNDO/2 and molecular mechanics computations. Normal coordinate analysis of both the molecules has been carried out and the force constants thus obtained have been employed to compute the energies of different conformers by the method of molecular mechanics. The computed conformational energy of methyl cyanoacetate is in close agreement with the experimental values. It has been concluded that for these molecules the *cis* conformers are most stable. The energy difference between *gauche-trans* and *cis-trans* conformers of ethyl cyanoacetate is computed to be 1.0 kcal mol^{-1}.

Conformational properties of substituted esters of acetic acid[1,2] have attracted much attention recently. In the present study a complete assignment of the fundamental modes of methyl cyanoacetate (MCA) and ethyl cyanoacetate (ECA) is attempted on the basis of normal coordinate analysis (NCA) and dipole moment data from CNDO/2 computations. The present study was undertaken because the earlier study of the vibrational spectra[3] of these molecules is mostly qualitative. Conformational behaviour of these molecules has been studied by the method of molecular mechanics with a view to computing the conformational energies of these molecules. This study has revealed that *cis* conformers of these molecules are the most stable.

Materials and Methods

MCA and ECA obtained from M/s Fluka AG were redistilled under vacuum and their purity was checked by TLC. The IR spectra of the samples in the region 4000-600 cm^{-1} were recorded on a Perkin-Elmer 377 IR spectrophotometer using NaCl optics. The Raman spectra of the samples in the region 4000-50 cm^{-1} were recorded on a Jobin-Yvon Ramanar HG-25 Raman spectrometer equiped with an Argon ion laser source. The bands below 600 cm^{-1} were taken from Raman spectra of the molecules and are shown in Fig. 1. The frequencies in all the measurements are believed to be accurate to $\pm$ 2 cm^{-1}.

Results and Discussion

Vibrational analysis

All the computations were performed on an ICIM-600 computer. Rotameric forms of MCA and ECA are shown in Figs 2 and 3 respectively. CNDO/2 computations were performed employing the computer programme of Hase and Schweig[4] using Slater type basis functions. The cartesian coordinates were computed using a computer programme of Crackett[5] employing geometrical parameters obtained from molecular mechanics computations of the present study. The computed dipole moments are listed in Table 1. It can be seen that in the case of ECA, rotation about $O-C_2H_5$ bond does not bring any large change in the dipole moment and is likely to have little effect on the splitting of IR bands. It is worth mentioning that the computed value of the dipole moment of ECA is very close to the experimental value reported by Krishna *et al.*[6]

Both the molecules considered here belong to C_s point group and classification of their normal modes is $19A + 11A'$ and $25A + 14A'$ for MCA and ECA respectively. The assignment of modes to different bands has been made on the basis of earlier studies on these and related molecules[7-11], dependence of IR peak intensities on solvent polarity in conjuction with dipole moment data of

†Department of Chemistry, Kurukshetra University, Kurukshetra

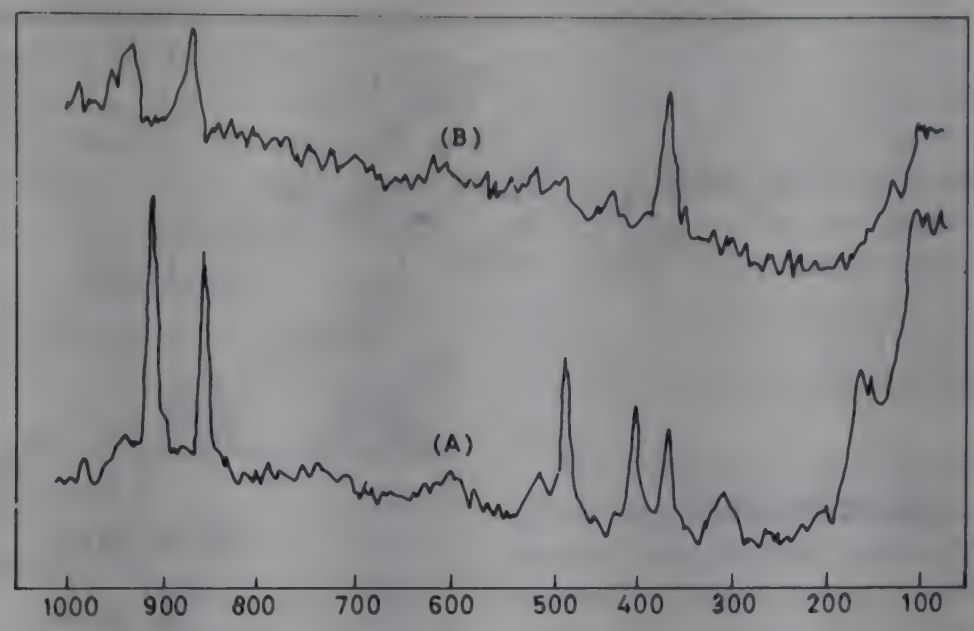

Fig. 1 – Raman spectra of methyl cyanoacetate (A) and ethyl cyanoacetate (B) in the region 1000-100 cm^{-1}

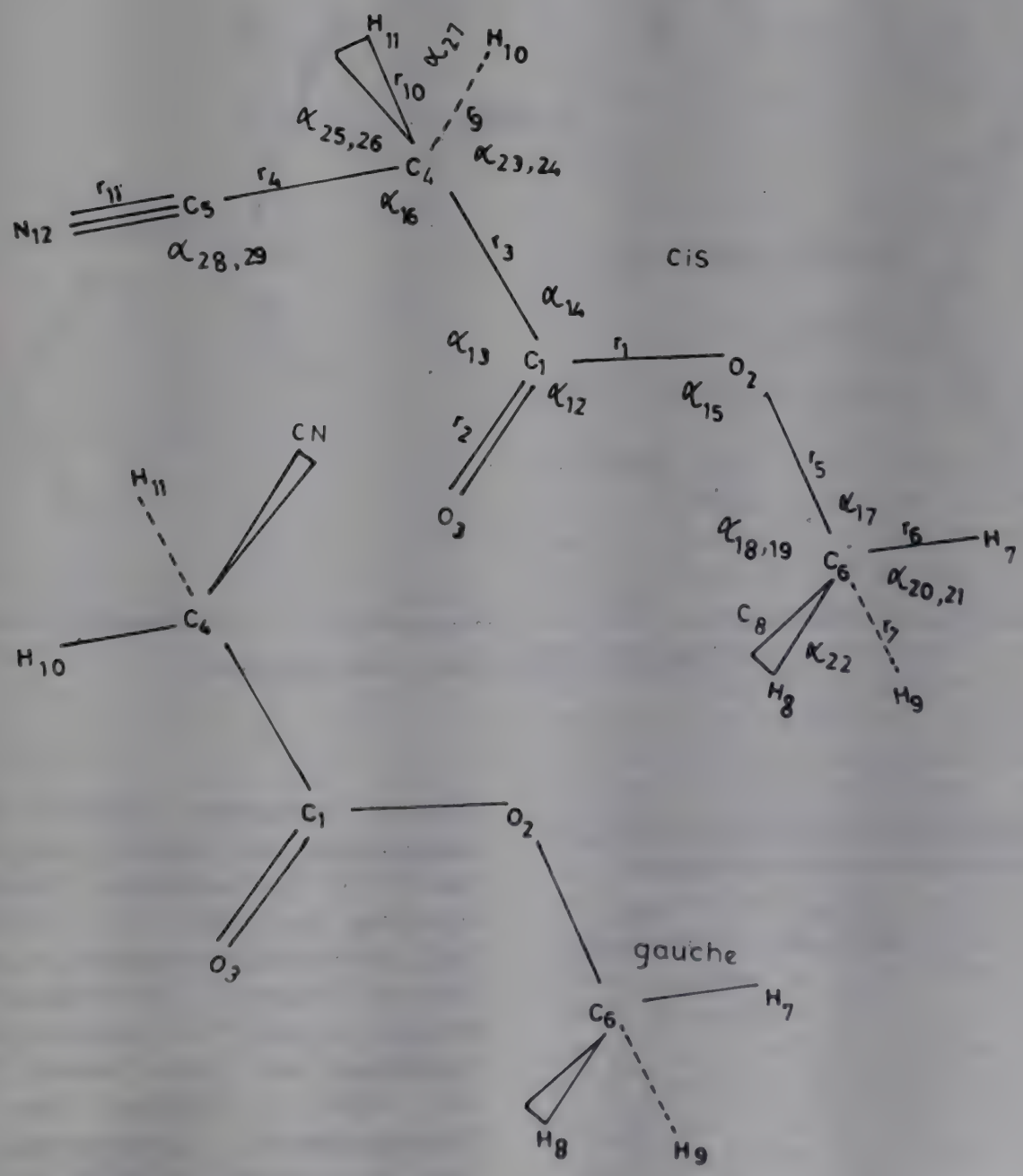

Fig. 2—Different rotameric forms of methyl cyanoacetate

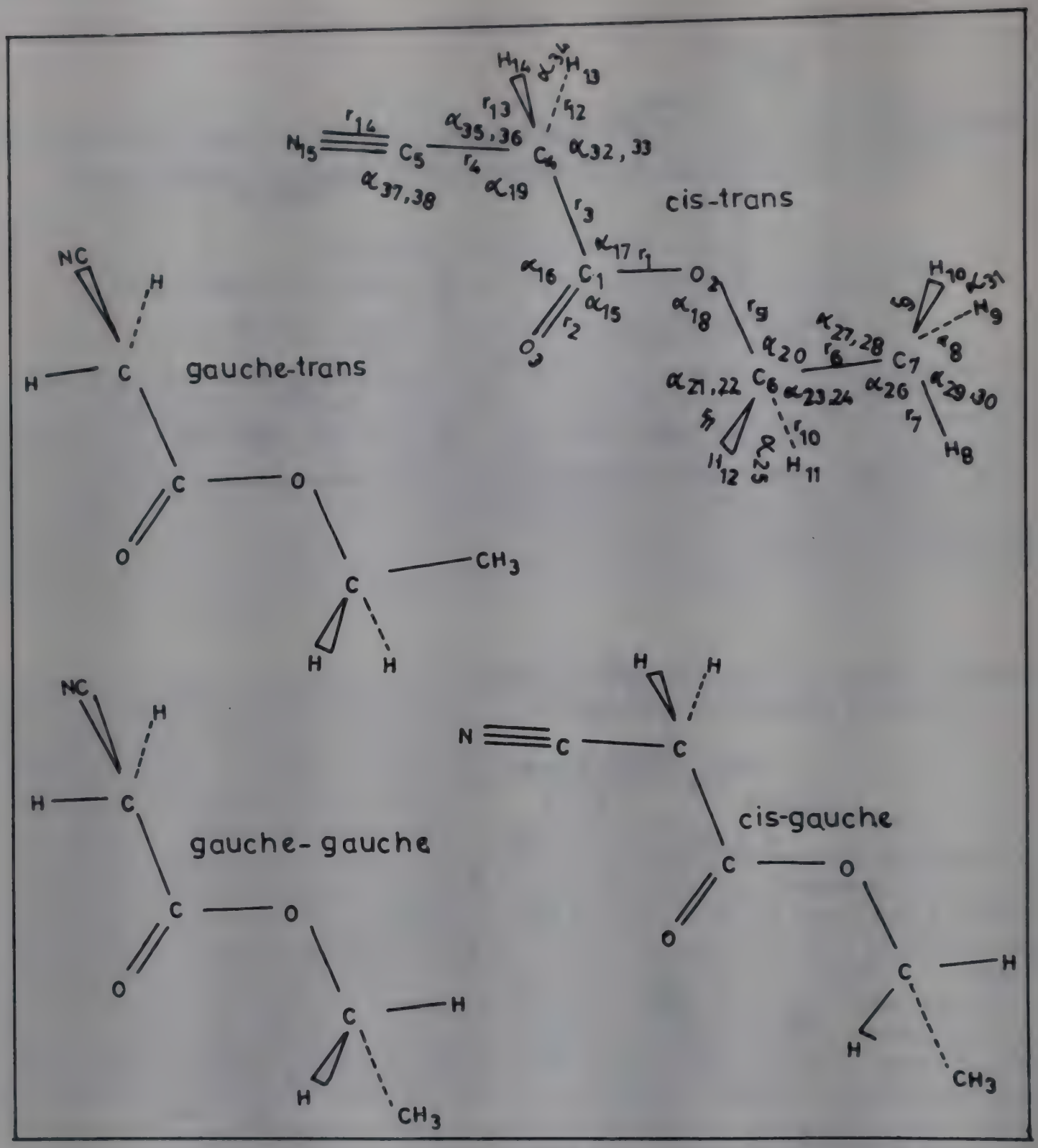

Fig. 3—Different rotameric forms of ethyl cyanoacetate

Table 1—Dipole moments (Debyes) of different conformers of methyl cyanoacetate and ethyl cyanoacetate

Conformers	methyl cyanoacetate	ethyl cyanoacetate
cis	4.06	—
gauche	2.52	—
cis-trans	—	4.48
cis-gauche	—	4.26
gauche-trans	—	2.65
gauche-gauche	—	2.80

different conformers obtained from CNDO/2 computations and present normal coordinate analysis (NCA). The calculation of normal frequencies, according to Wilson's FG matrix method was made employing a computer programme of McIntosh and Peterson[12]. The programme uses Hilderbrandt's method[13] of normalization of torsional coordinate and a new formula for out-of-plane wag which is different from that used by Schachtschneider[14]. Computations were performed only for *cis* isomer of MCA and *cis-trans* isomer of ECA. The structural parameters were based on

microwave work on ethyl formate[15,16]. The internal coordinates not included in the figure are: (i) out-of-plane C=O bending (π_{30}, π_{39} for MCA and ECA respectively) which involves the atoms 3, 1, 2, 4 and (ii) three torsions t_{31}, t_{32}, t_{33}, about bonds C_1-O_2, O_2-C_6 and C_1-C_4 respectively in MCA and four torsions t_{40}, t_{41}, t_{42}, t_{43} for torsions about bonds C_1-O_2, O_2-C_6, C_6-C_7 and C_1-C_4 respectively in ECA. Computations were first performed for MCA and the refined force constants for MCA were taken as initial set for ECA. The refinement of force constants was made employing the SIMPLEX optimization algorithm of Nelder and Mead[17] via a non-linear least squares analysis of calculated and observed eigenvalues. The best set of force constants thus obtained is presented in Table 2.

Table 2—Force constants of methyl cyanoacetate and ethyl cyanoacetate

Force constants	Methyl cyanoacetate	Ethyl cyanoacetate
$K_{C_1-O_2}$	4.34	4.33
$K_{C_1=O_3}$	8.75	8.74
$K_{C_1-C_4}$	2.57	2.57
$K_{C_4-C_5}$	2.95	2.95
$K_{O_2-C_6}$	3.83	3.52
$K_{C_6-C_7}$	—	3.00
$K_{C_6-H_7}=K_{C_6-H_8}=K_{C_6-H_9}$	5.05	—
$K_{C_7-H_8}=K_{C_7-H_9}=K_{C_7-H_{10}}$	—	5.06
$K_{C_6-H_{11}}=K_{C_6-H_{12}}$	—	5.10
$K_{C_4-H_{10}}=K_{C_4-H_{11}}$	4.96	—
$K_{C_4-H_{13}}=K_{C_4-H_{14}}$	—	5.0
$K_{C_5\equiv N_{12}}/K_{C_5\equiv N_{15}}$	18.25	18.25
$H_{O_3=C_1-O_2}$	2.0	2.20
$H_{O_3=C_1-C_4}$	0.72	0.72
$H_{C_4-C_1-O_2}$	1.45	1.55
$H_{C_1-O_2-C_6}$	1.68	1.60
$H_{C_1-C_4-C_5}$	2.50	2.50
$H_{O_2-C_6-C_7}$	—	2.10
$H_{O_2-C_6-H_7}=H_{O_2-C_6-H_8}=H_{O_2-C_6-H_9}$	0.57	—
$H_{O_2-C_6-H_{11}}=H_{O_2-C_6-H_{12}}$	—	0.56
$H_{H_{11}-C_6-H_{12}}$	—	0.57
$H_{C_7-C_6-H_{11}}=H_{C_7-C_6-H_{12}}$	—	0.58
$H_{H_7-C_6-H_8}=H_{H_7-C_6-H_9}=H_{H_8-C_6-H_9}$	0.55	—
$H_{H_8-C_7-H_9}=H_{H_8-C_7-H_{10}}=H_{H_9-C_7-H_{10}}$	—	0.57
$H_{C_6-C_7-H_8}=H_{C_6-C_7-H_9}=H_{C_6-C_7-H_{10}}$	—	0.56
$H_{C_1-C_4-H_{10}}=H_{C_1-C_4-H_{11}}$	0.65	—
$H_{C_1-C_4-H_{13}}=H_{C_1-C_4-H_{14}}$	—	0.65
$H_{C_5-C_4-H_{10}}=H_{C_5-C_4-H_{11}}$	0.61	—
$H_{C_5-C_4-H_{13}}=H_{C_5-C_4-H_{14}}$	—	0.64
$H_{H_{10}-C_4-H_{11}}$	0.51	—
$H_{H_{13}-C_4-H_{14}}$	—	0.49
$H_{C_4-C_5\equiv N_{12}}=H_{C_4-C_5\equiv N_{15}}$	0.13	0.13
$\pi_{O_3-C_1-O_2-C_4}$	0.42	0.46
$t_{C_1-O_2}$	0.57	0.53
$t_{O_2-C_6}$	0.58	0.68
$t_{C_6-C_7}$	—	0.20
$t_{C_4-C_1}$	0.38	0.38

Stretching constants are in units of mdyn $Å^{-1}$ and bending constants are in units of mdyn $Å/(rad)^{-2}$.

The calculated and observed frequencies together with potential energy distribution (PED) in internal coordinates from major contributions are shown in Tables 3 and 4 for MCA and ECA respectively. Comparable values of force constants for MCA and ECA demonstrate the transferability of force constants in the two molecules. The present NCA in general is in accord with the assignment of the observed spectra of MCA by Charles *et al.*[3] except that CH_3 symmetric stretch should be assigned at 2858 cm^{-1}. The present NCA has led to the assignment of the observed spectral bands to definite modes of vibrations.

In the earlier study on ECA Charles *et al.*[3] have discussed briefly some of the conformation-sensitive bands. In their study carbonyl band is reported to be asymmetric. However, the same is reported to be symmetric by Brown[10]. Therefore, it was decided to record the Raman spectrum of the molecule along with IR spectra in different solvents with a view to confirming the splitting of carbonyl band and making a complete assignment of the observed spectra. The assignment of C−H stretching modes was made in accordance with the results of Noline and Jones for deuterated esters[11] and the present NCA. The description of bands is given in Table 4. The IR band for C=O stretching mode is reproduced in Fig. 4. In CCl_4 solution the band splits into two peaks at 1745 and 1710 cm^{-1}. The intensity of the band at 1710 cm^{-1} is decreased considerably in CH_3CN solution. Based on solvent polarity and dipole moment data from CNDO/2 results these bands are assigned to C=O stretching modes of c-t and g-t conformers respectively. On the basis of studies on related esters, present NCA, solvent polarity studies and dipole moment data from CNDO/2 studies, the bands observed at 1300, 1260, 1230 and 1200 cm^{-1} are assigned to C−O stretching modes of c-g, c-t, g-t, and g-g conformers respectively of ECA. The PED values in Tables 3 and 4 show that except C−H and C≡N stretching modes, most of the modes show a mixed picture as they have contributions from other modes as well.

Table 3—Observed and calculated frequencies and PED (%) values for *cis* methyl cyanoacetate

Obs. (cm−1)	Calc. (cm^{-1})	PED in internal coordinates
3007	2990	$0.66r_6 + 0.16r_7 + 0.16r_8$
2970	2988	$0.49r_7 + 0.49r_8$
2960	2960	$0.49r_9 + 0.49r_{10}$
2910	2885	$0.49r_9 + 0.49r_{10}$
2882	2864	$0.33r_6 + 0.33r_7 + 0.33r_8$
2265	2247	$0.94r_{11}$
1755	1730	$0.61r_2$
1465	1442	$0.26\alpha_{22}$
1450	1428	$0.47\alpha_{20} + 0.47\alpha_{21}$
1440	1428	$0.23\alpha_{20} + 0.33\alpha_{21} + 0.39\alpha_{22}$
1405	1411	$0.11\alpha_{23} + 0.11\alpha_{24} + 0.27\alpha_{27}$
1360	1384	$0.12\alpha_{25} + 0.12\alpha_{26} + 0.43\alpha_{27}$
1270	1259	$0.21r_1 + 0.20\alpha_{12}$
1185	1188	$0.23\alpha_{23} + 0.23\alpha_{24} + 0.24\alpha_{25} + 0.24\alpha_{26}$
1015	1012	$0.11r_2 + 0.14\alpha_{15} + 0.13\alpha_{17} + 0.11\alpha_{18}$
935	938	$0.11r_4 + 0.12r_5 + 0.30\alpha_{16} + 0.10\alpha_{17}$
905	936	$0.44\alpha_{18} + 0.45\alpha_{19}$
885	881	$0.23\alpha_{23} + 0.23\alpha_{24} + 0.16\alpha_{25} + 0.16\alpha_{26}$
850	857	$0.16r_3 + 0.47r_5 + 0.11\alpha_{16}$
750	750	$0.11r_2 + 0.10r_4 + 0.22\alpha_{12} + 0.14\alpha_{17}$
710	677	$0.12r_2 + 0.40r_4$
575	573	$0.83\pi_{30}$
502	527	$0.29\alpha_{14} + 0.11\alpha_{16}$
425	417	$0.40t_{33}$
350	346	$0.12t_{31} + 0.21t_{32}$
318	313	$0.14\alpha_{12} + 0.19\alpha_{14} + 0.32\alpha_{15}$
300	308	$0.57\alpha_{28}$
200	193	$0.41\alpha_{29} + 0.30t_{31}$
160	168	$0.16\alpha_{14} + 0.28\alpha_{16}$
90	90	$0.30\alpha_{29} + 0.31t_{32}$

RMS error (wave number) = 12.64

Table 4—Observed and calculated frequencies and PED (%) values for *cis-trans* ethyl cyanoacetate

Obs. (cm−1)	Calc. (cm^{-1})	PED in internal coordinates
3000	3002	$0.46r_{10} + 0.46r_{11}$
2990	2993	$0.65r_7 + 0.16r_8 + 0.16r_9$
2980	2990	$0.46r_8 + 0.46r_9$
2970	2971	$0.49r_{12} + 0.49r_{13}$
2938	2926	$0.49r_{10} + 0.49r_{11}$
2915	2896	$0.49r_{12} + 0.49r_{13}$
2880	2865	$0.33r_7 + 0.33r_8 + 0.33r_9$
2270	2263	$0.92r_{14}$
1745	1725	$0.59r_2 + 0.10\alpha_{17}$
1475	1474	$0.55\alpha_{25}$
1462	1459	$0.47\alpha_{29} + 0.47\alpha_{30}$
1445	1459	$0.11\alpha_{29} + 0.11\alpha_{30} + 0.65\alpha_{31}$
1430	1448	$0.11\alpha_{32} + 0.11\alpha_{33}$
1405	1426	$0.11\alpha_{27} + 0.11\alpha_{28} + 0.11\alpha_{29} + 0.11\alpha_{30}$
1370	1370	$0.72\alpha_{36}$
1335	1326	$0.12\alpha_{12} + 0.72\alpha_{24}$
1260	1263	$0.18r_1 + 0.16\alpha_{15}$
1185	1205	$0.20\alpha_{32} + 0.20\alpha_{33} + 0.26\alpha_{34} + 0.26\alpha_{35}$
1125	1131	$0.21\alpha_{21} + 0.21\alpha_{22} + 0.23\alpha_{23} + 0.23\alpha_{24}$
1097	1085	$0.10r_5 + 0.10\alpha_{26} + 0.15r_6$
1030	1005	$0.12\alpha_{21} + 0.12\alpha_{22} + 0.16\alpha_{27} + 0.16\alpha_{28}$
935	919	$0.11r_2 + 0.21r_5 + 0.21\alpha_{19}$
910	892	$0.20\alpha_{32} + 0.20\alpha_{33} + 0.11\alpha_{34} + 0.11\alpha_{35}$
870	865	$0.36\alpha_{26}$
850	862	$0.21\alpha_{27} + 0.21\alpha_{28}$
815	833	$0.10r_3 + 0.24r_5 + 0.21r_6$
750	767	$0.15r_1 + 0.15r_3 + 0.14r_4 + 0.25\alpha_{25}$
710	685	$0.20t_4 + 0.14r_5 + 0.10\alpha_{19}$
565	565	$0.10\alpha_{37} + 0.20\alpha_{39}$
492	492	$0.15\alpha_{17} + 0.39\alpha_{19}$
475	464	$0.21\alpha_{18} + 0.20\alpha_{19}$
425	424	$0.39t_{43}$
365	393	$0.21t_{40} + 0.39t_{42}$
300	301	$0.37\alpha_{37} + 0.41\alpha_{26}$
240	241	$0.22\alpha_{18} + 0.12\alpha_{19} + 0.12\alpha_{20}$
230	227	$0.59\alpha_{38} + 0.29\pi_{39}$
160	162	$0.19\alpha_{17} + 0.21\alpha_{18} + 0.21\alpha_{19}$
130	136	$0.20\pi_{39} + 0.23t_{40}$
80	83	$0.32t_{41}$

Molecular mechanics computations

These computations were performed with a view to calculating conformational energies of the molecules under consideration. The initial geometry was constructed on the basis of microwave study on methyl formate[15], ethyl formate[16] and molecular mechanics computations on these molecules by Allinger and Chang[18]. Computations were performed using a computer programme of Allinger[19] with suitable modifications for CYBER-180 computer. In all the computations, we have used force constant data listed in Table 2. In the computation of torsional energy, V_3 term was ignored for dihedral angle ω greater than 60° if V_1 and V_2 terms were zero otherwise it was included for all values of ω. In the methodology of computation, the total energy was computed as a sum of terms corresponding to compression, bending, van der Waals and dipole energies. Minimization of these terms relative to a 'strainless' set by successive alteration in atomic coordinates lead to a configuration of minimum steric energy[20,21]. Optimized geometries thus obtained compared favou-

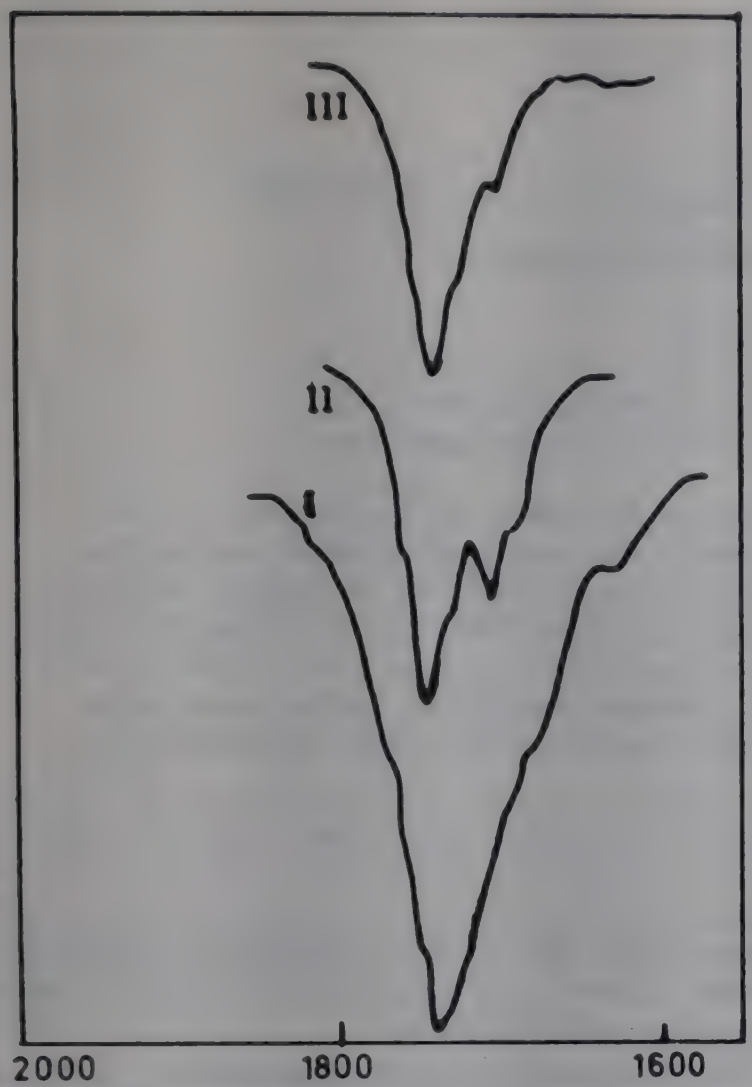

Fig. 4—IR spectra of ethyl cyanoacetate in the region 2000-1600 cm^{-1} showing bands corresponding to C=O stretching mode [I, liquid film; II, CCl_4 solution; III, CH_3CN solution]

rably with the reported geometries of esters obtained by microwave method[16,17].

During computation of torsional energy, the torsional parameter for dihedral angle $C_{sp}-C_{sp3}-C_{sp2}=0$ was needed. This parameter was computed by performing CNDO/2 computations at dihedral angles of 30, 60, 90 and 120 degrees. A plot of dihedral angles versus total energy for MCA gave V_3 barrier to be 1.5 kcal/mol. This was treated as the initial value for molecular mechanics computations; it was then varied in steps of 0.1 till the calculated conformational energy was in good agreement with the observed value. The final value of V_3 term was 2.1 kcal/mol. Using this value of V_3 term for $C_{sp}-C_{sp3}-C_{sp2}=0$ dihedral angle in ECA, we computed the conformational energy between *cis-trans* and *gauche-trans* conformers of ethyl cyanoacetate to be 1.0 kcal/mol. Unfortunately, this could not be compared with the experimental values as the same is not reported. In all these computations the energies of *cis* conformers were found to be lower which is in accord with the experimental finding on MCA[3]. The total barrier for rotation about C−C bond in the molecules will be 3.6 kcal/mol which is the sum of V_3 terms for three rotations: $C_{sp}-C_{sp3}=0$ and two rotations $H-C_{sp3}-C_{sp2}=0$.

References

1 Raso M A, Garcia M V & Morcillo J, *J molec Struct*, 115 (1984) 449.
2 Dube N, Porwal P & Prasad R, *J Raman Spectrosc*, 19 (1988) 189.
3 Charles S W, Jones G I L & Owen N L, *J chem Soc Faraday Trans*, II, 69 (1973) 1454.
4 Hase H L & Schweig A, *Quantum chemistry programme exchange*, 11 (1974) 261.
5 Crackett A, *Quantum chemistry programme exchange*, 11 (1970) 169.
6 Krishna B, Bhargwa S K & Prakash B, *J molec Struct*, 8 (1971) 195.
7 Wilmhurst J K, *J molec Struct*, 1 (1957) 201.
8 Williams G & Owen N L, *Trans Faraday Soc*, 67 (1971) 950.
9 Charles S W, Jones G I L, Owen S J, Cyvin S J & Cyvin B N, *J molec Struct*, 16 (1973) 225.
10 Brown T L, *Spectrochim Acta*, 18 (1962) 1615.
11 Nolin B & Jones R N, *Can J Chem*, 34 (1956) 1392.
12 McIntosh D F & Peterson M R, *Quantum chemistry programme exchange*, 11 (1977) 342.
13 Hilderbrandt R L, *J molec Spectrosc*, 44 (1972) 599.
14 Schachtschneider J H, Report 231 and 57 (Shell Development Co. USA) 1964.
15 Curl (Jr) R F, *J chem Phys*, 30 (1959) 1529.
16 Riverose J M & Wilson (Jr) E B, *J chem Phys*, 46 (1967) 4605.
17 Nelder J A & Mead R, *Computer Journal*, 7 (1965) 308.
18 Allinger N L & Chang S H M, *Tetrahedron*, 33 (1977) 1561.
19 Allinger N L, *Quantum chemistry programme exchange*, 11 (1976) 318.
20 Allinger N L, Tribble M T, Miller M A & Wertz D H, *J Am chem Soc*, 93 (1971) 1637.
21 Wertz D H & Allinger N L, *Tetrahedron*, 30 (1974) 1579.
22 Hernanz A, Garcia M V & Morcillo J, *J molec Struct*, 80 (1982) 335.

Indian Journal of Chemistry
Vol. 29A, July 1990, pp. 624-630

Adsorption and reactivity of thiophene on promoted molybdena and tungsta systems

M O Alias & V Srinivasan*

Department of Chemistry, Indian Institute of Technology, Madras 600 036

Received 24 April 1989; revised 5 October 1989; accepted 7 November 1989

The interaction of thiophene with Co and Ni promoted molybdena and tungsta catalyst systems has been studied with a view to interpreting surface activity for hydrodesulfurisation reaction. Gas-solid chromatography has been used for the study of adsorption of thiophene on catalysts. Adsorption isotherms and heat of adsorption have been evaluated. It is found that molybdena catalysts have good thiophene adsorption properties as compared to tungsta catalysts. The better thiophene adsorption properties obtained for molybdena catalyst is consistent with higher desulfurisation activities observed for these catalysts. Ni-Mo system is the most suitable catalyst system for hydrodesulfurisation reaction.

Molybdena and tungsta catalysts promoted by Co and Ni are most frequently used for hydrodesulfurisation (HDS) reactions. Adsorption of n-butylamine and 1-butene on reduced form of promoted molybdena and tungsta catalysts was reported by us in an earlier publication[1] in order to determine the contribution of surface acid sites to the desulfurisation activity of the catalysts. The present work attempts to draw some conclusions regarding the interaction of thiophene with Co and Ni promoted molybdena and tungsta catalysts with a view to making use of the results for interpreting surface activity for thiophene desulfurisation reaction. Low surface area support α-alumina used by many workers[2-6] has been used for the preparation of the catalysts in order to highlight the activity of active species. Low surface area support is virtually non-porous and consists of small discrete particles or may have coarse pore structure.

Gas-solid chromatographic technique has been used for thiophene adsorption study. Effort has also been made to study the temperature programmed desorption (TPD) of thiophene adsorbed reduced catalysts by gas chromatography using H_2 as the carrier gas. This is sometimes referred to as temperature programmed reduction. TPD has been used in evaluating differences in nature of adsorption sites in different catalyst systems of molybdena and tungsta promoted by Ni and Co.

Although under HDS condition the catalysts are in a sulfided state to a large extent, it is relevant to study the oxide precursors because it has been shown that a direct relationship exists between properties of oxidic catalysts and the corresponding sulfided catalysts[7-9].

Temperature programmed reduction (TPR), a sensitive technique for studying reducibility, has been applied successfully for the characterisation of hydrodesulfurisation (HDS) catalysts[10-14]. Low temperature oxygen chemisorption has recently come out as an important surface specific tool for characterising reduced[15,16] as well as sulfided[17-19] hydroprocessing catalysts.

Materials and Methods

Catalysts

A list of the catalysts studied is given in Table 1, together with catalyst compositions and specific surface areas. All catalysts were prepared with low surface area α-alumina carrier with a surface area of 6 m^2g^{-1}. Mo-Al_2O_3 and W-Al_2O_3 samples were prepared as described earlier[1] by impregnating α-alumina with ammonium paramolybdate and ammonium paratungstate solutions respectively. Ni and Co promoted molybdena and tungsta catalysts were prepared by coimpregnation technique. After the impregnation process, catalysts were dried in an air oven at 110°C for 3 hr and finally calcined at 500°C for 6 hr. The notation used for catalyst is as follows: For instance 3Ni-13Mo-Al_2O_3 indicates a sample containing 3 wt% NiO and 13 wt % MoO_3. For the sake of simplicity all catalyst concentrations are referred to in their oxidic form. In nickel tungsta catalyst (Cat. No. 12) and cobalt molybdena catalyst (Cat.

Table 1 – Composition and surface areas of various catalysts

No.		Composition (atomic ratio) (r)				Surface area (m^2g^{-1})
		Ni / Ni + Mo	Co / Co + Mo	Ni / Ni + W	Co / Co + W	
1	13Mo-Al_2O_3	0.00	0.00	—	—	7.2
3	3Ni-13Mo-Al_2O_3	0.31	—	—	—	9.1
4	3.9Ni-13Mo-Al_2O_3	0.37	—	—	—	7.5
10	3.5Co-13Mo-Al_2O_3	—	0.34	—	—	4.6
11	24W-Al_2O_3	—	—	0.00	0.00	4.4
12	4.5Ni-24W-Al_2O_3	—	—	0.37	—	7.0
13	2.8Co-24W-Al_2O_3	—	—	—	0.27	6.4

Carrier used was α-alumina having surface area, 6 $m^2 g^{-1}$ (BET, N_2)

No. 10), the atomic ratios of Ni/Ni + W and Co/Co + Mo are 0.37 and 0.34 respectively which were comparable to the Ni/Ni + Mo ratio of Cat. No. 4. The value of Co/Co + W ratio in cobalt tungsta catalyst was 0.27 and it was comparable to Ni/Ni + Mo ratio of Cat. No. 3.

BET surface areas of all samples were evaluated in a conventional volumetric set up[20] by N_2 adsorption at liquid N_2 temperature.

X-ray powder analysis

X-ray powder diffraction patterns of the catalysts were recorded on a Philips X-ray diffractometer using the CuK_α radiation. The diffraction patterns obtained were compared with relevant ASTM standards.

Thiophene adsorption

The apparatus used for thiophene adsorption by pulse flow was similar to that used earlier for *n*-butylamine adsorption[1]. Prior to adsorption experiments, the catalyst was heated in a stream of argon gas (1 atm and 10 ml/min) for 2 hr at 400°C. Catalyst was then reduced *in situ* in pure H_2 (20 ml/min for 4 hr at 400°C). After lowering the temperature to the required value, H_2 flow rate was raised to 36.5 ml/min. The stream of H_2 carrier gas from the reference channel of thermal conductivity detector flowed successively through the catalyst tube, measuring channel and the exit. Thiophene (1 μl) was injected through a rubber septum at the top of the catalyst tube. The detector temperature was maintained at 200°C and detector current was set at 200 mA. The part of the apparatus between the catalyst tube and the detector was held at 110°C to prevent any condensation of thiophene in the tube. Adsorption studies were carried out in the temperature range of 95-190°C. The retention volume calculated from the corrected retention time[21] for the total weight of catalyst used gave a measure of thiophene adsorption. Adsorption isotherms were constructed from elution chromatograms.

Temperature programmed desorption (TPD)

The equipment used was essentially a modification of gas chromatograph by replacing the chromatographic column with catalyst tube. Prior to the desorption experiments, the catalyst (0.37 g) was reduced in pure H_2 (20 ml/min at 400°C for 2 hr) after purging the catalyst at 400°C by argon (10 ml/min for 1 hr). The catalyst was cooled to room temperature in H_2 stream. The H_2 flow rate was raised to 30 ml/min and diverted to flow through thiophene bubblers (40°C). The adsorbate thiophene in H_2 passed over the catalyst at room temperature for 45 min. Then H_2 was diverted to bypass the thiophene bubblers, flowing directly to the catalyst tube. After 2 hr, H_2 flow rate was adjusted to 75 ml/min and temperature of the catalyst was raised linearly at a rate of 13.5°C/min from room temperature to 400°C. Desorption occurred as the temperature of catalyst increased. Successive TPD runs were carried out on the same sample to check for deactivation. The effluent stream could be sampled out using a sample valve at the time of peak emergence and separately analysed qualitatively and quantitatively by gas chromatography.

Thiophene reactivity

The extent of desulfurisation of thiophene by the catalyst was measured using a microcatalytic pulse reactor. Analysis of product stream was ac-

complished with a gas chromatograph. Before the reaction, the catalyst in the reactor was reduced (H_2 flow rate of 20 ml/min for 4 hr at 400°C). The reactant H_2 also served as the carrier gas in the reaction. A large number of thiophene pulses of 5 μl each were introduced at 10-min intervals in order to have steady state activity. Fractional conversion (x) of thiophene was calculated using the data obtained from the analysis of product stream. All conversions were normalised to 0.38 g of catalyst which was the average weight of all catalysts. The reaction temperature was 400°C.

Following the observations made earlier[22,23] under the conditions of thiophene desulfurisation by gas chromatographic method, first order kinetics was assumed to determine rate constants.

All chemicals were of AR grade (BDH/Merck).

Results and Discussion

Thiophene adsorption

The retention volumes (V_g) corresponding to various corrected retention times, t_r(corr), for the total weight of catalyst sample in the catalyst tube have been obtained using the Eq. (1)

$$V_g = t_r(\text{corr})F/M \qquad \ldots(1)$$

where F is the carrier gas flow rate and M is the weight of catalyst. The V_g values increase logarithmically with the reciprocal of the absolute temperature according to Eq. (2).

$$\log V_g = C - \frac{\Delta H}{2.303 R} \cdot \frac{1}{T} \qquad \ldots(2)$$

where C is a constant reflecting column dimensions, i.e. carrier gas flow rate and entropy of adsorption. The plot of V_g against 1/T is linear, the slope of which gives the heat of adsorption. Heats of adsorption evaluated are listed in Table 2. Equation (2) has been obtained by integrating Eq. (3).

$$\frac{\partial \ln V_g}{\partial T} = \frac{\Delta H}{RT^2} \qquad \ldots(3)$$

Table 2 – Heats of adsorption (q_{st}) of thiophene on catalysts, evaluated from log V_g versus 1/T plot

No.*	q_{st} (kJ mol^{-1})	No.*	q_{st} (kJ mol^{-1})
1	4.0	11	3.8
3	12.0	12	7.5
4	12.0	13	4.2
10	4.6		

*For catalyst notation see Table 1.

Since V_g appears as its logarithm, it is not necessary that it be used directly; any quantity proportional to V_g, such as t_r(corr) or the retention volume for the total weight of adsorbent in the column may be used provided this refers to flow rates or volumes corrected to a single temperature. Thus, the change in the characteristics of adsorption process with temperature is detected, not only from the adsorption isobars but also from the plot of log V_g against 1/T or from the plots of V_g versus T. Since the retention volume is proportional to the steady state amount adsorbed, the V_g versus T or t_r(corr) versus T plots in essence represent the adsorption isobars. The linearity of log V_g versus 1/T plot would be affected if there is a change in the value of entropy of adsorption which in turn may be due to a change in the mode of adsorption or in the activity of sites.

The adsorption isotherms constructed from the elution chromatograms after applying correction for the diffusional broadening are depicted in Figs 1-3. The method of Cremer and Bechtold[24] was used for correcting the chromatographic bands. Plot of the reciprocal values of Fig. 1 shows that these isotherms obey the equation of Langmuir isotherms (see Fig. 4). Extrapolation to $1/C = 0$ would give the number of thiophene sites. In order to obtain the strength distribution of the sites adsorbing thiophene, the isosteric heat of adsorption (q_{st}) was calculated at various coverages in the range of $0.54\text{-}3.43 \times 10^{-2}$ mmole of thiophene absorbed per gram of catalyst. The heat of adsorption at a given surface coverage was calculated in the usual manner by applying the Clau-

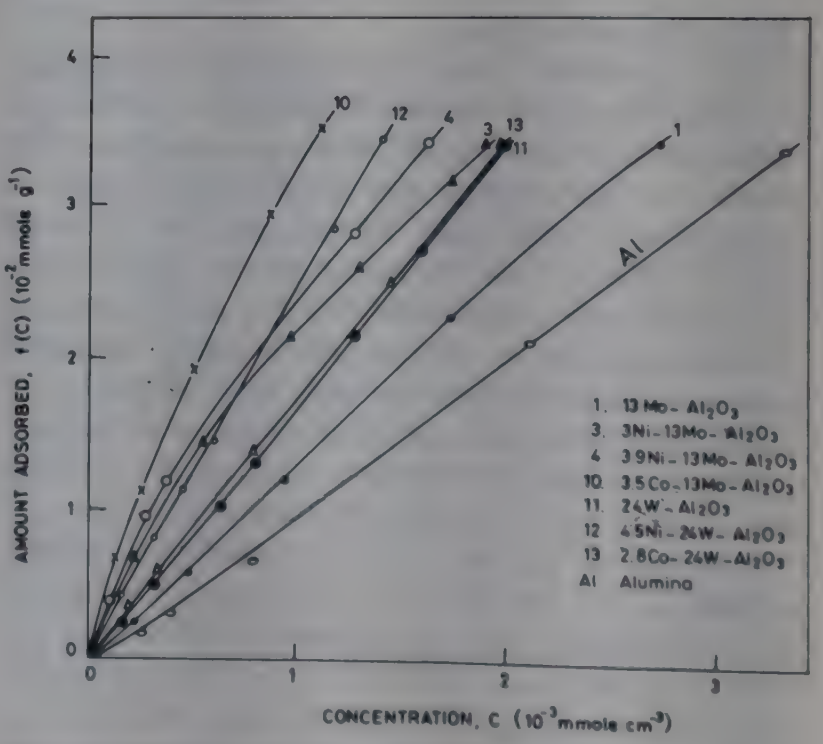

Fig. 1 – Adsorption isotherms of thiophene on catalysts at 95°C (catalyst No. 4 at 110°C)

sius-Clapeyron equation to a series of adsorption isotherms at different temperatures determined by gas chromatography. Figure 5 shows the variation of q_{st} value with coverage for various catalysts. Adsorption of thiophene on all catalysts was measured in the reduced state, using H_2 as the carrier gas. This was done in order to preserve the catalyst surface and to obtain results which would be relevant to reaction conditions.

On incorporation of Mo or W into alumina, there is an increase in the number of sites adsorbing thiophene (Figs 1-3). An increase in the strength of these sites may also occur (Fig. 5). Adsorption characteristics of molybdena and tungsta

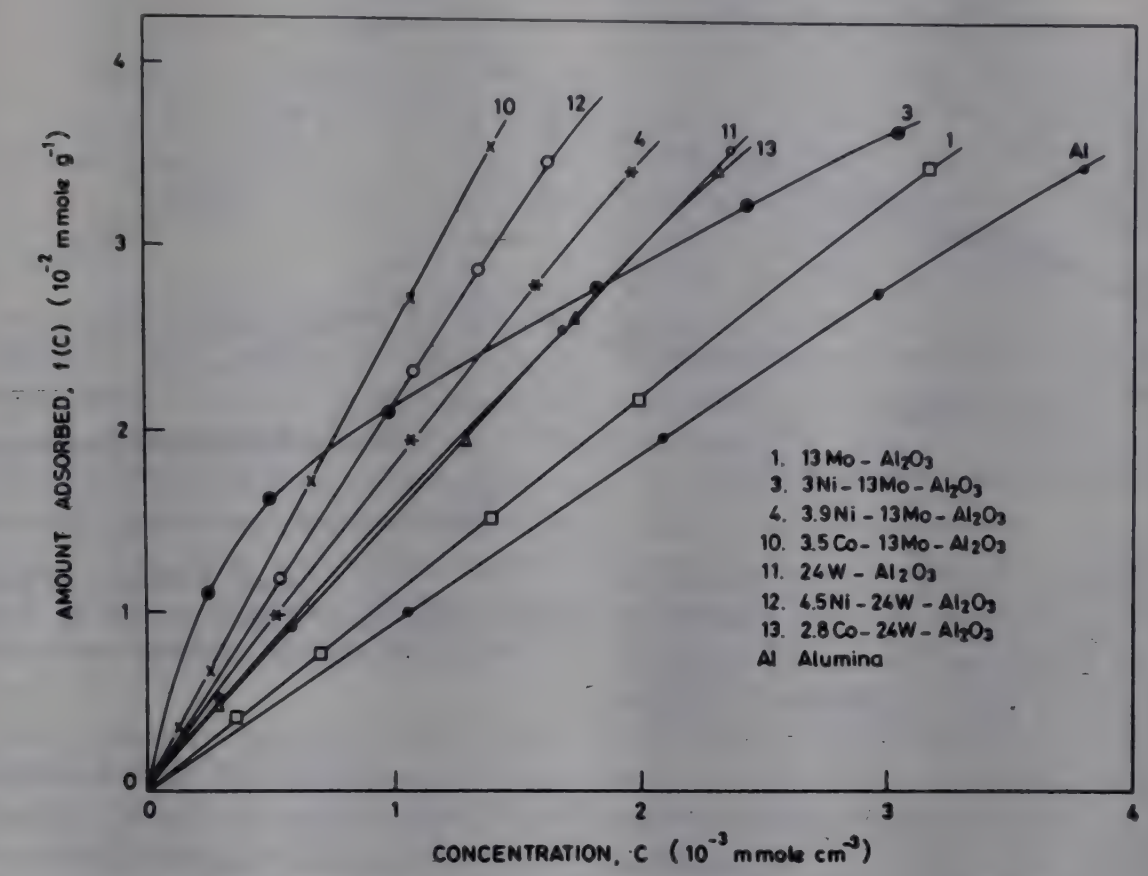

Fig. 2 – Adsorption isotherms of thiophene on catalysts at 155°C

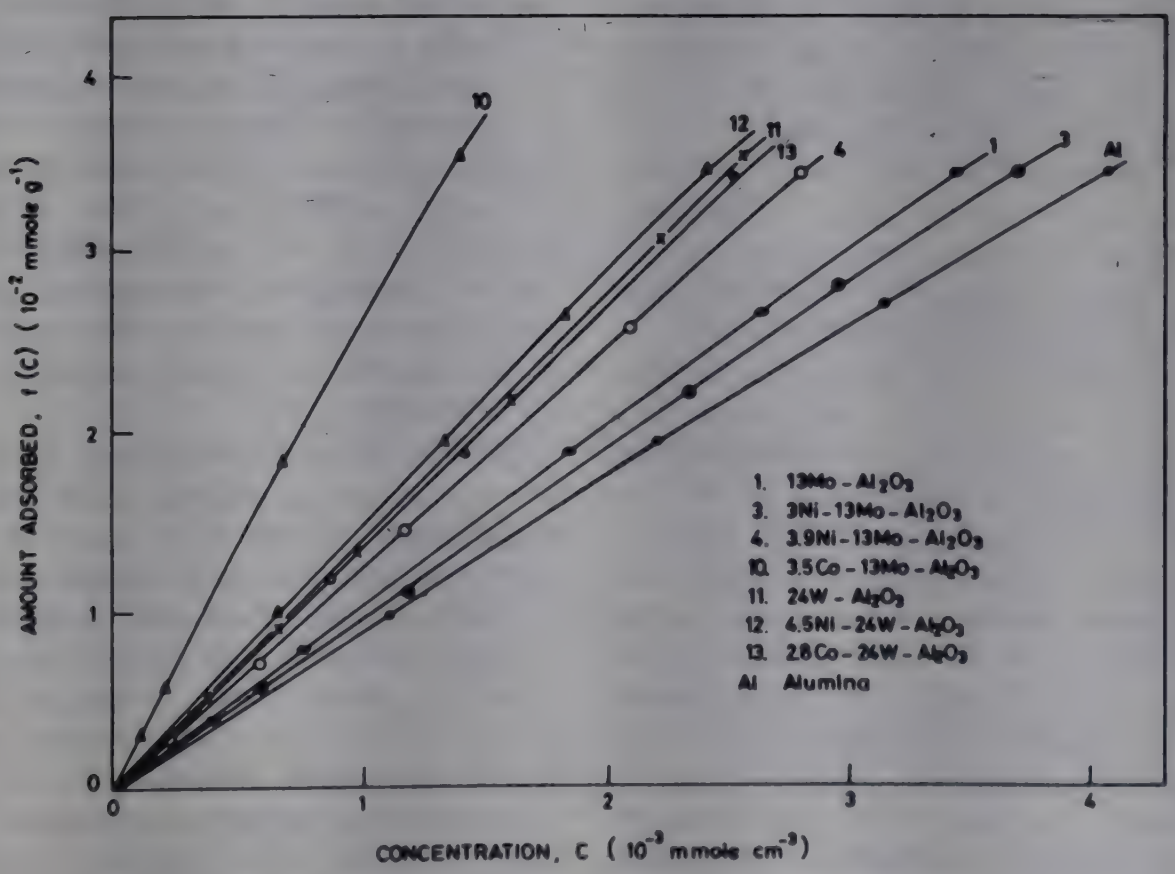

Fig. 3 – Adsorption isotherms of thiophene at 190°C

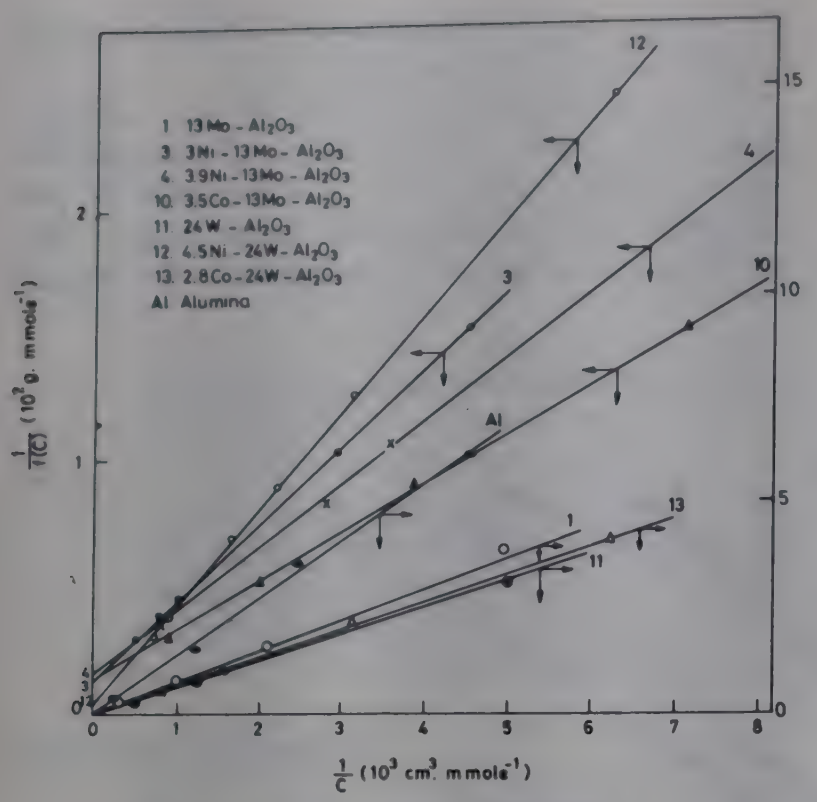
1 13Mo - Al2O3
3 3Ni - 13Mo - Al2O3
4 3.9Ni - 13Mo - Al2O3
10 3.5Co - 13Mo - Al2O3
11 24W - Al2O3
12 4.5Ni - 24W - Al2O3
13 2.8Co - 24W - Al2O3
Al Alumina
1/T(C) (10³ g. mmole⁻¹)
1/C (10³ cm³. mmole⁻¹)

Fig. 4 – Plot of the reciprocal values of Fig. 1

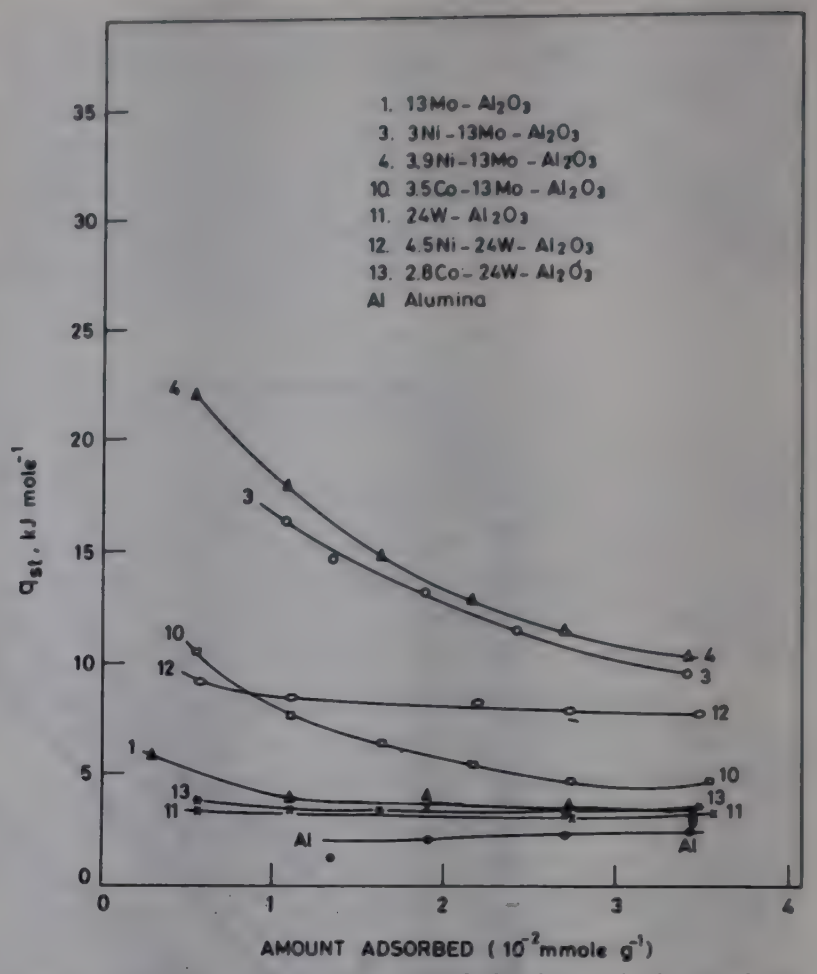
1. 13Mo - Al2O3
3. 3Ni - 13Mo - Al2O3
4. 3.9Ni - 13Mo - Al2O3
10. 3.5Co - 13Mo - Al2O3
11. 24W - Al2O3
12. 4.5Ni - 24W - Al2O3
13. 2.8Co - 24W - Al2O3
Al Alumina
qst, kJ mole⁻¹
AMOUNT ADSORBED (10⁻² mmole g⁻¹)

Fig. 5 – Calculated dependences of the isosteric heat of adsorption upon the adsorbed amount of thiophene

catalysts were greatly affected by the nature of promoter ions. The effect of different promoters like Co and Ni on thiophene adsorption could be examined in relation to their desulfurization activity. On incorporation of either Ni or Co into Mo-Al_2O_3 and W-Al_2O_3, there is an increase in both the number (Figs 1-3) and strength (Fig. 5) of sites adsorbing thiophene; the extent of this increase being different for Ni and Co promoted molybdena and tungsta catalysts. Figure 4 shows that the number of thiophene sites is more for nickel molybdena Cat No. 4 than that for cobalt molybdena Cat No. 10 or for cobalt tungsta Cat No. 12 under comparable compositions. The number of thiophene sites decreases in the order: Ni-Mo-Al_2O_3 > Co-Mo-Al_2O_3 > Ni-W-Al_2O_3. Similarly, the number of sites for nickel molybdena Cat No. 3 (r = 0.31) is high compared to that of cobalt tungsta catalyst (Cat No. 13; Co/Co + W = 0.27).

The results of effect of Ni and Co incorporation upon the strength of sites adsorbing thiophene in Mo-Al_2O_3 and W-Al_2O_3 systems are given in Table 2. The heat of adsorption of Ni and Co promoted catalysts are higher than those of unpromoted molybdena and tungsta catalysts. The heats of adsorption obtained from log V_g versus 1/T plots are believed to be representative of the average values over the range of concentrations involved. The dependence of isosteric heat of adsorption upon the adsorbed amount (Fig. 5) shows the changes as a result of Ni and Co incorporation on the strength distribution of thiophene sites in catalysts. The heats of adsorption (q_{st}) decrease with surface coverage, this effect being more pronounced with nickel molybdena catalysts (Cat Nos. 3 and 4). The q_{st} values do not vary much for tungsta catalysts and are higher in the region of higher adsorbed amounts. The trend in the variation of heats of adsorption with Ni content of the catalyst, obtained from the isotherms, is similar to that obtained from the log V_g versus 1/T plot. From the results obtained with Ni and Co promoted catalysts, it can be concluded that the strength of thiophene adsorption sites is more for nickel molybdena Cat No. 4 than for nickel tungsta Cat No. 12 or for cobalt molybdena Cat No. 10. Similarly the strength of adsorption sites for nickel molybdena Cat No. 3 (r = 0.31) is higher as compared to cobalt tungsta Cat No. 13 (Co/Co + W = 0.27).

On the basis of foregoing results from thiophene adsorption studies, it can be deduced that molybdena systems have good adsorption properties in comparison to tungsta catalysts. Ni-Mo system is superior to all other catalyst systems.

Examination of the activity data for different catalyst systems (Table 3) reveals that the activities decrease in the order: Ni-Mo-Al_2O_3 (Cat No. 4) > Co-Mo-Al_2O_3 > Ni-W-Al_2O_3. All these catalysts have comparable compositions. Similarly, activity of Co-W.Al_2O_3 catalyst is relatively very low as compared to that of Ni-Mo Cat No. 3, though

Table 3 – Reaction rate constants for various catalysts at 400°C

No.*	Rate constant (mol $atm^{-1} g^{-1} s^{-1}$)	
	Initial state (1st pulse)	Steady state (14th pulse)
1	2.18×10^{-6}	5.18×10^{-6}
3	1.05×10^{-5}	4.93×10^{-6}
4	1.43×10^{-5}	5.18×10^{-6}
10	5.80×10^{-6}	4.48×10^{-6}
11	1.00×10^{-7}	2.10×10^{-7}
12	4.50×10^{-7}	8.50×10^{-7}
13	1.00×10^{-7}	2.70×10^{-7}

*For catalyst notation see Table 2.

they have comparable atomic ratios. In general, molybdena catalysts have higher desulfurisation activities as compared to those of tungsta catalysts. Nickel promoted molybdena catalysts have maximum desulfurization activities. The better thiophene adsorption properties obtained from molybdena catalyst is consistent with higher desulfurisation activity of these catalysts. Ni-Mo system is the most suitable catalyst system for desulfurisation reaction.

Temperature programmed desorption

The results in Table 4 show that with Ni and Co promoted molybdena Cat Nos. 3,4 and 10, unpromoted molybdena Cat No. 1 and Ni promoted tungsta Cat No. 12 thiophene desorption is obtained while with cobalt tungsta Cat No. 13 and unpromoted tungsta catalyst, no desorption peak is observed suggesting negligible adsorption of thiophene on latter catalysts. Thiophene desorption from catalyst decreases in the order: Ni-Mo-Al_2O_3 (Cat No. 5) > Co-Mo-Al_2O_3 ≥ Ni-W-Al_2O_3 and Ni-Mo-Al_2O_3 (Cat No. 3) ≫ Co-W-Al_2O_3. These catalysts have comparable compositions. These desorption results are consistent with activity data. For catalysts with higher desulfurisation activity, the amount of thiophene desorbed is more. Thus with Ni-Mo catalysts, more amount of thiophene is found to desorb.

Only one peak is observed in the desorption chromatograms and this can be attributed to thiophene desorbed at 200°C. Successive TPD runs on the same sample do not show any desorption peak indicating marked deactivation of sites responsible for adsorption. It may be pointed out that during the process of adsorption of thiophene and subsequent desorption, the colour of the catalyst changes from dull white to black and formation of coke has been detected. Thus the deactivation could be attributed to coke formation. Concentration of sites adsorbing thiophene is thus considerably decreased by first TPD run itself.

Table 4 – Amount of thiophene desorbed (200°C) during TPD run on various reduced catalysts

No.*	Thiophene desorbed (mol. g^{-1})	No.*	Thiophene desorbed (mol. g^{-1})
1	1.1×10^{-4}	11	No desorption
3	8.9×10^{-4}	12	1.8×10^{-4}
4	9.4×10^{-4}	13	No desorption
10	3.5×10^{-4}		

*For catalyst notation see Table 1

X-ray powder patterns reveal the presence of MoO_3 and WO_3 in respective catalysts along with the diffraction bands of α-Al_2O_3. Cobalt and Ni molybdena catalysts indicate the signals corresponding to $CoMoO_4$ and $NiMoO_4$ respectively. Increase in intensity for Bragg reflections of $Al_2(MoO_4)_3$ has been observed in Co molybdena catalyst as compared to that in Ni molybdena sample. Cobalt and Ni tungsta catalysts show strong diffraction bands of $Al_2(WO_4)_3$ in addition to very weak bands corresponding to $CoWO_4$ and $NiWO_4$. Thus for active molybdena catalysts with high adsorption property, octahedral molybdenum due to $CoMoO_4$ or $NiMoO_4$ is easily detected. Corresponding species like $CoWO_4$ or $NiWO_4$ is not detected in less active tungsta catalysts with poor adsorption. It may be concluded that the octahedral phases are highly conducive for adsorption and reactivity. Ni and Co molybdena catalysts on reduction show strong diffraction patterns corresponding to MoO_2, signals due to MoO_3 or $Al_2(MoO_4)_3$ are not observed. Corresponding tungsta catalysts indicate strong diffraction bands of $Al_2(WO_4)_3$.

Acknowledgement

This work was supported by the CSIR, New Delhi.

References

1 Alias M O & Srinivasan V, *Indian J Chem*, 78 (IC 6144).
2 Ipatieffv, Monroe G S, Fischer L E & Meisinger E E, *Ind Eng Chem*, 41 (1949) 1802.
3 McKim F L W & Carbon A, *Can J Res*, B27 (1949) 813.
4 Wan Shen-Wu, *Ind Eng Chem*, 45 (1953) 234.
5 Todo N, Muramatsu K, Kurita M, Ogawa K, Sato T, Ogawa M & Kotera Y, *Bull Japan Petrol Ins*, 14 (1972) 89.
6 Magnusson J, *Ind Eng Chem Res*, 26 (1987) 877.
7 Mone R, *Preparation of catalysts*, ed by B Delmon, Jacobs P A & Poncelet G (Elsevier, Amsterdam) 1976, p. 381. 381.
8 Scheffer B, Arnoldy P, van Oers E M, de Beer V H J & Moulin J A, *Appl Catal*, 25 (1986) 303.

9 Topsoe N-Y, Topsoe H, *J Catal*, 77 (1982) 293.
10 Arnoldy P & Moulijn J A, *J Catal*, 93 (1985) 38.
11 Arnoldy P, de Booys J L, Scheffer B & Moulijn J A, *J Catal*, 96 (1985) 122.
12 Thomas R, deBeer V H J & Moulijn J A, *Bull Soc Chim Belg*, 90 (1982) 1349.
13 Arnoldy P, Franken M C, Scheffer B & Moulijn J A, *J Catal*, 96 (1985) 381.
14 Nag N K, Fraenkel D, Moulijn J A & Gates B C, *J Catal*, 66 (1980) 162.
15 Liu H C, Yuan L & Weller S W, *J Catal*, 61 (1980) 282.
16 Lopez Agudo A, Gil Llambias F J, Reyes P & Garcia Fierro J L, *Appl Catal*, 1 (1981) 59.
17 Zmierczak W, Muralidhar G & Massoth F E, *J Catal*, 77 (1982) 432.
18 Chung K S & Massoth F E, *J Catal*, 64 (1980) 332.
19 Candia R, Clausen B S, Bartholdy J, Topsoe N-Yu, Lengeler B & Topsoe H, *Proceedings 8th international congress on catalysis, Berlin (West)* 1984.
20 Srinivasan V, *Proc Indian Acad Sci*, 45A (1957) 120.
21 Greene S A & Pust H, *J phys Chem*, 62 (1958).
22 Habgood H W, *The solid-gas interface*, ed by E A Flood (Marcel Dekker, New York) 1967, p. 611.
23 Bassett D W & Habgood H W, *J phys Chem*, 64 (1960) 769.
24 Bechtold E, *Gas chromatography* 1962, ed by M Van Swaay (Butterworth, London), 1963, p. 49.

Indian Journal of Chemistry
Vol. 29A, July 1990, pp. 631-634

Electrical and magnetic properties of poly(N-ethylaniline)

A D Borkar & Mool C Gupta*
Chemistry Department, Nagpur University, Nagpur 440 010

Received 14 September 1989; revised and accepted 22 December 1989

Poly(N-ethylaniline) has been obtained by peroxodisulphate oxidation of N-ethylaniline in aqueous sulphuric acid solution. TGA shows an initial mass loss due to loss of water molecules; the activation energy and pre-exponential factor for thermal decomposition in air have been found to be 125 kJ mol^{-1} and 1.4×10^9 s^{-1} respectively. The polymer is paramagnetic and X-ray diffraction data show it to be an amorphous powder. The electrical conductivity has been measured at temperatures from 303 to 433 K. From the plot of log σ vs $1/T$, the activation energy of conductivity has been found to be 0.078 eV. It is suggested from the temperature dependence of the conductivity and magnetic moment that the conduction mechanism is possibly small polaron hopping conduction.

In recent years much attention has been bestowed upon electrically conducting materials which may be useful for rechargeable batteries[1-3], electrochromic display devices[4] and modified electrodes[5-11]. However, most of the studies in the field are confined to conjugated organic polymers, prepared by chemical and electrochemical synthesis, including poly(pyrrole) and poly(aniline). These polymers can be doped with either electron acceptors or donors to yield conducting polymers.

Poly(aniline) is known to be an electroactive polymer when it is obtained from electrochemical oxidation or peroxodisulphate oxidation of aniline in acidic aqueous solution. The structure of poly(aniline) is known as *para*-linked phenylene aminimine[9,12-14] (structure I).

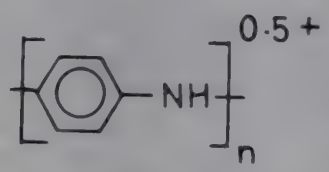

(I)

We have synthesized poly(N-ethylaniline) by peroxodisulphate oxidation of N-ethylaniline; we present here our results of TGA, electrical conductivity, magnetic susceptibility measurements and X-ray diffraction studies on poly(N-ethylaniline) and an explanation of electrical conduction mechanism.

Materials and Methods

Synthesis

Poly(N-ethylaniline) was synthesized by reacting 0.4 mol of N-ethylaniline and 0.12 mol of potassium persulphate in 1 *M* sulphuric acid medium. As the reaction progressed, the colour of the solution changed to black. The mixture was stirred for 60 min and a black precipitate was produced from the reaction. The product was removed, washed with sulphuric acid solution and finally with absolute ethanol and dried.

Chemical analysis of the black powder showed the presence of sulphate ions. The SO_4^{2-} anion could be exchanged on treatment with HCl and the gravimetric determination of sulphate showed that black powder was a polymer. IR spectrum of the polymer did not show absorption in the range 3000-3500 cm^{-1} where characteristic absorption due to N−H group is expected, thereby showing indirectly that bonding in poly(N-ethylaniline) is through N-atom.

Thermogravimetric analysis

The thermogravimetric analysis (TGA) was recorded using a Perkin-Elmer thermal analyser system. TGA was recorded in a nitrogen atmosphere at temperatures in the range 313-873 K with a heating rate of 10°C min^{-1}. TGA in air was carried out on a locally assembled TG apparatus with a slow heating rate of 4°C min^{-1}.

X-ray diffraction

X-ray diffraction pattern was recorded on a Phillips PW 7000 automated X-ray diffractometer, using an iron target, operated at 35 kV and 20 mA.

Magnetic susceptibility

Magnetic susceptibility measurements at room temperature were carried out by the Gouy method[15]. The experimental tube, made up of pyrex glass with a teflon stopper, was thoroughly washed with water and ethanol. A series of weighings were then made in different magnetic fields, using mercury(II) tetrathiocyanatocobalt(II) as the standard.

Electrical conductivity

Electrical conductivity of the polymer was measured using a BPL Megaohmmeter at 303-433 K. The polymer powder was made into a pellet, placed in a temperature controlled chamber and heated to the required temperature. The conductivity values were calculated directly from the measured resistance and sample dimensions.

Results and Discussion

TGA

TGA of the polymer sample (Fig. 1) in nitrogen atmosphere shows that the mass loss starts at 90°C and continues up to 185°C (9.7% mass loss); in the next stage mass loss occurs in the temperature range from 250°C to 510°C. The initial mass loss in the temperature range 90 to 185°C may be due to the loss of water molecules. Syed *et al.*[9] have also reported that poly(aniline) has very high water content (0.78 mol per monomer unit). The second stage mass loss is due to oxidative degradation of polymer in air. The activation energy and pre-exponential factor of thermal decomposition in air were found to be 125 kJ mol^{-1} and 1.4×10^9 s^{-1} respectively from TG data in air by using the Sharp-Wentworth method[16].

The results of chemical analysis (gravimetric determination of sulphate) and TGA indicate that the formula of poly(N-ethylaniline) sulphate should be $(-C_6H_4-N(Et))(SO_4)_{0.2}$ 0.8 H_2O in sulphuric acid medium (theoretical mass loss 9.4%; experimental mass loss from Fig. 1, 9.7%).

X-ray diffraction

X-ray diffraction pattern of the polymer revealed no peak in its spectrum, suggesting that it is an amorphous polymer. A diffuse broad peak corresponding to *d*-spacing of 0.5048 nm was obtained which may be caused by the characteristic distance between the ring planes of benzene rings in adjacent chains. This *d*-spacing value compares well with the *d*-spacing for poly(pyrrole) which is 0.34 nm[5].

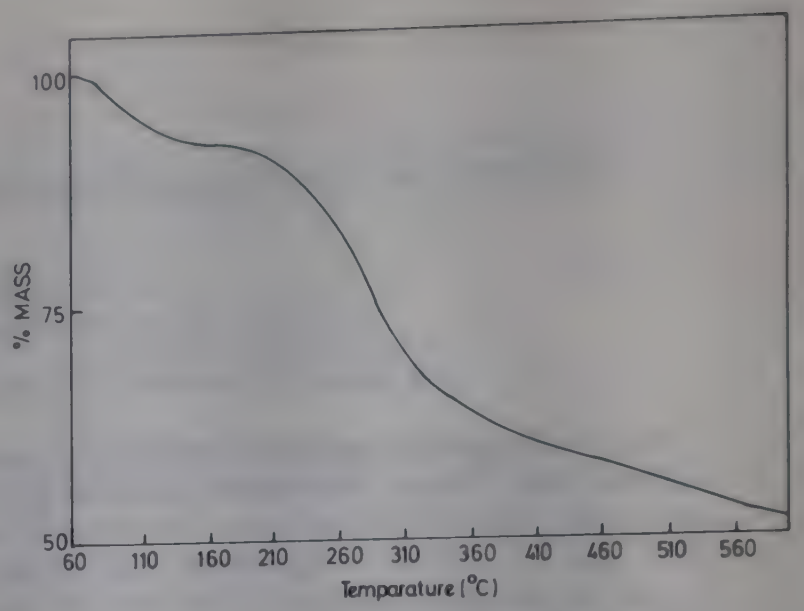

Fig. 1 – TG curve of poly(N-ethylaniline)

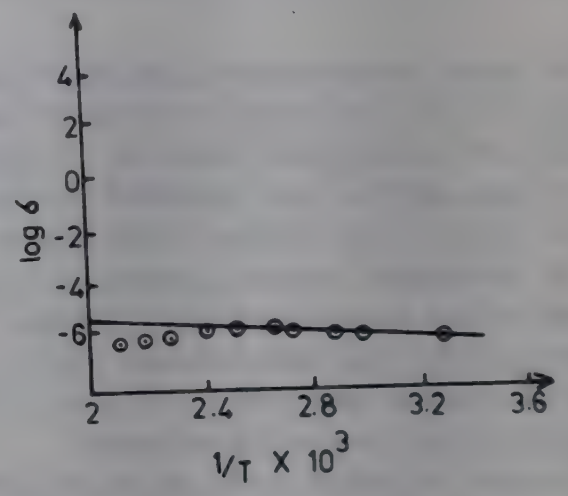

Fig. 2 – Conductivity of poly(N-ethylaniline) as a function of temperature

Magnetic susceptibility

Magnetic susceptibility of the polymer was measured by the Gouy method at room temperature and the magnetic moment was computed by using the expression[15],

$$\mu_{eff.} = 2.83 (\chi_M T)^{\frac{1}{2}} \text{ BM} \qquad \ldots (1)$$

where χ_M' is the molar magnetic susceptibility; $\mu_{eff.}$ for poly(N-ethylaniline) was found to be 4.25 BM at 309 K. This shows that poly(N-ethylaniline) is paramagnetic and has 4 unpaired electrons per chain which corresponds to 0.4 unpaired electron per monomer unit. This value compares well with the value of 0.5 electron per monomer unit in poly(aniline), predicted by Syed *et al.*[9].

Electrical conductivity

The temperature dependence of electrical conductivity can be described by an Arrhenius type

equation between 303 K and 433 K. The measured values are plotted semilog arithmetically in Fig. 2 as a function of reciprocal of temperature, $1/T$. The conductivity increases with temeprature. The measured points can be approximated by a straight line, indicating that the temperature dependence can be described by Eq. (2),

$$\sigma(T) = \sigma_0 \exp(-E_g/2kT) \quad \ldots (2)$$

at least in the temperature range investigated.

The activation energy of conductivity, E_g, has been calculated and found to be 0.078 eV. The activation energy of conductivity in poly(aniline) tetrafluoroborate has been reported to be 0.082 eV by Choi *et al.*[14]. This value is considerably higher than that measured for poly(pyrrole) (0.04 eV) and lower than that for modified poly(acetylene) (0.5 eV) and unmodified poly(acetylene) (1.5 eV)[17,18].

The conduction mechanism in poly(N-ethylaniline) could be explained by the well known band structure. Since organic polymers are generally insulators, as a result there are no mobile charge carriers in them to support conduction. However, appropriate charge carriers may be generated in organic polymers by partial oxidation (removal of electron from filled valence band) or partial reduction (addition of electrons to the conduction band) with appropriate oxidant or reductant. Thus, in poly(N-ethylaniline) sulphate, which is prepared by peroxodisulphate oxidation, oxidation creates a positive character and as a result electron assumes a polaron state (radical cation), and the polymer exhibits paramagnetism. However, such conduction mechanism is influenced by factors such as dopant level, the morphology of polymers, orientation of conducting species, density, temperature, shape and state of the polymer. Since poly(N-ethylaniline) sulphate has an amorphous matrix, the band structure cannot be considered.

Many investigators[19-21] have suggested equations relevant to various modes for electrical conduction in composites. In Greaves' equation[19] (Eq. 3), conductivity is a function of temperature in terms of hopping conduction mechanism,

$$\sigma T^{\frac{1}{2}} = \exp(-B/T^{\frac{1}{4}}) \quad \ldots (3)$$

where B is a constant. The Eq. (3) represents a variable range hopping conduction mechanism.

In Matare's equation[20] (Eq. 4), conductivity is a function of temperature in terms of electrical conduction including grain boundary barriers,

$$\sigma = AT^{\frac{1}{2}} \exp(-E_a/kT) \quad \ldots (4)$$

where A is a constant and E_a is the height of the potential barrier. Zeller's equation[21] for tunnelling conduction is expressed by Eq. (5),

$$\sigma = \sigma_0 \exp(-A/T^{\frac{1}{4}}) \quad \ldots (5)$$

Plots of the temperature dependence of the electrical conductivity have been made based on Eqs (3)-(5) for hopping, grain boundary and tunnelling conduction. The plot of $\ln(\sigma T^{\frac{1}{2}})$ vs $T^{-\frac{1}{4}}$ is linear whereas those for $\ln(\sigma T^{-\frac{1}{2}})$ vs $1/T$ and $\log\sigma$ vs $T^{-\frac{1}{4}}$ are not linear. This implies that the conduction in poly(N-ethylaniline) sulphate is predominantly carried out by hopping mechanism. Thus, the polarons act as charge carriers hopping from state to state in poly(N-ethylaniline).

Further, from Fig. 2, it is observed that electrical conductivity decreases from 393 to 433 K. This could be because the electrical conductivity in poly(aniline) is highly dependent on moisture content and the water content in poly(N-ethylaniline) sulphate is very high. As temperature increases, there is a loss of water, as is seen from Fig. 1 (TGA). Thus, conductivity decreases as the temeprature increases.

Conclusion

The chemical analysis and magnetic susceptibility measurements show that the oxidation reaction of N-ethylaniline containing SO_4^{2-} anions is a reaction involving 4 unpaired electrons. This means that polymerization should take place through previous production of N-ethylaniline piradical cation (as suggested by Syed *et al.*[9]) which could act as monomer for polymerization reaction with neighbouring N-ethylaniline molecules.

TGA data show the presence of bound water molecules, and X-ray diffraction data indicate that the polymer is amorphous powder in which *d*-spacing between chains is 0.5048 nm. From the temperature dependence of electrical conductivity, the activation energy of conductivity is found to be 0.078 eV. From these data, the conduction mechanism is suggested to be a polaron hopping conduction and the charge transfers are polarons.

Acknowledgement

Thanks are due to Dr K N. Somasekharan for his constructive suggestions for the improvement of the paper.

References

1 Syed A A, Dinesan M K & Genies E M, *Bull Electrochem*, 4 (1988) 737.

2 Syed A A, Genies E M & Santriein C in *Materials for solid batteries*, edited by B V R Chowdhari & S Radhakrishna (World Scientific Publishing Co, Singapore) 1986.

3 MacDiarmid A G, Mu S L, Somasiri N L D & Wu W, *Molec Cryst Liq Cryst*, 121 (1985) 187.

4 Paul E W, Ricco R J & Wrington M S, *J phys Chem*, 89 (1985) 1441.

5 Wegner G, *Agnew Chem Int Ed Eng*, 20 (1981) 361.

6 Diaz A P & Kanazawa K K, in *Extended linear chain compounds*, edited by J S Miller (Plenum, New York) 1983.

7 Umana M & Weller J, *Analyt Chem*, 58 (1986) 2979.

8 Tunney S E, Suenaga J & Stille J K, *Macromolecules*, 16 (1983) 1398.

9 Syed A A, Dinesan M K & Somasekharan K N, *Indian J Chem*, 27A (1988) 279.

10 Bakshi A K, *Sci Reporter*, March (1989) 141.

11 Focke W W, Wnek G E & Wei Y, *J phys Chem*, 91 (1987) 5813.

12 Lu F L, Wudl F, Nowa M & Heeger A J, *J Am chem Soc*, 108 (1986) 8311.

13 Vachon D J, Angus R O, Lu F L, Liu Z X, Shaefer H, Wudl F & Heeger A J, *Synth Met*, 18 (1987) 297.

14 Choi K M, Kin K H & Choi J S, *J phys Chem Solids*, 50 (1989) 283.

15 Inoue H & Yanagisawa S, *J inorg nucl Chem*, 35 (1973) 2561; 36 (1974) 1409.

16 Sharp J M & Wentworth S A, *Analyt Chem*, 41 (1969) 2060.

17 Katon J I, *Organic semiconducting polymers* (Marcel Dekker, New York) 1968.

18 Munstedt H, *Polymer*, 29 (1988) 296.

19 Mott N F, *J noncryst Solids*, 1 (1980) 1.

20 Matare M F, *J appl Phys*, 56 (1984) 2605.

21 Zeller H R, *Phys Rev Lett*, 28 (1972) 1452.

Indian Journal of Chemistry
Vol. 29A, July 1990, pp. 635-638

Electrochemical oxidation of sulphamethoxazole at pyrolytic graphite electrode: An example of free radical dimerization

R N Goyal* & Amit K Srivastava
Department of Chemistry, University of Roorkee, Roorkee 247 667

Received 12 June 1989; revised 18 September 1989; accepted 16 October 1989

The electrochemical oxidation of sulphamethoxazole (I) has been studied in the *p*H range of 2.23-9.94 (phosphate buffers) at pyrolytic graphite electrode by linear and cyclic sweep voltammetry, coulometry and spectral studies. It is found that I is oxidized in $2e^-$, $2H^+$ step to give azobenzene-4, 4′-(N-3-methoxazolyl) disulphonamide as the major product.

Electrochemical investigations provide an invaluable insight into the redox behaviour of biologically important compounds[1-3]. It was, therefore, considered interesting to elucidate the mechanism of electrooxidation of the well-known antibacterial drug, sulphamethoxazole (I) at pyrolytic graphite electrode.

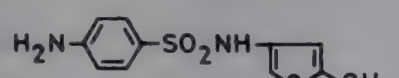

(I)

Materials and Methods

Sulphamethoxazole was a gift from Roche Products Ltd, Bombay, Azobenzene-4, 4′-(N-3-methoxazolyl) disulphonamide was synthesised by the method reported in the literature and its purity checked by TLC. All experiments were carried out at 25 ± 1.0°C in phosphate buffers of ionic strength 0.5 *M*. The IR spectra were recorded on a Beckmann IR-20 spectrophotometer and PMR spectra on a Jeol JMS D 300 instrument. All potentials were referred to SCE.

Procedure

Voltammograms of deaerated solution of sulphamethoxazole (2.0 m*M*) in phosphate buffers (*p*H 2.23-9.94) were recorded. For controlled potential electrolysis a solution of sulphamethoxazole (8-10 mg) in appropriate buffer (25 ml) was electrooxidised in an H-type cell at potentials about 100 mV more positive than the peak potential using pyrolytic graphite plate (6×1 cm^2), platinum gauze cylinder and SCE as working, auxiliary and reference electrodes respectively. The progress of electrolysis was monitored by recording cyclic voltammograms at different time intervals. When the oxidation peak I_a completely disappeared, the electrolysed solution was removed from the cell and lyopholised. The product obtained at *p*H 7.3 gave a single spot ($R_f = 0.46$) in TLC. However, two products were formed on carrying out electrolysis at *p*H 3.6 (R_f=0.27 and 0.48). These were separated as follows: The lyopholised material was dissolved in distilled water (1-2 ml) and passed through a glass column packed with Sephadex G-10 (Sigma, bead size 40-120 μ) using doubly distilled water as eluent, collecting 10 ml fractions. The absorbance of the fraction was monitored at 210 nm. The absorbance versus volume plot exhibited three peaks for the product obtained at *p*H 7.3 in GLC. The first peak obtained (fraction 6 to 15) corresponded to phosphate and was discarded. The fractions corresponding to other peaks were mixed, freeze-dried and characterized by m.p., IR, UV, PMR and mass spectra.

Results and Discussion

Linear sweep voltammetry of sulphamethoxazole (I) at a sweep rate of 10 mV s^{-1} exhibited a single well-defined, *p*H-dependent oxidation peak at the pyrolytic graphite electrode (PGE). The E_p versus *p*H plot exhibited two breaks at about *p*Hs 2.7 and 6.5

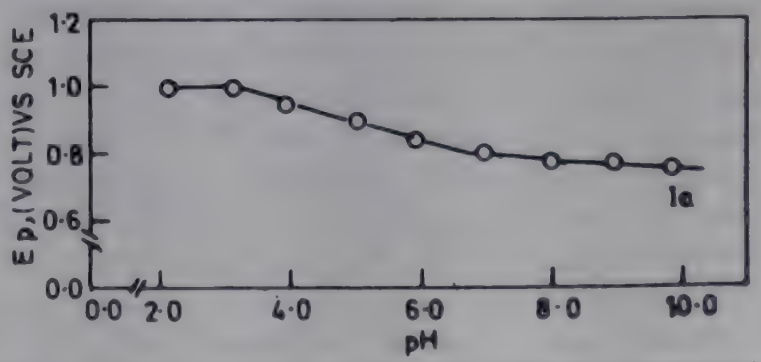

Fig. 1—Variation of peak potential with *p*H for the voltammetric peaks of sulphamethoxazole (I) (Sweep rate = 10 mV s^{-1})

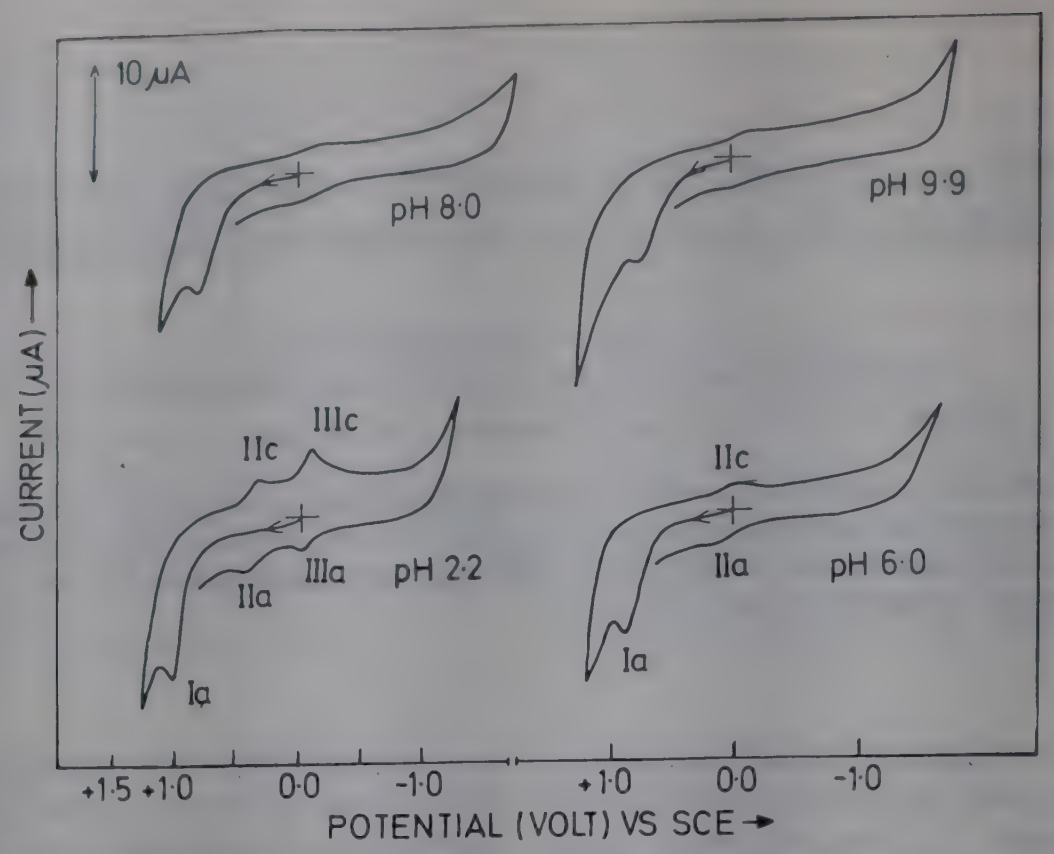

Fig. 2—Typical cyclic voltammograms observed for sulphamethoxazole (I) in phosphate buffers of different *p*H value (Sweep rate = 100 mV s^{-1})

(Fig. 1). The relation between E_p and *p*H can be expressed by equations (1-3):

E_p(*p*H 2.23-3.23) = (1.00 − 0.00 *p*H)V ... (1)
E_p(3.23 − 7.00) = (1.18 − 0.053 *p*H)V ... (2)
E_p(7.00 − 9.94) = (0.90 − 0.014 *p*H)V ... (3)

As sulphamethoxazole (I) possesses an aromatic amino group and a sulphonamide moiety, cyclic voltammogram of benzene sulphonamide at PGE was recorded. As benzene sulphonamide did not exhibit any peak at PGE, it was concluded that oxidation of the aromatic amino group not of sulphonamide group, occurred at PGE.

Cyclic voltammograms of I at a sweep rate of 100 mV s^{-1} exhibited a sharp oxidation peak (I_a) when the sweep was initiated in the positive direction. In the reverse sweep two reduction peaks (II_c and III_c) were observed which formed a quasi-reversible couple with peaks II_a and III_a observed in the subsequent sweep towards positive potentials (Fig. 2).

Peaks III_a/III_c were observed only below *p*H 4.0 at a sweep rate > 50 mV s^{-1}, whereas the couple IIa/II_c was observed in the entire *p*H range (2.2-9.9). The peak potentials of peaks II_a/II_c and III_a/III_c were also dependent on *p*H and E_p versus *p*H plot exhibited a linear relation with dE_p/dpH values as 63, 70, 100, 110 mV/*p*H for peaks II_a, II_c, III_a, III_c, respectively. The peak current of peak I_a was found to increase with increase in concentration of I in the range of 0.2 to 3.0 m*M*. Below concentration 1.5 m*M* the plot of i_p versus concentration was approximately linear whereas at concentration > 1.5 m*M*, the peak current more or less attained a constant value. This indicated complexity in the electrode reaction[4] due to adsorption of the depolariser. This was further supported by occasional splitting of the peak I_a and the increase in the values of the peak current function ($i_p/ACV^{1/2}$) with increase in sweep rate[5].

The value of n, i.e. the number of electrons involved in electrooxidation was determined by controlled potential coulometry of I at different *p*H values. Graphical integration of the current-time curve, reported by Lingane[6] gave n = 2.0 ± 0.1 in the entire *p*H range studied.

A 1 m*M* stirred solution of I generally took 3 hr for complete electrooxidation and at the end solution became light yellow from colourless. The cyclic voltammograms recorded at different time intervals indicated that while peak I_a systematically decreased in the entire *p*H range, peaks II_a/II_c and III_a/III_c did not exhibit any significant change at *p*H < 4.0. At *p*H > 4.0, only peaks II_a/II_c were observed in the exhaustively electrolysed solution. Thus, it is clear that products of electrooxidation of sulphamethoxazole are electroactive in nature.

Spectral studies

The UV spectra of a 0.05 m*M* solution of sulphamethoxazole (I), in the *p*H range of 2.2-9.9, exhibited a well-defined band at 267 nm below *p*H 5.21 while at *p*H > 5.21, this band shifted to 256 nm region. The plot of absorbance versus *p*H at λ_{max} showed two infl-

ections in the E_p versus *p*H plots, at around *p*H 2.7 and 6.5. The pK_a (1) at around *p*H 2.7 corresponds to the equillibrium of $-N^+H_3 \rightleftharpoons -NH_2 + H^+$, whereas the pK_a (2) at *p*H 6.5 suggests the acid dissociation of amide linkage. This is in accordance with the potentiometrically determined pK_a value[7].

The progress of electrolysis of compound I at *p*H values 3.6 and 7.3 was also monitored by recording the UV spectra at different time intervals. The absorbance of λ_{max} of I at 256 nm after electrolysis at *p*H 7.3 showed progressive decrease with time whereas the absorbance in the region 280 to 340 nm increased. After two-hour electrolysis another shoulder at around 250 nm appeared. Similarly the absorbance of λ_{max} at 270 nm at *p*H 3.6 also showed progressive decrease with time whereas the absorbances in the regions of 290 to 340 nm and 220 to 250 nm registered increases. At the end of electrolysis at *p*H 3.6 the solution exhibited a broad band at 240 nm. These observations indicated that the products of electrooxidation of sulphamethoxazole (I) at *p*Hs 3.6 and 7.3 are different.

Product characterization

For the identification of the products at *p*Hs 3.6 and 7.3, the electrolysed solution of sulphamethoxazole was lyopholised. The TLC of lyopholised solution of *p*H 7.3 exhibited a single spot indicating the formation of only one product during electrooxidation. The freeze-dried material obtained from GLC was analysed by IR, PMR and mass spectra.

Sulphamethoxazole (I) exhibits νNH_2 in the region of 3400-3120 cm^{-1} besides other sharp bands at 680, 830, 1150, 1310 and 1480 cm^{-1}. The product of oxidation at *p*H 7.3 did not exhibit the νNH_2, indicating that oxidation of I occurred at the amino group. Further, a strong band at 1610 cm^{-1} indicated the presence of azo group in the product. The IR spectrum was superimposable over that of the authentic azo compound.

The PMR spectrum of sulphamethoxazole displayed signals at: δ2.29 ($-CH_3$), 4.57 ($-NH_2$), 6.11 ($-CH=$), 6.63 and 7.66 (aromatic proton). The PMR spectrum of the product did not exhibit any signal for amino group suggesting the disappearance of amino group in the product. Finally, the azo structure of the product was confirmed by the molecular ion peak at m/z 502 in its mass spectrum.

The formation of an azo compound as a product was further supported by the cyclic voltammograms of authentic azo compound at different *p*H values, which were similar to those of the products. The UV spectrum of the authentic azo compound was similar to that of the exhaustively electrolysed solution of I at *p*H 7.3.

The exhaustively electrolysed solution of I at *p*H 3.6 on the other hand, exhibited two spots in TLC (R_f 0.27 and 0.48), indicating the presence of two products. One of the products, corresponding to R_f value 0.48 was found to be similar to the azo product obtained at *p*H 7.3. The other product (R_f 0.27) could not be characterized due to nonavailability of an authentic sample.

Redox mechanism

The evidences presented above clearly indicate that electrooxidation of sulphamethoxazole (I) involves a two-electron process. In order to account for the overall mechanism it seems reasonable to assume that 1e, $1H^+$ oxidation of sulphamethoxazole (I) gives a free radical species (II), which can be deactivated by a number of ways. Species (II) may further undergo 1e, $1H^+$ oxidation to give nitrene (III) which on dimerization results in the formation of an azo compound

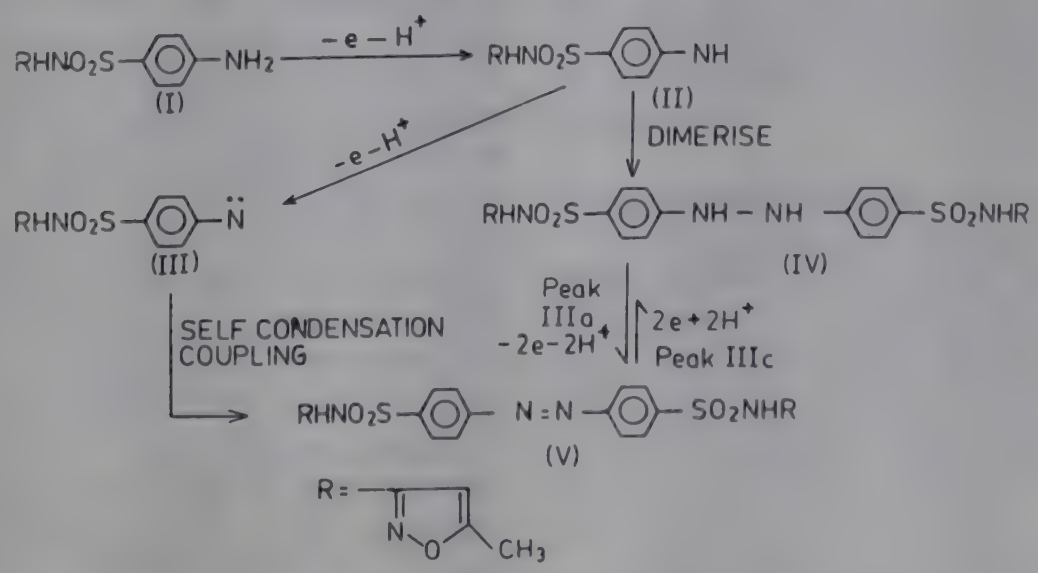

TENTATIVE MECHANISM PROPOSED FOR THE ELECTROOXIDATION OF SULPH-
-AMETHOXAZOLE

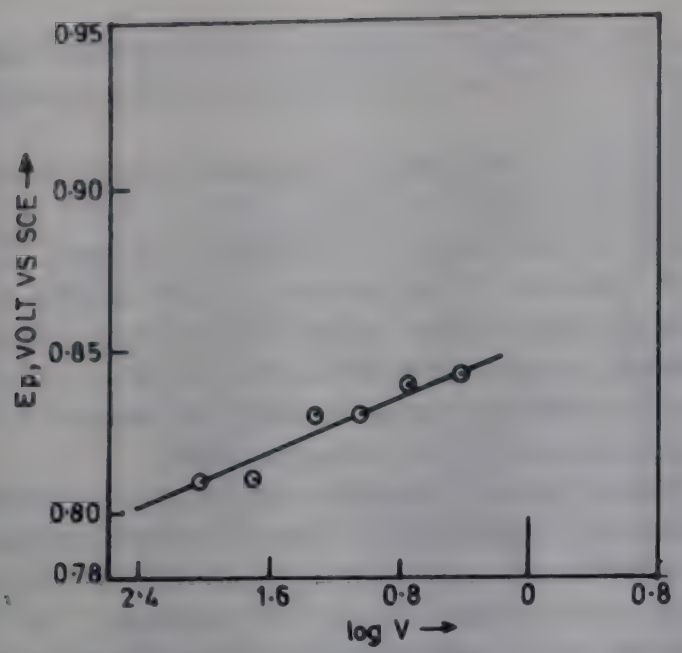

Fig. 3-Variation of the peak potential with log voltage sweep rate for 0.5 m*M* sulphamethoxazole (I) at *p*H 7.3

(V) (Scheme 1). On the other hand, the free radical species (II) may combine with another radical species to give a hydrazo compound (IV). As hydrazo compounds are more easily electrooxidisable than amino group, it undergoes further oxidation in a 2e, $2H^+$ reaction to give an azo product (V). The reduction of azo compounds in aqueous and non-aqueous systems is well-known[8], therefore the azo product (V) gets reduced in a 2e, $2H^+$ reaction to give back the hydrazo compound. Such an oxidation-reduction of azo-hydrazo compounds has been observed in cyclic voltammetry (peaks III_a/III_c).

Out of the two possible pathways for the electrode reaction, the electrodimerization is one of the most common process in organic electrochemistry and was confirmed in the present studies by determining the slope of E_p versus log V plot. Such a plot is linear (Fig. 3) with a slope of 20 mV. Experimental slope and the theoretical value corresponding to free radical dimerization as suggested by Andrieux *et al.*[9,10] were the same. It is, therefore, concluded that oxidation of sulphamethoxazole (I) proceeds through electrodimerization to give an azo product at the pyrolytic graphite electrode.

Acknowledgement

The authors are grateful to M/s Pfizer, USA for the gift of a pyrolytic graphite. One of the authors (AKS) thanks the ICMR, New Delhi, for the award of a junior research fellowship.

References

1 Dryhurst G, *Bioelectro Bioenerg*, **14** (1985) 281.
2 Peterson T E C & Toth A B, *J electroanal Chem*, 239 (1988) 161.
3 Subramanian P & Dryhurst G, *J electroanal Chem*, 224 (1987) 137.
4 Wopschall R H & Shain I, *Analyt Chem*, 39 (1967) 1514.
5 Brown E C & Large R F, *Techniques of chemistry*, edited by A Weissberger and B W Rossiter (Wiley-Interscience, New York), 1974 pp 423.
6 Lingane J J, Swain C G & Fields M, *J Am chem Soc*, 65 (1943) 1348.
7 Othmer K, *Encyclopedia of chemical technology*, Vol 2 (Wiley--Interscience, New York) 1969 pp 796.
8 Stradins J P & Glezer V Y, in *Encyclopedia of electrochemistry of the elements* edited by A J Bard and H Lund, Vol 13 (Marce Dekker, New York) 1979 pp 163.
9 Andrieux C P & Saveant J M, *J electroanal Chem*, 26 (1970) 223.
10 Andrieux C P, Nadjo L & Saveant J M, *J electroanal Chem*, 26 (1970) 147.

Indian Journal of Chemistry
Vol. 29A, July 1990, pp. 639-646

Complexation of hydrogen and alkali cations with 18Crown6 in 25 and 50% (v/v) methanol-water mixtures

A A Majmudar, K C Bhalla & A R Gupta*
Chemistry Division, Bhabha Atomic Research Centre, Bombay 400 085

Received 10 October 1988; revised and accepted 5 October 1989

The formation constants of complexes of K^+, Na^+ and H_3O^+ with 18Crown6 (18C6) (K_{Kc}, K_{Nac} and K_{Hc} respectively) in 25 and 50% (v/v) methanol-water mixtures have been determined by competitive ion exchange technique. K^+/H^+ and Na^+/H^+ exchanges on Dowex 50WX8 both in the absence and presence of 18C6 have been studied in these media. The values of K_{Kc} and K_{Nac} (212 ± 6 and 14 ± 2 in 25% and 2400 ± 200 and 236 ± 23 in 50% (v/v) methanol-water mixtures), are greater than those in pure aqueous medium. This behaviour is consistent with the generally observed enhancement of stability constants in media of lower dielectric constant. The values of K_{Hc} for H_3O^+-18C6 derived from the two exchange systems are in good agreement with each other. The K_{Hc} comes out to be 0.5 ± 0.5, in 25% (v/v) methanol-water medium which is lower than that in pure aqueous medium. On the other hand K_{Hc} in 50% (v/v) methanol-water mixture is 66 ± 10. This unusual behaviour in methanol-water mixture of low methanol content is explained in terms of structure of methanol-water mixtures of low methanol content. This also provides an instance where medium structure plays a dominant role in determining the stability constant. K_{Hc} in 50% (v/v) methanol-water mixture follows the normal trend as observed for alkali metal cations and is consistent with normal behaviour of methanol-water mixtures in this composition range. The free energies of transfer of K^+, Na^+ and H_3O^+-18C6 complexes from water to 25 and 50% (v/v) methanol-water mixtures also have been computed.

Complexation of hydrogen ions with 18Crown6 (18C6) in aqueous solution has recently been studied potentiometrically[1] and by ion exchange technique[2]. The formation constant (K_{Hc}) for $H_3O^+ - 18C6$ was found to be greater than the corresponding formation constants for Li^+ and Na^+ ions and it was concluded that the stability of the complex was due to formation of H-bonds between H atoms of H_3O^+ and alternate oxygens of ether ring of the 18C6. The complexation of alkali metal cations with crown ethers is strongly affected by the solvent composition. However, the effect of solvent composition on the complexation of hydrogen ions could be different from its usually observed effect on alkali metal cation-18C6 complexation because it is H_3O^+ which forms stable complexes with 18C6 while solvation shell of alkali metal cations is completely or partially removed on complexation. Therefore, hydrogen ion-cosolvent interactions as well as cosolvent-water interactions could play an important role in these systems. With this in view, we have undertaken a systematic study of the complexation of K^+ and H^+ ions with 18C6 in 25% and 50% (v/v) methanol-water mixtures based on the study of K^+/H^+ exchange equilibrium on Dowex 50WX8 in these media with and without 18C6. As both the formation constants, K_{Mc} and K_{Hc} are unknown in these media, the approach used for analysing the data in aqueous medium (where K_{Mc} is known) could not be used and has been modified to yield both the formation constants. Further, confirmation of K_{Hc} value has been provided by studying Na^+/H^+ exchange on the same resin in these solvent mixtures, where both K_{Nac} and K_{Hc} were obtained. K_{Nac} has been compared with the results obtained by Dishong and Gokel[3] in water-methanol mixtures by ion selective electrodes.

Materials and Methods

All the chemicals were of AR or equivalent grade. Methanol was of GR (BDH) grade. Crown ether (18C6) was obtained from Sigma Laboratories, USA (m.p. 37-38°, lit. m.p. 36-38°). Solutions (HCl, KCl and NaCl) were prepared in 25 and 50% (v/v) methanol-water media. Stock solutions of 18C6 in these media were prepared and standardized as described below:

A slight excess of potassium picrate was added to 18C6 solution, its *p*H adjusted to 9-10 by the addition of LiOH solution and the picrate deter-

mined spectrophotometrically at 356 nm on a Hitachi 330 spectrophotometer ($\varepsilon = 14000$). Potassium picrate-18C6 complex was extracted into dichloromethane. The difference in the picrate concentration in the stock solution before and after solvent extraction gave the amount of 18C6 initially present in the stock solutions. This was further checked by estimating 18C6 as a K-picrate complex in organic phase at 358 nm ($\varepsilon = 15000$). It was observed that traces of methanol present in the solution did not affect absorption (the stock solution needed to be diluted about 200 times before the extraction).

Resins

Strong acid cation exchanger Dowex 50WX8 was converted into H^+ form and its capacity determined by eluting with NaCl solution and estimating liberated H^+ ions. The batch technique was used for ion exchange studies as described earlier[2].

Analysis of experimental data

An ion exchange reaction for univalent cations, M^+ and H^+, viz. $M^+ + HR \rightleftharpoons H^+ + MR$ (R is ion exchange resin) has a selectivity coefficient $K_d = [H^+][MR]/[M^+][HR]$. When a ligand is present in solution and both the cations form complexes with it, two other equilibria are superimposed on the ion exchange equilibria. First, $M^+ + C \rightleftharpoons MC^+$ having equilibrium (formation) constant $K_{Mc} = [MC^+]/[M^+][C]$ and the second, $H^+ + C \rightleftharpoons HC^+$ having the formation constant $K_{Hc} = [HC^+]/[H^+][C]$. In an earlier[2] treatment of experimental data, K_{Mc} was known and the data were arranged in a quadratic equation in $[HC^+]$ as unknown, and K_{Hc} was obtained. In the present system, both the formation constants are unknown. Therefore the modified approach described in the sequel has been used. The experimental values of mol fraction of free metal ions in solution phase, denoted by $AZ_{obs(i)}$ $(i = 1,\cdots,n)$ were obtained in the following way.

The ion exchange experiments were carried out over a wide range of mol fractions in the absence of 18C6 and a plot of mol fraction of metal ions in resin phase, denoted by AMR(obs) versus AZ was obtained (exchange isotherm, Fig. 1). Similar experiments were carried out in the presence of 18C6 and the values of mol fraction of metal ion in resin phase, denoted by AMR(pre) were obtained. The values of AZ corresponding to these AMR(pre) were obtained from the exchange isotherm. These are called AZ(obs) $(i = 1,\cdots,n)$.

If M_T and H_T are total equilibrium concentrations (i.e. in both complexed and uncomplexed forms) of M^+ and H^+ ions respectively and C_T is the initial concentration of the ligand, then the two complexation equilibria in the solution phase lead to the cubic equation (1) in [C], the free ligand concentration at equilibrium

$$A[C]^3 + B[C]^2 + E[C] + D = O \qquad \ldots(1)$$

where

$A = K_{Mc} \cdot K_{Hc}$;

$B = -[K_{Mc}.K_{Hc}(C_T - K_T - H_T) - K_{Mc} - K_{Hc}]$;

$E = -K_{Mc}(C_T - K_T) + K_{Hc}(C_T - H_T) - 1]$ and

$D = -C_T$

These coefficients are functions of M_T, H_T, C_T and K_{Mc}, K_{Hc} of which K_{Mc} and K_{Hc} are unknown. For reasonable guess values of K_{Mc} and K_{Hc} and every set of M_T, H_T and C_T, the [C] value was obtained by solving Eq. (1). Each time, Eq. (1) gave only one real value of [C]. These [C] values were used in two different ways to fix K_{Mc} and K_{Hc} by the least error sum square method:

(1) From [C]'s the mol fractions of free ions in solution phase, denoted by AZ(calc.), were calculated using the definitions of K_{Mc} and K_{Hc}. Then the sum of the error square given by Eq. (2),

$$S = \sum_{i=1}^{n} (AZ^i_{obs} - AZ^i_{calc})^2 \qquad \ldots(2)$$

was minimized w.r.t. K_{Mc} and K_{Hc}.

(2) In this method the selectivity coefficient K_d were calculated using AZ (calc) by Eq. (3)

$$K_d = [(1/AZ) - 1]/[(1/AMR) - 1] \qquad \ldots(3)$$

and the sum of the error square S′, by Eq. (4)

$$S' = \sum_{i=1}^{n} (K^i_{d(obs)} - K^i_{d(calc)})^2 \qquad \ldots(4)$$

was minimized w.r.t. K_{Mc} and K_{Hc}.

The minimization was done on ND-500 computer using pattern search method. The K_{Kc} and K_{Hc} were varied upto the step size of 10E-4 and their optimized values were obtained by the above two methods were confined within a small range, which represented the accuracy of these values and essentially reflected the errors in the experimental measurements.

The method can also be used in a slightly modified way as follows:

As K_{Mc} and K_{Hc} differed widely, values of K_{Mc} were obtained for a fixed value of K_{Hc} in the narrow range and the error sum square values (ESS) determined. The plot of K_{Hc} versus ESS was a

smooth curve passing through a minimum. K_{Mc} and K_{Hc} corresponding to the minimum in ESS were taken as the real ones. K_{Hc} obtained from both K^+-H^+ and Na^+-H^+ systems were in good agreement, thus proving the reliability of the method.

Results and Discussion

Figure 1 shows the exchange isotherms for K^+/H^+ and Na^+/H^+ systems in 25 and 50% (v/v) methanol-water mixtures. Plots of log K_d (K_d is the selectivity coefficient), versus resin phase composition (AMR) for various exchange systems (K^+/H^+ and Na^+/H^+) were constructed. Figure 2 shows such plots for 25% (v/v) methanol-water mixture. The K_d values at low AMR were extrapolated using the calculated K_d values based on isotherms in Fig. 1. The thermodynamic equilibrium constants computed from Eq. (5)

$$\log K = \int_0^1 \log(K_d \gamma_{\pm}^2 HCl/\gamma_{\pm}^2 KCl)\, dAMR \qquad \ldots (5)$$

Log K values of 0.68 (0.70) for K^+/H^+ and 0.45 (0.47) for Na^+/H^+ systems in 25% (v/v) methanol-water and 1.26 (1.31) for K^+/H^+ and 0.87 (0.862) for Na^+/H^+ in 50% (v/v) methanol-water medium were in agreement with reported values[4] (given in the parentheses). As an example of the effect of 18C6 on log K_d, Fig. 2 also gives the plot of log K_d versus AMR in the presence of 18C6 in 25% (v/v) methanol-water mixture. It can

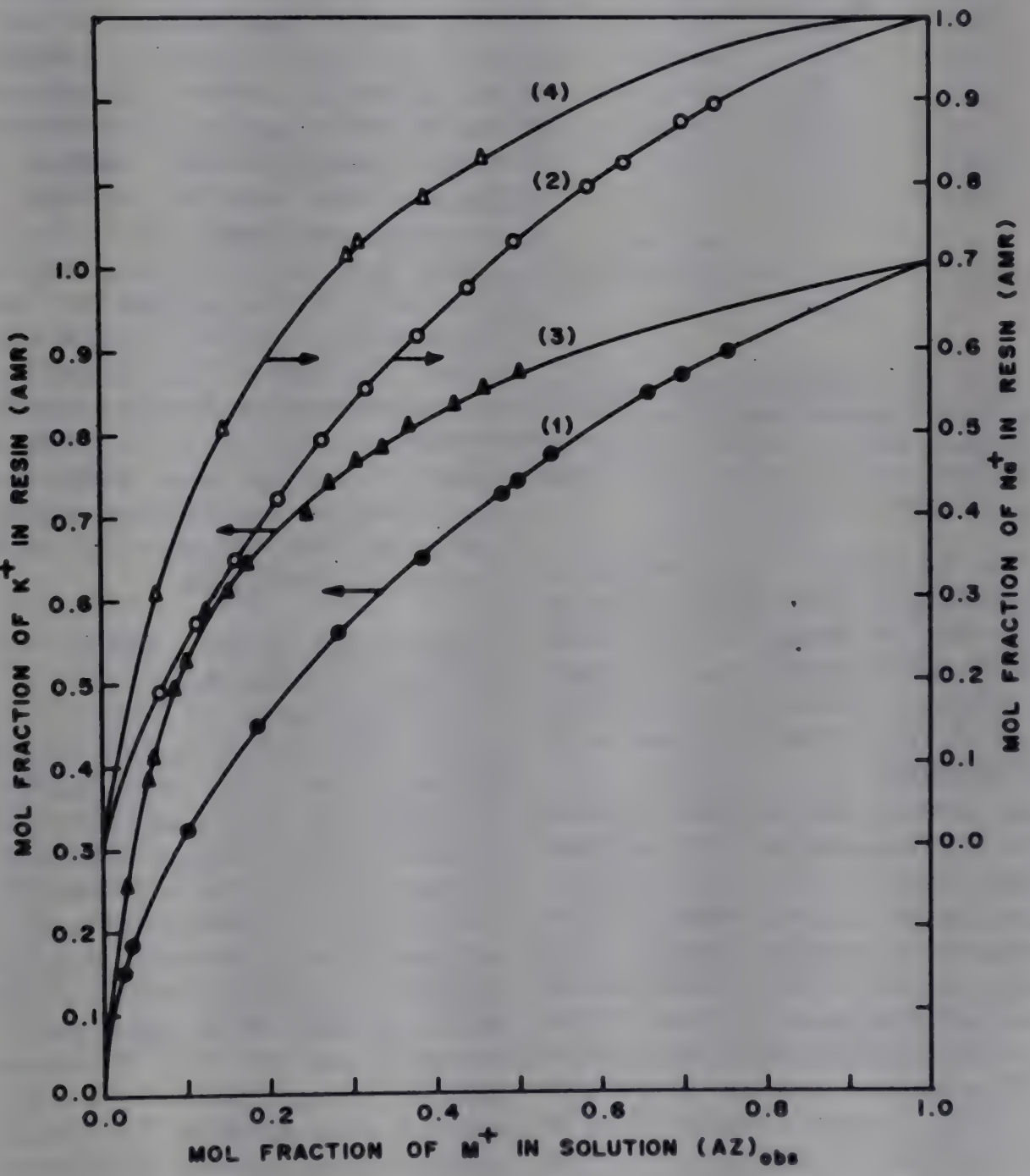

Fig. 1 – Plots of mol fraction of metal ion in solution (AZ) versus mol fraction of metal ion in resin phase (AMR) [(1) K^+/H^+ system in 25% (v/v) methanol-water; (2) Na^+/H^+ system in 25% (v/v) methanol-water; (3) K^+/H^+ system in 50% (v/v) methanol-water; and (4) Na^+/H^+ system in 50% (v/v) methanol-water]

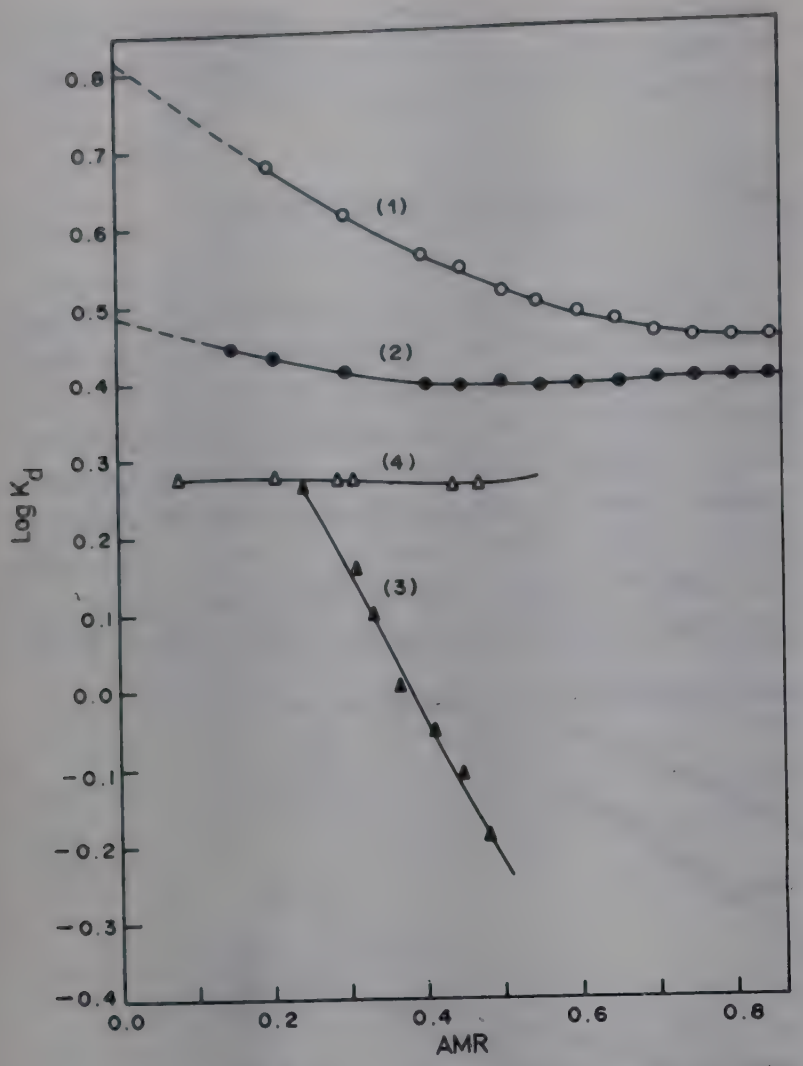

Fig. 2 – Plots of log K_d versus AMR in the absence and presence of 18C6 in 25% (v/v) methanol-water mixture [(1) K^+/H^+ system in absence of 18C6; (2) Na^+/H^+ system in absence of 18C6; (3) K^+/H^+ system in presence of 18C6; and (4) Na^+/H^+ system in presence of 18C6]

be observed that the shape of curve, both in the presence and absence of 18C6 remains the same for Na^+/H^+ system even though the actual values are different while the shape of curves for K^+/H^+ is drastically different, indicating that the complexation of 18C6 with Na^+ is very small while with K^+ it is of high order.

The sorption of 18C6 on resin phase for both K^+/H^+ and Na^+/H^+ systems was 10-11 mg/meq. of resins in both 25 and 50% (v/v) and was independent of solution phase composition. This loss of ligand was taken into account. When the initial ligand concentration was high, small changes in concentrations due to sorption of ligand at resin surface did not affect the final values to any significant extent. The application of Eqs (2) and (4) is illustrated in Table 1 where complete data for K^+/H^+ system in 25% (v/v) methanol-water mixture are given. Optimized values for K^+/H^+ and Na^+/H^+ in 50% (v/v) methanol-water mixture along with the experimental details are summarized in Table 2. The uncertainty in formation constants were estimated by K_{Hc} versus ESS plots for various systems taking ESS as indistinguishable beyond the fourth decimal place (Fig. 3). The best values for K_{Kc} and K_{Hc} in 25% (v/v) methanol-water mixture from K^+/H^+ data are 212 ± 6 and 0.5 ± 0.5 respectively. The optimum values for K_{Nac} and K_{Hc} from Na^+/H^+ data are 14 ± 2 and 0.5 ± 0.5 respectively. While the best values for K_{Kc}, K_{Hc} and K_{Nac} in 50% methanol-water mixture, given in Table 2, are 2400 ± 200, 66 ± 10 and 236 ± 23 respectively. The values of K_{Kc}, K_{Nac} and K_{Hc} for aqueous medium are 108 (refs 2,6), 6.3 (ref. 6) and 20 (ref. 1) respectively. In absolute terms enhancement of K_{Kc} values between aqueous and 25% methanol-water mixture is much greater than that in K_{Nac} values. However the enhancement in terms of percentage increase over values in pure aqueous medium is of similar order for both K^+ and Na^+ complexes. Dishong and Gokel[3] have reported the formation constants for Na^+-18C6 and Na^+-15C5 covering the whole range of methanol-water mixture compositions. However, the value for Na^+-18C6 in aqueous system is considerably higher than the ones reported in the literature. Also the formation constant values for this complex in 25 and 50% (v/v) methanol-water media are much higher than our values. The plots of log K_{Kc} and log K_{Nac} versus mol per cent methanol for the reported values for 0,70,90 and 100 (w/w) % methanol[5,6] and the present values are linear emphasising that our K_{Nac} values at low methanol concentrations are compatible with the reported values at higher methanol concentrations.

Complexation of Na^+ and K^+ with 18C6 in methanol-water mixtures

The larger stability of K^+-18C6 as compared to that of Na^+-18C6 in aqueous phase has been attributed to the greater envelopment of K^+ ion by the ligand due to ring size effect and the lesser hydration of K^+ complex compared to the Na^+ complex (ref. 7). One can therefore expect that solvation of the cations and complexed species will play a role in determining the stability of the complexes in different solvents. However the data on the solvation of the ligand and the complexed cation species M^+-18C6 in aqueous and non-aqueous solvents[8] indicate solvation to the same extent in both the media. This shows that the solvation does not play any significant role in the enhancement of log K_{Mc} in mixed solvent as against aqueous solutions. This is further supported by the work of Izatt and others[6] who studied the enthalpy and entropy changes for Na^+ and K^+ com-

Table 1 – Optimized parameters for K^+/H^+ system in 25% water-methanol medium

K_T	H_T	C_T	Free lig. con.	K_d obs.	K_d calc.	AZ obs.	AZ calc.	K_{Kc} (at $K_{Hc}=0$)
.03170	.01840	.12000	.08870	4.27000	4.24401	.08500	.08377	194.93
.03110	.01900	.09160	.06183	3.77800	3.76390	.10500	.10736	198.15
.02960	.02100	.04230	.01845	3.13360	3.12117	.22000	.22524	204.28
.02560	.02450	.03760	.01720	3.58990	3.56295	.18500	.18533	205.14
.02440	.02580	.02500	.00890	3.18560	3.20901	.25000	.24806	199.66
.02350	.02670	.02000	.00638	3.15780	3.17769	.27500	.27330	199.21
.02230	.02760	.06100	.04020	3.99900	3.95676	.08000	.07988	186.35
.02250	.02760	.01500	.00426	2.90010	2.95438	.30500	.30075	201.74
.02210	.02810	.03290	.01561	3.65000	3.67106	.15500	.15569	200.54
.02170	.02840	.01000	.00248	2.97760	2.98609	.33500	.33416	198.23
.01840	.03190	.02820	.01408	3.75270	3.74877	.12500	.12739	202.56
.01500	.03520	.06100	.04616	5.02000	5.08859	.04000	.03891	194.41
.01460	.03580	.02350	.01255	4.46400	4.46330	.10500	.10089	201.98
.01250	.03830	.02200	.01255	4.46000	4.45639	.08500	.08237	201.94
.01120	.03958	.01880	.01070	4.04050	4.01330	.08000	.08007	204.10
.00750	.04300	.01410	.00890	5.36390	5.32004	.06000	.05718	204.64
.00633	.04480	.02200	.01651	4.89300	4.88926	.03000	.03066	200.56
.00450	.04610	.00940	.00655	5.12620	5.18724	.04000	.03935	196.88

	K_{Kc}(av)	K_{Hc}(av)	ESS	Mean error
K_d (min)	211.13	0.790	0.0191	0.0335
AZ (min)	211.95	0.6675	0.0001	0.00243

Table 2 – Experimental conditions and optimized parameters for K^+/H^+ and Na^+/H^+ (50%) and Na^+/H^+ (25%) (v/v) methanol-water mixtures

K^+/H^+ (50%) K_T	H_T	C_T	Free lig. con.	Na^+/H^+ (50%) NA_T	H_T	C_T	Free lig. con.	Na^+/H^+ (25%) NA_T	H_T	C_T	Free lig. con.
.02800	.02190	.04870	.01175	.00124	.00876	.01347	.01874	.00124	.00876	.01347	.00929
.02800	.02200	.02650	.00169	.01834	.02976	.03128	.01354	.01834	.02976	.03128	.00843
.02730	.02270	.02740	.00200	.01932	.03085	.05387	.03423	.01932	.03085	.05387	.02025
.02590	.02410	.02360	.00141	.01541	.03174	.02737	.02977	.01541	.03174	.02737	.00730
.02460	.02540	.01960	.00094	.01652	.03352	.04718	.02379	.01652	.03352	.04718	.01654
.02404	.02570	.03704	.00645	.01226	.03394	.02346	.02523	.01226	.03394	.02346	.00625
.02395	.02590	.04700	.01201	.01307	.03697	.04040	.01890	.01307	.03697	.04040	.01352
.02324	.02686	.01570	.00062	.00682	.03748	.01564	.00931	.00682	.03748	.01564	.00417
.02220	.02790	.02650	.00273	.00451	.03884	.01173	.02058	.00451	.03884	.01173	.00314
.02200	.02800	.01200	.00040	.01018	.03988	.03367	.01325	.01018	.03988	.03367	.01031
.02110	.02900	.02120	.00168	.00248	.03992	.00782	.01574	.00248	.03992	.00782	.00211
.01920	.03080	.01590	.00090	.00770	.04237	.02693	.01971	.00770	.04237	.02693	.00769
.01790	.03210	.01060	.00040	.00560	.04448	.02020	.01068	.00560	.04448	.02020	.00539
.01698	.03250	.02800	.00456	K_{NaC}(av) = 236 ± 23				K_{NaC}(av) = 14 ± 2			
.01680	.03350	.02650	.00404	K_{Hc}(av) = 66 ± 10				K_{Hc}(av) = 0.5 ± 0.5			
.01650	.03350	.00530	.00017								
.01514	.03460	.02935	.00556								
.01169	.03800	.02348	.02348								
K_{Kc}(av) = 2400 ± 200											
K_{Hc}(av) = 66 ± 10											

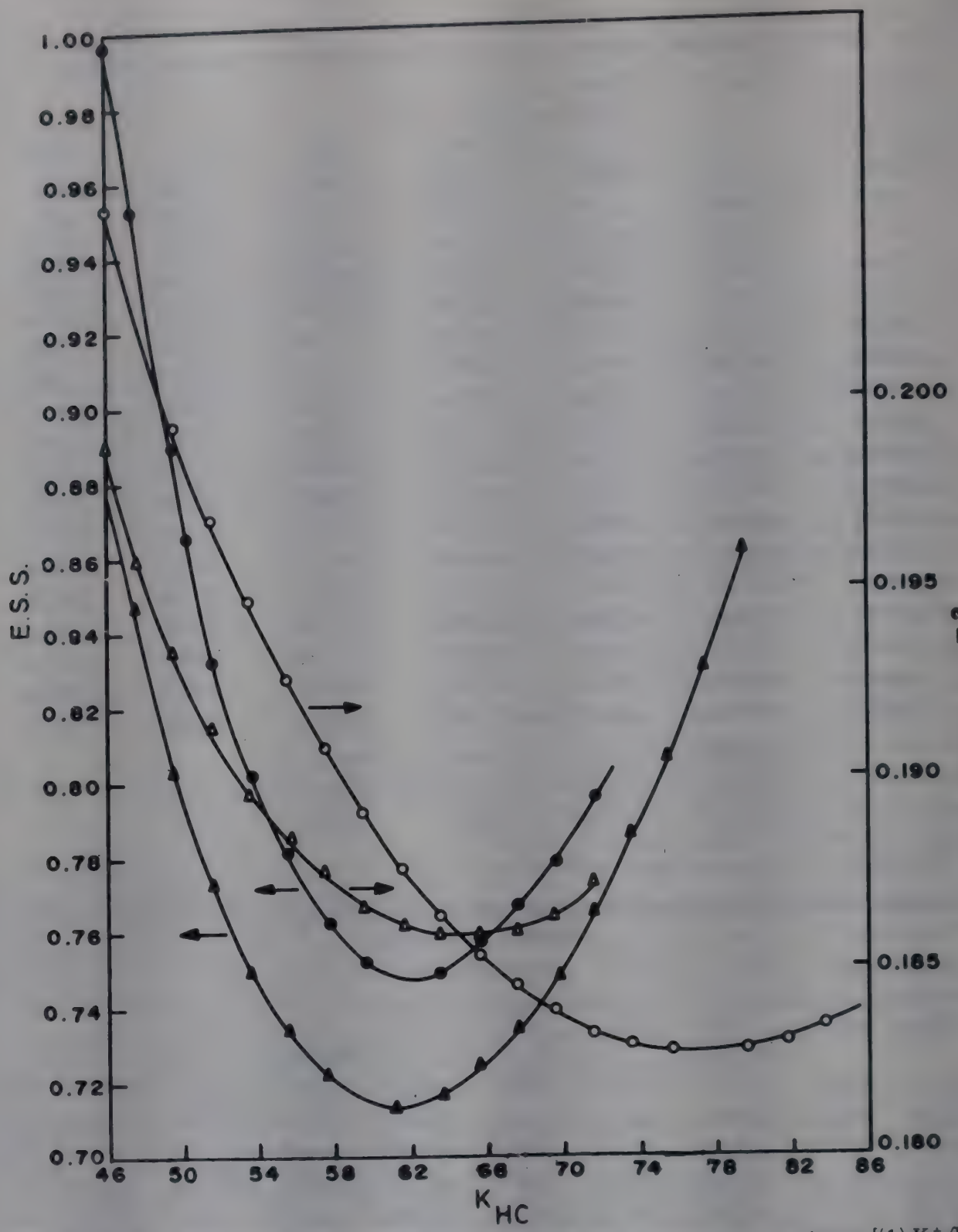

Fig. 3 – Plots of ESS versus K_{Hc} for K^+/H^+ and Na^+/H^+ systems in 50% (v/v) methanol-water mixture [(1) K^+/H^+ system (K_d minimization); (2) Na^+/H^+ (AZ minimization); (3) K^+/H^+ (K_d minimization); and (4) Na^+/H^+ (AZ minimization)]

plexes with B15C5 in 0-80 wt % methanol-water mixtures and Na^+ and K^+ complexes with 18C6 in 70 wt % methanol-water mixture. The entropy changes in aqueous and 70 wt % methanol-water mixture remain essentially constant, implying that the changes in cation solvation on complexation are similar in different solvents. Cations are less solvated in mixed solvent systems compared to that in water and this can lead to enhancement in stability constants in mixed solvent systems. Hence the enhancement in the stabilities of alkali metal ion complexes with B15C5 and 18C6 from aqueous to 70 wt % methanol was therefore attributed to an increasingly favourable enthalpic effect, i.e. greater electrostatic interactions between cation and ligand. The opposing entropic contributions remain constant and only at higher methanol concentrations these contributions increase. Similar explanation holds for increase in stability constants of Na^+-18C6 and K^+-18C6 in 25 and 50% (v/v) methanol-water mixtures as compared to that in pure aqueous medium.

Complexation of H_3O^+ with 18C6 in 25 and 50% methanol-water mixture

On the basis of above discussion, one would

expect the stability of H_3O^+-18C6 complex to increase in methanol-water mixtures as compared to that in aqueous medium. However, K_{Hc} is lower in 25% (v/v) but greater in 50% (v/v) methanol-water mixtures as compared to that in aqueous medium. The greater stability of H^+-18C6 complex compared to Na^+ or Li^+-18C6 complex in aqueous medium was explained by us earlier on the basis of H-bonding between three hydrogen atoms of H_3O^+ and three alternate oxygens of 18C6 ring. The unusual behaviour of K_{Hc} in methanol-water mixtures must also have its origin in the H-bonded structure of these media which would influence the H-bonding between H_3O^+ and 18C6.

A generally accepted view of water is that it exists as a mixture of bulky H-bonded, three-dimensional clusters, full of cavities and dense monomeric water which are in dynamic equilibrium with each other[9]. Unlike that of water[9] liquid alcohols have two dimensional H-bonded structure. The computer simulation studies of water-methanol mixtures[10] have shown that 5 mol per cent methanol stabilizes the water structure. Anamolies in the physicochemical properties of water-methanol mixtures of low methanol content have been discussed in terms of their structural features. Computer simulation studies have also indicated that methanol molecules though surrounded by water molecules do not effectively participate in H-bond formation with them and therefore possess free OH groups.

Frank[9] and Tourkey[11] have observed that methanol is more basic than water in water-methanol mixtures of low methanol content. The presence of free hydroxyl groups not involved in H-bonds is the basis for the greater basicity of methanol in water-methanol mixtures of low methanol content. Only at high methanol concentration water becomes more basic than methanol due to cleavage of this stabilized water structure. This means that the protons form $CH_3OH_2^+$ more readily at low methanol concentration (25% v/v) than H_3O^+, and at high methanol concentration (50% v/v) it forms H_3O^+ in preference to $CH_3OH_2^+$. This results in reduced availability of H_3O^+ for the formation of H_3O^+-18C6 complex ($CH_3OH_2^+$ having two H atoms and a CH_3 group cannot form as stable a complex with 18C6) in 25% methanol-water mixture. This is consistent with the observed lower stability of H_3O^+-18C6 complex in this medium. It can be further concluded that the combined effect of $CH_3OH_2^+$ and methanol in stabilising water structure at low methanol concentrations is greater than that of only methanol. Thus the negligible complex formation between hydrogen ions and 18C6 in 25% (v/v) methanol-water reflects the special structural features of methanol-water mixtures of low methanol content. Recently, Aksnes and Asaad[12] have discussed the role of changing water structure with temperature on some chemical reactions. The lowering of K_{Hc} in 25% (v/v) methanol-water mixture seems to be the first example where the effect of cosolvent on the medium structure plays a dominant role in determining the equilibrium constant of a chemical reaction.

Hydrogen ions predominantly exist as H_3O^+ in 50% (v/v) methanol-water mixtures (see above) and the normal enthalpic effect, as evident in the case of K^+ and Na^+ complexation, enhances the stability of H_3O^+-18C6 complexes. These results indicate that there is no simple correlation with the methanol concentration as in the case of alkali metal ions and every solvent composition presents its own peculiarities due to varying structure of the medium with changing methanol content.

Free energy of transfer of complexed species

The free energy of transfer ΔG_t° of M^+-18C6 from water to solvent S can be calculated from Eq. (6)[13].

$$\Delta G_t^\circ(M^+ - 18C6) = \Delta G_f^\circ(M^+ - 18C6)_s - \Delta G_f^\circ(M^+ - 18C6)_w + \Delta G_t^\circ(18C6) + \Delta G_t^\circ(M^+) \quad \ldots (6)$$

where ΔG_f°s are the free energies of formation in two solvents and ΔG_t°s are free energies of transfer of different species from water to solvent S.

We have obtained $\Delta G_t^\circ(M^+ - 18C6)$ for 25 and 50% (v/v) methanol-water as follows: For neutral molecules, a linear relationship for ΔG_t° and wt. % organic solvent is theoretically predicted. We have assumed the same relationship for $\Delta G_t^\circ(18C6)$ in methanol-water mixtures and evaluated $\Delta G_t^\circ(18C6)$ for 25 and 50% (v/v) methanol-water mixtures using ΔG_t° (18C6) from water to methanol reported by Abraham and How Chiong Ling[14]. The values of single cation free energy of transfer from water to methanol-water mixtures ($\Delta G_t^\circ(M^+)$ were evaluated from Feakins and Voice's[15] data by applying the assumption $\Delta G_t^\circ(Ph_4B^+) = \Delta G_t^\circ(Ph_4As)^-$ (ref. 16).

From our experimental results, $\Delta G_t^\circ(M^+ - 18C6)_s$ was calculated for K^+, Na^+ and H_3O^+ for both the solvent compositions and the values of $\Delta G_t^\circ(M^+ - 18C6)$ were calculated from Eq. (6) and are given in Table 3. ΔG_t° values for Na^+ and K^+ complexes are small supporting the conclu-

Table 3 – Free energies of transfer of the cations (in molal scale)

% (v/v) CH_3OH in H_2O-MeOH mixture	Cation	$\Delta G_t^\circ(M^+\text{-}18C6)$ (kJ/mol)	$\Delta G_t^\circ(MCl)$ (kJ/mol)	$\Delta G_t^\circ(M^+)$ (kJ/mol)	$\Delta G_t^\circ(M^+\text{-}18C6)$ (kJ/mol)
0%	K^+	−11.590	—	—	—
	Na^+	−4.565	—	—	—
	H^+	−7.422	—	—	—
25%	K^+	−13.53	3.500	3.270	2.735
	Na^+	−6.540	3.535	3.142	2.657
	H^+	0.711	1.540	1.309	10.581
50%	K^+	−19.100	8.083	6.033	1.197
	Na^+	−13.535	7.962	5.991	−0.343
	H^+	−10.381	2.887	0.010	−0.310

For these calculations 25 and 50% (v/v) methanol-water mixtures have been taken as equal to 20 and 44 wt % methanol-water mixtures respectively.

sion that the stabilization of these complexes in methanol-water mixtures is an enthalpic effect. This implies that the solvation of alkali metal ion complexes is similar in aqueous and the two methanol-water mixtures used in the present study. On the other hand, for $\Delta G_t^\circ(H_3O^+ - 18C6)$ have large positive values in 25% (v/v) methanol indicating that H^+-18C6 complex is more solvated (and more stable in aqueous compared to methanol-water mixtures). This emphasises that the entropic effects are predominant in this system. Whereas in 50% (v/v) methanol-water mixture, $\Delta G_t^\circ(H_3O^+\text{-}18C6)$ is small and positive as for alkali metal complexes. This clearly shows that enthalpic effects are important as in the case of alkali metal cation complexes. This means that 50% (v/v) methanol-water behaves like a normal fluid (as borne out by variations in the physico-chemical properties of methanol-water mixtures beyond 25% (v/v) compositions).

References

1 Majmudar A A & Gupta A R, *Indian J Chem*, 25A (1986) 861.

2 Majmudar A A & Gupta A R, *Indian J Chem*, 26(A) (1987) 721.

3 Dishong D M & Gokel G W, *J org Chem*, 47 (1982) 147.

4 Nandan D & Gupta A R, *Indian J Chem*, 11 (1973) 546.

5 Haymore B L, Lamb J D, Izatt R M & Christensen J J, *Inorg Chem*, 21 (1982) 469.

6 Izatt R M, Terry R E, Nelson D P, Chan Y, Eatough D J, Bradshaw J C, Hansen L D & Christensen J J, *J Am chem Soc*, 98 (1976) 7626.

7 (a) Hoiland H, Ringseth J J & Brun T S, *J solution Chem*, 8 (1979) 779.
(b) Yanabe T, Hori K, Akagi K & Fukui K, *Tetrahedron*, 35 (1979) 1065.

8 Michaux G & Reiss J, *J Am chem Soc*, 106 (1982) 6895.

9 (a) Franks F, *Hydrogen bonded solvents* edited by A K Covington and P Jones (Taylor and Francis, UK) 1968 pp. 31.
(b) Luck W A P, *Pure appl Chem*, 59 (1987) 1215.

10 Okazaki S, Touhara H & Nakanishi K, *J chem Phys*, 81 (1984) 890.

11 (a) Tourkey A R, Abdel-Hamid A A & Slim I Z, *Z phys Chem*, (*Leipzig*), 250 (1972) 49.
(b) Tourkey A R, Abdel-Hamid A A & Slim I Z, *Z phys Chem*, (*Leipzig*), 250 (1972) 61.

12 Asknes G & Asaad N, *Interaction of water in ionic and non-ionic hydrates*, edited by H Kleebung (Springer Verlag, Berlin Heidelberg) 1987, pp. 298.

13 Cox B G, *Kinetics and the thermodynamics studies on electrolyte solutions, Ann Rep Sec. C* (The Royal Society of Chemistry, London) 1981, pp. 3.

14 Abraham M H & How Chiong Ling, *Tetrahedron Lett*, (1982) 469.

15 Feakins D & Voice P J, *J chem Soc Faraday Trans*, 68 (1972) 1390.

16 Popovych O, *J phys Chem*, 88 (1984) 4167.

Indian Journal of Chemistry
Vol. 29A, July 1990, pp. 647-651

Volumetric and solvation behaviour of amino acids in some aqueous binaries: Part III—Glycine, DL-alanine and DL-α-aminobutyric acid in aqueous solutions of non-electrolytes at 298.15 K

I N Basumallick & R K Mohanty*

Department of Chemistry, Visva-Bharati Santiniketan 731235

and

Utsabananda Chakraborty

T.D.B. College, Raniganj

Received 23 May 1989; revised and accepted 31 October 1989

Apparent molal volumes, apparent molal adiabatic compressibilities and solvation numbers of glycine, DL-alanine and DL-α-amino-*n*-butyric acid have been determined at 298.15 K in aqueous solutions containing upto 50% (by wt) of ethylene glycol, propylene glycol and glycerol and also in aqueous dimethyl sulphoxide. The volumes and compressibilities of transfer and the solvation numbers at various compositions of the mixtures have also been obtained and interpreted in terms of the nature of the given binary systems and the hydration of amino acids.

In continuation of our studies[1,2] on the solvation behaviour of amino acids in various aqueous binary mixtures, we present here the apparent molal volumes, apparent molal adiabatic compressibilities and hydration numbers of glycine, DL-alanine and DL-α-aminobutyric acid in some aqueous non-electrolyte solutions. Aqueous non-electrolyte media are suitable for the study of weak non-bonding interactions existing in biological systems[3-7]. The cosolvents, viz., ethylene glycol (EG), propylene glycol (PG), glycerol (GL), are all hydrophilic in nature[8,9] while dimethyl sulphoxide (DMSO) is somewhat hydrophobic in character[10-13]. Although amino acids have been studied by different authors in various media[14-17], there are only a few studies on volumetric properties in non-electrolyte media[18-20]. Interestingly enough, EG, PG and GL seem to interact similarly with water, but behave differently with respect to protein stabilisation/destabilisation in solution[9-21]. As such, it will be interesting to see how these cosolvents influence the hydration of amino acids, which are protein components. Dimethyl sulphoxide (DMSO) shows a contrasting behaviour with respect to water and hence it will be interesting to compare the results of hydrophilic solvents and somewhat hydrophobic DMSO.

Materials and Methods

Glycine and DL-alanine were of chromatographic grade (BDH, England) and DL-α-amino-*n*-butyric acid was obtained from Sigma Chemicals, USA. These were dried in a vacuum desiccator for 8 days before use. Ethylene glycol (Merck), propylene glycol (Merck), glycerol (GR, Merck) and dimethyl sulphoxide (LR, BDM) were purified by standard methods.

The apparent molal volumes (ϕ_v), apparent molal adiabatic compressibilities (ϕ_k) and their limiting values and the solvation numbers of the amino acids at various compositions of the binary mixtures were obtained at 298.15K by methods described in our previous publication[1]. The concentrations of the amino acids were varied from 0.2 to 0.9 mol kg^{-1}.

Results and Discussion

The ϕ_v^0 and ϕ_k^0 values of the amino acids in various binary mixtures are presented in Table 1. The transfer values of these parameters from water to the various binary mixtures are presented along with the solvation numbers in Table 2.

In solutions of amino acids like glycine (Gly), DL-alanine (Ala) and DL-α-aminobutyric acid (Aba) interactions with the solvent will be mostly at the NH_3^+ and COO^- ends, i.e. their solvation will be mostly controlled by charge-dipole forces[22]. As such, the change, if any, in the solvation of the amino acids when they are transferred from water to the aquo-organic media, will be due to changes

Table 1—Limiting apparent molal volumes (ϕ_v^0) and adiabatic compressibilities (ϕ_k^0) of amino acids in different binary mixtures at 25°C

Mol fr. of cosolvent	ϕ_v^0 (ml mol^{-1})			$\phi_k^0 \times 10^4$ (ml mol^{-1}bar^{-1})		
	Gly†	Ala	Aba	Gly†	Ala	Aba
			Water + ethylene glycol			
0.000	43.2	60.5	75.4	−25.9	−23.9	−26.0
0.0312	43.7	60.6 (0.6)[a]	75.3 (0.5)	−20.7	−18.9 (2.2)	−20.4 (1.8)
0.0676	44.6	60.9 (0.5)	75.5 (0.5)	−16.5	−14.2 (1.2)	−15.9 (1.2)
0.1106	45.2	61.3 (0.6)	75.9 (0.5)	−12.8	−10.3 (1.8)	−11.0 (1.4)
0.1620	45.8	61.9 (0.4)	76.5 (0.3)	− 9.1	− 6.7 (0.8)	− 6.0 (0.6)
0.2248	—	62.5 (0.4)	77.2 (0.4)	—	− 3.3 (0.7)	− 1.0 (1.2)
			Water + propylene glycol			
0.0256	43.6 (1.0)[a]	60.4 (0.6)	75.0 (0.6)	−20.1 (1.7)	−18.3 (1.1)	−19.6 (1.5)
0.558	44.3 (0.8)	60.8 (0.5)	75.1 (0.7)	−14.8 (1.5)	−12.6 (0.7)	−13.3 (1.6)
0.0920	45.2 (0.8)	61.3 (0.6)	75.8 (0.5)	− 9.6 (1.0)	− 8.2 (1.3)	− 7.1 (2.5)
0.1362	46.1 (0.7)	62.1 (0.6)	76.7 (0.5)	− 6.5 (1.7)	− 3.6 (1.8)	− 0.5 (1.8)
0.1913	47.0 (0.7)	63.0 (0.8)	77.9 (0.6	− 3.6 (0.5)	+ 1.7 (0.2)	+ 5.7 (−0.6)
			Water + glycerol			
0.0212	43.8 (0.9)[a]	60.9 (0.5)	75.7 (0.5)	−21.4 (1.2)	−19.7 (1.1)	−20.4 (1.0)
0.0466	44.5 (0.9)	61.3 (0.5)	76.1 (0.5)	−17.9 (1.1)	−15.1 (0.8)	−15.3 (1.3)
0.0773	45.2 (0.8)	61.9 (0.5)	76.6 (0.5)	−13.5 (1.4)	−11.3 (1.2)	−10.5 (0.9)
0.1153	45.9 (0.9)	62.4 (0.5)	77.1 (0.5)	− 9.8 (1.5)	− 7.6 (1.3)	− 5.8 (0.8)
0.1635	46.6 (0.9)	63.1 (0.5)	77.8 (0.6)	−6.2 (1.0)	− 3.6 (2.3)	− 1.4 (1.5)
			Water + DMSO			
0.0249	43.5 (0.8)	60.3 (0.6)	75.0 (0.5)	−20.9 (2.1)	−18.9 (1.7)	−19.8 (1.0)
0.0544	43.9 (1.0)	60.4 (0.6)	74.9 (0.4)	−15.1 (1.7)	−13.3 (0.7)	−13.7 (0.3)
0.0898	44.6 (0.7)	60.6 (0.8)	74.9 (0.7)	−10.1 (1.1)	− 8.7 (1.1)	− 8.8 (1.3)
0.1330	45.5 (0.7)	61.4 (0.5)	75.7 (0.4)	− 6.8 (2.0)	− 4.0 (0.8)	− 4.3 (1.0)

Gly = Glycine; Ala = DL-alanine; Aba = DL-α-amino-*n*-butyric acid.

(a) Slope values given in the parentheses.

†Data for water + EG system calculated using data from ref. 31.

in such forces as we go from water to the binary solvent.

Water-glycol (EG and PG) and water-glycerol (GL) systems

From pure water to water-EG mixtures containing 50% by weight of EG, the dielectric constant of the binary mixtures changes from 78.5 to 63.2 at 25°C (ref. 23), and the water structure breaks down considerably[24]. Because of the reduction in intermolecular interaction in the medium with increase in mole fraction of EG, the cavity creation effect increases resulting in a gradual increase in positive contribution to ϕ_v^0 of the amino acid. The hydration of amino acids will also go on decreasing, and since this hydration is mostly electrostrictive, it will also have a positive contribution to volume. However, the cavity effect increases with increase in the size of the amino acid, whereas the electrostrictive/solvation effect remains almost

Table 2—Limiting apparent molal volume of transfer ($\phi^0_{v,tr}$), adiabatic compressibility of transfer ($\phi^0_{k,tr}$) of amino acids from water to various binary mixtures and hydration numbers (n_h) in these media at 25°C

Mol fr. of cosolvent	$\phi^0_{v,tr}$ (ml mol^{-1})			$\phi^0_{k,tr} \times 10^4$ (ml mol^{-1}bar^{-1})			n_h		
	Gly	Ala	Aba	Gly	Ala	Aba	Gly	Ala	Aba
				Water + ethylene glycol					
0.0312	0.5	0.1	−0.1	5.2	5.0	5.6	2.7	2.5	2.7
0.0676	1.4	0.4	0.1	9.4	9.7	10.1	2.3	2.0	2.2
0.1105	2.0	0.8	0.5	13.1	13.6	15.0	1.9	1.6	1.6
0.1620	2.6	1.5	1.2	16.7	17.1	19.9	1.4	1.1	0.9
0.2248	—	2.0	1.9	—	20.5	24.9	—	0.6	0.2
				Water + propylene glycol					
0.0256	0.4	0.0	−0.3	5.8	5.6	6.3	2.7	2.4	2.6
0.0558	1.1	0.3	−0.2	11.0	11.3	12.7	2.1	1.8	1.9
0.0920	2.0	0.9	0.5	16.2	15.7	18.9	1.5	1.3	1.1
0.1362	2.9	1.6	1.4	19.4	20.2	25.5	1.0	0.6	0.1
0.1913	3.7	2.6	2.5	22.2	25.6	31.7	0.6	−0.3	−0.9
				Water + glycerol					
0.0212	0.6	0.4	0.4	4.5	4.2	5.5	2.8	2.6	2.7
0.0466	1.3	0.9	0.7	8.0	8.8	10.7	2.6	2.2	2.2
0.0773	2.0	1.5	1.2	12.3	12.6	15.4	2.1	1.8	1.6
0.1153	2.6	2.0	1.7	16.0	16.3	20.2	1.7	1.3	1.0
0.1635	3.4	2.7	2.5	19.6	20.3	24.6	1.1	0.7	0.2
				Water + DSMO					
0.0249	0.3	−0.1	−0.3	5.0	5.0	6.1	2.8	2.5	2.6
0.0544	0.7	0.0	−0.4	10.7	10.6	12.3	2.2	1.9	1.9
0.0898	1.4	0.1	−0.4	15.7	15.2	17.2	1.5	1.3	1.3
0.1330	2.3	1.0	0.3	19.0	19.9	21.7	1.1	0.6	0.7
0.1872	3.2	1.8	1.2	23.3	22.2	29.4	0.4	0.3	−0.5

same among the present set of amino acids. Of course, for DL-alanine (Ala) and DL-α-aminobutyric acid (Aba) there will be some contribution from hydrophobic hydration, which will have a negative contribution to volume − being more negative for the more hydrophobic molecule[25]. As such, the combined effect of all these will result in a volume of transfer in the order: $\phi^0_{v,tr}$ (Gly) > $\phi^0_{v,tr}$ (Ala) > $\phi^0_{v,tr}$ (Aba). However, the order in the variation of ϕ^0_k and n_h is expected to be $\phi^0_{k,tr}$ (Aba) > $\phi^0_{k,tr}$ (Ala) ⩾/ $\phi^0_{k,tr}$ (Gly) and $n_{h,tr}$ (Aba) > $n_{h,tr}$ (Ala) ⩾ $n_{h,tr}$ (Gly), because of the contribution from hydrophobic hydrations in the case of DL-α-aminobutyric acid (Aba). This has actually been observed. It would be worthwhile to mention here that the nature of variation of above two functions is similar to that in other water + cosolvent systems studied. With increase in the mole fraction of EG, ϕ^0_v and ϕ^0_k should increase and n_h should decrease. This trend of variation in the above three functions is actually observed as can be seen from Tables 1 & 2.

The trends in variation in the above three functions in water + PG and water + GL systems are grossly similar to that in the water + EG system (vide Tables 1 and 2); and the small variations can be traced to the increased hydrophobicity in PG and increased hydrophilicity in GL.

Water-DMSO system

DMSO is known to enhance the three dimensional structure of water[10] and as such at the initial addition of DMSO to water, cavity creation factor for dissolution of amino acid will be minimised, resulting in negative volumes of transfer. As the DMSO concentration increases, the cage structures can no longer be sustained and will break down. Under the circumstances the DMSO-water system behaves like the water + glycol or water + glycerol system, so that after a particular concentration of DMSO, the volumes of transfer ($\phi^0_{v,tr}$) of the amino acids would increase, which is actually observed. The $\phi^0_{k,tr}$ and n_h values however show a more regular variation, indicating that the amino acids get more and more dehydrated with increase in DMSO concentration (see Table 2).

Comparison of different systems

It appears from the data in Tables 1 and 2 that while $\phi^0_{v,tr}$ for glycine increases with increase in cosolvent content of the medium, those of alanine and aminobutyric acid have some negative values at certain mole fraction of cosolvent. This indicates that the sign and magnitude of $\phi^0_{v,tr}$ for these amino acids in these systems depend on the nature of the amino acid and on the nature as well as concentration of the cosolvent. Thus, the volume of transfer decreases with increase in the hydrophobic nature of the cosolvent or the hydrophobic nature of amino acids.

A comparison of $\phi^0_{v,tr}$ of amino acids in presence of electrolytes[1] (KCl) at 0.8 *m* with those in non-electrolytes also at 0.8 *m* (obtained by intrapolation) indicates that $\phi^0_{v,tr}$ of amino acids are much greater in electrolyte solutions than in non-electrolyte solutions (Table 3). This appears to suggest that zwitterion-ion interactions are much stronger than zwitterion-nonelectrolyte interactions.

The positive values of $\phi^0_{k,tr}$ (Table 2) indicates that ϕ^0_k of the amino acid solution is determined by the combined effects of (i) reduction[27] or loosening of electrostricted hydration zone around zwitterionic ends and (ii) destruction of hydrophobic hydration around the carbon skeleton[27,28], in the presence of cosolvent. Since both these effects have positive contributions to ϕ^0_k, amino acids with larger carbon skeletons are likely to exhibit more positive values of $\phi^0_{k,tr}$. Again, among the cosolvents, the observed large values of $\phi^0_{k,tr}$ of the amino acids in the presence of PG, may be due to its efectiveness in reducing electrostriction around the zwitterionic ends through its hydrophilic centre and destruction of hydrophobic hydration zone of amino acid via interaction with hydration sphere of its hydrophobic moieties. Apart from these interactions (electrostriction or hydrophobic), the contribution of modified water structure by the solutes (amino acids) and cosolvents should be considered for the detailed analysis of $\phi^0_{k,tr}$.

Table 3—Limiting apparent molal volume of transfer ($\phi^0_{v,tr}$) of amino acids from water to 0.8*m* electrolyte (KCl) and 0.8*m* non-electrolyte solutions at 25°C

Salt/ cosolvent	Molality of the salt/cosolvent (mol kg^{-1})	$\phi^0_{v,tr}$ (ml mol^{-1})		
		Gly	Ala	Aba
KCl[a]	0.8	1.25	1.42	1.27
EG	0.8	0.25	0.05	−0.05
PG	0.8	0.20	0.0	−0.20
GL	0.8	0.40	0.30	0.25
DMSO	0.8	0.15	−0.10	−0.25

(a) Taken from ref. 1.

The limiting apparent molal compressibilities (ϕ^0_k) have been used to compute hydration numbers of amino acids in these media. It is to be noted that hydration numbers of amino acids decrease (as also in the present study) in all the aqueous binaries, except in cases where selective solvation is possible[29]. The reasons for the decreases in hydration number may be attributed to the removal of water molecules from the hydration zones of the amino acids because of interactions with the cosolvent.

It is very difficult at this stage to assess the relative contributions of various factors stated above and of any other possible phenomenon. However, by changing the interacting species (EG, PG, GL, DMSO) the variation in the hydration numbers of amino acids is not found to be that appreciable. This may be due to the fact that hydration at the zwitterionic ends is the major factor contributing to the hydration of these amino acids, and further that, it is hardly disturbed by the interactions with the non-electrolytes chosen in this study. Similar conclusions were also drawn earlier from volumetric studies of amino acids in aqueous urea[22,30].

References

1 Basumallick I, Mohanty R K & Chakraborty U N, *Indian J Chem*, 25A (1986) 1089.

2 Mohanty R K, Basumallick I & Chakraborty U N, *Indian J Chem*, 27A (1988) 338.

3 Barone G, Castronuovo G, Elia V, Stassinopuoluc K & Datta G D, *J chem Soc Faraday Trans-I*, 80 (1984) 3094.

4 Scheraga H A, *Acc chem Res*, 12 (1979) 7, and references 1-6 therein.

5 Arnett E M, in *Physico-chemical processes in mixed aqueous solvents*, edited by F Franks (Heinemann, London) 1967, p 105.
6 Ray A, *J Am chem Soc*, 91 (1969) 6511.
7 Tanford C, *Adv Protein Chem*, 23 (1968) 121.
8 Rowlinson J S, in *Liquids and liquid mixtures* (Butterworths, London) 1969.
9 Kundu K K & Basumallick I, *Can J Chem*, 57 (1979) 961.
10 Oakenfull D & Fenwick D E, *J chem Soc Faraday Trans-I*, 75 (1979) 636.
11 Safford G J, *J chem Phys*, 50 (1969) 2140.
12 Rallo F, Rodante F & Silvestroni P, *Thermochim Acta*, 1 (1970) 311.
13 de Visser C, Heuvelsland W J M, Dunn L A & Somsen G, *J chem Soc Faraday Trans-I*, 74 (1978) 1159.
14 Gekko K, *J Biochem*, 90 (1981) 1633.
15 Gekko K & Koga S, *Biochem-Biophys Acta*, 786 (1984) 151.
16 Nozaki Y & Tranford C, *J biol Chem*, 240 (1965) 3568.
17 Nozaki Y & Tanford C, *J biol Chem*, 246 (1971) 2211.
18 Chattopadhyay A K & Lahiri S C, *Electrochim Acta*, 27 (1982) 269.
19 Mishra A K & Ahluwalia J C, *J chem Soc Faraday Trans-I*, 77 (1981) 1469.
20 Ogawa T, Yasuda M & Mizutani K, *Bull chem Soc (Japan)*, 57 (1984) 662.
21 Kundu K K & Basumallick I, *Indian J Chem*, 18A (1979) 1.
22 Mishra A K, Prasad K P & Ahluwalia J C, *Biopolymers*, 22 (1983) 2397.
23 Arkhadov Y Y, in *Dielectric properties of binary solutions* (Pergamon, New York) 1981.
24 Mohanty R K, Sarma T S, Subramanian S & Ahluwalia J C, *Trans Faraday Soc*, 67 (1971) 305.
25 Mishra A K & Ahluwalia J C, *J phys Chem*, 88 (1984) 86.
26 Desnoyers J E, Arel M, Perron G & Jolicoeur C, *J phys Chem*, 73 (1969) 3347.
27 Kaulgud M V & Rao K S M, *J chem Soc Faraday Trans-I*, 75 (1979) 2237.
28 Bhowmik S & Mohanty R K, *Indian J Chem*, 25A (1986) 416.
29 Cox B G & Natarajan R, *J chem Soc Faraday Trans-I*, 75 (1979) 86.
30 Derosiers N, Perron G, Mathieson J C, Conway B E & Desnoyers J E, *J soln Chem*, 3 (1974) 784.
31 Bhowmik S & Mohanty R K, Submitted for publications elsewhere.

Indian Journal of Chemistry
Vol. 29A, July 1990, pp. 652-655

Evaluation of solute-solvent interactions of some nonelectrolytes with N-methylpyrrolidone by gas-liquid partition chromatography

B Rajeshwar Rao & S D Bhagat*
Indian Institute of Petroleum, Dehradun 248 005

Received 5 May 1989; revised 18 September 1989; rerevised and accepted 12 January 1990

Infinite dilution activity coefficients of some nonelectrolytes in N-methylpyrrolidone have been determined at 310 K by gas-liquid partition chromatography. The results are discussed in terms of thermodynamics of interactions between the components of the binary systems, and the nature of selectivity and solvent power.

The gas-liquid partition chromatography technique has been extensively used for determining thermodynamic properties of binary nonelectrolyte solutions[1] at infinite dilution in view of the usefulness of such data in petrochemical and industrial processes. Weak attractive interactions of the type of alkyl-phenyl[2], dipole-induced dipole[3], aromatic-aromatic[4], carbonyl-aromatic[5], and amino-aromatic[6] interactions in various systems are known to affect molecular conformations and chemical selectivity[7]. Therefore, in the present study the excess partial molar free energy and activity coefficients of some nonelectrolytes in N-methylpyrrolidone solvent have been estimated from the measurement of experimental retention volume at 310 K. The results have been discussed in terms of solute-solvent interactions in binary mixtures.

Materials and Methods

Gas chromatographic measurements were made using a Perkin-Elmer Sigma 2000 gas chromatograph with a flame ionization detector connected to a Perkin-Elmer 3600 Data Station. The detector, injection port, and column temperatures were maintained at 100, 90, and 37 ± 0.1°C respectively. N-Methylpyrrolidone (16% by weight, Fluka AG) was coated on the solid support chromosorb P, NAW 80-100 mesh, by the normal rotary evaporator technique, and packed uniformly in a 3.0 m long column of stainless steel tubing (2.1 mm I.D./3.0 mm O.D.). The column was preconditioned under nitrogen flow (12 ml min^{-1}) for 24 h at 26°C, having a presaturator which was filled with N-methylpyrrolidone and the solid support in series before column, to compensate for the loss of solvent during the experiment. The amount of stationary phase in the column was determined by weighing. All the solutes (Fluka AG/BDH AR) were used as such and injected with a 10 µl Hamilton syringe. The carrier gas was nitrogen with a flow rate of 36 ml min^{-1}. The pressure of the carrier gas at the column inlet was measured by means of a pressure gauge calibrated against a mercury manometer and the outlet pressure was read using a barometer. The adjusted retention time was measured from the methane peak to the corresponding sample peak maximum (t_R). Vapour pressure values (p^o) of the solutes were calculated from the Antoine equation constants. The specific retention volume (V_g^o) was determined through a precise control of the experimental variables like the gas flow rate (using mass flow controller), the pressure drop across the column, the column temperature, the dead volume of the column and the weight of the stationary phase. The measurements were reproducible within ±0.2%.

The activity coefficient (γ^o), the partition coefficient (K^o) and excess partial molar free energy (ΔG_e^o) may be determined with high accuracy in dilute solutions from the specific retention volume[8] (V_g^o). From this data, relative volatility[9] (α) and selectivity[10] (β) with reference to benzene and solvent power or solubility[11] (s) were estimated.

Results and Discussion

The data obtained for various solutes in N-methylpyrrolidone (NMP) solvent have been presented in Table 1. The values of various physicochemical parameters are dependent mainly on the intermolecular forces operating between the stationary phase and the solutes. The solution properties refer to the transfer of solute from the one atmosphere ideal vapour to the hypothetical pure liquid with the infinitely dilute state in solvent[12]. The reproducibility of V_g^o values within ±0.2% in the present study indicates precise control on the experimental parameters; bleeding eff-

Table 1—Physicochemical data on the interaction of some solutes with N-methylpyrrolidone at 310 K

Solute	t_R (min)	V_g^o (ml mol^{-1})	γ^o_{Exptl}	γ^o_{UNIFAC} (a)	Deviations of Exptl values from UNIFAC (b)	Deviations of Exptl values from UNIFAC (c)	K°	α	β	s	ΔG_c^o (kcal mol^{-1})
n-Pentane	1.16	25.09	8.736	8.60	22.3	1.5	28.986	35.03	7.21	0.114	1.335
n-Hexane	2.77	61.18	11.306	12.00	19.7	6.1	70.690	14.36	9.33	0.088	1.494
n-Heptane	6.48	144.36	14.724	16.60	15.9	12.7	166.791	6.08	12.15	0.068	1.657
n-Octane	14.52	324.61	19.826	22.60	23.3	13.9	375.054	2.71	16.36	0.050	1.840
n-Nonane	34.88	781.07	24.664	31.30	21.6	26.9	902.445	1.12	20.35	0.041	1.975
n-Decane	82.50	1848.67	31.638	42.30	66.2	33.7	2135.961	0.47	26.10	0.032	2.128
Cyclohexane	5.58	124.18	8.466	7.78	13.4	8:1	143.478	7.07	6.98	0.118	1.316
1-Heptene	8.67	193.46	8.980				223.520	4.54	7.41	0.111	1.352
1-Octene	22.60	505.76	10.416				584.353	1.74	8.59	0.096	1.443
Cyclohexene	10.23	228.43	5.023				263.929	3.85	4.14	0.199	0.994
Cycloheptene	27.50	615.61	6.369				711.279	1.43	5.25	0.157	1.140
Cyclooctene	76.56	1715.50	7.672				1982.095	0.51	6.33	0.130	1.255
Benzene	39.24	878.81	1.212	1.23	14.3	1.5	1015.384	1.00	1.00	0.825	0.118
Toluene	85.41	1913.91	1.746	1.67	13.5	4.4	2211.339	0.46	1.44	0.573	0.343
Carbon tetrachloride	25.22	564.50	1.596				652.219	1.56	1.32	0.626	0.288
Chloroform	98.71	2212.09	0.221				2555.853	0.40	0.18	4.525	−0.930
Methylene chloride	27.73	620.77	0.402				717.237	1.41	0.33	2.487	−0.561
Methanol	57.82	1295.36	0.575				1496.667	0.68	0.47	1.739	−0.341

(a) γ^o-values (UNIFAC-Model) were obtained from the plot of ln γ^o vs 1/T (b) ref. 13 (c) present work.

ects were found to be minimum. All solutes other than chlorocarbons and methanol showed marked deviations from Raoult's law ($\gamma^\circ > 1$). The dipolar structure (II) of NMP (dipole moment = 4.09 ± 0.04D) is expected to generate considerable dipole-induced dipole interactions with benzene and olefins, dipole-dipole interactions with chlorocarbons; methanol and toluene, and dispersion interactions with paraffins solutes. Dipole-dipole interactions are expected to occur between the C − Cl dipoles of chlorocarbons, O − H dipole of methanol or electron-rich aromatic part (π-base) of toluene and the C = O dipole of the NMP solvent.

The experimentally determined data have been compared in Table 1 with γ^o values calculated from the universal functional group activity coefficient (UNIFAC) equation for selected solute-NMP systems for which the UNIFAC parameters were available. Deviations of experimental γ^o values for these solutes reported by Ferriera *et al.*[13] from UNIFAC predicted values are also included in the table. It is seen that except for *n*-nonane, deviations of experimental γ^o values of the present study are significantly lower.

I II

γ^o is a measure of strength of solute-solvent interactions. A large positive value of γ^o for a solute in a particular solvent phase would suggest that the solute molecules are incompatible with the solvent molecules and are being forced out of that phase into the vapour phase whereas a value $\gamma^o < 1$ indicates the presence of some type of solute-solvent interaction.

The experimental γ^o data for alkane-NMP systems show that as the C − C chain length of the alkane is increased, γ^o increases reflecting the increasing tendency of the solute for being forced out of the solvent phase. This is also shown by the increase in the K° values with molecular weight of the alkane. As a result of these effects, the solubility (S) of the solute in NMP decreases with molecular weight, while selectivity of NMP for aromatics (benzene) over alkanes increases with increase in molecular weight of alkane. γ^o values of $CHCl_3$-NMP and CH_2Cl_2-NMP system are less than one. This indicates presence of some form of solute-solvent interactions in these systems. If there is H-bonding interaction operating in these systems then the strength of these interactions should

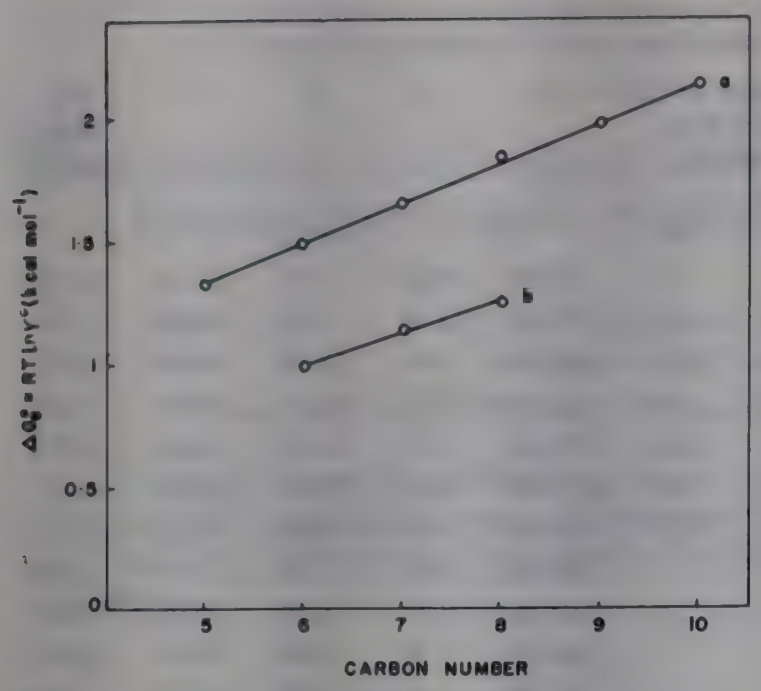

Fig. 1—Variation of ΔG_e^o with number of carbon atoms for (a) *n*-alkanes and (b) cycloalkenes at 310 K in NMP

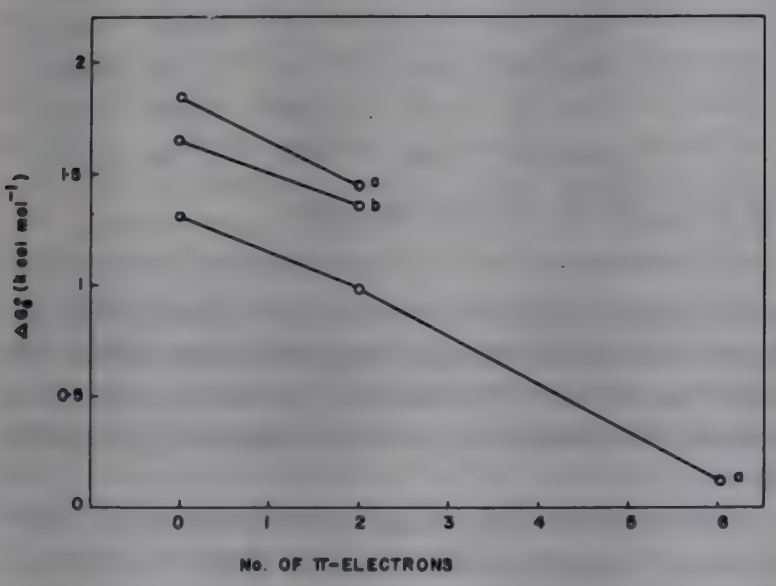

Fig. 2—Variation of ΔG_e^o with number of π-electrons for (a) C_6-, (b) C_7-, (c)and (c) -hydrocarbons at 310 K in NMP

decrease in the order, $CHCl_3 > CH_2Cl_2 > CCl_4$ which requires that γ^o, α and β for these systems should vary in the order $CHCl_3 < CH_2Cl_2 < CCl_4$, while S and K^o should vary in the order $CCl_4 < CH_2Cl_2 < CHCl_3$. The experimental data given in Table 1 show these trends, substantiating the assumption of H-bonding interactions for these systems.

Interaction of CH_3OH with NMP is indicated by the γ^o value of less than one for this system. This interaction may involve not only hydrogen bonding but also steric repulsion between bulky CH_3 groups present in both molecules. The solvent power (S), is found to decrease in the order: chlorocarbons > methanol > aromatics > cycloalkenes > *n*-paraffins. The solvent power is also found to decrease with ascending homologous hydrocarbons series on the basis of

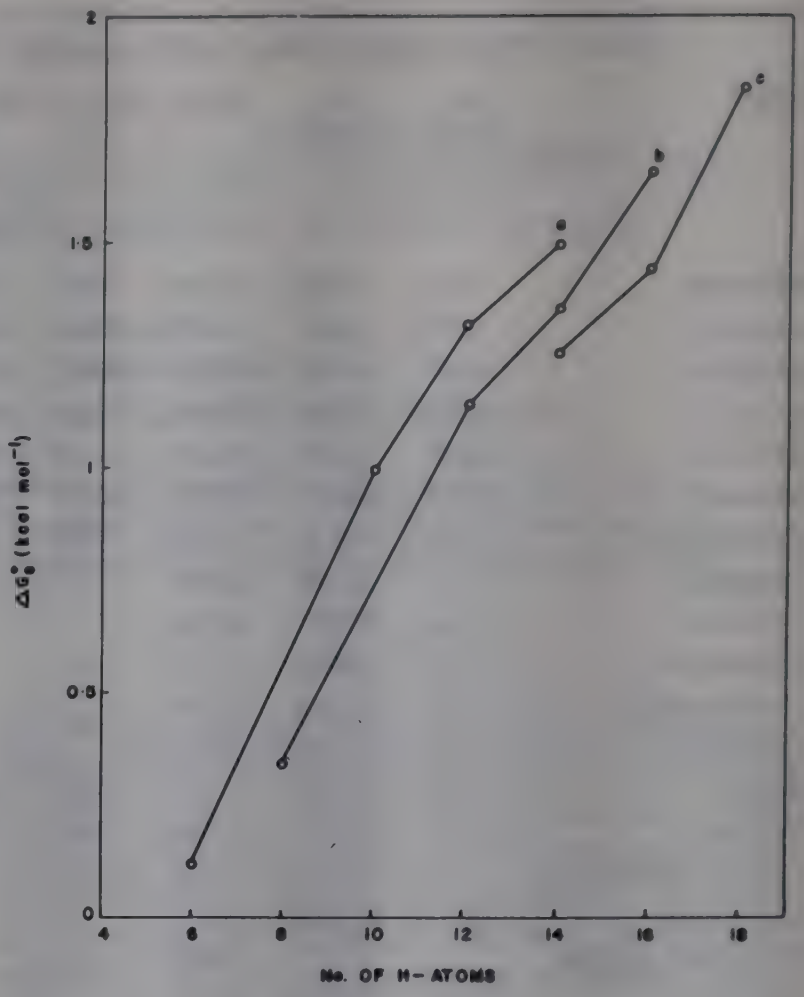

Fig. 3—Variation of ΔG_e^o with number of H-atoms for (a) C_6-, (b) C_7-, and (c) C_8-hydrocarbons at 310 K in NMP

difference in polarity. Partition coefficient (K^o) values can also be used to screen the solvent for liquid-liquid extraction, whereas the value of relative volatility (α) in a solvent gives better understanding for the vapour-liquid equilibrium. The GLC column essentially works like a multiple extractive distillates column with high loading of immobile liquid phase (solvent) and is ideal for determining the relative volatility of compounds.

Several attempts have been made earlier to relate the excess partial molar free energy ΔG_e^o, with solute-solvent interaction. Variation of ΔG_e^o with the carbon number is shown in Fig. 1. The effect of π-electrons in the solute on solute-solvent interactions is evident on examining the experimental excess partial molar free energy, ΔG_e^o, values for such solutes. The variation of ΔG_e^o with the number of π-electrons in -C_6, -C_7 and -C_8 hydrocarbons has been shown in Fig. 2, from which it is evident that the interaction increases with increase in number of π-electrons, with ΔG_e^o values decreasing by 0.3-0.4 kcal mol^{-1} per π-bond. Cyclization also decreases the ΔG_e^o values. Thus, for a pair of molecules having the same number of π-electrons like heptene, cycloheptene or octene, cyclooctene, cyclization reduces ΔG_e^o by about 0.188 to 0.212 kcal mol^{-1}. A reduction in ΔG_e^o on cyclization (0.178 kcal

mol^{-1}) is also shown in the pair *n*-hexane-cyclohexane where there are no π-electrons. In Fig. 3, we have plotted the variation in ΔG_e^o with the number of H-atoms for the same carbon number. As expected, ΔG_e^o values decrease with the decrease in the number of H-atoms, which reflects the contributions of weak interactions arising from dispersion forces.

In conclusion, we may state that in gas-liquid partition chromatography, we have a useful analytical technique that may be used to investigate the thermodynamics of solute-solvent interactions with a high degree of precision, and the technique is also quite fast. It is possible to draw useful inferences using only microgram quantities of solute as well as solvent. The experimentally measured thermodynamic parameters are in good agreement with those predicted using advanced solution models like the UNIFAC model.

Acknowledgement

The authors are thankful to the Director, Indian Institute of Petroleum, Dehradun 248 005 for encouragement. One of them (B R Rao) is grateful to the CSIR, New Delhi for financial assistance.

References

1 Conder J R & Young C L, *Physicochemical measurements by gas chromatography* (John Wiley, New York), 1979, 154.
2 Hiraki Y & Tai A, *Bull chem Soc Japan*, 56 (1983) 2330.
3 Stoddart J F, *Chem Soc Rev*, 8 (1979) 85.
4 Burley S K & Petsko G A, *J Am chem Soc*, 108 (1986) 7995.
5 Gould R O, Gray A M, Taylor P & Walkinshaw M D, *J Am chem Soc*, 107 (1985) 5921.
6 Burley S K & Petsko G A, *FEBS Lett*, 203 (1986) 139.
7 Berg U, Liljefors T, Roussel C & Sandstrom J, *Acc chem Res*, 18 (1985) 80.
8 Kenworthy S, Miller J & Martire D E, *J chem Educ*, 40 (1963) 541; Martin A J P & Synge R L M, *Biochem*, 35 (1941) 1358; Hardy C J, *J Chromatogr*, 2 (1959) 490; Kuchhal R K & Mallik K L, *J chem Engg Data*, 17 (1972) 49.
9 Vernier P, Raimbault C & Renon H, *J chim Phys*, 66 (1969) 429.
10 Deal C H & Derr E L, *Ind Eng Chem Process Design Develop*, 3 (1964) 394.
11 Voetter H & Kosters C G, *VI World Petroleum Congress*, 3 (1963) 131.
12 James M R, Giddings J C & Keller R A, *J gas chromatogr*, 3 (1963) 57; Meyer E F, *J chem Educ*, 50 (1973) 191.
13 Ferriera P O, Bostos J C & Medina A G, *J chem Engg Data*, 32 (1987) 25.
14 Katti P K & Prakash O M, *J chem Engg Data*, 11 (1966) 46; Reed T M & Taylor T E, *J phys Chem*, 63 (1959) 58.

Indian Journal of Chemistry
Vol. 29A, July 1990, pp. 656-660

Conductometric determination of dissociation constants of picric acid in 2-methoxyethanol, 1,2-dimethoxyethane and their aqueous binary mixtures

S K Ghosh & D K Hazra*
Department of Chemistry, North Bengal University, Darjeeling 734 430

Received 17 May 1989; revised 23 August 1989; accepted 18 September 1989

The conductances of picric acid have been measured in 2-methoxyethanol, 1,2-dimethoxyethane and also in their binary aqueous mixtures at 25 ± 0.01°C. The data have been analysed by the Shedlovsky and the Fuoss conductance equations and the dissociation constants of picric acid have been determined and discussed on the basis of the physical properties of the solvents. Thermodynamic transfer functions in the two solvent systems have also been evaluated and explained in terms of ion-solvent interactions.

2-Methoxyethanol (ME) and 1,2-dimethoxyethane (DME) have found varied applications in organic synthesis[1,2] as well as in different electrochemical[3] studies. As they are monomethyl and dimethyl ethers of ethylene glycol, it is very likely that their physico-chemical characteristics lie intermediate between protic and dipolar aprotic solvents. The conductometric method is well known to give valuable information regarding ion-solvent interactions. Although conductivity of picric acid in ME as solvent has been investigated recently[4], no information regarding the conductometric behaviour of picric acid in DME as well as in ME-water and DME-water mixtures is available and hence the title investigation. The standard Gibbs energies of transfer of picric acid [$\Delta G_t^{\P}(1)$] in the two solvent systems have been evaluated and explained in terms of ion-solvent interactions.

Materials and Methods

Purified 2-methoxyethanol (ME) and 1,2-dimethoxyethane (DME) were used. Triply distilled water (Sp cond $< 1 \times 10^{-6}$ Ω^{-1} cm^{-1}) was used. Solutions were prepared using freshly distilled solvents. Dielectric constants of the solvent mixtures were taken from the literature[5,6].

Picric acid (Glaxo) was recrystallised from ethanol-water mixture. The solvent mixtures were prepared by weight. Stock solution of picric acid in the appropriate solvent mixture was prepared by weight and the working solutions were obtained by dilution.

A Pye-Unicam conductivity meter (PW 9509) was used for measuring the conductances at 2 kHz with a dip-type cell of cell constant 0.73 cm^{-1} and having an accuracy of ±0.1%. The measurements were carried out in a thermostatic bath maintained at 25 ± 0.01°C. A 60 W heating element and a toluene-mercury thermoregulator were used to maintain the temperature of the experimental thermostat which was placed in a hot-cum-cold thermostat. The temperature of the hot-cum-cold thermostat was preset at the desired temperature using a contact thermometer and relay system. The absolute temperature was determined by a calibrated platinum resistance thermometer and Muller bridge.

Results

The measured equivalent conductances and the corresponding molar concentrations at different percentages of ME + H_2O and DME + H_2O mixtures at 25°C are given in Tables 1 and 2. The conductance data were analysed using Shedlovsky's method from the set of equations as reported previously[7].

The dissociation constants, K, and the limiting equivalent conductance (Λ_0) have been iteratively calculated and are recorded in Table 3. The low values of dissociation constants upto 80 wt% ME or DME suggest that the electrolyte is present as free ions in these solvent mixtures.

In order to improve our results, we have applied the recent method of computation suggested by Fuoss[8]. For a set of conductance data (C_j, Λ_j, $j = 1 \ldots n$), the three adjustable parameters Λ_0, K_A and R can be obtained by solving Eqs (1-6).

$$\Lambda = P[\Lambda_0(1 + RX) + EL] \quad \ldots (1)$$

$$P = [1 - \alpha\ (1 - \gamma)] \quad \ldots (2)$$

$$\gamma = 1 - K_A C \gamma^2 f^2 \quad \ldots (3)$$

$$-\ln f = \beta\kappa/2(1 + \kappa R) \quad \ldots (4)$$

Table 1 – Equivalent conductance (Λ) of picric acid in aqueous binary mixtures of ME at 25°C

20 Wt% ME		40 Wt% ME		60 Wt% ME	
10^4C (mol dm^{-3})	Λ (Ω^{-1} cm^2 mol^{-1})	10^4C (mol dm^{-3})	Λ (Ω^{-1} cm^2 mol^{-1})	10^4C (mol dm^{-3})	Λ (Ω^{-1} cm^2 mol^{-1})
2.470	236.95	2.776	144.40	2.593	82.45
6.176	235.75	5.552	143.80	3.629	82.10
11.117	234.78	9.716	143.07	6.482	81.46
18.528	233.40	16.656	142.29	11.667	80.70
29.645	232.08	27.759	141.21	18.148	79.85
43.233	230.38	44.415	139.82	25.926	79.07
80 Wt % ME		100 Wt% ME			
1.531	47.95	1.056	17.70		
3.062	47.36	2.641	15.68		
8.164	46.42	5.281	11.63		
12.603	45.75	7.922	9.49		
20.921	44.79	10.563	8.38		
27.563	44.15	26.407	5.57		

Table 2 – Equivalent conductance (Λ) of picric acid in aqueous binary mixtures of DME at 25°C

20 Wt% DME		40 Wt% DME		60 Wt% DME	
10^4C (mol dm^{-3})	Λ (Ω^{-1} cm^2 mol^{-1})	10^4C (mol dm^{-3})	Λ (Ω^{-1} cm^2 mol^{-1})	10^4C (mol dm^{-3})	Λ (Ω^{-1} cm^2 mol^{-1})
5.450	238.01	4.489	145.50	3.095	97.27
16.350	235.02	10.240	143.75	7.737	95.65
27.260	233.50	17.223	142.25	12.378	94.60
38.160	232.00	24.010	141.00	17.020	93.70
49.060	231.01	34.810	139.50	21.662	92.79
59.960	229.50	44.890	138.25	30.946	91.40
80 Wt% DME		100 Wt% DME			
3.413	72.40	0.123	12.50		
8.533	70.43	0.423	11.00		
13.653	68.63	0.986	8.50		
20.479	67.04	1.690	6.02		
30.719	65.11	2.103	4.70		
37.823	63.80	2.466	3.30		

$$\beta = e^2/\varepsilon kT \quad \ldots(5)$$

$$K_A = K_R/(1-\alpha) = K_R(1+K_s) \quad \ldots(6)$$

where RX and EL are relaxation and hydrodynamic terms respectively and other terms have their usual significance. The parameters Λ_0, K_A and R are obtained[9] from the above equations by finding the values of Λ_0 and α which minimize

$$\sigma^2 = \sum_j [\Lambda_j(\text{cal}) - \Lambda_j(\text{obs})]^2/(n-2) \quad \ldots(7)$$

for a sequence of R-values. From the plot of $\sigma\%$ ($=100\ \sigma/\Lambda_0$ against R, the best fit R corresponds to the minimum in σ % versus R curve. Initial Λ_0 value for the iteration procedure was taken from Shedlovsky extrapolations of the data.

As the dielectric constant of solvent mixtures is very low, a wide range of R-values reproduced the data equally well in most of the cases except in 60 wt% ME and 20 and 40 wt% DME where fairly well-defined minima in the σ % versus R curve were obtained.

In order to treat the data for which σ % versus R curve did not show a sharp minimum, R value was arbitrarily preset[8] at the centre-to-centre distance of the solvent separated pair, i.e., $R = a + d$ as $a + d > \beta/2$. Here 'a' is the sum of the crystallographic radii of the ions and 'd' is the average

Table 3 – Conductance parameters and dissociation constants (pK) of picric acid in ME-water and DME-water mixtures at 25°C from 1978 Fuoss equation

Wt%	Λ_0^a (Ω^{-1} cm^2 mol^{-1})	K_A (dm^3 mol^{-1})	$\Lambda_0\eta_0$	R (A°)	σ%	pK
			ME-water mixtures			
00	—	—	3.38[b]	—	—	0.42[c]
20	238.66(±0.06)	3.43(±0.13)	3.62	9.00	0.035	0.54(±0.02)
40	145.76(±0.03)	5.40(±0.09)	3.45	17.00	0.025	0.73(±0.01)
60	83.75(±0.04)	10.97(±0.39)	2.42	9.70	0.055	1.04(±0.01)
80	49.09(±0.03)	33.01(±0.69)	1.26	22.00	0.082	1.52(±0.02)
100[d]	41.09	21338.69	0.63	—	—	4.33
			DME-water mixtures			
20	240.69(±0.22)	4.35(±0.31)	3.90	9.50	0.101	0.64(±0.03)
40	147.94(±0.11)	10.46(±0.37)	3.14	9.60	0.082	1.02(±0.01)
60	99.69(±0.04)	19.62(±0.36)	1.62	14.00	0.047	1.29(±0.01)
80	76.78(±0.11)	55.28(±1.44)	0.71	23.00	0.144	1.74(±0.02)
100[d]	21.18	73561.38	0.08	—	—	4.87

(a) Initial Λ_0 values of picric acid for the iteration procedures are: 238.61,145.78, 83.68, 49.09 and 41.09 in20, 40,60, 80 and 100 wt% ME-water mixtures and 240.59, 147.82, 99.59, 76.89 and 21.18 in 20, 40, 60, 80 and 100 wt% DME-water mixtures respetively.
(b) From ref. 15; (c) from ref. 16; and (d) from Shedlovsky's method.

distance corresponding to the side of a cell occupied by a solvent molecule. The distance 'd' is given by Eq. (8)

$$d = (M/N\rho)^{1/3} = 1.183\,(M/\rho)^{1/3}\ \text{Å} \quad \ldots(8)$$

where M is the molecular weight of solvent and ρ is its density. For mixed solvents, M is replaced by the mole-fraction average molecular weight (M_{av}), which is given by Eq. (9).

$$M_{av} = M_1M_2/(W_1M_2 + W_2M_1) \quad \ldots(9)$$

In Eq. (9) W_1 is the weight fraction of the first component of molecular weight M_1. Though this is an over simplification which ignores possible selective solvation, it at least provides a self-consistent way to obtain an acceptable value for the parameter when a broad range of R-values fit the data. The values of Λ_0, K_A and R obtained by this procedure are recorded in Table 3.

Discussion

It is observed that the viscosity (η_0) of ME-water and DME-water mixtures increases rapidly to reach a maximum at about 60 wt% ME and 40 wt% DME and then decreases rapidly; at this stage η_0 is about three times the viscosity of water. This indicates that the three dimensional structure of water is increased with the addition of organic cosolvent due to hydrophobic interactions of $-CH_3$ groups in ME or DME with water[10,11]. The maximum structuredness seems to occur at 60 and 40 wt% of ME and DME respectively, due to formation of $ME-H_2O$[10] and $DME-H_2O$[11] complexes; thereafter cleavage of the complexes takes place.

The Λ_0 values obtained using Shedlovsky's and Fuoss' methods are in good agreement with each other with marginal variations. It is found that Λ_0 values decrease with increase in organic solvent component in the mixed solvent. The values always decrease with increase or decrease in viscosity (η_0) of solvent mixtures but the Walden product is found to be different. The results indicate that the difference in solvation of ions is responsible for the change in mobility of the ions and hence Λ_0.

It is to be expected that the hydrodynamic entity around the picrate ions is likely to be greater in water than in ME or DME but the higher Λ_0 values in water may be due to greater freedom of ions to move through the polar H-bonded solvent system having high dielectric constant. The three dimensional water structure has 'holes' through which the transfer of ions can occur rather easily and making or breaking of solvated chains is quick enough for a rapid transfer of ions through water. The transfer process is obviously difficult in $ME+H_2O$ or $DME+H_2O$ mixtures as the 'holes' may be blocked by ME/DME or $ME+H_2O/DME+H_2O$ complex and the structure making or breaking would be a slow process.

The data in Table 3 show that K_A values of picric acid are very low in 20, 40 and 60 wt% of ME-water and DME-water mixtures, indicating

Table 4 – Values of $\Delta G_t^\circ(1)$, $\Delta G_t^\circ(H^+)$ and $\Delta G_t^\circ(A^-) - \Delta G_t^\circ(HA)$ for picric acid in ME-water and DME-water mixtures at 25°C [ΔG_t° values are in kJ mol^{-1} (molar scale)]

Wt% cosolvent	Mol% cosolvent	$\Delta G_t^\circ(1)$	$\Delta G_t^\circ(H^+)$	$\Delta G_t^\circ(A^-) - \Delta G_t^\circ(HA)$
		ME + Water mixtures		
20	5.58	−0.68	−1.88	1.19
40	13.63	−1.77	−2.43	0.66
60	26.20	−3.54	−2.93	−0.61
80	48.64	−6.28	−2.25	−3.35
100	—	−22.31	—	—
		DME + Water mixtures		
20	4.75	−1.26	−2.57	1.31
40	11.75	−3.42	−3.99	0.57
60	23.08	−4.96	−4.57	−0.39
80	44.45	−7.53	−1.42	−6.11
100	—	−25.39	—	—

that picric acid is not associated but almost completely dissociated in these solvent mixtures having high dielectric constants. However in ME-water or DME-water containing >60 wt% organic cosolvent, K_A is comparatively high. The pK of picric acid ($pK = 4.33$) in ME is in good agreement with that obtained by Tosi and coworkers[4] ($pK = 4.62$). However, the pK values reported by Simon *et al.*[12] in ME and ME-water mixtures are much different from those obtained presently. Similar discrepancy in the acid dissociation constants of picric acid in other solvents has also been observed[13,14].

The Walden products ($\Lambda_0\eta_0$) of picric acid (Table 3) is maximum in 20 wt% of ME-water or DME-water. The corresponding values in water were taken from literature[15]. As the Walden product of an ion is inversely proportional to the effective radius of the ion in a solvent, the initial variation in the Walden product in mixed solvents can be explained in terms of selective solvation of ions (Pic^- and H^+) by ME, DME and water molecules respectively. The decrease in Walden product in solvent mixtures containing >20 wt% organic cosolvent indicates preferential solvation of ions by ME or DME and the different magnitudes of Walden product suggests that H^+ and Pic^- ions are solvated to different extents in these solvent mixtures. It is thus apparent that the selective solvation of ions depends upon the viscosity of the medium, the exchange of ions with neighbouring solvent molecules, and the movement of ions through the holes in H-bonded solvent systems.

The dissociation constants of picric acid in water and mixed solvents have been used to evaluate the changes in standard free energy accompanying the ionization of the acid in the solvent, $\Delta G_t^\circ(s)$, relative to that in water, $\Delta G_t^\circ(w)$, at 25°C on the molar scale using Eq. (10).

$$\Delta G_t^\circ(1) = \Delta G_t^\circ(s) - \Delta G_t^\circ(w) = 2.303\,RT[pK_s - pK_w] \quad \ldots(10)$$

The dissociation constant of picric acid in water ($pK = 0.42$) was taken from literature[16]. In ME-water and DME-water systems, $\Delta G_t^\circ(1)$ decreases with increase in mol% of ME or DME; the effect being greater in DME + H_2O (Table 4).

Solvent effect is also better understood in terms of $\Delta G_t^\circ(i)$ values (Eq. 11) of all the three species involved in the dissociation equilibrium[17,18].

$$\Delta G_t^\circ(1) = \Delta G_t^\circ(H^+) + \Delta G_t^\circ(A^-) - \Delta G_t^\circ(HA) \quad \ldots(11)$$

where $\Delta G_t^\circ(1)$ is the Gibbs energy change accompanying the transfer of one mole of species (i) from the standard state in water to the standard state in the solvent concerned, both on the molar scale. $\Delta G_t^\circ(H^+)$ values for the solvent systems under investigation have been taken from our previous work[19]. It can be observed from Table 4 that the values of $\Delta G_t^\circ(A^-) - \Delta G_t^\circ(HA)$ in ME + H_2O and DME + H_2O continuously decrease with increase in mol% of organic cosolvent.

The dispersion interaction contribution to the combined term is expected to be cancelled to a large extent, The solvents, however, differ in their dielectric constants (ε) and solvating capabilities. Again, ε value of ME-water being greater than that of DME-water containing similar mol% non-aqueous component, electrostatic interactions should impart less positive contribution to $\Delta G_t^\circ(A^-)$ in ME-water than that in DME-water. Almost similar behaviour is reflected in relative positions of $\Delta G_t^\circ(A^-) - \Delta G_t^\circ(HA)$ values upto 60 wt% of mixed solvents. The departure from the behaviour of higher mol% of organic cosolvent may be attributed to stronger anion desolvating capability of DME compared to that of ME.

Acknowledgement

One of the authors (SKG) thanks the authorities of the University of North Bengal for the award of a research fellowship.

References

1 Garst J F, in *Solute-solvent interactions*, edited by J F Coetzee & C D Ritchie (Marcel Dekker, New York) 1969.
2 Kreshkov A P, *Osnovy anal Khim*, (*Fundamentals of analytical chemistry*, Izd. Khimiya, Moscow) Vol. 5, 1970.
3 Schwartz A G & Barkar J B, *Talanta*, 22 (1975) 773.

4 (a) Franchini G C, Ori E, Preti C, Tassi L & Tosi G, *Can J Chem*, 65 (1987) 722.
(b)Franchini G C, Marchetti A, Tassi L & Tosi G, *J chem Soc Faraday Trans I*, 84 (1988) 4427.
5 Sadek H, Tadros Th F & El-Harakany A A, *Electrochim Acta*, 16 (1971) 339.
6 Renard E & Justice J, *J sol Chem*, 3 (1974) 633.
7 Das S & Hazra D K, *Indian J Chem*, 27A (1988) 1073.
8 Fuoss R M, *J phys Chem*, 82 (1978) 2427.
9 Dasgupta D, Das S & Hazra D K, *J chem Soc Faraday Trans I*, 84 (1988) 1057.
10 Guha P K & Kundu K K, *Can J Chem*, 63 (1985) 798.
11 Roy R N, Swensson E E, Lacross G & Kruegek O W, *Advances in chemistry series*, edited by W F Furter (American Chemical Society, Washington DC) 1976.
12 Simon W & Heilbronner E, *Helv chim Acta*, 61 (1955) 508.
13 Iwachido T, Oosawa S & Toei K, *Bull chem Soc Japan*, 58 (1985) 2415 and references therein.
14 D'Aprano A & Fuoss R M, *J phys Chem*, 73 (1969) 400.
15 Spiro M, in *Physical chemistry of organic solvent systems*, edited by A K Covington & T Dickinson (Plenum Press, New York) 1973, p. 638.
16 Albert A & Serjeant E P, *The determination of ionization constants*, (Chapman & Hall, London) 1984, p. 145.
17 De A L & Atta A K, *Can J Chem*, 63 (1985) 3129.
18 Bates R G, in *Hydrogen-bonded solvent systems*, edited by A K Covington & P Jones (Taylor & Francis, London) 1968, p. 49.
19 Ghosh S K, Hazra D K & Lahiri S C, *Thermochim Acta*, 147 (1989) 41.

Indian Journal of Chemistry
Vol. 29A, July 1990, pp. 661-665

Synthesis and NMR spectral studies of polynuclear complexes of rhodium(I) with bridging benzimidazole derivatives

R Halesha, N M N Gowda* & G K N Reddy
Department of Chemistry, Central College, Bangalore University, Bangalore 560 001

Received 3 April 1989; accepted 26 July 1989

Reaction of $[Rh(diolefin)(\mu\text{-}Cl)]_2$ (diolefin = cycloocta-1, 5-diene or norbornadiene) with 2-substituted benzimidazoles (R-bztH; R = H, Me, Et, *n*-Pr or *n*-Bu) in the presence of triethylamine yields trinuclear complexes of the type $[Rh(diolefin)(\mu\text{-}R\text{-}bzt)]_3$. The latter compounds undergo displacement of diolefin with CO to give tetranuclear complexes of the formula $[Rh(CO)_2(\mu\text{-}R\text{-}bzt)]_4$. NMR spectral studies have been useful in assigning the structures of the complexes.

There has been a growing interest in the study of polynuclear complexes of rhodium in view of their possible use as multicentered catalysts[1-7]. Polynuclear complexes, in general are also of significance, since such systems could function as models for intramolecular electron transfer reactions and could also behave as one dimensional conductors[8,9].

Noriaki *et al.*[10] have patented the synthesis of trinuclear complexes of rhodium of the type $[RhL_2(\mu\text{-}N\text{-}N)]_3$($L_2$ = cytcloocta-1, 5-diene (cod); N-N = imídazolate or benzimidazolate; L = C_2H_4; N-N = imidazolate) which are prepared by reacting $[RhL_2(\mu\text{-}Cl)]_2$ in tetrahydrofuran with an appropriate nitrogen heterocycle in the presence of BuLi at $-60°C$. Structural assignments for these complexes have not been revealed. Nevertheless the imidazolate complex containing cod has been found to be a hydroformylation catalyst for the conversion of olefins to aldehydes[11]. Synthesis of some tri and tetra-nuclear complexes of rhodium containing imidazolate and its derivatives have also been described by Uson and co-workers[12]. Earlier we have reported[13,14] a number of binuclear complexes of rhodium containing bridging nitrogen heterocycles. As an extension of our earlier work, synthesis and NMR spectral investigations of polynuclear complexes of rhodium stabilised by substituted benzimidazole derivatives are reported in this paper.

Materials and Methods

The complexes such as $[Rh(cod)(\mu\text{-}X)]_2$, $[Rh(nbd)(\mu\text{-}Cl)]_2$ and $[Rh(CO)_2(\mu\text{-}X)]_2$ were prepared by published methods[15-17]. Infrared (in nujol and CH_2Cl_2) and ^1H and ^{13}C NMR spectra (in $CDCl_3$) were recorded on a specord 75 IR spectrophotometer and Bruker WH-270 spectrometer, respectively. Solid state ^{13}C NMR spectrum was recorded on a Bruker MSL-300 spectrometer. Conductivity measurements were carried out using a Toshniwal conductivity bridge type CL 01.02. Molecular weight measurements were made using KNAUER vapour pressure osmometer.

Tris[cycloocta-1, 5-diene (cod) or norbornadiene (nbd)] tris-[μ-R-benzimidazolato (R-bzt)] trirhodium (1) *(for cod, R = H, Me, Et; n-Pr or n-Bu; for nbd, R = Me or n-Pr)*

The nitrogen heterocycle, R-bztH(1.0 mmole) followed by triethylamine (1.0 ml) was added to a hot solution of $[Rh(diolefin)(\mu\text{-}X)]_2$ (0.5 mmole) in acetone (30 ml). The resultant solution was refluxed for 3 hr, when shining yellow crystals of the desired product separated out. The crystals were filtered off, washed with water, acetone and dried *in vacuo*.

Octacarbonyl tetrakis(μ-R-benzimidazolato)tetrarhodium(1) $[Rh(CO)_2(\mu\text{-}R\text{-}bzt)]_4$ *(R = H, Me, Et, n-Pr or n-Bu): Method*-1

Carbon monoxide was bubbled through a suspension of $[Rh(cod)(\mu\text{-}R\text{-}bzt)]_3$ in benzene (30 ml) for 4-5 hr. The resulting yellow solution was concentrated under reduced pressure to about 0.5 ml and ethanol was added when pale yellow microcrystals of the desired products separated out. The crystals were washed with ethanol and dried *in vacuo*.

Method-2

To an alcoholic solution (25 ml) of $[Rh(CO)_2(\mu\text{-}X)]_2$ (0.4 mmole), R-bztH (0.8 mmole) was added and the mixture was stirred for 1.5 hr in the presence of triethylamine (1.0 ml) to get pale yellow crystals of the desired product. The crystals were filtered off, washed with water, ethanol and dried *in vacuo*.

Table 1—Physical properties and elemental analyses of polynuclear complexes

[All the complexes are yellow crystalline solids]

	Complex	m.p. (°C)	Mol. weight[a]	Found (%) (calc.)		
				C	H	N
I	$[Rh(cod)(\mu\text{-bzt})]_3$	200	—	54.19	5.91	8.26
				(54.88)	(5.22)	(8.53)
II	$[Rh(cod)(\mu\text{-2-Me-bzt})]_3$	250	897	56.13	5.76	7.86
			(1026)	(56.14)	(5.59)	(8.18)
III	$[Rh(cod)(\mu\text{-2-Et-bzt})]_3$	164	—	56.20	5.62	7.54
				(57.17)	(5.92)	(7.84)
IV	$[Rh(cod)(\mu\text{-2-n-Pr-bzt})]_3$	200	1076	58.45	6.10	7.54
			(1110)	(58.37)	(6.26)	(7.56)
V	$[Rh(cod)(\mu\text{-2-n-Bu-bzt})]_3$	164	—	58.80	6.37	7.15
				(59.40)	(6.54)	(7.29)
VI	$[Rh(nbd)(\mu\text{-2-Me-bzt})]_3$	172	—	54.96	5.04	8.58
				(55.23)	(4.63)	(8.58)
VII	$[Rh(nbd)(\mu\text{-2-n-Pr-bzt})]_3$	186	—	57.45	5.50	7.76
				(57.63)	(5.40)	(7.91)
VIII	$[Rh(CO)_2(\mu\text{-bzt})]_4$	160	—	38.00	2.37	9.15
				(39.15)	(1.83)	(10.14)
IX	$[Rh(CO)_2(\mu\text{-2-Me-bzt})]_4$	156	1346	41.39	2.28	9.40
			(1160)	(41.40)	(2.43)	(9.67)
X	$[Rh(CO)_2(\mu\text{-2-n-Bu-bzt})]_4$	164	—	47.65	4.07	8.13
				(46.96)	(3.91)	(8.43)

[a] Calculated value in parentheses

Results and Discussion

The halo-bridged binuclear complexes of the type $[Rh(cod)(\mu\text{-X})]_2$ (X = Cl or Br) react with benzimidazole or its 2-substituted derivatives (I: R = H, Me, Et, *n*-Pr or *n*-Bu) to give pale yellow products the elemental analyses of which correspond to the composition Rh(cod)X(R-bztH). Obviously the benzimidazole derivative cleaves the halo-bridges of the dimer to give simple mononuclear derivatives (these systems are being investigated). On the contrary, if the *p*H of the above reaction system is raised by using triethylamine (Et_3N) yellow crystalline products are obtained, the analytical data and other physical properties of which suggest that these should be formulated as $[Rh(diolefin)(\mu\text{-R-bzt})]_n$) for cod, R = H, Me, Et, *n*-Pr or *n*-Bu; for nbd, R = Me or *n*-Pr). Some physical properties and analytical data of the isolated compounds are listed in Table 1.

The complexes are soluble in common organic solvents (excepting the Et-bzt containing complex) and are non-electrolytes in nitrobenzene. The IR spectra of these complexes either in nujol or in dichloromethane do not exhibit any peak assignable to νNH implying that the R-bztH ligand undergoes deprotonation at the pyrrole nitrogen during the reaction in the presence of Et_3N. This is further confirmed

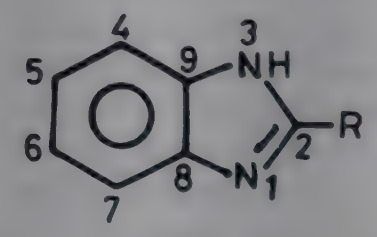

I

by their ^1H NMR spectra which do not exhibit the presence of NH resonance signal around δ11.0. The resonanace signals due to the coordinated diolefin and R-bzt groups are easily discernible. Each of these $[Rh(cod)(\mu\text{-R-bzt})]_n$ complexes (except when R = H) shows six sets of resonance signals (Fig. 1), three of these sets (which are complex) in the range of δ1.2 to 3.0 correspond to the diolefin ligands and the other three (labelled as a, b and c)† in the range δ6.8 to 8.4 due to the bzt groups (Table 2). These results suggest that not only there are three diolefin molecules and three R-bzt groups per molecule of the complex but also the groups are in three different chemical environments (probably oriented in different directions caused by steric effects arising from the R group). On the basis of these results the complexes may be proposed

† Assignments a, b etc are tentative

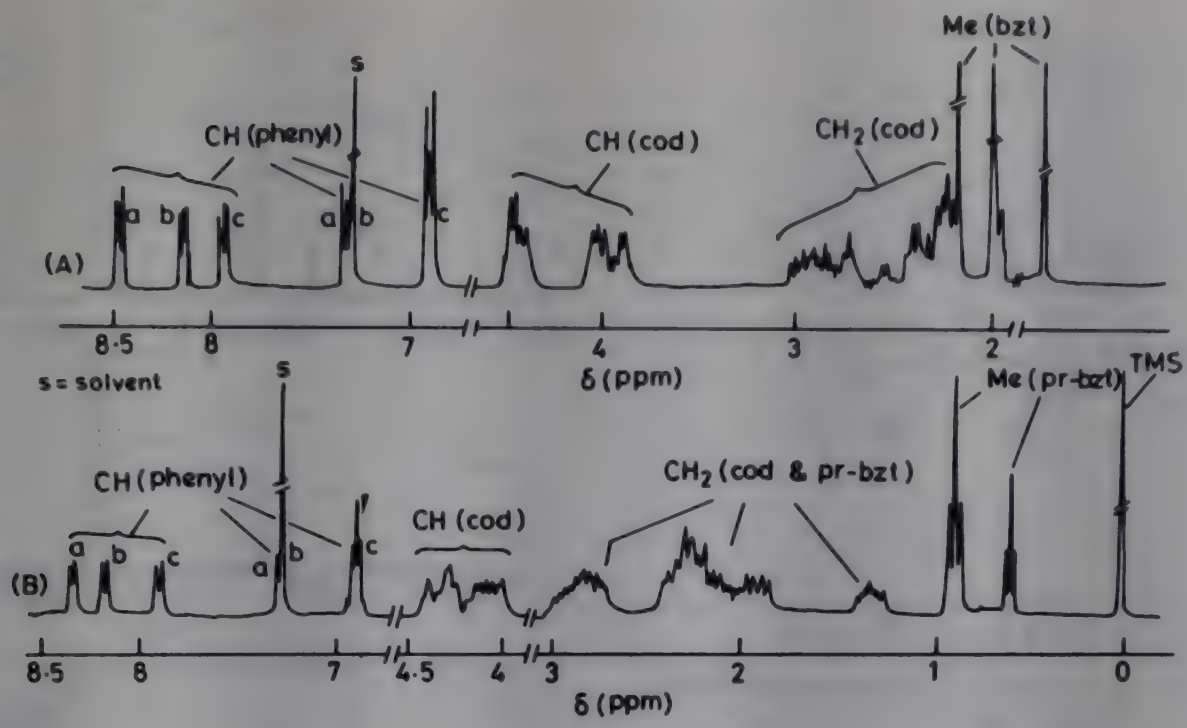

Fig. 1—^{1}H NMR spectra (in $CDCl_3$) of (a) [Rh(cod) (μ-Me-bzt)]$_3$ and (b) [Rh(cod)(μ-Pr-bzt)]$_3$

Table 2—IR (cm^{-1}) and ^{1}H NMR (δ in ppm) spectral data

Complex	νC=C νC=N	νCH(def)	Diolefin/νCO	cod		Nitrogen heterocycle
				CH_2	CH	
I	1600	735, 715	1285, 1232, 1160 1067	1.89m 2.53m	4.28s	6.78s(CH), 6.97m and 7.8m (phenyl)
II	1600	735, 730	1270, 1200, 1140 1060, 620	1.25-2.5m 2.73-3.0m	3.8-4.0m 4.36-4.46m	0.95s, 1.96s, 2.15s (Me) 6.8m, 6.9m, 7.3m, 7.9m, 8.12m and 8.42m (phenyl)
III	1595	740, 730	1270, 1150, 1060 960, 620			
IV	1510	735, 720	1270, 1140, 980 940, 620	1.82-2.53m 2.75-2.91m	3.98-4.13m 4.25-4.36m	0.58, 0.71m and 0.88m (propyl) 6.9m, 7.26m, 7.88m, 8.18m and 8.35m (phenyl)
V	1600	750, 720				
VIII	1605	735, 705	2010, 2090			6.53s(CH) 7.23m and 7.72m (phenyl)
IX	1605	732, 710	2010, 2070			0.42s, 1.56s, 1.91s (Me) 7.0m, 7.18m, 7.31m, 7.48m, 7.7m and 7.88m (phenyl)
X	1605	735, 710	2005, 2080			
[Rh(CO)$_2$-(μ-2-Et-bzt)]$_4$	1596	715	2005, 2070			

to have a trinuclear structure(II). The ^{13}C NMR spectrum of [Rh(cod) (μ-Me-bzt)]$_3$ complex (Fig. 2)‡ in $CDCl_3$ also exhibits six sets of resonance signals, three of these due to the diolefin ligands and the other three due to Me-bzt groups (Table 3) supporting the trimeric formula for the complex. The solid state ^{13}C NMR spectrum of this compound (Fig. 3) also exhibits spectral features which are more or less comparable to those in the solution spectrum implying that the trimeric form exists both in the solid state and in solution. Molecular weight measurements in chloroform further support the trimeric nature of the complexes (Table 1).

Surprisingly both the ^{1}H (Fig. 1B) and ^{13}C NMR spectra of the benzimidazolate complex exhibit only two sets of resonance signals, one set assignable to the diolefin ligands and the other to the bzt groups (Table 2). Presumably the bzt complex also has a trimeric structure and in this case it is likely that all the three diolefin ligands are in identical chemical environments, so also all the three bzt groups owing to the reduced steric hindrance by hydrogen on C-2 (I, R = H).

‡ For comparison the ^{13}C NMR spectra of [Rh(cod) (μ-bzt)]$_3$, [Rh(cod) (μ-Cl)]$_2$ and Me-bztH along with assignments are also included

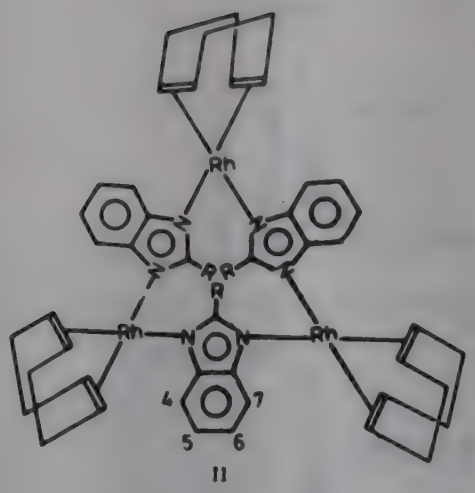

II

Table 3—^{13}C NMR spectra (δ in ppm)

Compound	cod		Nitrogen heterocycle*
	CH_2	CH	
2-Me-bztH	—	—	14.82(R) 114.59(5,6) 122.23(4, 7) 138.99(8, 9), 151.63(2)
$[Rh(cod)(\mu\text{-}Cl)]_2$	30.97	78.62	-
$[Rh(cod)(\mu\text{-bzt})]_3$	31.8	80.48	116.69(5,6), 120.10(4, 7) 149.20(2), 143.25(8, 9)
$[Rh(cod)(\mu\text{-2-Me-bzt})]_3$	28.22	75.76	19.49, 18.52 (Me) 115.64, 117.41 and 118.01 (5,6)
	31.14	79.83	118.39, 119.30 and 119.50 (4,7)
	34.50	84.04	143.20, 143.72 and 144.52 (8,9) 148.67, 158.13 and 161.02(2)

* Numbers in parentheses correspond to the labellings

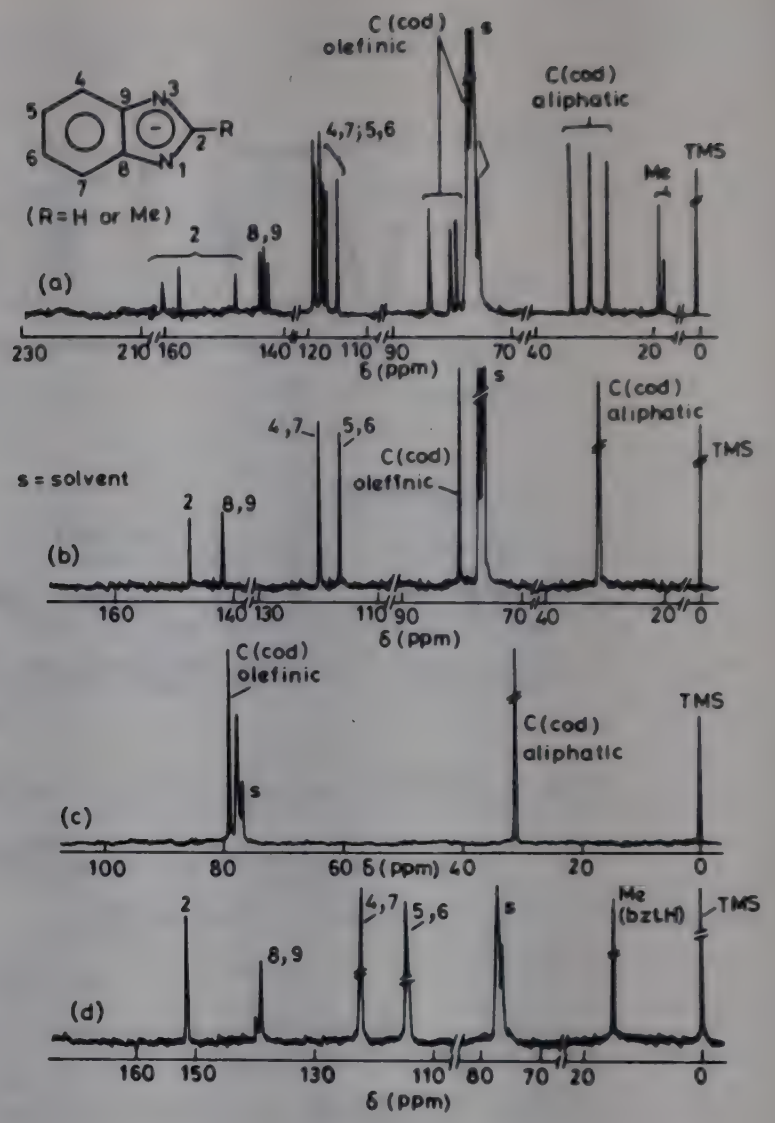

Fig. 2—^{13}C NMR spectra(in $CDCl_3$) of (a) $[Rh(cod)(\mu\text{-Me-bzt})]_3$, (b) $[Rh(cod)(\mu\text{-bzt})]_3$, (c) $[Rh(cod)(\mu\text{-Cl})]_2$, (d) Me-bztH

That is the bzt groups are oriented in such a way that all of them experience an equivalent chemical environment in the complex. Molecular model studies on the complexes containing benzimidazolate and methylbenzimidazolate groups support the above deductions.

It has been found earlier[14] that the nitrogen heterocycle-bridged dinuclear complexes of the type $[\{Rh(diolefin)(X)\}_2(\mu\text{-N-N})]$ react with CO to give carbonyl complexes of the type $[\{Rh(CO)_2X\}_2(\mu\text{-N-N})]$ by the displacement of each of the diolefin group by two CO molecules. Carbonyl complexes of the formula $[Rh(CO)_2(\mu\text{-R-bzt})]_n$ have also been obtained presently by bubbling CO through benzene solution of trimers. These carbonyl complexes could also be obtained by treating halo-bridged carbonyl dimers of the type $[Rh(CO)_2(\mu\text{-X})]_2$ (X = Cl or Br) with benzimidazole derivatives in ethanol in the presence of Et_3N.

The carbonyl complexes are freely soluble in common organic solvents and behave as non-electrolytes in nitrobenzene. Satisfactory elemental analyses have been obtained for all the complexes and the analytical data along with some physical properties are given in Table 1. The IR spectra of the complexes exhibit, in addition to bands due to the coordinated bzt groups, two very intense bands around 2000 cm^{-1} assignable to *cis* carbonyl groups (Table 2).

The ^{1}H NMR spectra of the carbonyl complexes do not exhibit peaks due to the diolefin ligands, but exhibit four sets of resonance signals due to the R-bzt groups suggesting the presence of at least four such heterocyclic groups per molecule of the complex situated in different chemical environments (Table 2). In the case of the benzimidazolate complex only one set of resonance signals have been observed (Table 2) suggesting that the bzt groups are oriented in such a way that they experience an equivalent chemical environment as in the case of the parent diolefin complex. On the basis of these results, a tetrameric structure

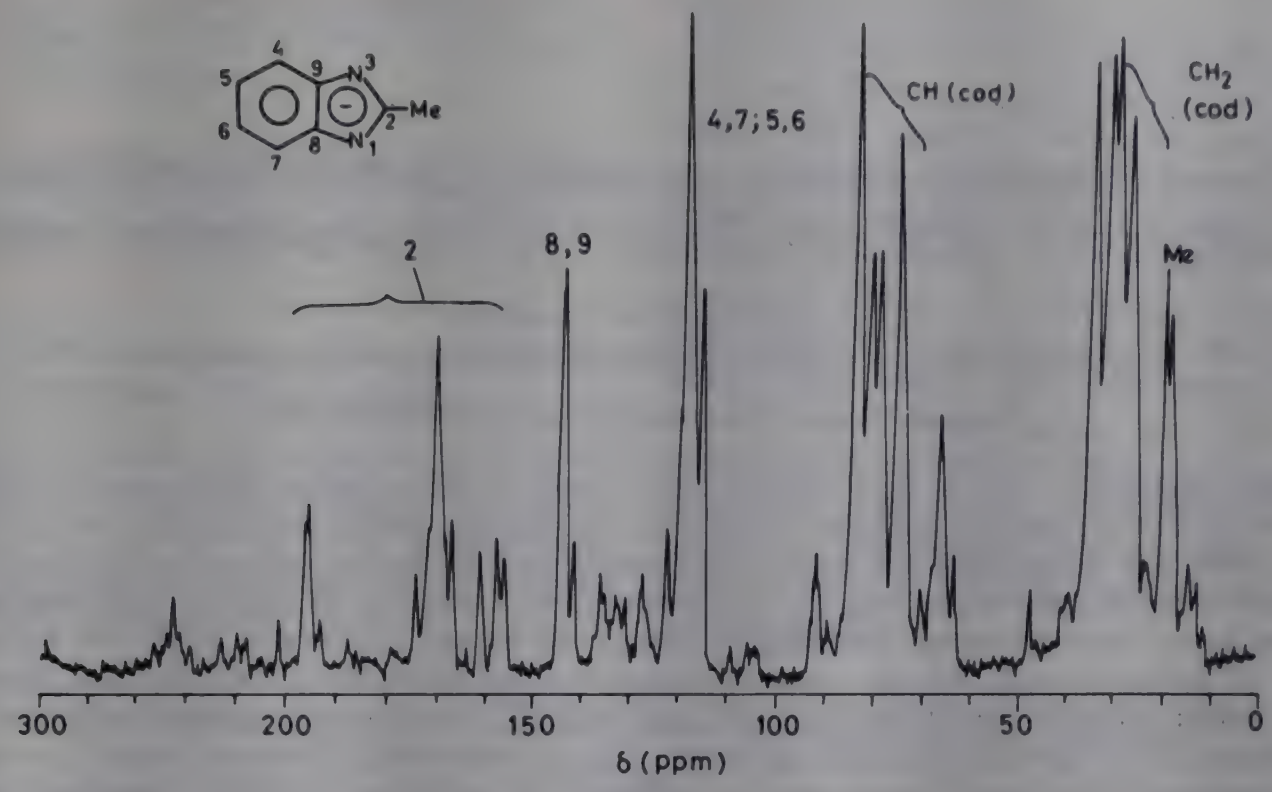

Fig. 3—^{13}C NMR spectrum (solid state) of $[Rh(cod)(\mu\text{-Me-bzt})]_3$

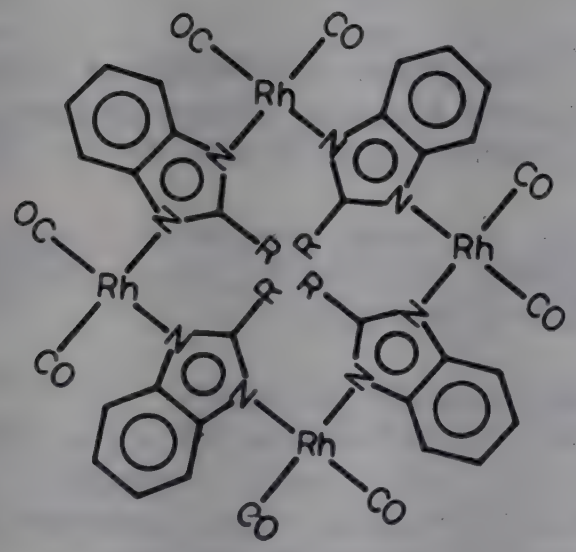

III

(III) may be proposed for the complexes. Molecular weight measurements in chloroform also support the tetrameric nature of the complexes (Table 1). The above results indicate that the trinuclear diolefin complexes on carbonyl substitution get converted into tetranuclear complexes. Such a conversion is perhaps due to changing the terminal ligand from cod to carbonyls. This modifies the electron density on the metal atom in such a way that a change in the molecular geometry is necessary for stabilising the system[18]. Formation of such tetranuclear structures has been confirmed by Uson and co-workers[12] and Rasmussen and co-workers[18] by X-ray crystal structure studies.

Acknowledgement

The authors are thankful to Prof. C.L. Khetrapal, SIF, Indian Institute of Science, Bangalore, India for NMR spectral measurements, and to UGC, New Delhi, for financial assistance.

References

1 James B R, *Adv Organometal Chem*, 17 (1979) 319.
2 Masters C, *Adv Organometal Chem*, 17 (1979) 61.
3 Mestroni G, Zassinovich G & Camus A, *J Organomet Chem*, 140 (1977) 63.
4 Farmetti E, Vinzi F & Mestroni G, *J molec Catal*, 24 (1984) 147.
5 Uson R, Oro L A & Esteruelas M A, *Trans Metal Chem*, 7 (1982) 242.
6 Clavar C, Marco E, Oro L A, Royo M &Pastor E, *Trans Metal Chem*, 7 (1982) 246
7 Mahajan D, Cruetz C & Sutin N, *Inorg Chem*, 24 (1985) 2063.
8 Pruchnik F & Wazda K, *J organomet Chem*, 164 (1979) 71.
9 Morton S & Nixon J F, *J Organomet Chem*, 282 (1985) 123.
10 Noriaki K, Seaki K & Toda Y, *Japan Kokai*, 76, 141, 866; *Chem Abstr*, 86 (1977) 171604e.
11 Tanaka M, Seaki K & Kihara N, *Japan Kokai*, 77, 83, 311; *Chem Abstr*, 87 (1977) 200792t.
12 Tiripicchio A, Camellini M T, Uson R, Oro L A, Ciriano M A & Pinillos M T, *J Organomet Chem*, 224 (1982) 207.
13 Reddy G K N & Ramesh B R, *J Organomet Chem*, 87 (1975) 347.
14 Halesha R, Reddy G K N, Sudhakar Rao S P & Manohar H, *J organomet Chem*, 252 (1983) 231.
15 Chatt J & Vananzi L M, *J chem Soc*, (1957) 4735.
16 Abel E W, Bennet M A & Wilkinson G, *J chem Soc*, (1959) 3178.
17 Deeming A J & Sharratt P J, *J Organomet Chem*, 99 (1975) 347.
18 Kaiser S W, Saillant R B, Butler W M & Rasmussen P G, *Inorg Chem*, 15 (1976) 2688.

Indian Journal of Chemistry
Vol. 29A, July 1990, pp. 666-669

Synthesis and characterisation of copper(II), nickel(II), cobalt(II) and zinc(II) complexes of 3-(1-hydroxy-2-naphthyl)-5-(4-X-phenyl)pyrazolines

C Natarajan* & P Tharmaraj

Department of Inorganic Chemistry, Madurai Kamaraj University, Madurai 625 021

Received 13 June 1989; revised and accepted 3 October 1989

Metal complexes of the type ML_2nB, [M = Cu(II), Ni(II), Co(II), Zn(II); L = 3-(1-hydroxy-2-naphthyl)-5-(4-X-phenyl) pyrazoline (HONXPP); X = H, Me, MeO; B = H_2O, Py; n = 0, 2] have been synthesized through different routes and characterized on the basis of analysis, infrared, ligand field and ^1H NMR spectra and magnetic susceptibility measurements. IR and ^1H NMR data indicate that the ligands act as bidentate, coordinating through the oxygen of phenolic group and tertiary nitrogen of pyrazoline ring. All the copper(II) complexes are obtained in the anhydrous form with square-planar configuration whereas cobalt(II) and nickel(II) complexes are isolated as diaquates and dipyridinates with high-spin octahedral geometry. The corresponding anhydrous nickel(II) complexes are diamagnetic with square-planar structure, whereas the anhydrous cobalt(II) complexes are polymeric with cobalt in an octahedral environment. Enhanced π-bonding between nickel and C = N in the square complexes increases the LFSE.

Chalcones and flavonones react with hydrazine hydrate to form 3,5-diphenyl substituted pyrazolines[1,2] as the more facile products rather than the usual hydrazones. Similarly, 1-hydroxy-2-naphthyl(4-X-styryl)ketones (HONXSK) and 7,8-benzoflavonone[3], on reaction with hydrazine hydrate, yield 3-(1-hydroxy-2-naphthyl)-5-(4-X-phenyl)pyrazolines (HONXPP). Biocidal activity of pyrazolines is well documented in the literature[4-6]. Some naphthylpyrazolines[3,7] have been reported as antipyretic and analgesic agents. Therefore, it was thought of interest to investigate the coordinating ability of HONXPP and in this paper are described the preparation and characterization of its metal complexes and their pyridine adducts.

Materials and Methods

All the metal salts (BDH, AR) and hydrazine hydrate ($N_2H_4.H_2O$, 80%) (BDH, LR) were used as such for synthesis. Elemental analyses were performed at VHNSN College, Virudhunagar, India. The ^1H NMR spectra were obtained on an R-32 Perkin-Elmer 90 MHz spectrometer in $CDCl_3$. Metal contents and other physical measurements were determined as reported elsewhere[8].

Synthesis of ligands: 3-(1-*hydroxy*-2-*naphthyl*)-5-(4-*X*-*phenyl*)*pyrazolines* (*HONXPP*) (*X* = *H*, *Me*, *MeO*)

They were obtained from 1-hydroxy-2-naphthyl(4-X-styryl)ketone (HONXSK) or 7,8-benzoflavonone and hydrazine hydrate adopting the literature method[3] (m.p. 133-134°, lit.[3] m.p. 131°).

Synthesis of metal complexes: *Cu*(*ONXPP*)$_2$, *Zn*(*ONHPP*)$_2$, *Co*(*ONXPP*)$_2$.2H_2O, *Ni*(*ONXPP*)$_2$.2H_2O (*X* = *H*, *Me*, *MeO*):

(*i*) *From pyrazolines* (*HONXPP*)

To an ethanolic solution (80 ml) of HONXPP (5 mmol) was added metal(II) acetate $M(CH_3COO)_2nH_2O$ (2.5 mmol) in water (20 ml). The resulting solid was collected in a filter, washed with aqueous EtOH followed by Et_2O and dried *in vacuo*.

(*ii*) *From ketone HONXSK or* 7,8-*benzoflavonone* (*in situ*)

HONXSK or 7,8-benzoflavonone (10 mmol) in EtOH (40 ml) was heated to reflux with slight excess of hydrazine hydrate (3 ml). To this was added an aqueous solution of metal(II) acetate (5 mmol) in water (30 ml). On cooling, the complex separated was suction-filtered, washed successively with aqueous EtOH and Et_2O and dried *in vacuo*.

(*iii*) *From preformed keto complexes*: *M*(*ONXSK*)$_2$.*n*H_2O (*X* = *H*)

To a suspension of $Cu(ONHSK)_2$ or $Ni(ONHSK)_2$. $2H_2O$ in EtOH was added slight excess of hydrazine hydrate (5 ml) and stirred

well for an hour. The complex obtained on standing was collected in a filter washed with aqueous ethanol and dried *in vacuo.*

Synthesis of anhydrous complexes and pyridine adducts: $Ni(ONXPP)_2$, $Co(ONXPP)_2$, $Ni(ONXPP)_2.2Py$ and $Co(ONXPP)_2.2Py$ (X = H, Me, MeO)

The anhydrous complexes were obtained by heating the dihydrates at 140° in an air oven.

The pyridine adducts were obtained by dissolving the anhydrous complexes in excess of pyridine and allowing to evaporate at room temperature. The resulting solids were washed with petroleum ether (b.p. 60-80°) and dried *in vacuo.*

Results and Discussion

The elemental analyses, colour, magnetic moment and electronic spectral data are given in Table 1. The analytical data and spectral data of the complexes synthesised through different routes are consistent with the assigned molecular formulae (structure I). All the complexes are insoluble in water. The cobalt(II) complexes are fairly well soluble in most of the organic solvents whereas the others have very poor solubilities. Conductance measurements on the cobalt(II) complexes in chloroform show them to be non-electrolytes. The weight loss experiments indicate the loss of coordinated water in aquo complexes around 140°C and that of pyridine around 80° in pyridine adducts.

Table 1 – Analytical, magnetic moment and electronic spectral data of metal(II) complexes

Complex (Colour)	Found (Calc.) %				$\mu_{eff.}$ (B.M.)	ν_{max} (cm^{-1})
	M	C	H	N		
$Cu(ONHPP)_2$	9.32	70.81	3.92	8.14	2.00	13157
(Gray green)	(9.96)	(71.51)	(4.74)	(8.78)		17543
$Cu(ONMePP)_2$	9.24	72.53	5.22	8.71	1.93	15151
(Gray green)	(9.54)	(72.11)	(5.14)	(8.41)		
$Cu(ONMeOPP)_2$	9.82	69.10	4.73	7.62	2.03	14285
(Gray green)	(9.10)	(68.80)	(4.91)	(8.02)		18181
$Ni(ONHPP)_2.2H_2O$	9.30	68.91	5.43	9.25	2.40	15290
(Yellow)	(8.77)	(68.18)	(5.12)	(8.37)		19920
$Ni(ONMePP)_2.2H_2O$	9.27	70.08	5.52	8.83	2.95	15105
(Yellow)	(8.42)	(68.88)	(5.49)	(8.03)		20080
$Ni(ONMeOPP)_2 \cdot 2H_2O$	8.72	66.82	4.74	7.91	2.56	16094
(Yellow)	(8.05)	(65.86)	(5.25)	(7.68)		22222
$Ni(ONHPP)_2$	9.54	73.24	5.22	9.14	dia	15873
(Brown)	(9.27)	(72.06)	(4.77)	(8.85)		22222
$Ni(ONMeOPP)_2$	8.80	70.30	4.94	8.53	dia	15551
(Brown)	(8.47)	(69.28)	(4.94)	(8.08)		20000
$Ni(ONHPP)_2.2Py$	7.83	72.84	5.51	11.15	2.79	15873
(Brown)	(7.42)	(72.83)	(5.09)	(10.62)		20408
$Ni(ONMePP)_2.2Py$	8.07	72.92	5.12	10.51	2.63	14814
(Brown)	(7.16)	(73.27)	(5.41)	(10.25)		20000

(contd.)

Table 1 – Analytical, magnetic moment and electronic spectral data of metal(II) complexes—(contd.)

Complex (Colour)	Found (Calc.) %				$\mu_{eff.}$ (B.M.)	ν_{max} (cm^{-1})
	M	C	H	N		
$Ni(ONMeOPP)_2.2Py$	7.32	71.24	5.81	10.13	2.82	15923
(Brown)	(6.89)	(70.52)	(5,21)	(9.87)		20242
$Co(ONHPP)_2.2H_2O$	9.51	69.02	4.82	8.53	5.00	14749
(Brown)	(8.80)	(68.16)	(5.12)	(8.37)		20242
$Co(ONMeOPP)_2.2H_2O$	8.80	66.21	4.37	7.54	4.30	13586
(Brown)	(8.08)	(65.84)	(5.25)	(7.68)		20283
$Co(ONHPP)_2$	9.84	73.06	5.42	9.21	4.21	16393
(Brown)	(9.30)	(72.03)	(4.77)	(8.84)		19600
$Co(ONMeOPP)_2$	8.23	70.33	4.13	8.72	4.30	17093
(Brown)	(8.50)	(69.26)	(4.94)	(8.08)		19700
$Co(ONHPP)_2.2Py$	7.04	72.91	5.83	10.12	4.65	16722
(Brown)	(7.44)	(72.81)	(5.09)	(10.61)		20408
$Co(ONMeOPP)_2.2Py$	7.25	70.54	6.10	10.23	4.35	16783
(Brown)	(6.92)	(70.50)	(5.21)	(9.87)		19650
$Zn(ONHPP)_2$	10.44	71.16	4.91	8.46	—	—
(Yellow)	(10.21)	(71.31)	(4.72)	(8.75)		

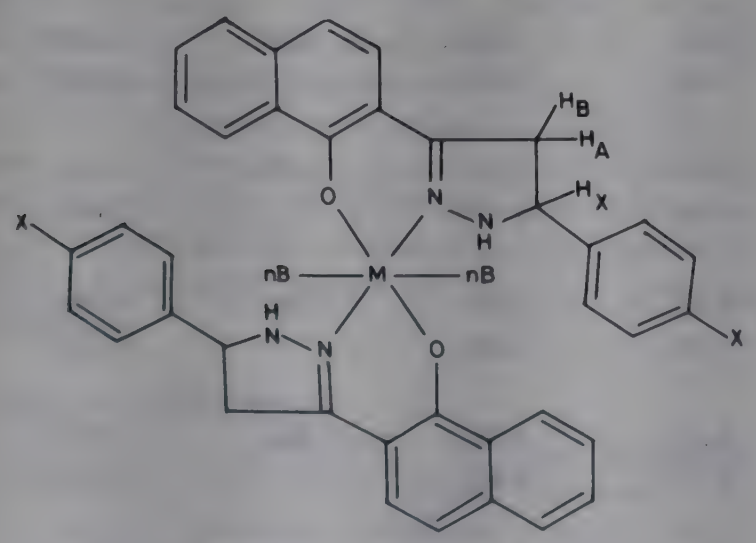

(I)

Magnetic properties and ligand field spectra

The magnetic moments of all the copper(II) complexes fall in the range 1.93-2.03 BM which is characteristic of square-planarity. Their electronic absorption spectra in $CHCl_3$ (Table 1) show bands in the regions 13157-15151 and 17543-18181 cm^{-1} assignable respectively to the transitions $^2B_{1g} \rightarrow {}^2B_{2g}$ and $^2B_{1g} \rightarrow {}^2E_g$ of square-planar structure[9]. The dihydrates and dipyridinates of nickel(II) complexes possess magnetic moments in the range 2.40-2.95 BM which are somewhat lower than the expected value for regular octahedral complexes. The lowering may be ascribed to distortion of structure due to lattice forces. The ligand field bands in the regions 15105-15923 and 19920-20408 cm^{-1} arising respectively from $^3A_{2g}(F) \rightarrow {}^3T_{1g}(F)$ (ν_2) and $^3A_{2g}(F) \rightarrow {}^3T_{1g}(P)$ (ν_3) transitions are characteristic of octahedral geometry. Surprisingly the corresponding anhydrous compounds are diamagnetic, which is a characteristic of a square-planar structure. Their electronic spectra manifest bands in the regions 15551-15873 and 20000-22222 cm^{-1} assignable respectively to $^1A_{1g} \rightarrow {}^1B_{1g}$ (ν_2) and $^1A_{1g} \rightarrow {}^1A_{2g}$ (ν_3) transitions which are consistent with square-planar geometry[10]. In the anhydrous nickel(II) bis chelates, enhanced d_π-p_π back-bonding involving the π^* orbital of C=N bond occurs. This leads to an increase in Δ due to lowering[11]

of the energy of d_π orbitals (d_{yz}, d_{xz}). Thus, the ligand field produced is strong enough to stabilize the MN_2O_2 coordination structure and effect spin-pairing. The magnetic moments for the diaquo and dipyridinato cobalt(II) complexes lie in the range 4.30-5.00 BM; the lower values may presumably be due to the distortion from the regular octahedral geometry. Their electronic spectra show two bands in the regions 13586-16783 and 19650-20408 cm^{-1} which are assigned to the transitions $^4T_{1g}(F) \rightarrow {}^4A_{2g}(F)$ (ν_2) and $^4T_{1g}(F) \rightarrow {}^4T_{1g}(P)$ (ν_3) respectively, which are characteristic of octahedral geometry. The corresponding anhydrous complexes have still lower magnetic moments (4.21, 4.30 BM) and ligand field bands in the regions 16393-17093 and 19600-19700 cm^{-1} which are suggestive of pseudo-octahedral geometry[12]. For nickel(II) and cobalt(II) complexes the low energy band could not be recorded in our spectrophotometer. In contrast to the nickel(II) anhydrous complexes, these anhydrous complexes achieve octahedral environment probably through oligomerization. The zinc(II) complex is diamagnetic and does not have ligand field transitions. The 1:2 complex is likely to have tetrahedral structure characteristic of the metal ion.

Infrared spectra

The IR spectra of ligands and complexes obtained by different routes are identical. The free ligands exhibit strong bands in the region 3300-3310 cm^{-1} assignable to NH stretching vibrations. The hydrogen bonded OH appears as a broad band in the range 2890-2960 cm^{-1}. The $\nu(C=N)$ appears[2] as a doublet in the region 1590-1627 cm^{-1}. The absorptions around 1234-1240 and 832-849 cm^{-1} may be assigned respectively to phenolic $\nu(C-O)$ and $\nu(N-N)$[13].

On coordination, the intensity of both the C=N bands is reduced much and the higher frequency band suffers a negative shift (1-35 cm^{-1}). In most cases the lower frequency band disappears. The negative shift in $\nu(C=N)$ and positive shift in $\nu(N-N)$ (15-55 cm^{-1}) are indicative of coordination of the tertiary nitrogen of pyrazoline to the metal. The increased $\nu(N-N)$ in the complexes may be attributed to the loss of lone pair-lone pair repulsive forces on the nitrogen atom[14]. The $\nu(NH)$ shows irregular variations in the complexes which rules out the possibility of its coordination and this is supported by the ^1H NMR data. The change in $\nu(NH)$ may occur at the expense of change in $\nu(N-N)$. The $\nu(C-O)$ registers an increase in the complexes (4-20 cm^{-1}) indicating the participation of phenolic oxygen in coordination. The replacement of water by pyridine results in a considerable decrease in $\nu(C=N)$ (2-34 cm^{-1}) which is attributed to the strong π-acceptor property of pyridine.

^1H NMR spectra

The ^1H NMR spectrum of HONXPP in $CDCl_3$ shows signals at the following δ values: 3.2 (dd, 1H, H_A), 3.65 (dd, 1H, H_B), 4.9 (t, 1H, H_X), 8.6 (br, 1H, NH), 7-8 (m, 6H, Ar−H), 12.0 (br, 1H, OH). The occurrence of OH peak at much lower field suggests the presence of hydrogen bonding with azomethine nitrogen of pyrazoline ring. The zinc complex $Zn(ONHPP)_2$ in pyridine (d_5) shows signals at 3.40 δ (dd, 1H, H_A), 3.84 δ (dd, 1H, H_B), 4.9 δ (t, 1H, H_X), 8.92 δ (s, 1H, NH), 7-8 δ (m, 6H, Ar−H). The absence of the signal at 12.0 δ in the complex indicates the deprotonation of phenolic oxygen on coordination and the almost unchanged nature of the NH signal in the complex confirms the non-involvement of secondary nitrogen in coordination.

Acknowledgement

We thank the CSIR, New Delhi for the award of SRF to one of us (PT). Our thanks are also due to USIC for providing instrumental facilities.

References

1 Kallay F, *The reaction of flavonoid compounds with hydrazines*, edited by R Bognar, V Bruckner & Cs Szantay (Hungarian Academy of Sciences, Budapest) 1973.
2 Thakare V G & Wadodkar K N, *Indian J Chem*, 25B (1986) 610.
3 Sammour E Abd, Elkasaby & Mohamed, *J Chem UAR*, **12** (1969) 1.
4 Kerdawy M M El & Agemy A A El, *J drug Res*, 7 (1975) 105.
5 Roushd I M, Schai I A El & Habib N S, *Egypt J pharm Sci*, 16 (1975) 407.
6 Brown F C, *J Am chem Soc*, 78 (1956) 6189.
7 Bayouki El, Khairy A H M, Abdul H & Mohamoud M, *Egypt J Chem*, 22 (1977) 37.
8 Natarajan C & Tharmaraj P, *Transition Met Chem*, 12 (1987) 553.
9 Figgis B N, *Introduction to ligand fields* (Wiley, New York) 1967.
10 Lever A B P, *Inorganic electronic spectroscopy*, (Elsevier, Amsterdam) 1968.
11 Basolo F & Pearson R G, *Mechanism of inorganic reactions* (John Wiley, New York) 1958.
12 Singh B, Singh R N & Aggarwal R C, *Polyhedron*, 4 (1985) 401.
13 Saha N & Datta K M, *J inorg nucl Chem*, 43 (1981) 1405.
14 Radecka P W, Jankowska E & Luks E, *Polyhedron*, 7 (1988) 439.

Indian Journal of Chemistry
Vol. 29A, July 1990, pp. 670-675

Reactions in micellar solutions: Part 9† – Kinetics of base hydrolysis of *cis*-(imidazole)(salicylato)bis(ethylenediamine)cobalt(III) and (αβS)-(sulphito)(tetraethylenepentamine)cobalt(III) in the presence of neutral, anionic and cationic surfactants in aqueous medium

Anadi C Dash* & Jayashree Prusti
Department of Chemistry, Utkal University, Bhubaneswar 751004

Received 24 May 1989, revised and accepted 20 September 1989

The base hydrolysis of *cis*-(imidazolato)(salicylato)bis(ethylene-diamine)cobalt(III) is moderately catalysed by CTAB (cationic), retarded by SDS (anionic) and influenced only a little by Triton X-100 (neutral). The rate retardation by SDS is due to the less reactive phenol species, *cis*-$[Co(en)_2(im)SalH]^+$, in which form the complex exists exclusively in the micellar pseudo-phase of SDS. The rate of base hydrolysis of (αβS)-(tetraethylenepentamine)(sulphito)cobalt(III)(stable S-bonded isomer) is retarded by Triton X 100, SDS and CTAB, the effect increasing with increase in [surfactant] in the order SDS > > Triton-X-100 > CTAB. The rate data for this substrate at varying [SDS] and [Triton X 100] are interpreted in terms of pseudo-phase equilibrium model taking into account ion-exchange in the case of SDS. The rate retardation by CTAB is due to the formation of less reactive premicellar aggregate (1:1 ion pair) of this substrate with the CTA^+ cation. The roles of electrostatic and hydrophobic effects of the micelles on the hydrolysis reactions of the micelle-bound Co(III) substrates under consideration are discussed.

Both hydrophobic and electrostatic effects of the micelles play significant role in the reactions of coordination complexes in micellar media[1-6]. Also the pre-miceller aggregates of anionic and cationic surfactants have been reported to catalyse the racemisation and ligand dissociation reactions of a limited number of iron(II) and nickel(II) complexes[7,8].

The title investigation has been undertaken in order to further elucidate the effects of Triton X100 (neutral), sodium dodecyl sulphate (SDS) (anionic) and cetyltrimethylammonium bromide (CTAB) (cationic) micelles on the kinetics and equilibria of some model octahedral cobalt(III) complexes.

Materials and Methods

Tetraethylenepentamine (BDH), ethylenediamine (E Merck), imidazole (Fluka, AG), salicylic acid (BDH, AR), cetyltrimethylammonium bromide (CTAB, 99% pure, E Merck, GR), sodium dodecyl sulphate (SDS; 99% pure GC assay, LOBA, GR) and Triton X 100 ($C_8H_{17}Ph(OC_2H_2)_{9.5}OH$) (BDH, LR) were used as received. All other chemicals used were of AR grade. Solutions were prepared in doubly distilled conductivity water.

Cis-(imidazole)(salicylato)bis(ethylenediamine) cobalt(III) diperchlorate and (αβS)(sulphito)(tetraethylenepentamine)cobalt(III) perchlorate (the stable S-bonded isomer) were prepared as described by Dash and Mohanty[9] and Harris *et al.*[10], respectively.

The surface tension measurements were made at ambient temperature (~30°C) with a Du Nuoy surface tensiometer. The critical micelle concentration (cmc) of SDS and CTAB agreed well with those reported in literature[11]. The values of cmc for SDS and CTAB in 0.050 mol dm^{-3} NaOH were 0.002 and 0.0002 mol dm^{-3} respectively in agreement with the fact that added electrolytes reduce the cmc's of these surfactants[11].

The base hydrolysis reactions were investigated spectrophotometrically as described earlier[5] using a Varian UV-visible spectrophotometer model 634S, the cell compartment of which was thermostatted to the desired temperature. The pseudo-first order rate constants were calculated from the gradients of the plots of $\log(A_t - A_\infty)$ versus t(s).

Results and Discussion

1. *Effects of micelles on base hydrolysis of cis-(imidazolato)(salicylato)bis(ethylenediamine) cobalt(III)*

The rate of base hydrolysis of this complex was

† For Part 8, see ref. 1

Table 1 – Effect of varying [CTAB] and [SDS] on the rate of base hydrolysis of *cis*-(imidazolato)(salicylato)bis(ethylenediamine)cobalt(III)

([complex]$_T$ = (2.1-2.3) × 10^{-4} mol dm^{-3}; λ = 330 nm; temp. = 38.0 ± 0.1°C)

$[NaOH]_T$ (mol dm^{-3})	$10^4 k_\psi$ (s^{-1})[a]	$[Surfactant]_T$ (mol dm^{-3})	$10^4 k_\psi$ (s^{-1})[b]		
			CTAB		SDS
0.025	5.89 ± 0.20				
0.050	6.34 ± 0.22	0.002			6.38 ± 0.14
0.100	6.98 ± 0.25	0.004	6.72 ± 0.12	(7.41 ± 0.10)	4.37 ± 0.33
0.15	8.25 ± 0.25	0.006	6.96 ± 0.12	(7.61 ± 0.10)	3.36 ± 0.08
0.20	8.82 ± 0.15	0.010	7.38 ± 0.15	(8.15 ± 0.15)	3.08 ± 0.06
		0.020	7.38 ± 0.15	(8.90 ± 0.25)	2.07 ± 0.06
		0.040	8.98 ± 0.16	(10.2 ± 0.4)	1.54 ± 0.08
		0.050	8.95 ± 0.19	(11.3 ± 0.3)	–
		0.080	–	(12.2 ± 0.3)	1.14 ± 0.05
		0.100	11.1 ± 0.3	(13.0 ± 0.5)	0.96 ± 0.03
		0.150	11.6 ± 1.2	(13.2 ± 0.3)	–

(a) In the absence of surfactant.

(b) $[NaOH]_T$ = 0.10 mol dm^{-3} for values of k_ψ under parentheses; all other values of k_ψ at $[NaOH]_T$ = 0.050 mol dm^{-3}.

accelerated by CTAB and retarded by SDS (see Table 1) while Triton X 100 had no significant effect. The (salicylato)(imidazol) complex will exist in the doubly deprotonated form in aqueous medium under the experimental conditions as pK_{NH} (for the coordinated imidazole) is 10.2 and pK_{OH} (for the unbound phenolic OH group) is 11.1 (30°C, I = 0.3 mol dm^{-3})[9]. Binding of this doubly deprotonated species to cationic CTAB micelles will further decrease its proton affinity both at N^- and O^- sites[12]. Such a binding resulted in decrease in the absorbance of the species in the range of λ = 270-320 nm with no appreciable shift of its λ_{max} (= 300 nm) and λ_{min} (= 285 nm). However, small spectral change observed even for large variation of [CTAB] (= 0.005-0.1 mol dm^{-3}) at $[OH^-]$ = 0.05 mol dm^{-3}, could not be useful for satisfactory evaluation of the micellar binding constant.

Scheme 1 is proposed to interpret the rate data in the presence of CTAB. In Scheme 1 C = cis$[Co(en)_2(im)CO_2CC_6H_4O]$, Dn = micellised surfactant, the subscripts (superscripts) W and M denote the aqueous or micellar pseudo-phase respectively and k_i^j is the rate constant (i = H_2O or OH^- for spontaneous aquation and second order base hydrolysis respectively) in the pseudo-phase j. Under the experimental condition the products are (*cis* + *trans*)$[Co(en)_2(im)OH]^+$ and $\{C_6H_4(CO_2)O\}^{2-}$; the latter is likely to be bound to the cationic micellar pseudo-phase while the former will exist predominantly in the aqueous

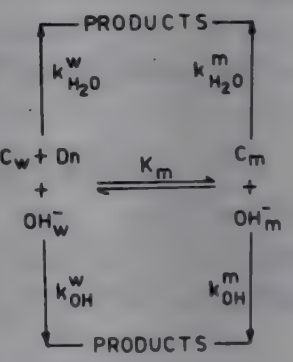

SCHEME -1

pseudo-phase. The partitioning of $[OH^-]_T$ between the aqueous and the cationic micellar pseudo-phase is assumed to be controlled by the pseudo-phase ion exchange equilibrium[13] (1).

$$OH^-_M + Br^-_W \overset{K^{OH}_{Br}}{\rightleftharpoons} OH^-_W + Br^-_M \quad \ldots (1)$$

In accord with Scheme 1, the pseudo-first order rate constant of base hydrolysis (k_ψ) is given by Eq. (2)

$$k_\psi = \frac{k^W_\psi + \{k^M_{H_2O}K_M + (k^M_{OH}K_M - k^W_{OH})m^s_{OH}\}[Dn]}{1 + K_M[Dn]} \quad \ldots (2)$$

where $m^s_{OH} = [OH^-_M]/[Dn]$; $[Dn] = [CTAB]_T - cmc$; $[C]_T = [C_W] + [C_M]$, $k^W_\psi = k^W_{H_2O} + k^W_{OH}[OH^-_W]$ ($= k_\psi$ at $[CTAB]_T = 0$), and K_M is the micellar binding constant. The concentrations are expressed in terms of total solution volume.

It is possible to calculate[14] the values of m^s_{OH} based on the known values of cmc, β and K^{OH}_{Br}.

With cmc = 2.0×10^{-4} mol dm^{-3} (see Materials & Methods), $K_{Br}^{OH} = 14$ and $\beta = 0.75$ (ref. 14), the calculated values of m_{OH}^{s} for $0.004 \leq [CTAB]_T \leq 0.15$ mol dm^{-3} ranged from 0.4184 to 0.0479 and from 0.5187 to 0.0832 at [OH] = 0.050 and 0.10 mol dm^3 respectively. Correspondingly the ionic strength of the aqueous pseudo-phase varied but marginally $\{I_{calc}^{W} = 0.06 \pm 0.01$ or 0.11 ± 0.01 for $[NaOH]_T = 0.050$ or 0.10 mol dm^{-3}, $[CTAB]_T = 0.0040$ to 0.150 mol dm$^{-3}\}$. Considering overall zero charge of the species *cis* [Co(en)$_2$(im)Sal], the effect of small variation of ionic strength on k_ψ can be neglected[15]. The plot of k_ψ^W versus $[OH^-]_T$ in the range of $[OH^-]_T = 0.0250$ to 0.200 mol dm^{-3} at $[CTAB]_T = 0$ (see Table 1) is linear, the intercept and gradient of which yield, $k_{H_2O}^{W} = (5.46 \pm 0.12) \times 10^{-4}$ s^{-1} and $k_{OH}^{W} = (17.0 \pm 0.9) \times 10^{-4}$ dm^3 mol^{-1} s^{-1}. As a first approximation, $(k_{OH}^{M} K_M - k_{OH}^{W})\, m_{OH}^{s} << k_{H_2O}^{M}$ was assumed and the rate data at $[OH^-]_T = 0.050$ and 0.100 mol dm^{-3} and varying $[CTAB]_T$ were fitted to Eq. (3), a linearized form of Eq. (2)

$$(k_\psi - k_\psi^W)^{-1} = (k_{H_2O} - k_\psi^W)^{-1} + [(k_{H_2O}^M - k_\psi^W) K_M]^{-1} [Dn]^{-1} \quad \ldots (3)$$

The plots of $(k_\psi - k_\psi^W)^{-1}$ against $[Dn]^{-1}$ were linear (corr. coeff. = 0.996 and 0.999 for $[OH^-]_T = 0.050$ and 0.100 mol dm^{-3} respectively) the intercepts and gradients of which yielded $K_M = 14.6 \pm 4.2$, 9.2 ± 1.9 dm^3 mol^{-1} and $k_{H_2O}^{M} = (13.8 \pm 2.1) \times 10^{-4}$, $(19.6 \pm 6.8) \times 10^{-4}$ s^{-1} for $[OH^-] = 0.050$ and 0.100 mol dm^{-3} respectively. The weighted mean value of $K_M = 10.1$ dm^3 mol^{-1} yielded $k_{H_2O}^{M} = (17.6 \pm 1.7) \times 10^{-4}$ s^{-1} from the rate data at $[OH^-]_T = 0.050$ and 0.100 mol dm^{-3}‡. Since $(m_{OH}^{s})_{calc} \neq 0$ and Eq. (3) holds good, an approximate value of $k_{OH}^{M} = 1.70 \times 10^{-4}$ s^{-1} could be obtained by setting $(k_{OH}^{M} K_M - k_{OH}^{W}) = 0$ (see Eq. 2). The estimated value of the Sterm layer of the micelles in which the substrate is likely to be positioned may be taken to be 0.14 dm^3 mol^{-1} (ref. 14). Hence the estimated second order base hydrolysis rate constant in the cationic micellar pseudo-phase $\{(k_2^M)_{OH} = k_{OH}^{M} \times 0.14\}$ is 2.4×10^{-5} dm^3 mol^{-1} s^{-1}.

‡ The rate data were also fitted to Eq. (2) by a nonlinear least squares program adopted to an IBM 1130 computer by varying the parameters $(k_{H_2O}^{M} K_M)$, $(k_{OH}^{M} K_M - k_{OH}^{W})$ and K_M. The sum of the weighted residuals $\Sigma^n[(k_{calc} - k_\psi)/\sigma(k_\psi)]^2$ were minimised for each set of values of K_{Br}^{OH} (= 12-16), β (= 0.70-0.85) and cmc (= 0.0002-0.0008 mol dm^{-3}). The fit was poor and the values of K_M (= 1.38 to 1.50 mol dm^{-3}) were found to be too small to be consistent with the satisfactory double reciprocal plot of $(k_\psi - k_\psi^W)^{-1}$ versus $[D_n]^{-1}$.

Noteworthy is the fact that the doubly deprotonated (imidazolato)(salicylato) species undergoes aquation ~3 times faster ($k_{H_2O}^{M}/k_{H_2O}^{W} \simeq 3.2$) in the cationic micellar pseudo-phase of CTAB than in aqueous medium; micellar binding, however, appears to decelerate its second order base hydrolysis rate (calc $k_{OH}^{W}/(k_2)_{OH}^{M} \simeq 70$). Similar observation has been made by Dash and Nayak[16] in a preliminary study of the base hydrolysis of ($\alpha\beta$S) (tetren) (3-NO_2 salicylato) cobalt(III) in the presence of CTAB ($k_{H_2O}^{M}/k_{H_2O}^{W} = 2$ and $k_{OH}^{W}/(k_2)_{OH}^{M} = 14$ at 30°C). The relatively higher rate of spontaneous aquation of the micelle-bound species is consistent with the operation of the internal conjugate base mechanism (SNICB) suggested earlier[9,17]. The formation of reactive conjugate base (ICB) via the intramolecular phenoxide assisted NH − deprotonation of the coordinated ethylenediamine,

cis-[Co(en)$_2$(im)($O_2CC_6H_4O$)] ⇌ [Co(en)(en-H)(im)($O_2CC_6H_4OH$)] (ICB)

may be more favourable and the replacement of the salicylate monoanion ($HSal^-$) by H_2O at the cobalt(III) centre may not be significantly retarded in the micellar pseudo-phase of CTAB relative to the aqueous pseudo-phase. This is quite reasonable considering the low dielectric constant ($D \simeq 40$)[18] of the intermicellar microenvironment of the substrate which favours the internal conjugate base equilibrium and also the intramolecular H-bonding interaction of the phenol group with the Co(III) bound carboxylate function in the ICB to assist the removal of the salicylate monoanion from the Co(III) centre. The situation, however, is quite different for the second order base hydrolysis path which is likely to involve equilibrium-controlled formation of amine conjugate base (due to NH deprotonation of the coordinated ethylenediamine by OH^-) followed by rate-determining loss of salicylate dianion from the resulting conjugate base. It appears likely that retardation of second order base hydrolysis by the cationic micelles is predominantly a kinetic effect, i.e. the rate of dissociation of salicylate dianion ($CO_2^- C_6H_4^- O$) from the Co(III) centre of the corresponding conjugate base $\{[Co(en)(en\text{-}H)(im)(O_2CC_6H_4O)]^-\}$ is appreciably slower in the cationic micellar surface of CTAB than in aqueous pseudo-phase.

The uncharged species, *cis*-[Co(en)$_2$(im)Sal]°, having anionic centres (N^- and O^-) will have the least tendency of binding to the anionic micelles of SDS. However, the UV-visible spectrum of this

substrate at *p*H 13 is strongly modified by SDS {the absorbance of the complex in the presence of SDS (pH = 13, $[SDS]_T = 0.10$, $[Complex]_T = 2.20 \times 10^{-4}$ mol dm^{-3}) was lower than that in the absence of SDS over the range of wavelength 320 to 460 nm} indicating micelle-substrate interaction. Further ε_{obs} (330 nm) decreases with $[SDS]_T$ (see Fig. 1) tending to attain a limiting value at high $[SDS]_T$ which is significantly higher than the value of ε (300 nm) (= 363 dm^3 mol^{-1} cm^{-1}) for the fully protonated dipositive complex, *cis*-$[Co(en)_2(imH)SalH]^{2+}$. Since the partitioning of OH^- to the anionic micelle surface is not favourable[19] the intermicellar *p*H is significantly lower than that of the aqueous pseudo-phase under the experimental condition. Hence it is reasonable to assume that the substrate bound to the anionic micelle surface exists predominantly as the less absorbing monoprotonated phenol form ($[Co(en)_2(im)SalH]^+$) and the micelle-substrate interaction equilibrium is best represented by Eq. (4) for which

$$C_W + D_n \overset{K'_M}{\rightleftharpoons} CH^+_M + OH^-_W \qquad \ldots (4)$$

the forward equilibrium constant (K'_M) is given by Eq. (5)

$$K'_M = \frac{[CH^+_M][OH^-_W]\gamma_W(OH^-)\gamma_M(CH^+)}{[C_W][D_n]\gamma_W(C)\gamma_M(D_n)} \qquad \ldots (5)$$

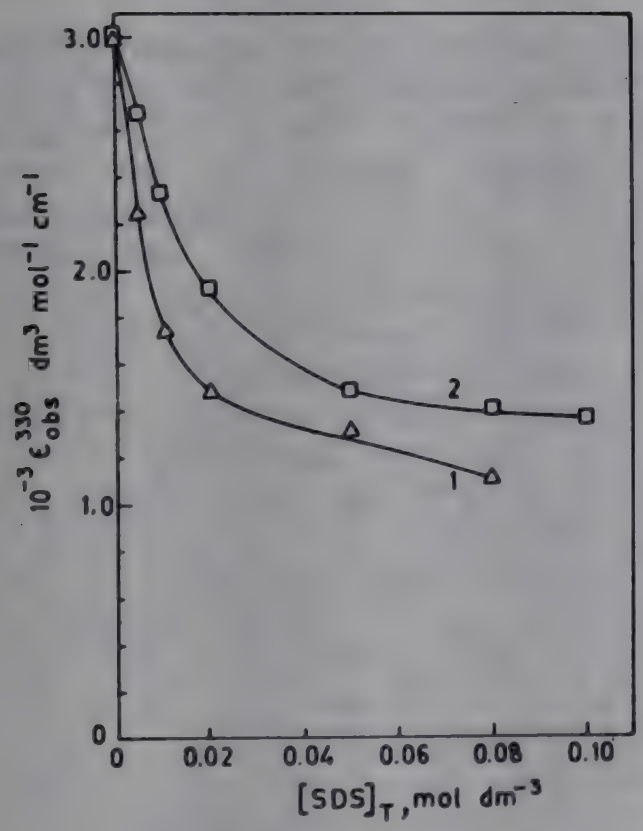

Fig. $1 - 10^{-3}\ \varepsilon^{330}_{obs}$ (dm^3 mol^{-1} cm^{-1}) versus $[SDS]_T$ plot for *cis*-$[Co(en)_2(im)Sal]$ at $[NaOH]_T = 0.050$ (1) and 0.10 (2) mol dm^{-3}.

where $\gamma_j(i)$ denotes the activity coefficient of species 'i' in the pseudo-phase j. Assuming $\gamma_M(CH^+) = \gamma_M(D_n) = \gamma_W(C) = 1$ and using Eq. (5) ε_{obs} (330 nm) takes the form given in Eq. (6).

$$\varepsilon_{obs} = \frac{\varepsilon_W + \varepsilon_M K'_M[D_n]/\{[OH^-_W]\gamma_W(OH^-)\}}{1 + K'_M[D_n]/\{[OH^-_W]\gamma_W(OH^-)\}} \qquad \ldots (6)$$

In Eq. (6) ε_W and ε_M denote the molar extinction coefficients of C and CH^+ species in aqueous and micellar pseudo-phases respectively. The ionic strength of the aqueous pseudo-phase was equated to $[NaOH]_T$ and the activity coefficient of OH^-, i.e. $\gamma_W(OH^-)$, was calculated from the Davis' equation[20]. Taking cmc = 0.0020 mol dm^{-3} (see Materials and Methods), ε_{obs} at varying $[SDS]_T$ and fixed $[OH^-]_T$ were then fitted to the linearized form of Eq. (6). We obtained $K'_M = 7.6 \pm 1.2$ and $\varepsilon_M = 1138 \pm 35$ dm^3 mol^{-1} cm^{-1}.

The observed retardation of base hydrolysis (see Table 1) of *cis*-$[Co(en)_2(im)Sal]$ by SDS is compatible with the reduced reactivity of its monoprotonated phenol form in the micellar pseudo-phase. Neglecting the reaction pathways involving CH^+_M, OH^-_W and CH^+_M, OH^-_M (see Scheme 1), Eq. (2) can be transformed to Eq. (7).

$$k_\psi = \frac{k^W_\psi + k^{M'}_{H_2O}K'_M[D_n]/\{[OH^-_W]\gamma_W(OH^-)\}}{1 + K'_M[D_n]/\{[OH^-_W]\gamma_W(OH^-)\}} \qquad \ldots (7)$$

where $k^{M'}_{H_2O}$ is the pseudo-first order aquation rate constant of the monoprotonated species, CH^+ (i.e. *cis*-$[Co(en)_2(im)SalH]^+$), in the micellar pseudo-phase and all other terms have their usual meaning. The rate data at $[SDS]_T = 0.0020$ to 0.10 mol dm^{-3} (see Table 1) were fitted to Eq. (7). We obtained $(k^{M'}_{H_2O}K'_M) = (5.57 \pm 0.80) \times 10^{-4}$ dm^3 mol^{-1} s^{-1}, $K'_M = 7.71 \pm 0.65$ dm^3 mol^{-1} and $k^{M'}_{H_2O} = (7.2 \pm 1.2) \times 10^{-5}$ s^{-1} (38°C). Excellent agreement between the values of K'_M from the analysis of equilibrium and kinetic data support the proposed micelle-substrate interaction (see Eq. 4).

Effect of micelles on base hydrolysis of $(\alpha\beta S)[Co(tetren)(SO_3)]^+$

The surfactants at concentration greater than cmc retard the base hydrolysis of this S-bonded sulphito complex in the order SDS > > Triton X 100 > CTAB (see Table 2). The observed rate versus $[surfactant]_T$ profile for SDS and Triton X 100 is reconciled to the following facts: (i) the complex cation is partitioned between the aque-

Table 2 – Effect of varying [surfactant] on rate of base hydrolysis of S-bonded (αβS)(tetren)$CoSO_3^+$ ($[complex]_T = (3.6 \pm 0.1) \times 10^{-4}$, $[NaOH]_T = 0.10$ mol dm^{-3}; $\lambda = 330$ nm; temp. = 35.8 ± 0.1°C)

$[Surfactant]_T$ (mol dm^{-3})	$10^4 k_\psi$ (s^{-1})[a]		
	CTAB	SDS	Triton X 100
0	0.98 ± 0.02[b]	0.98 ± 0.02[b]	0.98 ± 0.02[b]
0.002	0.70 ± 0.01	0.97 ± 0.02	1.07 ± 0.10
0.004	0.70 ± 0.02	0.88 ± 0.01	0.90 ± 0.05
0.006	0.77 ± 0.05	0.79 ± 0.03	0.78 ± 0.01
0.010	0.65 ± 0.01	0.51 ± 0.06	0.72 ± 0.06
0.020	0.76 ± 0.12	0.35 ± 0.01	0.67 ± 0.09
0.050	0.66 ± 0.04	0.235 ± 0.005	0.56 ± 0.03
0.100	0.70 ± 0.11	0.15 ± 0.01[c]	0.45 ± 0.05

(a) Average of duplicate runs and the errors quoted are the average deviation from the mean.

(b) $10^4 k_\psi$ s^{-1} = 0.94, 0.93, at $[NaCl]_T$ = 0.050 and 0.10 mol dm^{-3} respectively for $[SDS]_T = 0$ and $[NaOH]_T = 0.10$ mol dm^{-3}.

(c) $10^4 k_\psi$ s^{-1} = 0.36, 0.58 at $[NaCl]_T$ = 0.050 and 0.10 mol dm^{-3} respectively for $[SDS]_T = 0.10$ and $[NaOH]_T = 0.10$ mol dm^{-1}.

ous and micellar pseudo-phases; and (ii) it undergoes base hydrolysis predominantly in the aqueous pseudo-phase. For SDS added NaCl also increases the value of k_ψ at fixed $[NaOH]_T = 0.100$ mol dm^{-3} and $[SDS]_T = 0.100$ mol dm^{-3} (see foot note of Table 2) which further indicates that both Na^+, and $[Co(tetren)SO_3]^+$ compete for micellar binding and increase in $[Na^+]_T$ favours displacement of Co(III) substrate from the micellar pseudo-phase to the aqueous pseudo-phase in which it undergoes base hydrolysis. This view is supported by the observation that added NaCl in the absence of SDS at fixed $[NaOH]_T = 0.100$ mol dm^{-3} (see foot note *b* of Table 2) retards the base hydrolysis reaction to a small extent which must be ascribed to the ionic strength effect[15]. Hence it is reasonable to interpret the rate data in the presence of SDS with the pseudo-phase ion-exchange equilibrium model as given below

$$C_W^+ + Na_M^+ \overset{K_{ex}}{\rightleftharpoons} C_M^+ + Na_W^+ \quad \ldots (8)$$

$$C_W^+ + OH_W^- \xrightarrow{k_{OH}^W} [Co(tetren)OH]^{2+} + SO_3^{2-} \quad \ldots (9)$$

where $C^+ = [Co(tetren)SO_3]^+$ and all other terms have their usual meaning. The observed rate law (Eq. 10).

$$d[C^+]/dt = k_{OH}^W [OH_W^-][C_W^+] \quad \ldots (10)$$

in combination with the expression (11) for C_W^+],

$$(C_W^+] = [C^+]_T/(1 + K_{ex}[Na_M^+]/[Na_W^+]) \quad \ldots (11)$$

based on $\gamma^i(CoSO_3^+) = \gamma^i(Na^+)$, yields Eq. (12) for the observed pseudo-first order rate constant.

$$k_\psi = k_{OH}^W [OH_W^-]/(1 + K_{ex}[Na_M^+]/[Na_W^+]) \quad \ldots (12)$$

The ratio $[Na_M^+]/[Na_W^+]$ can be expressed by Eq. (13)

$$[Na_M^+]/[Na_W^+] = (\beta - m_{Co}^s)[D_n]/\{[Na^+]_T - (\beta - m_{Co}^s)[D_n]\} \quad \ldots (13)$$

where β, the overall micellar binding parameter is given by Eq. (14)

$$\beta = m_{Co}^s + m_{Na}^s = [C_M^+]/[D_n] + [Na_M^+]/[D_n] \quad \ldots (14)$$

and the concentrations are expressed in terms of total solution volume. The value of β is usually taken to be 0.7 ± 0.1 (refs 5, 21). For the complete micellar binding of the substrate ($= 3.6 \times 10^{-4}$ mol dm^{-3}), the maximum values of m_{Co}^s turn out to be 0.090 and 0.0036 at $[SDS]_T = 0.0060$ and 0.100 mol dm^{-3} respectively for $\beta = 0.7$ and cmc = 0.002 mol dm^{-3}. Hence with a reasonable approximation $\beta - m_{Co}^s = \beta$, K_{ex} was calculated from the rate data by combining Eqs (12) and (13) and taking $k_\psi^W = k_\psi$ at $[SDS]_T = 0$, $\beta = 0.70$ and cmc = 0.002 mol dm^{-3}. Further refinement of K_{ex} was made by an interactive procedure using the values of $[Na_M^+]/[Na_W^+]$ calculated by Eq. (13) with the estimates of m_{Co}^s (see ref. 5). The final values of K_{ex} turn out to be 15.0 ± 4.0, 12.6 ± 3.5 and 10.7 ± 3.0 for $\beta = 0.6$, 0.7 and 0.8 respectively indicating that K_{ex} is insensitive to the chosen value of β. The mean value of $K_{ex} = 12.6 \pm 1.2$ is comparable to that for *cis*-$[Co(en)_2(im)N_3]^+$/SDS (15.0 ± 1.6) and *cis*-$[Co(en)_2(im)NCS]^+$/SDS (13.8 ± 1.0) ion-exchange equilibria at 40°C (ref. 5).

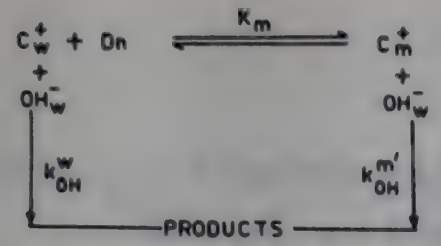

SCHEME-2

The pseudo-phase ion-exchange model does not apply for Triton X 100 as the micelles are uncharged. It is assumed that hydrophilic OH^-, unlike Co(III) substrate, prefers the aqueous pseudophase. Scheme 2 is assumed to interpret the rate data for the base hydrolysis of this S-bonded sulphito complex at varying $[\text{Triton X 100}]_T$.

Accordingly the pseudo-first order rate constant (k_ψ) is given by Eq. (15),

$$k_\psi = \frac{(k_{OH}^W + k_{OH}^{M'} K_M[D_n])[OH^-]_T}{1 + K_M[D_n]} \quad \ldots (15)$$

where $k_{OH}^{M'}$ is the second order rate constant for base hydrolysis of the micelle bound substrate with OH^- in the aqueous pseudo-phase. The cmc for Triton X 100 is $\sim 10^{-4}$ mol dm^{-3} (ref. 22). $[\text{Triton X 100}]_T = [D_n]$ was assumed and the rate data at fixed $[OH^-]_T$ and $[\text{Triton X 100}]_T = 0.0020\text{-}0.100$ mol dm^{-3} were fitted to Eq. (15). We obtained $k_{OH}^{M'} K_M = (38.8 \pm 10.0) \times 10^{-3}$ dm^6 mol^{-2} s^{-1}, $K_M = 91.2 \pm 14.2$ dm^3 mol^{-1}. It is noteworthy that the substrate bound to the neutral micelle surface undergoes base hydrolysis somewhat slower than that in aqueous medium ($k_{OH}^{M'}/k_{OH}^W = 0.25$). The value of the binding constant, K_M is comparable to those for binding of $Co(bpy)_3^{2+}$ (bpy = bipyridyl) and similar other substrates to the Triton X 100 micelles[22]. The hydrophobic interaction between $[Co(tetren)SO_3]^+$ and the neutral micelle favours strong binding.

Preliminary calculation showed that the observed rate retardation by CTAB (see Table 2) is not due to increase in ionic strength or slight decrease in $[OH_W^-]$ as a result of pseudo-phase ion-exchange equilibrium as depicted in Eq. (1). Almost asymptotic limit of k_ψ is reached at $[\text{CTAB}]_T = 0.0020$ mol dm^{-3} with k_ψ^W/k_ψ (limit) = 1.4 where k_ψ^W and k_ψ (limit) denote the rate constant at $[\text{CTAB}]_T = 0$ and the limiting rate constant respectively both at $[OH^-]_T = 0.100$ mol dm^{-3}. Attempts to fit the rate data to the pseudo-phase ion-exchange model with the micelle-bound substrate undergoing base hydrolysis was unsuccessful. The observed reactivity trend at varying $[\text{CTAB}]_T$ may be ascribed to the formation of a premicellar aggregate, an ionpair of the type {(tetren) $Co^{2+} - SO_3^-$, $CH_3(CH_2)_{15}N^+(CH_3)_3$} which, we believe, is less susceptible to base hydrolysis relative to the complex. The hydrophobic interaction between the tetren moiety and the hydrocarbon tail of CTA^+ presumably hinders, atleast partly, formation of reactive conjugate base via OH^- promoted NH− deprotonation of coordinated tetren moiety resulting in small rate retardation.

Acknowledgement

This work is supported by a research grant to one of the authors (ACD) by the UGC, New Delhi. Miss J Prusti is thankful to the UGC, New Delhi for a junior research fellowship.

References

1 Dash A C & Mohanty A K, *Indian J Chem*, 28A (1989) 989.
2 Dash A C & Nayak R C, *Indian J Chem*, 25A (1986) 234; 27A (1988) 862.
3 Dash A C & Mohanty A K, *Indian J Chem*, 28A (1989) 868, 661.
4 Murphy K J & Reinsborough, *J Sur Sci and Technol*, 5 (1989) 21.
5 Dash A C & Nayak R C, *J chem Soc, Faraday Trans* 1, 83 (1987) 1307; Dash A C & Nayak R C, *Indian J Chem*, 26A (1987) 293.
6 Tachiyashiki S & Yamatera H, *Inorg Chem*, 25 (1988) 3043.
7 Fletcher P D & Robinson B H, *J chem Soc Faraday Trans* 1, 80 (1984) 2417.
8 Tachiyashiki S & Yamatera H, *Bull chem Soc Japan*, 87 (1984) 1061, 1067, 1070; 58 (1982) 759.
9 Dash A C & Mohanty B, *Transition Met Chem* (*Weinheim*), 5 (1980) 183.
10 Dash A C, El Awady A A & Harris G M, *Inorg Chem*, 20 (1981) 3160.
11 Cordes E H & Gitler C in *Progress in bio-organic chemistry*, Vol. 1 edited by E T Kaiser and F J Kezdy (Wiley, New York) 1973, p. 1.
12 Hirose C & Sepulveda L, *J phys Chem*, 85 (1981) 3689; Bunton C A & Sepulveda L, *J phys Chem*, 83 (1979) 680.
13 Romsted L S, *Surfactants in solution* edited by K L Mittal & B Lindman (Plenum 1982) Vol II p. 1015.
14 Al-Lohedan H, Bunton C A & Romsted L S, *J phys Chem*, 85 (1981) 2123.
15 Eyring H, Lin S H & Lin S M, *Basic chemical kinetics* (Wiley New York) 1980, pp. 414.
16 Dash A C & Nayak R C, *Inorg Chem*, 25 (1986) 2237.
17 Dash A C & Harris G M, *Inorg Chem*, 20 (1981) 4011.
18 Mukherjee P & Roy A, *J phys Chem*, 70 (1966) 2144.
19 Kurz J L, *J phys Chem*, 66 (1962) 2239; Bunton C A & Robinson L, *J org Chem*, 34 (1969) 773.
20 Davies C W, *J chem Soc*, (1938) 2093.
21 Garnett C J, Lambie A J, Beck W H & Liler M, *J chem Soc Faraday Trans* 1, 79 (1983) 953, 965.
22 Carbone A I, Cavasino F P, Sbriziolo C & Pelizzette E, *J phys Chem*, 89 (1985) 3578.

Indian Journal of Chemistry
Vol. 29A, July 1990, pp. 676-679

Kinetics of oxidation of cinnamaldehyde by chloramine-T in perchloric acid and in alkaline medium catalysed by Os(VIII)

C K Mythily, K S Rangappa* & D S Mahadevappa
Department of Studies in Chemistry, University of Mysore, Manasagangotri, Mysore 570 006

Received 22 December 1988; revised 21 September 1989; accepted 11 December 1989

Kinetics of chloramine-T (CAT) oxidation of cinnamaldehyde in acid medium and in alkaline medium (catalysed by OsO_4) have been investigated at 313 K. In acid medium, a Michaelis-Menten kinetics is obeyed with a first order dependence of rate on [CAT] and a fractional order in [aldehyde] which becomes zero at higher [aldehyde]. Rate dependence on $[H^+]$ varies from inverse fractional to fractional order. In alkaline medium the reaction is first order each in [CAT] and [Os(VIII)] and inverse first order in $[OH^-]$. Solvent isotope effect, effects of added chloride ion, and *p*-toluenesulphonamide and varying ionic strength and dielectric constant of medium have been investigated. Activation parameters have been computed.

Oxidation of aldehydes, in particular of aliphatic aldehydes by N-haloamines in acidic and alkaline media has already been reported[1-5]. But, there is meagre information about the oxidation of aromatic aldehydes. Hence the title investigation.

Materials and Methods

Aqueous solution of CAT was standardised by iodometric method. Cinnamaldehyde (Wilson Laboratories, Bombay) was distilled, its purity checked by NMR and its solution was prepared in ethanol. Heavy water (D_2O, 99.2%) was obtained from Bhabha Atomic Research Centre, Bombay. All the other reagents were of AR grade. Triply distilled water was used throughout the investigation. The ionic strength of the system was kept fixed using sodium perchlorate.

For kinetic runs, a measured amount of CAT pre-equilibrated at 40°C was rapidly added to the thermally equilibrated mixture containing appropriate amounts of the aldehyde, acid/alkali, sodium perchlorate solutions, water and ethanol. The progress of the reaction was monitored for two half lives by iodometric determination of unreacted CAT in a measured aliquot withdrawn at regular intervals of time. The pseudo-first order rate constants were reproducible within ± 3%.

Stoichiometry and product analysis

Stoichiometric runs indicated that one mole of the aldehyde consumed one mole of the oxidant in both acidic medium and in alkaline medium catalysed by Os(VIII) in accordance with Eqs (1) and (2):

$$PhCH=CH-CHO + ArSO_2NClNa + H_2O \rightarrow PhCH=CH-COOH + ArSO_2NH_2 + NaCl \quad \ldots (1)$$

In alkaline medium,

$$Ph\,CH=CH-CHO + ArSO_2NClNa + NaOH \rightarrow PhCH=CH-COONa + ArSO_2NH_2 + NaCl \ldots (2)$$

p-Toluene sulphonamide ($ArSO_2NH_2$) was detected by paper chromatography. The other product was identified as cinnamic acid by comparing its NMR with that of an authentic sample.

Results and Discussion

(i) *Kinetics in acid medium*

The reaction is first order in [CAT] at all concentrations of the reactants and log titre-time plots were linear upto two half lives. Values of k_1 decrease with increase in $[H^+]$ in the range of 0.01 to 0.04 mol dm^{-3} and thereafter k_1 increases with increase in $[H^+]$ from 0.01 to 0.04 mol dm^{-3} (Fig. 1). Further, a fractional order at lower [aldehyde] becomes zero at higher [aldehyde], obeying the Michaelis-Menten kinetics. Addition of ethanol decreases the rate and a plot of log k_1 versus 1/D (D = dielectric constant of the medium) is linear with a negative slope. Added chloride ion increased the rate and a fractional order dependence (0.56) of rate on [chloride ion] was observed. However, the added reaction product, *p*-toluenesulphonamide had no effect on the rate.

The reaction was studied at different temperatures at varying [substrate] and from the Mechaelis-Menten plots activation parameters for the rate limiting step have been computed (Table 1).

The first order dependence of rate in [CAT] and the nil effect of added *p*-toluenesulphonamide on the reaction rate, indicate that $ArSO_2NCl_2$ and HOCl are not the reactive species in the present set of experiments[6,7]. Since the effect of change in ionic

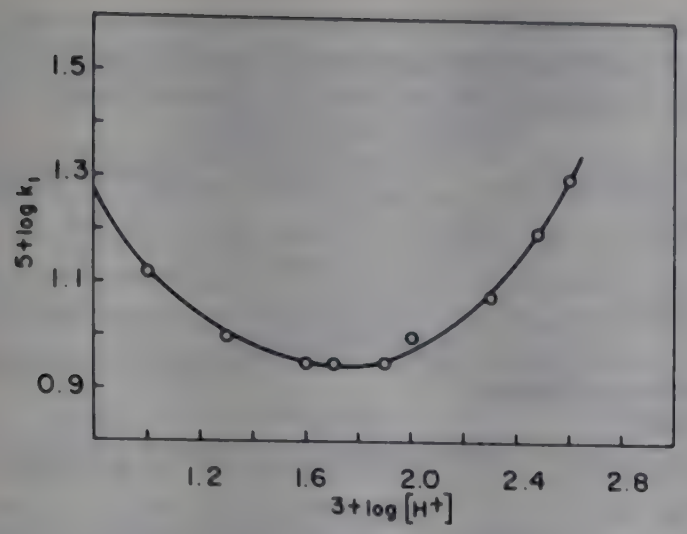

Fig. 1—Plot of log k_1 versus log $[H^+]$ ($[CAT]_0 = 0.005$ mol dm^{-3}, $[Cinn] = 0.05$ mol dm^{-3}, EtOH = 40%, $\mu = 0.05$ mol dm^{-3}, t = 40°C)

strength on the rate is negligible, it may be inferred that neutral species are involved in the rate-limiting step. Therefore, the $ArSO_2NHCl$ is the likely oxidising species which is involved in the deprotonation equilibrium[8] with $ArSO_2\overset{+}{N}H_2Cl$ (Scheme 1).

$$ArSO_2\overset{+}{N}H_2Cl \overset{K_1}{\rightleftharpoons} ArSO_2NHCl + H^+ \text{ (fast)} \quad \ldots \text{(i)}$$

$$ArSO_2NHCl + S \overset{K_2}{\rightleftharpoons} X \text{ (fast)} \quad \ldots \text{(ii)}$$

$$X \xrightarrow{k_3} \text{Products (slow)} \quad \ldots \text{(iii)}$$

Scheme 1

Scheme 1 leads to rate law (3)

$$\text{Rate} = k_3[X] = \frac{k_3K_1K_2[S][CAT]_t}{K_1 + [H^+] + K_1K_2[S]} \quad \ldots (3)$$

where $[CAT]_t$ is the total concentration of CAT given by Eq. (4).

$$[CAT]_t = [ArSO_2NHCl] + [ArSO_2\overset{+}{N}H_2Cl] + [X] \quad \ldots (4)$$

Since K_1 (~ 0.01) can be neglected compared to $[H^+] = 0.05$ mol dm^{-3}, Eq. (3) reduces to Eq. (5).

$$\text{Rate} = \frac{k_3K_1K_2[S][CAT]_t}{[H^+] + K_1K_2[S]} \quad \ldots (5)$$

If k_1 is the observed rate constant, then,

$$\frac{1}{k_1} = \frac{[H^+] + K_1K_2[S]}{k_3K_1K_2[S]}$$

or

$$\frac{1}{k_1} = \frac{[H^+]}{k_3K_1K_2[S]} + \frac{1}{k_3}$$

Table 1—Effect of varying substrate concentration at different temperatures in acid medium

$[H^+] = 0.05$ mol dm^{-3} EtOH = 40% $\mu = 0.5$ mol dm^{-3}

$[Cinn] \times 10^3$ mol dm^{-3}	$k_1 \times 10^5$ s^{-1} at				
	308.1	313	317.2	322.5	328.6
10	4.87	7.04	8.59	11.38	17.06
20	5.29	7.72	9.72	13.22	19.77
40	5.43	8.62	10.97	14.22	22.58
80	5.70	8.86	10.93	14.79	23.18
100	5.79	8.91	10.97	15.02	23.33

Table 2—Effect of temperature on the rate

$[CAT] = 0.005$ mol dm^{-3}, $[Cinn] = 0.1$ mol dm^{-3} in acid medium, $[Cinn] = 0.05$ mol dm^{-3} in alkaline medium, EtOH = 40%, $\mu = 0.5$ mol dm^{-3}

Acid medium $[H^+] = 0.05$ mol dm^{-3}			Alkaline medium $[OH^-] = 0.05$ mol dm^{-3}	
Temp. (K)	$k_3^* \times 10^5$ (s^{-1})	$K_1K_2^{**}$	Temp. (K)	$k_1^{***} \times 10^3$ (s^{-1})
308.1	5.88	23.17	313	1.74
313.0	9.09	16.81	318	2.30
317.2	11.36	15.62	323	3.76
322.5	15.38	14.89	328	5.16
328.6	25.00	11.00	333	9.53

*,**Rate constants and equilibrium constants for the rate determining steps.

***Rate constant for the overall reaction.

From the slope and intercept of the double reciprocal plot of $1/k_1$ versus $1/[S]$ at fixed $[H^+]$, values of K_1K_2 and k_3 were calculated at each temperature and the values are listed in Table 2.

Equation (5) supports the experimental results of fractional order in [S] becoming zero at higher [S], since $K_1K_2[S] \gg [H^+]$ under these conditions. The $[H^+]$-rate profile shown in Fig. 1 indicates a gradual change in mechanism and could be explained by assuming a reversal of step (i) in Scheme 1.

In order to determine the activation parameters for the rate-limiting step, the [substrate] was varied at each temperature and k_3 was calculated. From the plot of log k_3 versus 1/T, values of $\Delta H^{\neq}$, $\Delta G^{\neq}$, $\Delta S^{\neq}$ were calculated (Table 3).

Addition of chloride ion in the form of NaCl (0.005 to 0.10 mol dm^{-3}) increases the rate of reaction. Chloride ion catalysis in the present case can be explained by the mechanism given in Scheme 2 where the loose intermediate X′ formed in step (i) interacts with the substrate followed by the rate limiting step forming the products:

$$ArSO_2NHCl + Cl^- \overset{K_3}{\rightleftharpoons} ArSO_2NHCl \ldots Cl^- \text{ (fast)} \quad (X^1) \quad \ldots \text{(i)}$$

$$X' + S \overset{K_5}{\rightleftharpoons} Y \quad \text{(fast)} \quad \ldots \text{(ii)}$$

$$Y \overset{k_6}{\rightarrow} \text{Products} \quad \text{(slow)} \quad \ldots \text{(iii)}$$

Scheme 2

The rate law based on Scheme 2 is given by Eq. (6), which is in agreement with the observed experimental results.

$$\text{Rate} = \frac{k_6 K_1 K_4 K_5 [S][Cl^-][CAT]_t}{1 + K_1 + K_1 K_4 [Cl^-] + K_1 K_4 K_5 [S][Cl^-]} \quad \ldots (6)$$

Solvent isotope effect

Kinetics studies were carried out in D_2O containing $HClO_4$ and k_1 (D_2O) was found to be 6.82×10^{-5} s^{-1} while the corresponding $k_1(H_2O)$ was 7.90×10^{-5} s^{-1} leading to the normal solvent isotope effect $k_1(H_2O)/k_1(D_2O) = 1.16 \pm 0.02$. Since D_3O^+ is ~3 times stronger than H_3O^+ (refs 9, 10) for acid catalysed reactions, the inverse solvent isotope effect $k_1(D_2O)/k_1(H_2O)$ should be greater than unity. But for reactions retarded by H^+ ions, this ratio should be less than unity, as has been observed in the present investigations and hence supports the proposed mechanism and the derived rate expressions.

Effect of changing the solvent composition

A good account of effect of solvent on rate has been given by Entelis and Tiger[11]. For the limiting case of zero angle of approach between two dipoles or ion-dipole system, Amis[12] has shown that a plot of log k_1 versus 1/D is linear with a negative slope for a reaction between a negative ion and a dipole or between two dipoles, while a positive slope results for a positive ion-dipole interaction. The negative dielectric effect observed in the present investigations clearly supports the dipole-dipole nature of the rate determining step in Scheme 1.

The observed values of kinetic and thermodynamic parameters support the rate mechanism and the fairly high negative value of $\Delta S^{\neq}$ (Table 3) indicates the formation of a rigid transition state.

(ii) *Kinetics in alkaline medium catalysed by Os(VIII): Effect of varying [reactant]*

At fixed [alkali] with the substrate in excess, plots of log $[CAT]_0/[CAT]$ versus time were linear, indicating a first order dependence of rate on $[CAT]_0$. The values of k_1 were unaffected with increase in $[aldehyde]_0$, indicating that the rate was independent of $[aldehyde]_0$. The rate decreased with an increase in $[OH^-]$ and plots of log k_1 versus log $[OH^-]$ were linear, indicating an inverse first order dependence of rate on $[OH^-]$.

Table 3—Kinetic orders in [oxidant], [S] and $[H^+]$ or $[OH^-]$ and activation parameters for oxidation of cinnamaldehyde by CAT in acid and alkaline media

Orders observed in	Acid medium	Alkaline medium
[oxidant]	1.0	1.0
[S]	0.15 to zero	0
$[H^+/OH^-]$	−0.4 to 0.5 inverted bell type	−1.0
Activation parameters		
E_a (kJ mol^{-1})	58.32	61.25
$\Delta H^{\neq}$ (kJ mol^{-1})	55.53 ± 0.017	58.56 ± 0.013
$\Delta G^{\neq}$ (kJ mol^{-1})	102.26 ± 0.22	100.46 ± 0.18
$\Delta S^{\neq}$ (JK^{-1} mol^{-1})	−145.63 ± 0.13	−129.72 ± 0.25

The rate increased with increase in $[OsO_4]$ and a plot of log k_1 versus log $[OsO_4]$ was linear, with unit slope, indicating a first order dependence of rate on $[OsO_4]$.

It was observed that decrease in ethanol content of the reaction medium increased the rate of reaction. A plot of log k_1 versus 1/D was linear with a negative slope.

Variation of ionic strength of the medium by adding sodium perchlorate or addition of the reaction product toluenesulphonamide had no significant effect on the rate. Solvent isotope effect $k_1(H_2O)/k_1(D_2O)$ is found to be 2.08.

The reaction was studied at different temperatures (313-333 K; Table 2) and the activation parameters were computed (Table 3).

Mechanism of oxidation in alkaline medium catalysed by Os(VIII)

Several workers have observed the retarding influence of OH^- ions on the rate of CAT reactions with diverse substrates[13-15]. It has been suggested that the reactivity of CAT in weakly alkaline solutions is due to the formation of conjugate acid $ArSO_2NHCl$ from $ArSO_2NCl^-$ in a OH^- retarding step, Eq. (7)

$$ArSO_2NCl^- + H_2O \rightleftharpoons ArSO_2NHCl + OH^- \quad \ldots (7)$$

The possible oxidant species of CAT in alkaline solutions are $ArSO_2NCl^-$ and OCl^- [$ArSO_2NCl^- + H_2O \rightleftharpoons ArSO_2NH_2 + OCl^-$] which would be transformed into more reactive oxidising species $ArSO_2NHCl$ and HOCl, in the course of the reaction in OH^- retarding steps (Eqs 7 and 8).

$$ArSO_2NHCl + H_2O \rightleftharpoons ArSO_2NH_2 + HOCl \quad \ldots (8)$$

$$K_h = 4.88 \times 10^{-8} \text{ at } 25°C$$

The first order dependence of reaction rate in $[OsO_4]$ and $[CAT]_0$, an inverse first order in $[OH^-]$ and zero order dependence in cinnamaldehyde in the present investigations, indicate that the formation of an intermediate species from Os(VIII) and $ArSO_2NHCl$ is the most probable rate controlling step, as reported by the previous workers[16]. In view of these results two kinetically indistinguishable mechanisms (Schemes 3 and 4) can be suggested:

$$ArSO_2NCl^- + H_2O \overset{K_7}{\rightleftharpoons} ArSO_2NHCl + OH^- \quad \ldots (i)$$

$$OsO_4 + ArSO_2NHCl \overset{k_8}{\rightarrow} Z \quad \text{(slow)} \quad \ldots (ii)$$

$$Z + S \overset{k_9}{\rightarrow} \text{Products} \quad \text{(fast)} \quad \ldots (iii)$$

Scheme 3

$$[OsO_4(OH)_2]^{2-} + H_2O \overset{K_{10}}{\rightleftharpoons} [OsO_3(OH)_3]^- + OH^- \text{ (fast)} \quad \ldots (i)$$

$$[OsO_3(OH)_3]^- + ArSO_2NHCl \overset{k_{11}}{\rightarrow} Z' \quad \text{(slow)} \quad \ldots (ii)$$

$$Z' + S \overset{k_{12}}{\rightarrow} \text{Products} \quad \text{(fast)} \quad \ldots (iii)$$

Scheme 4

Schemes 3 and 4 lead to rate law (9)

$$-\frac{d}{dt}[\text{Chloramine-T}]$$

$$= \frac{k_8 K_7 [\text{Os(VIII)}][\text{CAT}][H_2O]}{[OH^-]}$$

$$= \frac{k_{11} K_{10} [\text{Os(VIII)}][\text{CAT}][H_2O]}{[OH^-]} \quad \ldots (9)$$

Equation (9) is in complete agreement with the experimental observations where a first order dependence each on [CAT] and [Os(VIII)] and an inverse first order in $[OH^-]$ are observed.

The solvent isotope effect $k_1(H_2O)/k_1(D_2O) = 2.08$ is noted in alkaline medium. This is generally correlated with the greater basicity of OD^- compared to OH^- ions which supports the initial equilibrium and the rate determining step in Scheme 3. It is also seen that the rate increases with an increase in dielectric constant of the medium, confirming the ion-dipole nature of the rate limiting step.

Further the mechanism is supported by the low enthalpy of activation. The value of $\Delta S^{\neq}$ shows that there is the formation of more ordered transition state.

Acknowledgement

One of us (CKM) gratefully acknowledges the award of junior research fellowship by the UGC, New Delhi.

References

1 Agrawal M C & Mushran S P, *Z Naturforsch*, 26b (1972) 401.
2 Goswami C & Banerji K K, *Z Naturforsch*, 26b (1971) 383.
3 Mahadevappa D S & Naidu H M K, *J Indian chem Soc*, 58 (1981) 454.
4 Radhakrishna Murthy P S & Sahu B, *Indian J Chem*, 15A (1977) 700.
5 Ram Sanehi, Agrawal M C & Mushran S P, *Indian J Chem*, 12 (1974) 311.
6 Campbell M M & Johnson G, *Chem Rev*, 78 (1978) 65.
7 Banerji K K, Jayaram B & Mahadevappa D S, *J Sci Ind Res*, 46 (1987) 65-67.
8 Narayanan S S & Rao V R S, *Radio chim Acta*, 32 (1983) 211.
9 *Isotope effects in chemical reactions*, edited by C J Collins & N S Bowman (Van Nostrand, New York) (1970) 267.
10 Wiberg K B, *Chem Rev*, 55 (1955) 713; Physical organic chemistry (Wiley, New York) 1964.
11 Entelis S G & Tiger R P, *Reaction kinetics in the liquid phase* (Wiley, New York) 1976.
12 Amis E S, *J Chem Educ*, 30 (1953) 351; *Anal Chem*, 27 (1955) 1672; *Solvent effects on reaction rates and mechanisms* (Academic Press, New York) 1966.
13 Higuchi T & Hussain A, *J chem Soc B*, (1967) 549.
14 Bernanose A & Simon J, *Bull Soc Pharm Nancy*, 24 (1955) 6.
15 Hardy F F & Johnston J P, *J Chem Soc Perkin* 2, (1973) 742.
16 Agrawal M C & Upadhyay S K, *J Sci Ind Res*, 42 (1983) 508.

Indian Journal of Chemistry
Vol. 29A, July 1990, pp. 680-685

Kinetics and mechanism of oxidation of carbohydrazide by N,N-dichlorotoluene-*p*-sulphonamide in water-methanol medium

B Thimme Gowda* & P Ramachandra

Department of Post-Graduate Studies and Research in Chemistry, Mangalore University, Mangalagangothri 574 199

Received 29 May 1989; revised 3 October 1989; accepted 15 November 1989

Kinetics of oxidation of carbohydrazide (CH) by N,N-dichlorotoluene-*p*-sulphonamide (DCT) in 1:1 (v/v) water-methanol medium have been studied over a wide range of [$HClO_4$] (0.0001-0.10 mol dm^{-3}). The reaction is first order in [DCT] and fractional order in [CH] in the entire range of [H^+]. But the dependence in [H^+] varies from zero order in [H^+] range of 0.0001 to 0.0005 mol dm^{-3}, to an inverse fractional order in [H^+] range of 0.0005 to 0.005 mol dm^{-3} and increases again in [H^+] range of 0.005 to 0.030 mol dm^{-3}. Variation in ionic strength of the reaction medium or addition of the reduced product of oxidant has no significant effect on the rate of oxidation. Increase in methanol content of the medium slightly increases the rate. Mechanisms consistent with the observed results have been suggested and the related rate laws deduced.

In continuation of earlier work[1-6] from our laboratory on oxidation kinetics of semicarbazide, carbohydrazide and their derivatives, we report herein the kinetics of oxidation of carbohydrazide by N,N-dichlorotoluene-*p*-sulphonamide (dichloramine-T or DCT) in 1:1 (v/v) water-methanol medium, in the presence of perchloric acid.

Materials and Methods

Stock solution (0.05 mol dm^{-3}) of DCT in pure methanol was standardised by iodometric method and preserved in amber coloured bottles.

Carbohydrazide (CH) was prepared in the laboratory and its purity checked (m.p. 154°). Stock solution (0.5 mol dm^{-3}) of CH was prepared in doubly distilled water. All other reagents employed were of AR grade.

Kinetic measurements

Kinetic studies were made under pseudo-first order conditions with [CH] ⩾ [DCT] (20-200 fold excess). The reaction was initiated by rapid addition of requisite amount of oxidant solution (5×10^{-4} to 5×10^{-3} mol dm^{-3}), thermally pre-equilibrated at a desired temperature, to a solution containing known amount of CH (0.02 to 0.20 mol dm^{-3}) and perchloric acid (0.0001 to 0.10 mol dm^{-3}), pre-equilibrated at the same temperature. The progress of the reaction was monitored for at least two half-lives by iodometric estimation of unreacted DCT at regular time intervals. The pseudo-first order rate constants (k_{obs}) were computed by the graphical methods and the values are reproducible within ± 4% error.

Stoichiometry and product analysis

Stoichiometry was determined by thermally equilibrating varying ratios of reactants at different [$HClO_4$] (0.0005-0.10 mol dm^{-3}) and estimating unreacted DCT in the reaction mixture. It was found that one mole of the substrate reacted with two moles of oxidant in accordance with Eq. (1).

$$NH_2NHCONHNH_2 + 2ArSO_2NCl_2 + H_2O \rightarrow$$
$$2ArSO_2NH_2 + 2N_2 + CO_2 + 4H^+ + 4Cl^- \quad \text{where } Ar = CH_3C_6H_4 \quad \ldots (1)$$

Nitrogen evolved, determined quantitatively using Schiff's nitrometer, was close to the theoretical value. Toluene-*p*-sulphonamide (TSA), the reduced product of the oxidant was detected by paper chromatography.

Results

At fixed [H^+] with several fold (20-200 fold) excess of the substrate, the plots of $\log[DCT]_0/[DCT]$ versus time were linear for at least two half-lives and k_{obs} computed from the plots remained unaffected by changes in $[DCT]_0$ (Table 1), establishing first order dependence in [DCT]. The effect of varying [H^+] on the rate of oxidation was investigated over a wide range of [H^+] (0.0001 to 0.10 mol dm^{-3}) (Table 1). At fixed [DCT] and

Table 1—Pseudo-first order rate constants (k_{obs}) for the oxidation of carbohydrazide by dichloramine-T (DCT) in 1:1 (v/v) water-methanol medium in the presence of perchloric acid (283 K)

$10^3[HClO_4]$ (mol dm^{-3})	$10^4 k_{obs}$ (s^{-1})	$10^3[DCT]_0$ (mol dm^{-3})	$10[CH]$ (mol dm^{-3})	$10^4 k_{obs}$(s^{-1}) at $[HClO_4]$(mol dm^{-3})		
				0.0002	0.002	0.02
0.1	22.5					
0.2	21.8	0.5	1.0	21.7	15.4	12.7
0.5	20.8	1.0	1.0	21.8	15.7	12.7
1.0	19.1	2.0	1.0	21.8	15.6	12.8
2.0	15.7	4.0	1.0	21.9	15.7	12.8
3.0	13.9	5.0	1.0	21.9	15.6	12.9
4.0	12.4	1.0	0.2	8.9	5.8	4.0
5.0	10.6	1.0	0.5	13.6	10.0	7.5
10.0	11.8	1.0	1.0	21.8	15.7	12.7
20.0	12.7	1.0	1.5	28.0	22.3	18.8
30.0	14.2	1.0	2.0	35.6	28.2	24.7
50.0	25.8					
70.0	36.3					
100.0	51.4					

Table 2—Kinetic data and activation parameters for oxidation of carbohydrazide by dichloramine-T (DCT) in 1:1 (v/v) water-methanol medium in the presence of perchloric acid

Order (n) observed in	Orders in $[HClO_4]$(mol dm^{-3}) range of		
	0.0001-0.0005	0.0005-0.005	0.005-0.03
[DCT]	1.0	1.0	1.0
[CH]	0.64	0.68	0.73
$[H^+]$	−0.06	−0.33	+0.08

	Activation parameters calculated using				
	k_1	K	k_5	k_1	k_2
E_a (kJ mol^{-1})	48.4	48.6	25.4	49.0	55.3
log$A$	7.05	7.26	1.18	6.20	8.21
$\Delta H^{\ddagger}$ (kJ mol^{-1})	46.3	45.9	24.1	46.8	48.4
$\Delta S^{\ddagger}$(JK^{-1}mol^{-1})	−116.5	−115.3	−226.6	−136.7	−111.3
$\Delta G^{\ddagger}$ (kJ mol^{-1})	79.3	77.9	88.2	84.6	79.9

[CH], the rate was almost insensitive to variation in $[H^+]$ up to 0.0005 mol dm^{-3}, decreased with increase in $[H^+]$ in the range 0.0005-0.005 mol dm^{-3} and increased beyond $[H^+]$ of 0.005 mol dm^{-3} (Table 1). The plot of k_{obs} versus $[H^+]$ was inverted bell shaped, while the plot of log k_{obs} versus log$[H^+]$ was zig zag (Fig. 1). $[CH]_0$ and $[DCT]_0$ were varied in all the four ranges of $[H^+]$ (up to 0.0005, 0.0005-0.005, 0.005-0.03, and $\geqslant$0.03 mol dm^{-3}) (Table 1). The rate increased with increase in [CH] in the first three ranges of $[H^+]$ (Table 1) with fractional order dependence in [CH] (Table 2), while it decreased with increase in [CH] at $[H^+]$ > 0.03 mol dm^{-3} (values not shown).

Variation in ionic strength of the reaction medium had no significant effect on the rate of oxidation. Increase in methanol content of the solvent medium slightly increased the rate. Addition of the reduced product of the oxidant, toluene-*p*-sulphonamide to the reaction mixture had negligible effect on the rate of oxidaion.

The rates were measured at different temperatures and varying acidities and [substrate]. Activation parameters in all the cases were computed from the Arrhenius plots (Table 2).

Discussion

Mechanism of oxidation: (*i*) *At* $[HClO_4]$ *in the range of* 0.0001-0.0005 *mol dm*$^{-3}$

The first order dependence in [DCT], fractional order in [CH] and almost zero order in $[H^+]$ in the

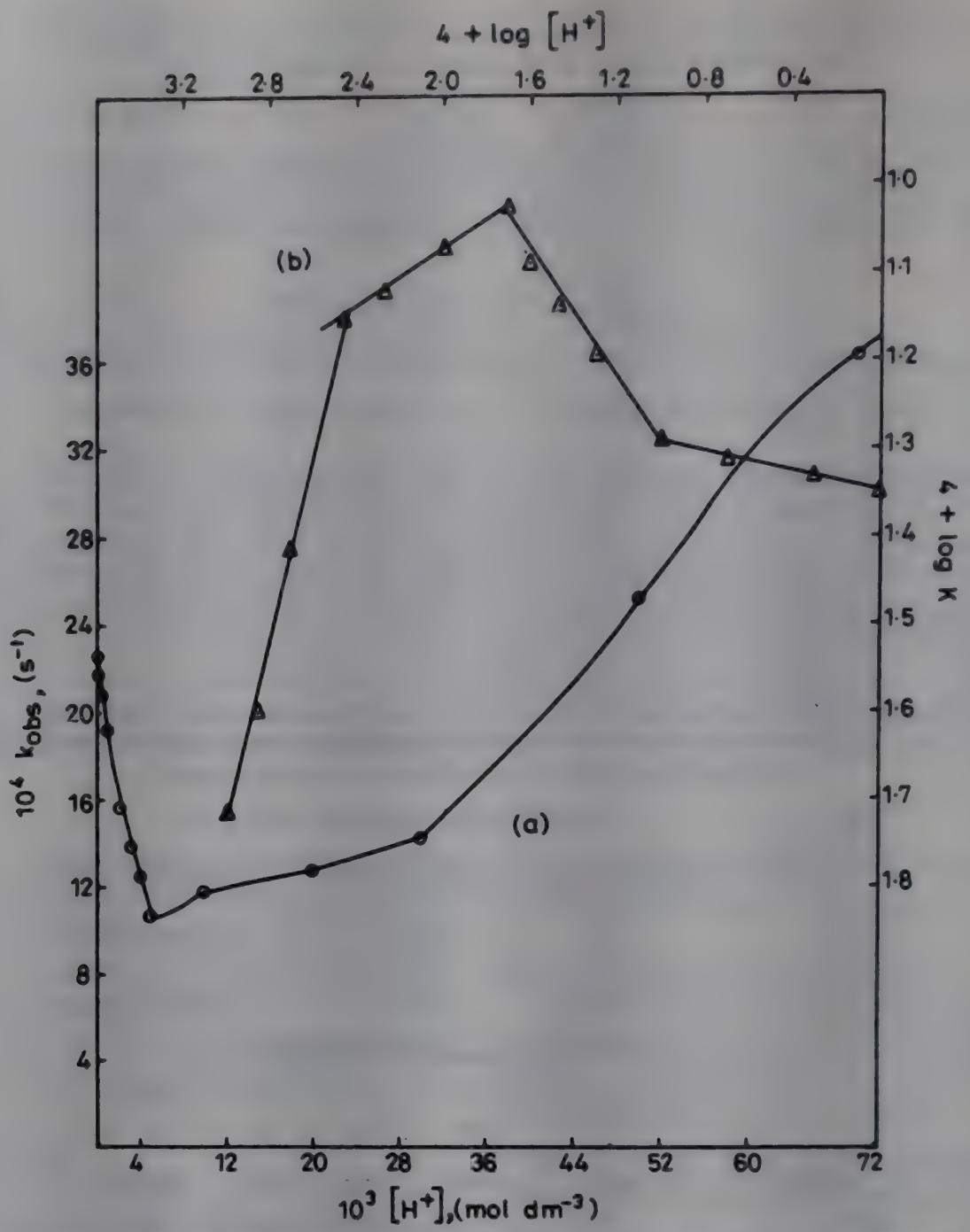

Fig. 1—Plots of (a) k_{obs} versus $[H^+]$, (b) $\log k_{obs}$ versus $\log[H^+]$ ($10^3[DCT]_0 = 10[CH]_0 = 1.0$ mol dm^{-3}, temp. 283K)

above acidity range may be explained by a two-pathway mechanism (Schemes 1 and 2). Since the plots of k_{obs} versus [CH] were linear with finite intercepts on the ordinate, and the double reciprocal plots wer non-linear, it is likely that most of the oxidant exists in the unprotonated form since $[DCT] > [H^+]$.

$$ArSO_2NCl_2 + CH \xrightarrow{k_1} \text{Products} \quad \ldots \text{(slow)}$$

Scheme 1

$$ArSO_2NCl_2 \xrightarrow{k_2} ArSO_2NCl^- + Cl^+ \quad \ldots \text{(slow)}$$

$$CH + Cl^+ \rightarrow \text{Products} \quad \ldots \text{(fast)}$$

$$ArSO_2NCl^- + H^+ \rightarrow ArSO_2NHCl \quad \ldots \text{(fast)}$$

Scheme 2

where $CH = (H_2NHNCONHNH_2)$

Combined rate law (Eq. 2) is in accord with Schemes 1 and 2.

$$-\frac{d[DCT]}{dt} = k_1[DCT][CH] + k_2[DCT] \quad \ldots (2)$$

or

$$-\frac{1}{[DCT]}\frac{d[DCT]}{dt} = -\frac{d\ln[DCT]}{dt} = k_{obs}$$

$$= k_1[CH] + k_2 \quad \ldots (3)$$

The plots of k_{obs} versus [CH] were linear (Fig. 2) in conformity with the rate law (3). The sl[illegible] and intercept of the plot gave the values of k_1 [illegible]

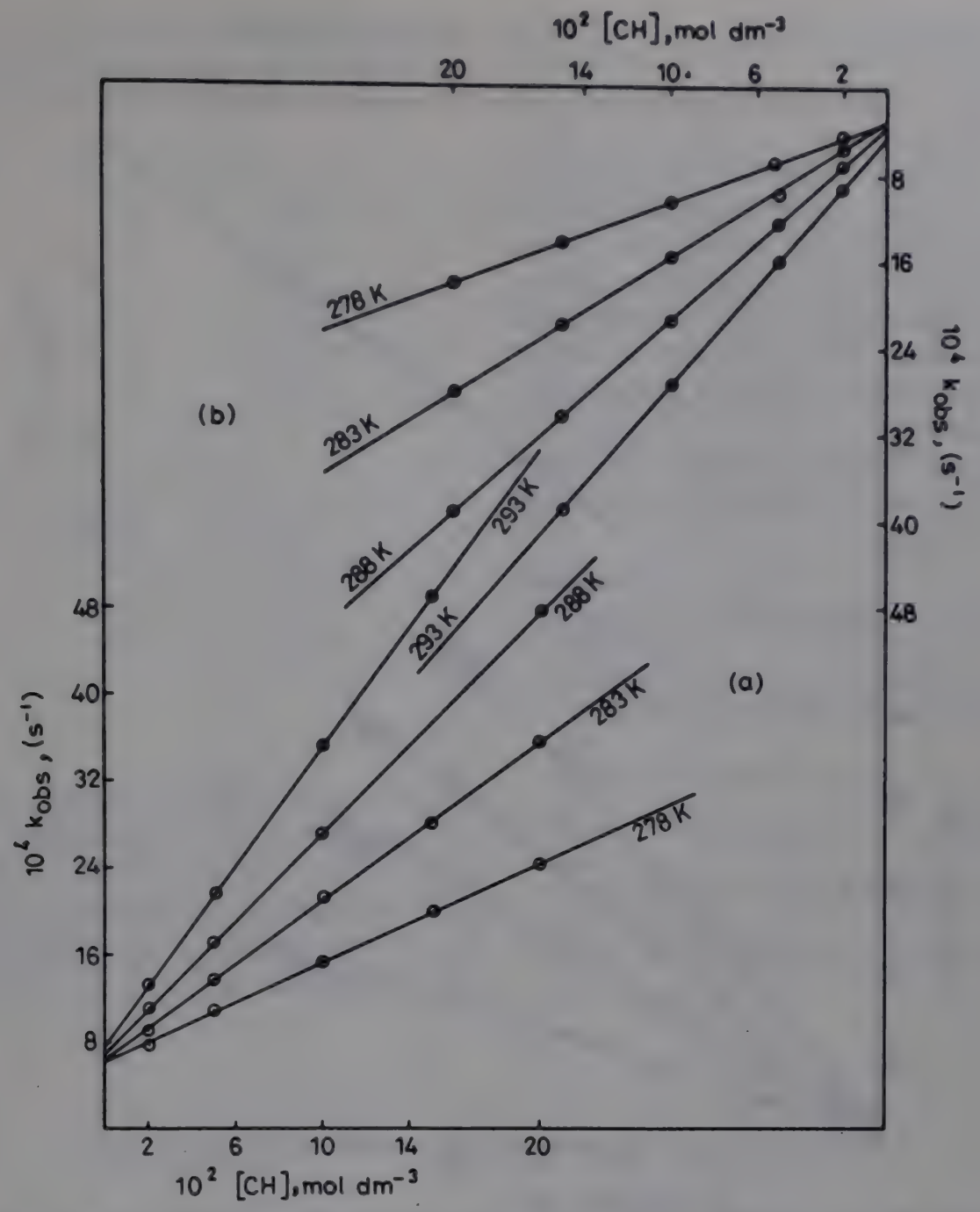

Fig. 2—Plots of k_{obs} versus $[CH]_0$, $10^3[DCT]_0 = 1.0$ mol dm^{-3}, temp. 283K ($10^4[H^+]$ (mol dm^{-3})= (2.0 (a), 20.0 (b))

k_2 respectively. Further CH concentrations were varied at different temperatures and the constants k_1 and k_2 were calculated at each temperature. The latter constants were used to compute the activation parameters from the plots of $\log k_x$ versus $1/T$ and $\log(k_x/T)$ versus $1/T$ (Table 2).

(ii) At $[HClO_4]$ in the range of 0.0005-0.005 mol dm^{-3}

At $[H^+] > 0.0005$ mol dm^{-3}, the rate decreased with an inverse fractional order dependence in $[H^+]$, orders in [DCT] and [CH] being first and fractional respectively. These results can also be accounted for by a two-pathway mechanism (Schemes 3 and 4). Under these conditions the oxidant may exist mostly in the protonated form.

$$ArSO_2NHCl_2^+ \rightleftharpoons^{K_3} ArSO_2NCl_2 + H^+ \quad \ldots \text{(fast)}$$

$$ArSO_2NCl_2 + CH \xrightarrow{k_4} \text{Products} \quad \ldots \text{(slow)}$$

Scheme 3

$$ArSO_2NHCl_2^+ \xrightarrow{k_5} ArSO_2NHCl + Cl^+ \quad \ldots \text{(slow)}$$

$$Cl^+ + CH \rightarrow \text{Products} \quad \ldots \text{(fast)}$$

Scheme 4

Based on Schemes 3 and 4 the combined rate law (4) has been deduced.

$$-\frac{d[DCT]}{dt} = \frac{K_3 k_4 [DCT]_0 [CH]}{K_3 + [H^+]} + k_5[DCT] \quad \ldots (4)$$

or

$$k_{obs} = \frac{K_3 k_4 [CH]}{K_3 + [H^+]} + k_5 \quad \ldots (5)$$

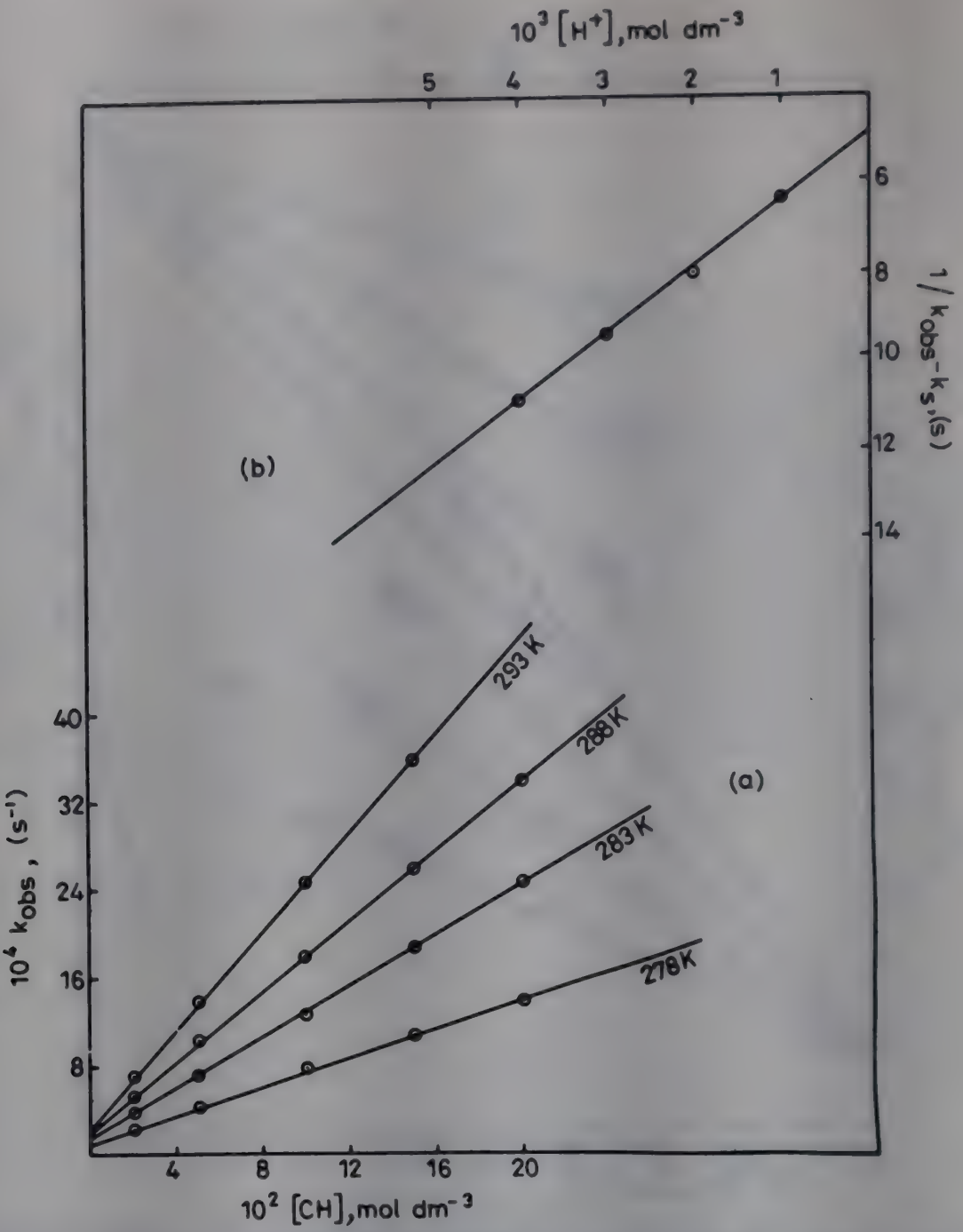

Fig. 3(a)—Plots of k_{obs} versus $[CH]_0$, ($10^3[DCT]_0 = 50[H^+] = 1.0$ mol dm^{-3}, temp. 283K.)

Fig. 3(b)—Plots of $1/(k_{obs} - k_5)$ versus $[H^+]$, ($10^3[DCT]_0 = 10[CH]_0 = 1.0$ mol dm^{-3}, temp. 283K.)

The plots of k_{obs} versus [CH] at fixed $[H^+]$ were linear (Fig. 2) with intercepts on the ordinate (k_5). Equation (5) may be rearranged as

$$\frac{1}{(k_{obs} - k_5)} = \frac{[H^+]}{K_3 k_4 [CH]} + \frac{1}{k_4 [CH]} \quad \ldots (6)$$

At fixed [CH], the plot of $1/(k_{obs} - k_5)$ versus $[H^+]$ was linear (Fig. 3), in conformity with rate law (6). The ratio of intercept to slope of the plot gave K_3, and k_4 was calculate from the intercept at fixed $[CH]_0$. To check the consistency of rate law (5), the constants K_3, k_4 and k_5 were used to calculate the rate constants at varying [CH] and $[H^+]$ (Table 3). Reasonable agreement between calculated and experimental values prove the validity of rate law (5). Further the constants $K(= K_3 k_4 / K_3 + [H^+])$ and k_5 were calculated at different temperatures at varying [CH] and two sets of activation parameters corresponding to K and k_5 paths were computed (Table 2).

Although one may think that the kinetic results under these conditions may as well be explained by a steady state mechanism, this possibility is ruled out as the plots of $1/k_{obs}$ versus 1/[CH] were non-linear. But, instead, the direct plots were perfectly linear (Fig. 2b).

(iii) At $[HClO_4]$ in the range of 0.005-0.030 *mol dm^{-3}*

At this acidity equilibrium step in Scheme 3 lies towards left. Hence the reactive species is likely to

Table 3—Comparison of calculated and experimental rate constants for oxidation of carbohydrazide by dichloramine—T as [CH] and [H^+] were varied

$10[CH]_0$ (mol dm^{-3})	$10^4 k_a(s^{-1})$	
	Calc.	Expt.
0.2	5.7	5.8
0.5	9.9	10.0
1.0	15.9	15.7
1.5	22.3	22.3
2.0	28.6	28.2
$10^3[H^+]$ (mol dm^{-3})		
1.0	19.0	19.1
2.0	15.9	15.7
3.0	13.8	13.9
4.0	12.3	12.4

[a]Please see Eq. (5)

be $ArSO_2NHCl_2^+$ instead of $ArSO_2NCl_2$. The first order in [DCT], fractional order in [CH] and almost zero order in [H^+] observed under these conditions may be explained by mechanisms similar to those represented by Schemes 1 and 2, (replacing $ArSO_2NCl_2$) in the latter scheme by $ArSO_2NHCl_2^+$). The end product of the oxidant under these conditions would be $ArSO_2NH_3^+$.

The [substrate] was varied at different temperatures even under these conditions. The constants k_1 and k_2 at different temperatures were calculated from the plots of k_{obs} versus [CH] (Fig. 3). The latter values were employed to compute the activation parameters which are listed in Table 2. The free energies of activation are almost constant (Table 2) indicating that similar mechanisms are operative in all the cases. Relatively larger negative entropies of activation may indicate that the transition states are more ordered than reactants due to decrease in the number of degrees of freedom.

References

1 Gowda B T & Ramachandra P, *J chem Soc, Perkin Trans* 2, (1989) 1067.

2 Gowda B T & Bhat J I, *Tetrahedron*, 43 (1987) 2119; *Indian J chem*, 27A (1988) 597; *Int J chem Kinet*, 21 (1989) 621.

3 Gowda B T & Rao R V, *J chem Soc, Perkin Trans* 2, (1988) 355.

4 Gowda B T & Sherigara B S, *Int J chem Kinet*, 21 (1989) 31.

5 Gowda B T & Sherigara B S, *Indian Acad Sci*, (Chem Sci), 101 (1989) 155.

6 Gowda B T & Sherigara B S, *J Indian chem Soc*, 66 (1989) 91.

Indian Journal of Chemistry
Vol. 29A, July 1990, pp. 686-692

A study of ternary metal-xanthosine complexes in solution—Thermodynamic aspects

P Rabindra Reddy*, K Venugopal Reddy, M Harilatha Reddy & K Sudhakar

Department of Chemistry, Osmania University, Hyderabad 500 007

Received 19 June 1989; revised 3 October 1989; accepted 15 November 1989

The stability constants of the ternary complexes (1:1:1) of Cu(II), Ni(II), Zn(II), Co(II), Mn(II), Mg(II) and Ca(II) with xanthosine and a secondary ligand (histidine, histamine, catechol and glycine) have been determined potentiometrically at 25, 35 and 45°C at an ionic strength $\mu = 0.10$ M (KNO_3). These ternary complexes have been found to be more stable than the corresponding binary complexes as shown by the positive value of $\Delta \log K$. The enthalpy (ΔH_f^0) changes associated with the ternary complexes of xanthosine have been calculated from the 1:1:1 stability data by the temperature coefficient method. With the help of these thermodynamic parameters, we have evaluated $\Delta\Delta H_f^0$ and $\Delta\Delta S_f^0$, to explain the extra stability found in these ternary complexes.

The current interest in ternary metal ion-nucleoside complexes can be attributed to the fact that these complexes can be regarded as simple models for many metalloenzyme reactions. We have been interested in the study of such metal nucleoside complexes for sometime[1-9]. The role of secondary ligands seems to be most important in controlling the structure and stability of metal-nucleoside complexes. The extra stability of these ternary complexes is usally measured in terms of $\Delta \log K$, the $\Delta \log K$ being the difference between the stability constants of ternary and binary systems. However, this stabilization can also be quantised in terms of $\Delta\Delta H_f^0$ and $\Delta\Delta S_f^0$ (ref. 3, 10-13), the difference in the corresponding ternary and binary enthalpy and entropy changes. Since these quantities directly measure the differences in the energies of bond breaking and bond making, the knowledge of these quantities will lead to a more comprehensive understanding of metal-ligand interactions in solution.

In the present paper, we report the results of our studies on the interactions of Cu(II), Ni(II), Zn(II), Co(II), Mn(II), Mg(II) and Ca(II) with xanthosine as primary ligand and histidine, histamine, catechol and glycine as secondary ligand. Based on temperature coefficient data, the thermodynamic parameters have been evaluated. An attempt has been made to discuss various aspects of metal-nucleoside interactions in solution.

Materials and Methods

Xanthosine, histidine and glycine were obtained from M/s Sigma Chemical Company (USA) while catechol was a Fluka (Switzerland) reagent. Transition and alkaline earth metal ions were of AR grade and the concentrations of metal stock solutions were determined by volumetric titration with disodium salt of EDTA in the presence of a suitable indicator as outlined by Schwarzenbach[14].

The experimental method employed consisted of potentiometric titration of the metal ion-xanthosine and the secondary ligands-histidine, histamine, catechol and glycine in a 1:1:1 ratio with standard carbonate free NaOH. All the titrations were carried out at 25, 35 and 45° ±0.1°C and $\mu = 0.10$ M (KNO_3), the details of which have been reported elsewhere[3].

Calculations

Dissociation constants

The acid dissociation constants of the ligands-xanthosine, histidine, histamine, catechol and glycine were calculated[15] by the usual algebraic method (Table 1). Briefly the acid dissociation constants for the two dissociable protons of H_2L or H_2A are related to the equilibrium expressions:

$$H_2L \overset{K_a}{\rightleftharpoons} HL^- + H_+ \quad \ldots (a)$$

$$HL^- \overset{K_{2a}}{\rightleftharpoons} L^{2-} + H^+ \quad \ldots (b)$$

The constants K_a and K_{2a} were calculated by the following expressions

Table 1—Proton dissociation constants of various ligands [Temp = 25-45°; μ = 0.10*M* (KNO_3)]

Ligand	Temp. °C	pK_a	pK_{2a}
Xanthosine	25	5.58 ± 0.04	9.92 ± 0.02
	35	5.56 ± 0.04	9.90 ± 0.02
	45	5.43 ± 0.04	9.47 ± 0.02
Glycine	25	2.51 ± 0.02	9.87 ± 0.02
	35	2.33 ± 0.02	9.75 ± 0.02
	45	2.19 ± 0.02	9.67 ± 0.02
Histidine	25	6.26 ± 0.02	9.18 ± 0.02
	35	6.00 ± 0.04	9.00 ± 0.04
	45	5.74 ± 0.01	8.81 ± 0.01
Histamine	25	6.03 ± 0.02	9.97 ± 0.02
	35	5.87 ± 0.02	9.63 ± 0.02
	45	5.67 ± 0.02	9.51 ± 0.02
Catechol	25	9.42 ± 0.04	11.16 ± 0.04
	35	9.21 ± 0.05	11.00 ± 0.05
	45	8.99 ± 0.05	10.90 ± 0.05

$$K_a = \frac{[H^+](aT_L + [H^+] - [OH^-])}{T_L - (aT_L + [H^+] - [OH^-])}$$

$$K_{2a} = \frac{[H^+]\{(a-1)T_L + [H^+] - [OH^-]\}}{T_L - \{(a-1)T_L + [H^+] - [OH^-]\}}$$

where 'T_L' and 'a' represent the total concentration of ligand species and the number of moles of base added per mole of ligand, respectively.

Formation constants

To calculate the stability constants of the ternary complexes of Cu(II), Ni(II), Zn(II), Co(II) and Mn(II) with xanthosine and histamine in a 1:1:1 ratio the following equations were used (charges are not shown):

$$M + H_2L + H_2A \rightleftharpoons [M(HL)A] + 3H^+ \quad \ldots (1)$$

or

$$M + HL + A \overset{K^{M}_{M(HL)A}}{\rightleftharpoons} [M(HL)A] \quad \ldots (2)$$

where

$$K^{M}_{M(HL)A} = \frac{T_M - [L]X_A}{[L]^3 X_A^2} \cdot X_L \quad \ldots (3)$$

$$[L] = \frac{6T_M - (2mT_M - 2[H^+] + 2[OH^-]}{\alpha_A + 3\alpha_L(X_A/X_L) + (X_A/X_L)}$$

$$X_A = \frac{[H^+]}{K_a K_{2a}} + \frac{[H^+]}{K_{2a}} + 1$$

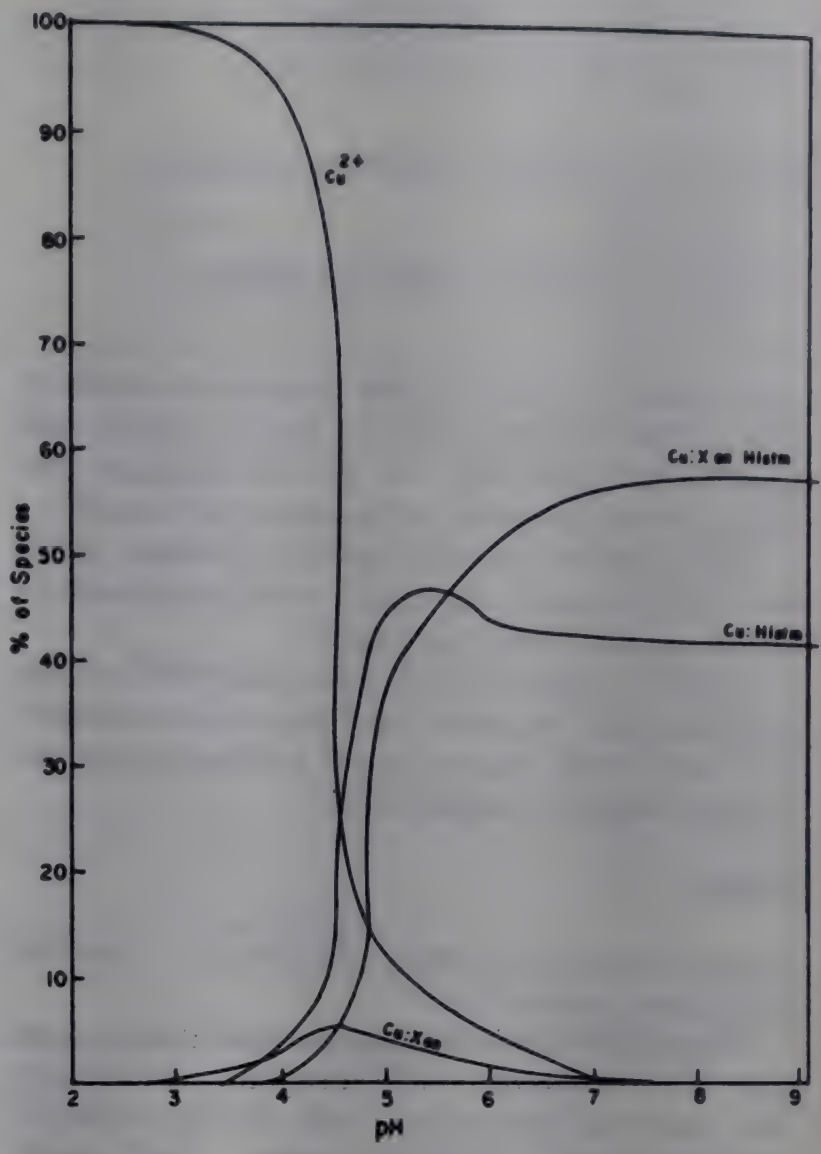

Fig. 1—Species distribution curve of Cu(II): xanthosine:histamine (1:1:1) ternary system

$$\alpha_A = \frac{3[H^+]^2}{K_a K_{2a}} + \frac{[H^+]}{K_{2a}} - 1$$

$$\alpha_L = \frac{[H^+]}{K_a} \text{ and } X_L = \frac{[H^+]}{K_a} + 1$$

T_M = total metal ion concentration and m = moles of base added per mole of metal ion.

The subscripts L and A represent xanthosine and histamine respectively. The constants K^{M}_{MH2LA} and $K^{MH_2LA}_{MLA}$ for the ternary complexes of Mg(II) and Ca(II) with xanthosine and histamine were calculated using Eqs. (4-6) and equations from ref. 4.

$$M + H_2L + H_2A \rightleftharpoons [MH_2LA] + 2H^+ \quad \ldots (4)$$

$$M + HA + HL \overset{K^{M}_{MH_2LA}}{\rightleftharpoons} [MH_2LA] \quad \ldots (5)$$

$$K^{M}_{MH_2LA} = \frac{T_M - [HL]}{[HL]^3[X]^2} \cdot X \quad \ldots (6)$$

where

$$[HL]=\frac{(2-m)T_M-[H^+]+[OH^-]}{([H^+]/K_{aL})+(X/Y)([H^+]/K_{aA})}$$

$$X=\frac{[H^+]}{K_{aL}}+1 \text{ (using } K_a \text{ value of xanthosine)}$$

$$Y=\frac{[H^+]}{K_{aA}}+1 \text{ (using } K_a \text{ value of histamine)}$$

The stability constants of the ternary complexes of Cu(II), Ni(II), Zn(II), Co(II), Mn(II), Mg(II) and Ca(II) with xanthosine and glycine, histidine and catechol were calculated as described previously[5].

The pertinent thermodynamic constants ΔH_f^0, ΔG_f^0, ΔS_f^0, $\Delta\Delta H_f^0$ and $\Delta\Delta S_f^0$ were calculated using temperature coefficient data[3].

Stability constants were calculated with suitable computational programs and the species distribution curves with respect to *p*H were calculated using the computer program BEST[16].

Results

Metal-xanthosine-histidine, -histamine, −catechol and glycine systems (1:1:1)

The mixed ligand titration curves of xanthosine with Cu(II)-histidine, Ni(II)-histidine, Zn(II)-histidine and Co(II)-histidine, with Cu(II)-histamine, Ni(II)-histamine, Zn(II)-histamine, Co(II)-histamine, Mn(II)-histamine and with Cu(II)-catechol in a 1:1:1 ratio at 25, 35 and 45°C gave inflection at $m=3$ indicating simultaneous formation of 1:1:1 mixed ligand complexes between $m=0$ and $m=3$. This assumption is further substantiated by the species distribution curves (Fig. 1). The corresponding tentative structure is shown as (I). The

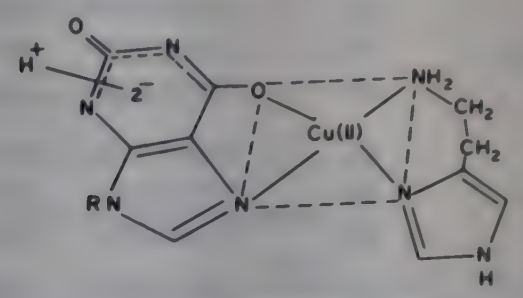

R= Ribose

(I)

mixed ligand titration curves of Cu(II)- and Ni(II)-xanthosine and -glycine showed inflection at $m=2$ indicating the formation of 1:1:1 mixed ligand complex in the region between $m=0$, $m=2$. The constant K^M_{MHLA} was calculated using Eqs (1-5). The titration curves of xanthosine with Mn(II)-histidine, Mg(II)-histidine, Ca(II)-histidine gave inflections at $m=2$ and $m=3$ whereas titration curves of xanthosine with Zn(II)-glycine, Co(II)-glycine, Mn(II)glycine, Mg(II)-glycine, Ca(II)-glycine showed inflections at $m=1$ and $m=2$ indicating the formation of a monoprotonated 1:1:1 species from the normal 1:1 metal-histidine or -glycine. Accordingly, the constants K^{MA}_{MHLA} were calculated. However, in the case of Mg(II)-, Ca(II)-xanthosine and -histamine, inflection was obtained at $m=2$.

Table 2—Stability constants and thermodynamic parameters of the ternary (1:1:1) metal complexes of xanthosine with histidine [$\mu=0.10$ $M(KNO_3)$]

Metal ion	25°		35°		45°	
	$\log K^{MA}_{MHLA}$	$\log K^{M}_{MHLA}$	$\log K^{MA}_{MHLA}$	$\log K^{M}_{MHLA}$	$\log K^{MA}_{MHLA}$	$\log K^{M}_{MHLA}$
Cu(II)	—	13.36 ± 0.02	—	13.19 ± 0.08	—	12.84 ± 0.06
		(−47.75 ± 2.17)†	—	(−76.23 ± 0.07)‡		(+96.16 ± 1.98)††
Ni(II)	—	12.06 ± 0.04	—	11.84 ± 0.06	—	11.67 ± 0.04
		(−35.30 ± 1.13)†		(−68.83 ± 0.17)‡		(+112.46 ± 3.30)††
Zn(II)	—	9.14 ± 0.04	—	9.05 ± 0.06	—	8.76 ± 0.04
		(−34.89 ± 3.76)†		(−52.13 ± 0.17)‡		(+57.86 ± 12.09)††
Co(II)	—	10.23 ± 0.04	—	10.11 ± 0.05	—	10.01 ± 0.04
		(−19.92 ± 0.33)†		(−58.37 ± 0.17)‡		(+129.03 ± 0.54)††
Mn(II)	2.98 ± 0.05	—	2.90 ± 0.06	—	2.80 ± 0.06	—
	(−16.37 ± 0.90)†		(−17.00 ± 1.01)‡		(+2.08 ± 0.02)††	
Mg(II)	2.58 ± 0.05	—	2.79 ± 0.06	—	2.88 ± 0.06	
	(+26.97 ± 3.35)†		(−14.73 ± 0.21)‡		(+139.99 ± 10.37)††	
Ca(II)	2.82 ± 0.05	—	2.76 ± 0.03	—	2.66 ± 0.06	—
	(−14.60 ± 1.17)†		(−16.08 ± 2.01)‡		(+4.98 ± 0.81)††	

†ΔH_f^0 values in kJ mol^{-1}; ‡ΔG_f^0 values of kJ mol^{-1} at 25°C; ††ΔS_f^0 values at 25°C in J mol^{-1} degree^{-1}.

Table 3—Stability constants and thermodynamic parameters of the ternary (1:1:1) complexes of xanthosine with histamine

[$\mu = 0.10 M(KNO_3)$]

Metal ion	25° $\log K^{M}_{MHLA}$		35° $\log K^{M}_{MHLA}$		45° $\log K^{M}_{MHLA}$	
Cu(II)	—	13.06 ± 0.02	—	12.48 ± 0.08	—	12.08 ± 0.02
		(−88.62 ± 4.52)†		(−74.52 ± 0.08)‡		(−47.32 ± 14.47)††
Ni(II)	—	10.92 ± 0.03	—	10.63 ± 0.08	—	10.23 ± 0.08
		(−62.84 ± 4.06)†		(−62.30 ± 0.13)‡		(−1.84 ± 13.18)††
Zn(II)	—	9.18 ± 0.06	—	8.87 ± 0.08	—	8.47 ± 0.08
		(−64.60 ± 2.22)†		(−52.38 ± 0.25)‡		(−41.00 ± 6.61)††
Co(II)	—	8.88 ± 0.06	—	8.62 ± 0.08		8.22 ± 0.08
		(−60.21 ± 3.72)†		(−50.67 ± 0.25)‡		(−32.00 ± 11.69)††
Mn(II)	—	8.96 ± 0.06	—	8.72 ± 0.08	—	8.32 ± 0.08
		(−58.41 ± 3.76)†		(−51.13 ± 0.25)‡		(−24.43 ± 11.79)††
	$\log K^{M}_{MH_2LA}$	$\log K^{MH_2LA}_{MLA}$	$\log K^{M}_{MH_2LA}$	$\log K^{MH_2LA}_{MLA}$	$\log K^{M}_{MH_2LA}$	$\log K^{MH_2LA}_{MLA}$
Mg(II)	7.14 ± 0.04	8.17 ± 0.08	7.24 ± 0.06	8.27 ± 0.08	7.35 ± 0.06	8.42 ± 0.08
	(+18.99 ± 1.01)†	(+22.80 ± 1.71)†	(−40.58 ± 0.25)‡	(−46.61 ± 0.35)‡	(+199.66 ± 10.21)††	(+232.92 ± 6.86)††
Ca(II)	7.90 ± 0.05	9.11 ± 0.06	7.67 ± 0.06	8.89 ± 0.07	7.47 ± 0.05	8.61 ± 0.06
	(−40.88 ± 3.51)†	(−45.22 ± 2.24)†	(−44.89 ± 0.25)‡	(−51.97 ± 0.25)‡	(+13.47 ± 4.01)††	(+21.63 ± 7.03)††

†ΔH^0_f values in kJ mol^{-1}; ‡ΔG^0_f values in kJ mol^{-1} at 25°C; ††ΔS^0_f values at 25°C in J mol^{-1}deg^{-1}.

Table 4—Stability constants and thermodynamic parameters of the ternary metal complexes (1:1:1) of xanthosine with catechol

[$\mu = 0.10\ M(KNO_3)$]

Metal ion	25°		35°		45°	
	$\log K^{M}_{MH_2LA}$	$\log K^{M}_{MHLA}$	$\log K^{M}_{MH_2LA}$	$\log K^{M}_{MHLA}$	$\log K^{M}_{MH_2LA}$	$\log K^{M}_{MHLA}$
Cu(II)	—	16.58 ± 0.04	—	16.36 ± 0.09	—	16.14 ± 0.04
		(−39.92 ± 0.42)†		(−94.60 ± 0.17)‡		(+184.51 ± 1.84)††
Ni(II)	10.38 ± 0.04	—	10.13 ± 0.05	—	9.88 ± 0.06	—
	(−45.39 ± 0.50)†		(−59.20 ± 0.17)‡		(+46.32 ± 1.13)††	
Zn(II)	10.54 ± 0.04	—	10.28 ± 0.05	—	10.02 ± 0.05	—
	(−47.19 ± 0.50)†		(−60.12 ± 0.17)‡		(+43.39 ± 1.13)††	
Co(II)	9.24 ± 0.04	—	9.08 ± 0.06	—	8.96 ± 0.04	—
	(−23.35 ± 0.96)†		(−52.72 ± 0.17)‡		(+91.84 ± 2.68)††	
Mn(II)	9.13 ± 0.04	—	8.94 ± 0.08	—	8.83 ± 0.06	—
	(−27.07 ± 1.05)†		(−52.09 ± 0.17)‡		(+83.97 ± 2.93)††	
Mg(II)	7.06 ± 0.06	—	7.27 ± 0.06	—	7.49 ± 0.06	
	(+39.04 ± 0.84)†		(−40.29 ± 0.25)‡		(+266.18 ± 3.65)††	
Ca(II)	5.62 ± 0.04	—	5.45 ± 0.03	—	5.34 ± 0.06	—
	(−25.31 ± 0.08)†		(−32.05 ± 0.17)‡		(+22.59 ± 2.38)††	

†ΔH^0_f values in kJ mol; ‡ΔG^0_f values in kJ mol^{-1} at 25°; ††ΔS^0_f values at 25°C in J mol^{-1}deg^{-1}.

Therefore, the formation of a diprotonated (MH_2LA) ternary complex was assumed between $m = 0$ and $m = 2$ and the constant $K^{M}_{MH_2LA}$ was calculated. In the buffer region between $m = 2$ and $m = 4$ simple dissociation of the diprotonated ternary complex was assumed and the constant $K^{MH_2LA}_{MLA}$ calculated. Ni(II)-catechol, Zn(II)-catechol, Co(II)-catechol, Mn(II)-catechol, Mg(II)-catechol, Ca(II)-xanthosine-catechol system followed pattern similar to that of Mg(II)-xanthosine-histamine system. All the stability constants and thermodynamic parameters are given in Tables 2-5.

Table 5—Stability constants and thermodynamic parameters of the ternary (1:1:1) metal complexes of xanthosine with glycine [$\mu = 0.10\ M(KNO_3)$]

Metal ion	25°		35°		45°	
	$\log K^{MA}_{MHLA}$	$\log K^{M}_{MHLA}$	$\log K^{MA}_{MHLA}$	$\log K^{M}_{MHLA}$	$\log K^{MA}_{MHLA}$	$\log K^{M}_{MHLA}$
Cu(II)	—	12.96 ± 0.08 (−43.89 ± 2.17)†	—	12.82 ± 0.10 (−73.93 ± 0.33)‡	—	12.48 ± 0.08 (+100.79 ± 6.19)††
Ni(II)	—	11.08 ± 0.06 (−28.95 ± 0.92)†	—	10.91 ± 0.10 (63.22 ± 0.25)‡	—	10.76 ± 0.06 (+114.98 ± 2.26)††
Zn(II)	2.86 ± 0.04 (−11.84 ± 0.46)†	—	2.81 ± 0.09 (−16.32 ± 0.17)‡	—	2.73 ± 0.04 (+15.02 ± 0.96)††	—
Co(II)	3.15 ± 0.06 (−17.26 ± 0.75)	—	3.06 ± 0.10 (−17.97 ± 0.31)‡	—	2.96 ± 0.05 (+2.32 ± 0.86)††	—
Mn(II)	2.86 ± 0.05 (−12.76 ± 1.59)†	—	2.80 ± 0.08 (−16.32 ± 0.21)‡	—	2.72 ± 0.06 (+11.92 ± 4.64)††	—
Mg(II)	2.39 ± 0.05 (+15.35 ± 1.38)†	—	2.52 ± 0.08 (−13.64 ± 0.21)‡	—	2.56 ± 0.04 (+96.92 ± 7.45)††	—
Ca(II)	2.72 ± 0.06 (−14.35 ± 2.30)†	—	2.64 ± 0.08 (−15.51 ± 0.25)‡	—	2.56 ± 0.04 (+3.34 ± 0.91)††	—

†ΔH^0_f values in kJ mol^{-1}; ‡ΔG^0_f values in kJ mol^{-1} at 25°; ††ΔS^0_f values at 25°C in J mol^{-1}deg^{-1}.

Table 6—$\Delta \log K$ values

Systems	Temp °C	Cu	Ni	Zn	Co	Mn	Mg	Ca
Metal-xanthosine-histidine	25	+0.15	+0.56	+0.41	+0.94	+0.50	+0.36	+0.45
	35	+0.11	+0.50	+0.49	+0.60	+0.33	+0.56	+0.55
	45	+0.53	+0.96	+0.40	+1.38	+0.27	+0.49	+0.35
Metal-xanthosine-histamine	25	+0.99	+1.48	+0.60	+0.57	—	+2.60	+3.11
	35	+0.44	+1.35	+0.55	+0.13	—	+2.57	+3.14
	45	+0.47	+1.27	+0.36	+0.22	—	+2.44	+3.00
Metal-xanthosine-catechol	25	+1.55	+2.72	+3.12	+2.48	—	—	—
	35	+1.35	+2.62	+2.99	+2.17	—	—	—
	45	+1.59	+2.65	+2.84	+2.52	—	—	—
Metal-xanthosine-glycine	25	+1.14	+2.18	+0.60	+0.97	+0.38	+0.17	+0.35
	35	+1.15	+2.07	+0.60	+0.51	+0.23	+0.59	+0.43
	45	+1.32	+2.25	+0.57	+0.70	+0.23	+0.17	+0.35

Discussion

Our results on the dissociation and 1:1 stability constants of histidine, histamine, catechol and glycine with metal ions agree well with those reported in the literature[17-23].

All the ternary complexes studied in this investigation have been found to be more stable than the corresponding binary complexes as seen by the positive $\Delta \log K$ values (Table 6). The ternary complexes of metal-xanthosine with aromatic ligands-(histidine, histamine or cathechol) are more stable than those with the aliphatic ligand-(glycine). This is because of the fact that the ligands (histidine, histamine and catechol) can take part in stacking interactions with xanthosine, whereas glycine being aliphatic cannot take part in such interactions. Another reason for greater stability of histidine, histamine and catechol complexes compared to those of the glycine complexes is due to the difference in π-accepting capacities of the ligands concerned. The former ligands are good π-acceptors whereas the latter is a poor one.

The thermodynamic data for the mixed ligand complexes of Cu(II), Ni(II), Zn(II), Co(II), Mn(II), Mg(II) and Ca(II) with xanthosine and various secondary ligands-histidine, histamine, catechol and

Table 7—Differences of enthalpy and entropy changes between the binary and ternary complexes of xanthosine in solution [$\mu = 0.10M(KNO_3)$]

Metal ion	$\Delta\Delta H_f^0$ (kJ mol^{-1})			$\Delta\Delta S_f^0$ (J mol^{-1}degree^{-1})		
	$K^{MA}_{MHLA} - K^{M}_{MHL}$			$K^{MA}_{MHLA} - K^{M}_{MHL}$		
	M-xan-gly	M-xan-histi	M-xan-hista	M-xan-gly	M-xan-histi	M-xan-hista
Cu(II)	—	—	—	—	—	—
Ni(II)	—	—	—	—	—	—
Zn(II)	−2.64	—	—	+2.05	—	—
Co(II)	−28.66	—	—	+5.98	—	—
Mn(II)	−10.67	−17.99	—	+2.72	+5.10	—
Mg(II)	−0.13	+11.51	+8.70	+1.95	+44.60	+137.53
Ca(II)	−7.66	−7.36	−38.83	+4.27	+2.43	+3.14

glycine-given in Tables 2, 3, 4 and 5 in general, show negative enthalpy (ΔH_f^0) values except for Mg(II) and positive entropy (ΔS_f^0) values for all the 1:1:1 systems studied except for Cu(II), Ni(II), Zn(II), Co(II) and Mn(II)-xanthosine-histamine systems, where the entropy values are negative. The values of enthalpy do not show a regular trend of variation for the systems studied. The positive value of ΔH_f^0 for Mg(II) is due to a very high heat of hydration for Mg(II) with smallest ionic radius compared to the other metal ions, a trend also observed in the binary 1:1 complexes.

The comparison of the enthalpy values of these systems indicates that the values for catechol system (Table 4) are less exothermic compared to those for histamine system (Table 3) and the corresponding values for histidine and glycine systems (Table 2 and 5) are intermediate. In the ternary complex formation, the solvent molecules will be displaced from the coordination sphere of the metal-xanthosine (1:1) complex, followed by the coordination of a secondary ligand. Among the secondary ligands studied in this investigation, the driving forces for the formation of mixed ligand complexes with catechol seems to be the entropy contribution rather than enthalpy. This is because the amount of energy required to form the metal-ligand bond in the place of the metal-solvent bond is expected to be similar, since in both the cases oxygen is the donor atom. In the case of histamine system (N−N donor ligand), there is a difference in the energies of the two bonds concerned. So the formation of these complexes seem to be favoured by an enthalpy factor. The enthalpy values for histidine and glycine complexes are intermediate because of the involvement of mixed N/O donor atoms in bonding.

As far as the entropies of formation (ΔS_f^0) of mixed ligand complexes are concerned, they vary from negative values [histamine system] except for Mg(II) and Ca(II)] to highly positive values (catechol system). In the histamine system, the formation of ternary complexes with alkaline earth metal ions seems to be favoured by an entropy factor and this is due to charge neutralization effects, where the overall charge of the ternary complex is uninegative.

In Table 7 are given $\Delta\Delta H_f^0$ and $\Delta\Delta S_f^0$ values for metal-xanthosine with histidine, histamine and glycine systems. It can be seen from the values that in general the $\Delta\Delta H_f^0$ values are negative and $\Delta\Delta S_f^0$ values are positive which indicate that the ternary complexes are stabilized by enthalpy and entropy factors. The more negative values of $\Delta\Delta H_f^0$ for histidine systems compared to those of glycine systems are in accord with the aromaticity of the former ligand, but the values for histidine system are less negative compared to the values for histamine system. This may be explained on the basis of the relative flexibilities of the ligands concerned. The more flexible histamine will stack more effectively with the binary metal-xanthosine complex than histidine, thus resulting in the formation of the more stable ternary complexes of histamine in solution. Previous observations about the dependence of stability[13] and kinetic[24] data on flexibility also support this view. The other ternary systems could not be discussed as the similar data are not available for the binary systems.

Acknowledgement

One of the authors (K S) is grateful to the CSIR, New Delhi, for financial assistance.

References

1 Rabindra Reddy P, Venugopal Reddy K & Taqui Khan M M, *J inorg nucl Chem*, 41 (1979) 423.

2 Rabindra Reddy P & Venugopal Reddy K, *Inorg chim Acta*, 80 (1983) 95.

3 Rabindra Reddy P, Harilatha Reddy M & Venugopal Reddy K, *Inorg Chem*, 23 (1984) 974.

4 Rabindra Reddy P & Harilatha Reddy M, *Polyhedron*, 2 (1983) 1171.

5 Rabindra Reddy P & Harilatha Reddy M, *J chem Soc, Dalton Trans*, (1985) 239.

6 Rabindra Reddy P & Malleswara Rao V B, *Polyhedron*, 4 (1985) 1603.

7 Rabindra Reddy P, Harilatha Reddy M & Prasad Reddy P R, *Proc Indian Acad Sci (Chem Sci)*, 95 (1985) 547.

8 Rabindra Reddy P & Malleswara Rao V B, *J chem Soc Dalton Trans*, (1986) 2331.

9 Rabindra Reddy P & Malleswara Rao V B, *Inorg chim Acta*, 125 (1986) 191.

10 Taqui Khan M M, Satyanarayana M, Jyoti M S & Abraham Lincolon Ch, *Indian J Chem*, 22A (1983) 357.

11 Arena G, Cali R, Cucinotta V, Musumeci S, Rizzarelli E & Sammaratano S, *J chem Soc Dalton Trans*, (1983) 1271.

12 Arena G, Cali R, Cucinotta V, Musumeci S, Rizzarelli E & Sammaratano S, *Thermochim Acta*, 74 (1984) 77.

13 Arena G, Cali R, Cucinotta V, Musumeci S, Rizzarelli E & Sarmmaratano S, *J chem Soc Dalton Trans*, (1984) 1651.

14 Schwarzenbach G, *Complexometric titrations* (Interscience, New York) 1957, 77.

15 Richard C F, Gustafson R L & Martell A E, *J Am chem Soc*, 81 (1959) 1033.

16 Motekaitis R J & Martell A E, *Can J Chem*, 60 (1982) 2403.

17 Gregely A, Nagypal I & Majzes J, *Acta chim Sci hung*, 51 (1967) 381.

18 Martin R P & Paris R A, *Bull Soc chim France*, (1964) 3170.

19 a) Sharma V S, Mathur H B & Kulkarni P S, *Indian J Chem*, 3 (1965) 156.
b) Sharma V S, Mathur H B & Kulkarni P S, *Indian J Chem*, 3 (1965) 475.

20 Heuveux G A L & Martell A E, *J inorg nucl Chem*, 28 (1966) 481.

21 Jameson R J & Neillie W J S, *J inorg nucl Chem*, 28 (1966) 2667.

22 Perrin D D & Sharma V S, *J chem Soc A*, (1967) 724.

23 Chakravorthy A & Cotton F A, *J phys Chem*, 67 (1963) 2878.

24 Cayley G R & Margerum D W, *J chem Soc Chem Commun*, (1974) 1002.

Indian Journal of Chemistry
Vol. 29A, July 1990, pp. 693-696

Notes

Solvation behaviour of some tetraalkylammonium ions in acetonitrile + dimethyl sulphoxide mixtures: Conductance and viscosity measurements at 25°C

V K Syal*, S Chauhan & M S Chauhan
Department of Chemistry, Himachal Pradesh University, Summer Hill, Shimla 171 005

Received 26 May 1989; revised and accepted 21 July 1989

Precise values of conductance and viscosity of Et_4NBr, Pr_4NBr and Bu_4NBr have been measured in the concentration ranges $(1\text{-}30)\times10^{-4}$ and $(20\text{-}200)\times10^{-4}$ $dm^3\ mol^{-1}$, respectively, in acetonitrile (AN), dimethyl sulphoxide (DMSO) and AN + DMSO mixtures at 25°C. The conductance data have been analyzed by the Shedlovsky conductance equation. The limiting ionic conductances (λ_i^0) for Et_4N^+, Pr_4N^+ and Bu_4N^+ ions have been evaluated to calculate the solvated radii (r_i) and the ionic Walden product ($\lambda_i^0\,\eta_0$). The viscosity data have been analyzed by the Jones-Dole equation to evaluate A and B-coefficients. Ionic B_+ values for Et_4N^+, Pr_4N^+ and Bu_4N^+ ions have been calculated from viscosity B-coefficients of the electrolytes and A-coefficients have been compared with theoretically calculated A_η-coefficients. The variation of r_i, B_+ and $\lambda_i^0\,\eta_0$ values have been measured as a function of solvent composition to interpret the solvation pattern of tetraalkylammonium ions in AN + DMSO mixtures.

Most of the physicochemical investigations on tetraalkylammonium ions have been reported either in pure nonaqueous[1-6] or in mixed aqueous + nonaqueous media[7-10]. Only very little experimental data on the solvation behaviour of these ions are available in mixed nonaqueous solvents[11-14]. Therefore, in the present work an attempt has been made to study the solvation behaviour of Et_4N^+, Pr_4N^+ and Bu_4N^+ ions in acetonitrile (AN), dimethyl sulphoxide (DMSO) and in AN + DMSO mixtures on the basis of conductance and viscosity measurements of Et_4NBr, Pr_4NBr and Bu_4NBr.

Experimental

Tetraethylammonium bromide (Et_4NBr) (Sisco, AG), tetrapropylammonium bromide (Pr_4NBr) and tetrabutylammonium bromide (Bu_4NBr) (both Fluka, AG) were dried *in vacuo* at 50-60°C over P_2O_5 for 48 hr. Açetonitrile (AN) (E. Merck) and dimethyl sulphoxide (DMSO) (Sisco, GR) were purified by the method reported earlier[15]. Binary mixtures of these solvents were prepared by weight. The physical properties of these binary solvent mixtures such as dielectric constant (D), viscosity (η_0), density (d) and Bjerrum critical distances[15,16] (q) have been reported elsewhere[17]. The details of conductivity cell, viscometer and the experimental procedure for the conductance and viscosity measurements were the same as reported earlier[15,18]. The overall accuracy of conductance and viscosity measurements was found to be ±0.2% and ±0.1% respectively.

Results and discussion

Conductances and viscosities of Et_4NBr, Pr_4NBr and Bu_4NBr have been measured in the concentration ranges $(1\text{-}30)\times10^{-4}$ $dm^3\ mol^{-1}$ and $(20\text{-}200)\times10^{-4}$ $dm^3\ mol^{-1}$ in AN, DMSO and AN + DMSO mixtures containing 12.0, 33.2, 58.2, 73.4 and 93.2 mol % AN. The conductance data have been analyzed by Shedlovsky conductance equation[19,20] with the help of a computer using a least-squares program suggested by Saloman[21]. The derived values of limiting molar conductance (Λ_0) and the ion-association constants (K_A) of the electrolytes have been reported in Table 1.

Since the precision of present conductance measurements was found not better than ±0.2%, there-

Table 1—Λ_0 ($ohm^{-1}\ cm^2\ mol^{-1}$) and K_A^* ($mol\ dm^{-3}$) values for some tetraalkylammonium salts in AN, DMSO and AN + DMSO mixtures at 25°C derived from the Shedlovsky conductance equation.

Solvent (mol % AN)	Λ_0 ($ohm^{-1}\ cm^2\ mol^{-1}$)		
	Et_4NBr	Pr_4NBr	Bu_4NBr
0.0	41.2	37.7	35.8
	(41.12)[a]	(37.45)[a]	(35.65)[a]
12.0	51.0	46.5	44.3
33.2**	68.1	62.3	58.3
58.2†	100.5	92.6	87.3
73.4‡	123.5	113.9	107.4
93.2††	165.7	151.9	143.0
100.0‡‡	186.5	172.1	163.9
	(185.5)[b]	(171.1)[c]	(162.1)[c]

*K_A values ≤ 10 have no physical significance[20] and have not been reported in this table.

**K_A = 22, †K_A = 20, ‡K_A = 28, ††K_A = 30, ‡‡K_A = 38. (values for Bu_4NBr).

[a]Ref. 34, [b]Ref. 35; value obtained indirectly by adding $\Lambda_0 = \lambda_+^0 + \lambda_-^0$; [c]Ref. 36.

fore, it was thought inappropriate to analyze this conductance data by a complete conductance equation which requires a precision in conductance data much better than ±0.1%. Fuoss and coworkers[22,23] have also preferred to analyze their conductance data in some mixed solvents by a semiempirical conductance equation similar to that given by Shedlovsky instead of using a complete conductance equation. Moreover, the main purpose of the present work was to study the solvation behaviour of ions which is based entirely on the Λ_0 values of the electrolytes. It is well known that all conductance equations (complete or semiempirical) give, after analysis, almost the same Λ_0 values for an electrolyte but different K_A values[24].

The entire viscosity data have been analyzed using the Jones-Dole equation[25] in the form:

$$\frac{\eta/\eta_0 - 1}{C^{1/2}} = BC^{1/2} + A \qquad \ldots (1)$$

where η is the viscosity of electrolyte solution and η_0 is the viscosity of pure solvent or solvent mixture. Since K_A values of Et_4NBr, Pr_4NBr and Bu_4NBr (obtained from their conductance data) were found to be negligible, the analysis of present viscosity data by an extended form of the Jones-Dole equation for associated electrolytes[17] was not thought to be necessary. The plot of $(\eta/\eta_0 - 1)C^{1/2}$ versus $C^{1/2}$ were found to be linear over the whole concentration range of the electrolytes in AN, DMSO and AN + DMSO mixtures. However, the viscosity A- and B-coefficient reported in Table 2 were evaluated by the least-squares treatment. Experimentally determined A-coefficients are compared with A_η-coefficients calculated theoretically using Falkenhagen-Vernon equation. The agreement between A and A_η-coefficients for all the electrolytes in AN, DMSO and AN + DMSO mixtures is reasonably good (Table 2).

The precision of the present conductance and viscosity measurements can be checked by comparing the Λ_0 and B values of Et_4NBr, Pr_4NBr and Bu_4NBr with the corresponding available literature values in AN and DMSO (literature Λ_0 and B values are reported in parentheses in Tables 1 and 2).

Ion solvation in AN + DMSO mixtures

In order to derive information about the solvation behaviour of ions from experimentally determined Λ_0 and B values of the electrolytes, it is essential to resolve these functions into the ionic λ_i^0 and $B_\pm$ components. λ_i^0 and $B_\pm$ values have been used as probes for getting insight into the dynamic aspect of ion-solvent interactions, because cation-solvent and anion-solvent interactions are known to be different[26].

Taking previously evaluated λ_i^0 values of Br^- ion in AN, DMSO and AN + DMSO mixtures[27], we have computed the λ_i^0 values of Et_4N^+, Pr_4N^+ and Bu_4N^+ ions from the Λ_0 values of Et_4NBr, Pr_4NBr and Bu_4NBr by using Kohlrausch's law of independent ionic conductances. Similarly, B_+ values of Et_4N^+, Pr_4N^+ and Bu_4N^+ ions have been obtained from B values of Et_4NBr, Pr_4NBr and Bu_4NBr by substracting B_- values of Br^- ion already reported from our laboratory in AN, DMSO and AN + DMSO mixtures[27]. The λ_i^0 and B_+ values thus obtained have been reported in Table 3. The λ_i^0 and B_+ values in AN and DMSO are also found to agree fairly well with the available literature values. Literature values are reported in parentheses in Table 3.

Using λ_i^0 values of Et_4N^+, Pr_4N^+ and Bu_4N^+ ions from Table 3, we have calculated the solvated radii

Table 2—Viscosity B* ($dm^3\ mol^{-1}$) and A* $(dm^3\ mol^{-1})^{1/2}$-coefficients of the Jones-Dole equation and theoretically calculated A_η-coefficients of some tetraalkylammonium salts in AN, DMSO and AN + DMSO mixtures at 25°C

Solvent (mol % AN)	Et_4NBr			Pr_4NBr			Bu_4NBr		
	B	10^2 A	10^2 A_η	B	10^2 A	10^2 A_η	B	10^2 A	10^2 A_η
0.00	0.78	1.0	1.08	0.86	1.2	1.20	0.97	1.3	1.28
12.0	0.79	1.0	1.1	0.87	1.3	1.22	0.98	1.3	1.30
33.2	0.77	1.2	1.18	0.85	1.4	1.35	0.96	1.3	1.44
58.2	0.75	1.3	1.28	0.82	1.5	1.47	0.95	1.6	1.56
73.4	0.76	1.4	1.38	0.83	1.7	1.56	0.95	1.6	1.65
93.2	0.73	1.6	1.55	0.81	1.7	1.69	0.94	1.7	1.80
100.0	0.70	1.8	1.57	0.79	1.7	1.71	0.93	1.8	1.81
	(0.69)[a]			(0.77)[a]			(0.93)[a]		

[a]Ref. 37

*The maximum uncertainty of viscosity B and A-coefficients reported in this table is ±0.03 $dm^3\ mol^{-1}$ and ±10% respectively.

Table 3—λ_i^0 (ohm^{-1} cm^2 mol^{-1}), r_i (Å), B_+ (dm^3 mol^{-1}) and ionic Walden product ($\lambda_i^0\,\eta_0$) values for some tetraalkylammonium ions in AN, DMSO and AN + DMSO mixtures at 25°C

Solvent (mol % AN)	λ_i^0	r_i	B_+	$\lambda_i^0\,\eta_0$
		Et_4N^+		
0.00	17.1	4.0	0.46	0.340
	(17.4)[a]			
12.0	21.0	4.0	0.45	0.336
33.2	29.4	4.0	0.44	0.323
58.2	44.1	4.0	0.43	0.313
73.4	55.5	4.0	0.42	0.305
93.2	75.9	4.0	0.40	0.296
100.0	85.2	4.0	0.37	0.291
	(84.8)[b]	(4.1)		
		Pr_4N^+		
0.00	13.6	4.6	0.54	0.271
	(13.71)[a]	(4.6)		
12.0	16.6	4.7	0.53	0.266
33.2	23.8	4.6	0.52	0.262
58.2	35.6	4.6	0.50	0.253
73.4	45.5	4.6	0.49	0.250
93.2	62.6	4.6	0.48	0.244
100.0	70.8	4.6	0.46	0.241
	(70.3)[b]	(4.6)		
		Bu_4N^+		
0.00	11.7	5.1	0.65	0.233
	(11.8)[a]	(5.1)		
12.0	14.4	5.1	0.64	0.230
33.2	20.5	5.1	0.63	0.226
58.2	31.3	5.1	0.63	0.222
73.4	39.4	5.1	0.61	0.217
93.2	55.0	5.1	0.60	0.215
100.0	62.6	5.1	0.60	0.213
	(61.7)[c]	(5.1)		

[a]Ref. 39; [b]Ref. 35; [c]Ref. 38.

(r_i) by Gill's modification of the Stoke's law[2] and ionic Walden product ($\lambda_i^0\,\eta_0$) for these ions in AN, DMSO and AN + DMSO mixtures (Table 3).

Before deriving any information about the solvation behaviour of tetraalkylammonium ions from the results of Table 3, we have to consider the fact that the dipole moment data of AN and DMSO ($\mu_{AN} = 3.37$D and $\mu_{DMSO} = 3.90$D)[18] indicate large cationophilicity of DMSO compared to that of AN. However, perusal of Table 3 reveals that the r_i values of Et_4N^+, Pr_4N^+ and Bu_4N^+ ions (r_i value is the measure of ion-solvent interaction) remain practically constant and equal to the corresponding crystallographic radii (r_c) ($Et_4N^+ = 4.0$, $Pr_4N^+ = 4.6$ and $Bu_4N^+ = 5.0$Å)[28] in AN, DMSO and in AN + DMSO mixtures. Eventually, the ionic Walden products and viscosity B_+-coefficients of Et_4N^+, Pr_4N^+ and Bu_4N^+ ions are found to decrease linearly with increasing mole fraction of AN in AN + DMSO mixtures.

It is known that a linear variation of ionic Walden product ($\lambda_i^0\,\eta_0$) and $B_\pm$ values in binary solvent mixture is due to invariance of solvation of ions with cosolvent composition[17,29,30]. Thus, present results also indicate non-solvation of Et_4N^+, Pr_4N^+ and Bu_4N^+ ions in AN, DMSO and AN + DMSO mixtures, which is further substantiated by the fact that the solvated radii of these ions show invariance in AN, DMSO and AN + DMSO mixtures.

It may, therefore, be concluded that the solvation behaviour of tetraalkylammonium ions in pure and in mixed nonaqueous solvents differs qualitatively from the solvation behaviour of inorganic ions due to the fact that such complex ions cannot form donor-acceptor bonds with solvent molecules and they experience comparatively weak electrostatic ion-dipole type of interactions owing to their very small charge density.

Since DMSO possesses an ordered structure which breaks down sharply between 40 and 60°C, or rearranges when a hydrogen donor is added[31-33], further investigation into the solvation behaviour of these ions in AN + DMSO mixtures at higher temperature is needed to clarify the situation.

Acknowledgement

S Chauhan thanks the CSIR, New Delhi for the award of a JRF. The authors also thank Prof. M Salomon, U.S. Army FT and DL (LABCOM) FT monmduth. 07703500 (USA) for providing a least-squares computer program of Shedlovsky conductance equation.

References

1 Gill D S, *Electrochim Acta*, 22 (1977) 491; 24 (1979) 701.
2 Gill D S, *J chem Soc Faraday Trans I*, 77 (1981) 751.
3 Krumgalz B S, *J chem Soc Faraday Trans I*, 76 (1980) 1887; 76 (1980) 1275; 78 (1982) 437; 79 (1983) 571.
4 Gupta D D, Das S & Hazara D K, *J chem Soc Faraday Trans I*, 84 (1988) 1057.
5 Nandi D, Das S & Hazara D K, *Indian J Chem*, 27A (1988) 574.
6 Danil de Namora A F & de Ponce H B, *J chem Soc Faraday Trans I*, 84 (1988) 1671.
7 Petrella G, Castagnolo M, Sacco A & Petrella M, *J soln Chem*, 9 (1980) 331.
8 Petrella G, Sacco A, Castagnolo M, Monica M D & DeGiglio A, *J soln Chem*, 6 (1977) 13.
9 Petrella G, Petrella M, Castagnolo M, Dell'Atti A & DeGiglio A, *J soln Chem*, 10 (1981) 129.

10 Petrella G & Petrella M, *Electrochim Acta*, 27 (1982) 1733.
11 Papadopoulos N, *Electrochimica Acta*, 31 (1986) 1811.
12 Papadopoulos N & Ritzoulis G, *J soln Chem*, 16 (1987) 31.
13 Syal V K & Ranowt P C, *Indian J Chem*, 24A (1985) 16.
14 Pathak R N & Dixit R S, *J Indian chem Soc*, 66 (1989) 81.
15 Gill D S, *J soln Chem*, 8 (1979) 691.
16 Bjerrum N, *Kgl Danske Vidensk Selskab*, 7 (1926); 22 (1928) 1263.
17 Gill D S & Sharma A N, *J chem Soc Faraday Trans I*, 78 (1982) 475.
18 Gill D S, Chauhan S & Chauhan M S, *Z phys Chem NF*, 150 (1986) 113.
19 Fuoss R M & Shedlovsky T, *J Am chem Soc*, 71 (1949) 1496.
20 Fuoss R M & Accascina F, *Electrolytic conductance* (Interscience, New York) 1959.
21 Saloman M, US Army FT & DL (LABCOM) FT MONMDUTH, NJ. 07703500 USA.
22 Janes C J & Fuoss R M, *J soln Chem*, 4 (1975) 91.
23 Aprano A D & Fuoss R M, *J soln Chem*, 4 (1975) 175.
24 Beronious P, *Acta chem scand*, 28A (1974) 77; 29A (1975) 289; 30A (1976) 115.
25 Jones G & Dole M, *J Am chem Soc*, 51 (1929) 2950.
26 Parker A J, *Chem Rev*, 69 (1969) 1.
27 Syal V K, Chauhan S & Chauhan M S, *Z phys Chem NF*, 159 (1988) 49.
28 Coetzee J F & Cunningham G P, *J Am chem Soc*, 87 (1965) 2529.
29 Gill D S, Sharma A N & Schneider H, *J chem Soc Faraday Trans I*, 78 (1982) 465.
30 Accascina F, Aprano A D & Fuoss R M, *J Am chem Soc*, 81 (1959) 1059.
31 Parker A J, *Q Rev*, 16 (1962) 163.
32 Szmatt H H, *Dimethyl sulphoxide*, edited by S W Jacob, E E Rosenbaum & D C Wood (Marcel Dekker, New York) 1971.
33 Kissinger J B, Tannahill M M, Greenbery M S & Popov A I, *J phys Chem*, 77 (1973) 2444.
34 Arrington D E & Griswold E, *J phys Chem*, 74 (1970) 123.
35 Springer C H, Coetzee J F & Key R L, *J phys Chem*, 73 (1969) 471.
36 Evans D F, Zawosk C & Kay R L, *J phys Chem*, 69 (1965) 3878.
37 Tuan D F T & Fuoss R M, *J phys Chem*, 67 (1963) 1343.
38 Krumgalz B S & Fleischer Z, *J chem Soc Faraday Trans I*, 81 (1985) 241.
39 Gopal R & Jha J S, *J phys Chem*, 78 (1974) 2405.

Indian Journal of Chemistry
Vol. 29A, July 1990, pp. 697-699

Kinetics of nonaqueous polymerization of methyl methacrylate by manganic laurate – *n*-hexanethiol redox system in carbon tetrachloride

Dipa Nandi, Prabir Kumar Pal & Ajit Kumar Chaudhuri*

Polymer Science Unit,
Indian Association for the Cultivation of Science,
Calcutta-700032

Received 28 April 1989; revised 25 August 1989;
accepted 11 September 1989

The polymerization of methyl methacrylate (MMA) has been studied in carbon tetrachloride with manganic laurate-*n*-hexanethiol as the initiator system. The rate of polymerization is proportional to [manganic ion]$^{1/2}$ and [thiol]$^{1/2}$. The order in [monomer] is 1.5. A reaction scheme involving initial complex formation between manganic laurate and MMA and subsequent reaction of the complex with the thiol to produce the free radicals has been postulated to account for the observed results. The activation energy and different kinetic constants for the system have also been evaluated.

Metal ions such as Ce(IV), Fe(III), Mn(III) etc. in the presence of various organic reducing agents are known to form effective redox initiator systems in the polymerization of vinyl monomers, usually in aqueous systems only. We have successfully used metallic soaps (ferric laurate[1] and manganic laurate[2,3]) in combination with organic thiols for initiating polymerization in an organic medium. Title investigation is in continuation of our earlier work.

Experimental

The polymerization was carried out in sealed glass ampoule under vacuum. Polymers were isolated by precipitation from benzene solution and dried to constant weight at 50°C in an oven *in vacuo*. The molecular weight ($\bar{M}_n$) of the polymers were determined by viscometric measurements in benzene at 35°C using the equation[4], $[\eta] = 8.69 \times 10^{-5}\ \bar{M}_n^{0.76}$ where $[\eta]$ is the intrinsic viscosity.

Results and discussion

A typical set of reaction curves showing the effect of varying [*n*-hexanethiol] on the polymerization of methyl methacrylate (MMA) in CCl_4 at 40°C at fixed [manganic laurate] is shown in Fig. 1. All the curves pass through the origin, indicating that there is no induction period involved. The rate of polymerization increases with increase in [thiol] and polymerization is completely inhibited by 2,2′-diphenyl-1-picrylhydrazyl indicating the free radical nature of the reaction. Manganic laurate or *n*-hexanethiol alone cannot initiate polymerization.

The rate of polymerization is proportional to [manganic ion]$^{1/2}$ and [*n*-hexanethiol]$^{1/2}$, in accordance with free radical polymerization involving bimolecular termination of free radicals. The order in [monomer] is 1.5, similar to that observed earlier[3] with Mn(III)-1-propanethiol and Mn(III)-2-propanethiol initiated systems, but the rate with manganic laurate-*n*-hexanethiol system is higher than that of the former and lower than that of the latter system under otherwise identical conditions.

Thiols are known to be easily oxidized to disulphides by various oxidizing agents. Wallace[5] found that thiols and ferric octanoate undergo rapid oxidation-reduction reaction producing thiyl radicals (RS) which can be trapped by olefins. It is expected that in the present system a similar oxidation-reduction reaction will occur between Mn(III) ion and *n*-hexanethiol producing *n*-hexanethiyl ($C_6H_{13}\dot{S}$) radicals which initiate po-

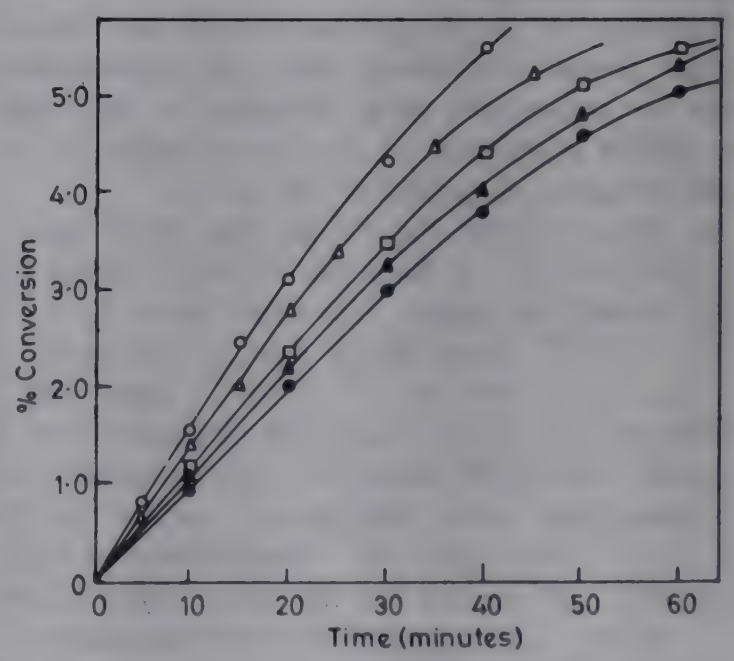

Fig. 1 – Manganic laurate – *n*-hexanethiol initiated polymerization of methyl methacrylate in CCl_4 at 40°C: Effect of varying *n*-hexanethiol concentration. ([Manganic laurate] = 1×10^{-3}; [MMA] = 4.7; [*n*-hexanethiol]: (○) 2.0×10^{-3}, (△) 1.6×10^{-3}, (□) 1.2×10^{-3}, (▲) 1.0×10^{-3}, (●) 8.0×10^{-4} mol dm^{-3}).

lymerization. The formation of a complex between manganic laurate and the monomer (MMA), was shown earlier on the basis of spectroscopic studies. Thus in analogy with the Mn(III)-propanethiol system[3], the following reaction mechanism may be visualized in the present system,

$$Mn(III) + M \overset{K}{\rightleftharpoons} C\ (complex)$$

$$C + RSH \overset{k_d}{\rightarrow} R\dot{S} + C' + H^+$$

$$RS + M \overset{k_i}{\rightarrow} \dot{M}$$

followed by normal propagation, transfer and bimolecular termination of polymer radicals.

By applying steady-state assumptions to the above scheme, the rate of polymerization (R_p) is given by Eq. (1)

$$R_p = (k_p/k_t^{1/2})(k_d K f)^{1/2}[M]^{3/2}[Mn(III)]^{1/2}[T]^{1/2} \quad \ldots (1)$$

and the average degree of polymerization ($\overline{DP}$) is given by Eq. (2)

$$1/\overline{DP} = C_M + C_T[T]/[M] + C_S[S]/[M] + \delta^2/[M]^2 \cdot R_p \quad \ldots (2)$$

where f is the initiator efficiency, K the equilibrium constant of the complex formation reaction, k_d the rate constant for the interaction between the complex C and the thiol RSH or T, and S the solvent (CCl_4). All the other symbols have the usual meanings.

Equation (1) is in agreement with our experimental results indicating that the assumptions made are reasonably valid. Initiation by thiyl radicals ($R\dot{S}$) is confirmed by the incorporation of thiyl end groups in the polymer (see ref. 2).

As expected from Eq. (1) the plot of R_p against $\{[Mn(III)][RSH]\}^{1/2}$ at fixed [monomer] is linear passing through the origin. The slope gives $(k_p/k_t^{1/2})(k_d K f)^{1/2}[M]^{3/2}$, from which $k_d K f$ is calculated to be 7.22×10^{-3} dm^3 mol^{-1} at 40°C, since [M] is known and the $k_p/k_t^{1/2}$ has been obtained from literature[6]. The $k_d K f$ values for 2-propanethiol and 1-propanethiol were determined earlier[3] to be 7.91×10^{-3} and 5.92×10^{-3} respectively at 40°C. Thus the $k_d K f$ values for the three thiols follow the order 2-propanethiol > *n*-hexanethiol > 1-propanethiol, i.e., same as the order of R_p obtained with these thiols under otherwise identical conditions. This is also expected from Eq. (1) which indicates that R_p will be determined by $k_d K f$ or rather by $k_d f$ since K is the same in all the cases. If we further assume that f is the same for all the thiols investigated so far, then the R_p's for the different thiols will follow the order of their respective k_d's. Now k_d refers to the reaction between the Mn(III)-monomer complex and thiol, and involves an electron transfer from thiol to the manganic ion. The reactivity of thiol will thus be dependent on electron-donating or electron-withdrawing influence of the attached groups. The relative activities of *n*-hexanethiol and 1-propanethiol can be explained on the basis of the electron-donating capabilities of their respective substituents. The highest rate observed with 2-propanethiol may be due to the presence of two electron-donating methyl groups.

From the plot of log R_p versus 1/T (Fig. 2) the overall activation energy for the rate of polymerization for the present system is found to be 31.2 kJ mol^{-1}. This is of the same order as is usually observed in redox polymerizations. From Eq. (1), it follows that $E_{overall} = E_p + 1/2\ E_{k_dK} - 1/2\ E_t$. Using literature value[7] of E_p (26.3 kJ mol^{-1}) and E_t (11.7 kJ mol^{-1}) in the above equation we get $E_{k_dK} = 21.5$ kJ mol^{-1}. The $E_{overall}$ and E_{k_dK} values for *n*-hexanethiol are lower than those (36.3 and 31.6 kJ mol^{-1}) for 1-propanethiol system[3]. This is in agreement with the higher rate observed with *n*-hexanethiol system compared to that with 1-propanethiol system.

The degree of polymerization ($\overline{DP}$) obtained in the present system is usually of the order of 10^3, and increases with increase in [monomer] and decreases with [manganic laurate] and [*n*-hexanethiol].

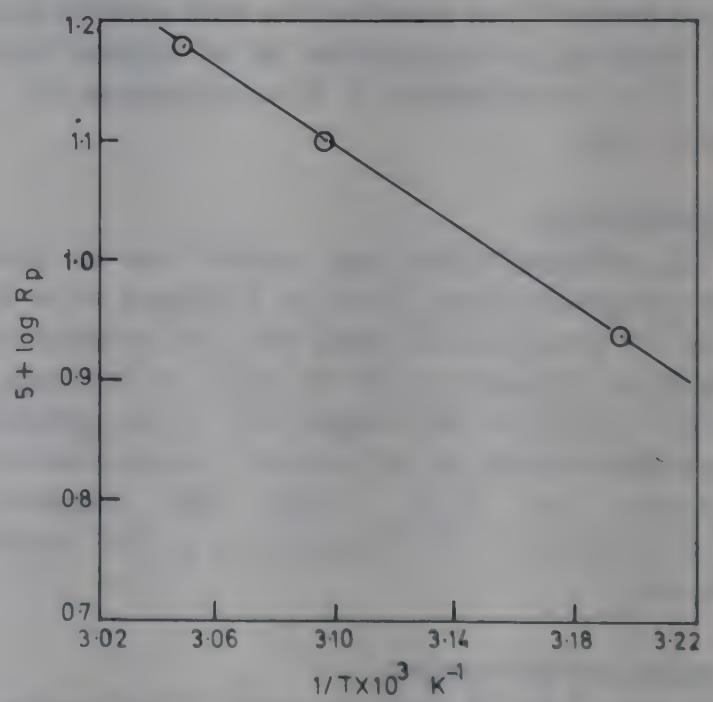

Fig. 2 – Dependence of initial rate of polymerization on absolute temperature. ([Mn(III)] = 1×10^{-3}; [*n*-hexanethiol] = 1×10^{-3}; [MMA] = 4.7 mol. dm^{-3} and solvent = CCl_4).

Thiols are known to be good chain transfer agents and transfer constant (C_T) of *n*-hexanethiol can be determined with the help of Eq. (2). As expected, the plot of $1/\overline{DP} - C_S[S]/[M] - \delta^2 \cdot R_p/[M]^2$ versus [T]/[M] at fixed [manganic laurate] is linear, the slope giving C_T and the intercept C_M, the chain transfer constant with respect to monomer. Literature values of C_S (for CCl_4) ($=3.09 \times 10^{-5}$ at 40°C)[8] and δ ($=10.6$ at 40°C)[6] were used for calculations. The value of C_M for MMA at 40°C comes out to be 1.00×10^{-5} agreeing with the literature value[9]. The C_T value for *n*-hexanethiol comes out to be 0.72. This is higher than those for 1-propanethiol (0.46)[3] and 2-propanethiol (0.35)[3]. Transfer reaction with the thiols involves abstraction of a H-atom from the S−H bond. So normally electron-donating groups should increase and electron-withdrawing groups should decrease the transfer activity of a primary thiol. Thus the relative transfer activities of *n*-hexanethiol and 1-propanethiol may be explained as due to relative electron-donating capacity of the attached groups. As was explained earlier[3] the lower activity of 2-propanethiol can be attributed to steric restriction due to methyl group substitution at the α-carbon atom.

The value of δ can also be determined with the help of Eq. (2). The plot of $1/\overline{DP}$ versus R_p at fixed [monomer] and [thiol] is linear, the slope giving $\delta^2/[M]^2$. From this, the value of $\delta (= k_t^{1/2}/k_p)$ is calculated to be 10.78 at 40°C agreeing well with the literature value of 10.6 at 40°C (ref. 6).

References

1 Ghosh S K, Ph.D. Thesis, Calcutta University (1980).
2 Saha S K, Chakraborty N K & Chaudhuri A K, *J polym Sci* (Polym Lett edn.) 21 (1983) 963.
3 Nandi D, Pal P K & Chaudhuri A K, *Eur Polym J*, 22 (1986) 979.
4 Fox T G, Kinsinger J B, Mason H F & Schuele E M, *Polymer*, 3 (1962) 71.
5 Wallace T G, *J org Chem*, 31 (1966) 3071.
6 Nandi U S, *J Colloid Sci*, 12 (1957) 321.
7 Matheson M S, Auer E E, Bevilacqua E B & Hart E J, *J Am chem Soc*, 71 (1949) 497.
8 Chadha R N, Shukla J S & Misra G S, *Trans Faraday Soc*, 53 (1957) 240.
9 Brandrup J & Immergut E H, *Polymer handbook*, (Interscience, New York) 1966, pp. 11-80.

Indian Journal of Chemistry
Vol. 29A, July 1990, pp. 700-702

Kinetics and mechanism of oxidation of aromatic amines by N-bromoacetamide

P R Sharadamani & V Jagannadham*
Department of Chemistry, Nizam College (Osmania University)
Hyderabad 500 001

Received 24 May 1989; revised 22 September 1989;
accepted 15 November 1989

Kinetics of oxidation of unsubstituted and substituted anilines by N-bromoacetamide (NBA) in methanol-water (50:50 v/v) mixture has been investigated in the presence of mercuric acetate and excess acetamide (AA). Electron-releasing substituents in the aromatic ring accelerate the reaction rates and electron-withdrawing substituents retard them. The value of the reaction constant (ρ) at 303 K, obtained from the Hammett's plot (corr. coeff. = 0.998) is -0.785. The Brönsted plot is also linear with a β value of 0.186 at 303 K. A mechanism involving an electrophilic attack of the oxidant on the amino group has been proposed to explain the observed results. Thermodynamic and activation parameters have also been evaluated.

Kinetics of oxidation of aromatic amines by a variety of oxidants have been studied extensively. With N-halo compounds such as CAT, BAT and NBS a nuclear halogenation[1] and oxidation of the amino group have been observed[2-10]. Neither oxidation nor bromination of anilines by N-bromoacetamide (NBA) has been reported so far, and hence the title investigation.

Experimental

All the chemicals used were of AR Grade. NBA (E Merck, GR) was used as such. All the anilines were either distilled or recrystallised before use. The reaction between NBA and aniline was instantaneous. However, addition of acetamide rendered the reaction slow. In addition, the reaction between aniline and NBA was followed at temperature as low as 273K. The reactions were conducted in binary solvent mixtures of water and methanol (50:50 v/v) in the absence of mineral acid and in the presence of added mercuric acetate. The course of the reaction was followed by estimating unreacted NBA iodometrically at suitable intervals of time.

Solutions of 4-nitroaniline and NBA in 1:2 molar ratio were mixed and kept aside for 2 to 3 days. The resulting precipitate was filtered off and washed with distilled water until free from NBA. TLC of the precipitate using benzene as an irrigant revealed the presence of two compounds. The major product (85%) was identified as 4,4′-dinitroazobenzene by IR and mixed melting point determination with an authentic specimen. The stoichiometry was found to be 1:1 in accordance with Eq. (1)

$$2C_6H_5NH_2 + 2CH_3CONHBr \rightarrow C_6H_5-N=N-C_6H_5 + 2CH_3CONH_2 + 2HBr \quad \ldots (1)$$

Results and discussion

Under the condition [NBA] < < [substrate], plot of log [NBA] versus time was linear (Fig. 1A) indicating a first order dependence on [NBA]. The observed pseudo-first order rate constants were obtained from the slopes of the above plots. The plots of log k_{obs} versus log [substrate] were linear (Fig. 1B). Slopes of such plots gave the orders in aniline and substituted anilines as one.

The rates of reaction decreased with increase in [acetamide] (Fig. 1C). No induced polymerisation was observed when acrylonitrile was added to the reaction mixture ruling out a radical mechanism. It has been reported earlier in the case of N-halo oxidants that in the absence of mineral acids, HOBr is the reactive oxidant species[11,12]. Since water is a much weaker acid than HOBr, existence of H_2OBr^+ was entirely ruled out in the present studies.

The rates were unaffected by added Na_2SO_4 indicating that the reaction may be between two dipoles, i.e. aniline and HOBr. In order to confirm this, the reaction was carried out in methanol-water mixtures of different compositions. Plot of log k versus 1/D was linear with a negative slope (Fig. 1D) suggesting a reaction between two dipoles. Based on the above observations, the mechanism in Scheme 1 has been proposed for the oxidation of aniline by NBA.

$$NBA + H_2O \overset{K_h}{\rightleftharpoons} CH_3CONH_2 + HOBr \quad \ldots (2)$$

$$HOBr + C_6H_5NH_2 \xrightarrow[\text{slow}]{k} C_6H_5NH^+ + H_2O + Br^- \quad \ldots (3)$$

$$C_6H_5NH^+ + C_6H_5NH_2 \xrightarrow{\text{fast}} C_6H_5\overset{+}{N}H_2 - NHC_6H_5 \quad \ldots (4)$$

$$C_6H_5\overset{+}{N}H_2 - NHC_6H_5 \xrightarrow{\text{fast}} C_6H_5NH - NHC_6H_5 + H^+ \quad \ldots (5)$$

$$C_6H_5NH - NHC_6H_5 \xrightarrow[\text{fast}]{HOBr} C_6H_5N=NC_6H_5 + H_2O + HBr \quad \ldots (6)$$

Scheme 1

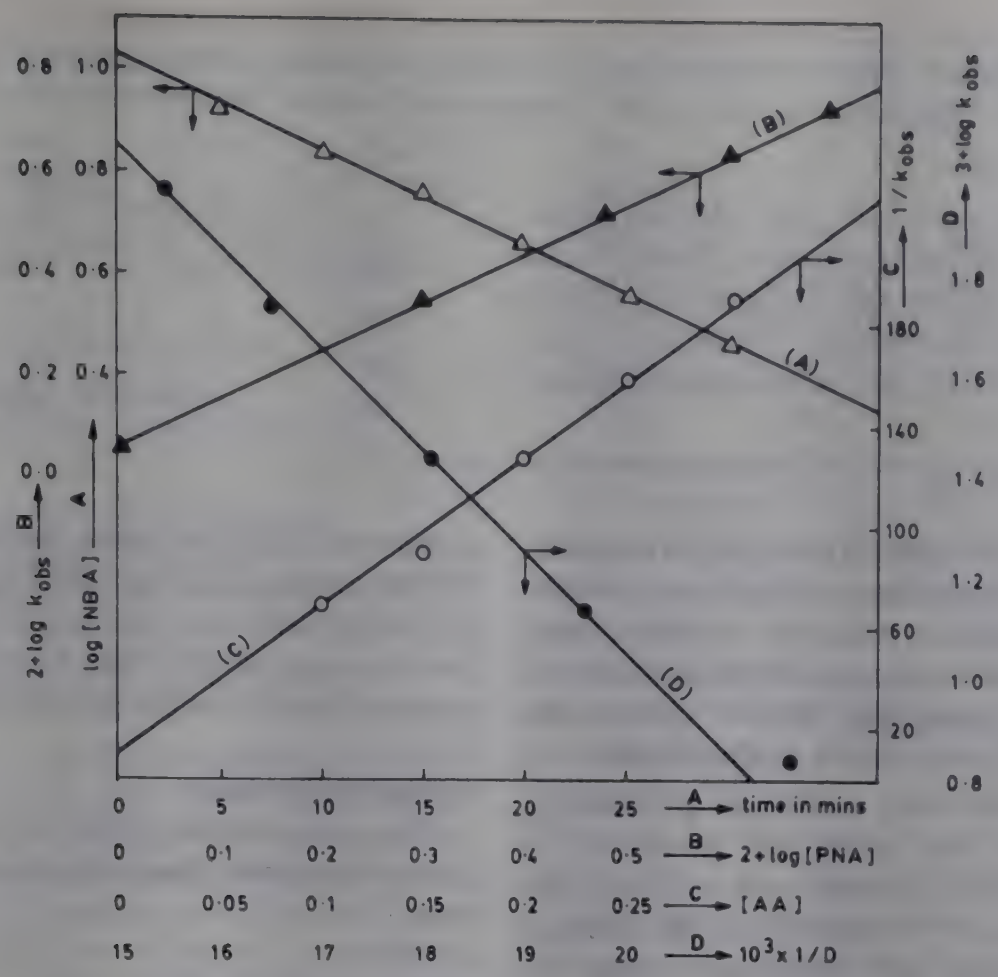

Fig.1—(A) Plot of log [NBA] versus time ([NBA] = 0.001 mol dm^{-3}; MeOH:H_2O = 50:50 (v/v); [$Hg(OAc)_2$] = 0.005 mol dm^{-3}; temp. = 308 K; [AA] = 0.1 mol dm^{-3}; [PNA] = 0.01 mol dm^{-3})

(B) Plot of $2 + \log k_{obs}$ versus $2 + \log$ [PNA], (Conditions same as in *A*, except [PNA] was varied from 0.01 mol dm^{-3} to 0.05 mol dm^{-3}; temp. = 308 K).

(C) Plot of $1/k_{obs}$ versus [AA], ([NBA] = 0.001 mol dm^{-3}; [PNA] = 0.01 mol dm^{-3}; [$Hg(OAc)_2$] = 0.005 mol dm^{-3}; [AA] was varied from 0.1 mol dm^{-3} to 0.3 mol dm^{-3}; temp. = 308 K).

(D) Plot of $(3 + \log k_{obs})$ versus $10^3 \times 1/D$, (temp = 300 K; (PNA] = 0.01 mol dm^{-3}; [NBA] = 0.001 mol dm^{-3}; [$Hg(OAc)_2$] = 0.005 mol dm^{-3}; [AA] = 0.1 mol dm^{-3}).

Scheme 1 leads to the rate expression (7)

$$\text{Rate} = \frac{kK_h[\text{aniline}][\text{NBA}]}{([\text{AA}] + K_h)} \quad \ldots (7)$$

where K_h is the hydrolysis constant for step 2 and k is the rate constant for step 3

$$\frac{-2.303\, d\log[\text{NBA}]}{dt} = k_{obs} = \frac{kK_h[\text{aniline}]}{([\text{AA}] + K_h)} \quad \ldots (8)$$

By taking reciprocals of Eq. (8), we get Eq. (9)

$$\frac{1}{k_{obs}} = \frac{[\text{AA}]}{kK_h[\text{aniline}]} + \frac{1}{k[\text{aniline}]} \quad \ldots (9)$$

Plots of $1/k_{obs}$ versus [AA] were found to be linear (Fig. 1c). From the ratio of the intercept and slope, K_h was calculated for the hydrolysis of NBA and from the intercept, k, the rate constant for the slow step was calculated.

The order of reactivities of various substituted anilines was found to be *p*-toluidine > aniline > *p*-chloroaniline > *m*-nitroaniline > *p*-nitroaniline. In the bromination of anilines by NBS[1] it was reported that it was a C-halogenation process. If in the present work such an attack were to take place, then a plot of log k versus σ_p for *meta* substituents and σ_m for *para* substituents would be linear. Such a linearity was not observed. In fact a fairly good correlation between log k and σ_m and σ_p for *meta* and *para* substituents respectively with a slope of -0.785 and a correlation coefficient $r = 0.998$ was observed. This suggested an electrophilic attack at the nitrogen of the amino group. The negative sign of ρ indicates that electron donating substituents accelerate the reaction rates and electron withdrawing substituents retard them. This is found to be so in the present investigation. It also suggests the development of an electron deficient centre in the activated complex leading to the transfer of a hydride

Table 1—Effect of substituents on K_h, k and thermodynamic/activation parameters

[NBA] = 0.001 mol dm^{-3}; [$Hg(OAc)_2$] = 0.005 mol dm^{-3}; [aniline] = 0.01 mol dm^{-3}; MeOH: H_2O = 50:50 (v/v); temp. = 303 K

Substituent	σ	pK_a	K_h	ΔH (kJ mol^{-1})	ΔS (J mol^{-1} K^{-1})	$k \times 10$ (s^{-1})	$\Delta H^{\neq}$ (kJ mol^{-1})	$\Delta S^{\neq}$ (J mol^{-1} K^{-1})
H	0.00	4.62	21.9	102	−115	15.8	20.4	−176
4-NO_2	0.78	1.00	1.44×10^{-2}	14.4	−233	3.48	33.9	−143
3-NO_2	0.71	2.40	3.98×10^{-2}	4.55	−258	6.30	32.4	−142
4-Cl	0.23	4.18	2.29	9.83	−207	10.0	6.95	−232
4-Me	−0.17	5.00	3.02	31.7	−132	19.9	50.4	−74.3

ion[7,14]. The value of ρ obtained presently is less than those reported for the oxidation of anilines by earlier workers[7,13,14]. However, similar ρ values have been reported for the oxidation of benzaldehydes and bromination of phenols by NBA[11,15], where the reaction takes place between two similar dipoles.

The thermodynamic and activation parameters were evaluated and the values are presented in Table 1. Since activation energies are not large, the low rate constants at 303K result from the strongly negative activation entropies. In addition, these values could be interpreted in terms of a loss of entropy due to the solvation of Br^- ion. The observed highly negative $\Delta S^{\neq}$ values are comparable to that of hydration of proton transfer to solvent (−105 J mol^{-1} K^{-1}). The high negative $\Delta S^{\neq}$ values could also be explained as due to the formation of an ionic transition state with an extensive charge separation resulting from the transfer of either two electrons or hydride ion in the rate-determining step[14] as shown below. Transition state is formed from two neutral molecules, viz. the substrate and HOBr.

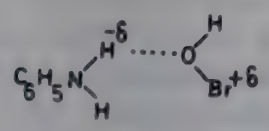

The plot of $\Delta H^{\neq}$ versus $\Delta S^{\neq}$ was linear which suggests that oxidation of all the aromatic amines occurs by an identical mechanism. The β-value is 269 K which is close to the lowest experimental temperature (273 K) indicating that the present reaction series is an entropy-controlled one.

The Brönsted plot (log k versus pK_a) is fairly linear with β = +0.186 at 303 K indicating that there is extensive bond formation between aniline and the HOBr centre in the transition state. The positive value of the Brönsted coefficient and the negative value of ρ point out that the rate increases with the increasing basicity of the nucleophile.

Acknowledgement

One of the authors (PRS) is grateful to the authorities of Kasturba Gandhi College, Secunderabad for help.

References

1 Radhakrishnamurthi P S & Sahu S N, *Indian J Chem*, 15A (1977) 785.
2 Srivastava S P, Gupta R C & Shukla A K, *Indian J Chem*, 15A (1977) 605.
3 Gupta R C & Srivastava S P, *Indian J Chem*, 10 (1972) 706.
4 Boyland E & Peter-Sims, *J chem Soc*, Part I (1954) 980.
5 Panigrahi G P & Mahapatro D D, *Int J chem Kinet*, 14 (1982) 977.
6 Radhakrishnamurthi P S & Ramakrishna Panda, *Indian J Chem*, 9 (1971) 1247.
7 Vedavrath R, Sethuram B & Navaneeth Rao T, *Proc Natl Acad Sci India*, 51A(4) (1981) 443.
8 Prasada Rao M D & Padmanabha J, *Indian J Chem*, 19A (1980) 984.
9 Vijayalakshmi & Sundaram E V, *Indian J Chem*, 17A (1979) 495.
10 Subas Pati C, Dev B R, Narasingh Behera & Minakshi Mishra, *Proc Ind Natl Sci Acad*, 49A(5) (1983) 538.
11 Venkateshwarlu S & Jagannadham V, *Indian J Chem*, 27A (1988) 314.
12 Radhakrishnamurthi P S & Prasada Rao M D, *Indian J Chem*, 14B (1976) 790.
13 Prasada Rao M, Sethuram B & Navaneeth Rao T, *Indian J Chem*, 17A (1979) 52.
14 Sreenivasulu P V, Adinarayana M, Sethuram B & Navaneeth Rao T, *Oxidn Communs*, 8 (1985) 199.
15 Venkateshwarlu S & Jagannadham V, *Oxidn Commun*, 8 (1985) 149.

Indian Journal of Chemistry
Vol. 29A, July 1990, pp. 703-706

Synthesis and reactivity of diorganotellurium(IV) β-diketonates

T N Srivastava & Jai Deo Singh
Chemistry Department,
Lucknow University, Lucknow 226 007
and
Sanjay Kumar Srivastava* & S Srivastava
School of Studies in Chemistry,
Jiwaji University, Gwalior 474 011

Received 24 April 1989;
revised and accepted 23 October 1989

Diorganotellurium(IV) bis-(β-diketonates) of the formula $R_2Te(acac)_2$ {R = CH_3, C_6H_5, *p*-$CH_3OC_6H_4$} and $R_2Te(dpm)_2$ (acacH = 2,4-pentanedione; dpmH = 2,2,6,6-tetramethylheptane-3,5-dione) have been prepared by the reaction of $R_2Te(OMe)_2$ with (acacH) and (dpmH) in anhydrous conditions. $R_2Te(acac)_2$ reacts with halocarboxylic acids (R′COOH) (R′ = CF_3, CCl_3, $CHCl_2$ or CH_2Cl) to give mixed ligand complexes of the type $R_2Te(acac)(R'COO)$. A weak coordination of the β-diketone group with tellurium atom in the solid state is concluded. The geometry around the central tellurium atom is suggested on the basis of physicochemical studies.

Reactions of $TeCl_4$ with 1,3-diketones are reported to yield cyclic and linear condensation products of the types [$CH_3C(OH)$:$CHC(O)CH_2TeCl_3$] and [$Cl_2TeCH_2COCH_2COCH_2$][1-3]. The reactions of diorganotellurium dihalides and 1,1-dimethyl-3,5-cyclohexanedione in presence of Et_3N in benzene yield ylid derivatives[4]. Recently, triphenyltellurium β-diketonates have been also reported[5]. In continuation of our studies on the synthesis and reactivity of organotellurium(IV) compounds containing chelating ligands[6,7], we report herein the synthesis and reactions of diorganotellurium(IV) bis-(β-diketonate) derivatives. Instead of ylid derivatives, we have obtained Te−O bonded β-diketonate derivatives.

Experimental

All manipulations were conducted under dry nitrogen. $TeCl_4$(BDH) was used as such. Me_2TeI_2 (ref. 8), Ph_2TeCl_2 (ref. 9) (*p*-$MeOC_6H_4)_2TeCl_2$ (ref. 10), Ph_2TeO (ref. 11), (*p*-$MeOC_6H_4)_2TeO$ (ref. 12), and $R_2Te(OMe)_2$ (ref. 13) were prepared according to established procedure. (acacH)(BDH), (dpmH)(Fluka), CF_3COOH (Koch-Light), R′COOH (R′ = CCl_3, $CHCl_2$ and CH_2Cl) (BDH) were purified by conventional methods before use. Solvents were purified by standard methods. Other physicochemical studies were made as described earlier[14]. Experimental details are given below and analytical data are listed in Table 1.

(a) Reaction of $R_2Te(OMe)_2$ with acacH

To a solution of Ph_2TeCl_2 (3.51 g; 10 mmol) in absolute methanol (50 ml) was added dropwise a solution of sodium methoxide (20 mmol) [prepared by the reaction of sodium (0.46 g; 20 mmol) and absolute methanol at 0°C]. The resulting mixture was stirred and the precipitated sodium chloride was filtered off. To the filtrate was then added dropwise a solution of acacH (2.0 g; 20 mmol) in the same solvent and contents were stirred for 2 hr. The solvent was removed under reduced pressure to induce crystallisation. The product was recrystallised from $CHCl_3$/pet. ether (40-60°C) (1:3) mixture.

Identical products were obtained by stirring a mixture of R_2TeO and acacH in 1:2; molar ratio in a mixture of absolute methanol and 2,2′-dimethoxypropane as solvent.

(b) Reaction of $R_2Te(acac)_2$ with R′COOH

To a stirring solution of $Ph_2Te(acac)_2$ (4.80 g; 10 mmol) in dry solvent ether, CF_3COOH (2.28 g; 20 mmol) in the same solvent was slowly added over a period of 2 hr. The precipitated compound was filtered off and washed with solvent ether. It analysed for $Ph_2Te(acac)(OCOCF_3)$.

Results and discussion

The reactions leading to the formation of present complexes may be represented by Eqs 1 and 2.

$$R_2Te(OMe)_2 + 2\ acacH/2\ dpmH \xrightarrow[-2MeOH]{} R_2Te(acac)_2/R_2Te(dpm)_2 \quad \ldots (1)$$

$$R_2Te(acac)_2 + R'COOH \xrightarrow[-2acacH]{} R_2Te(acac)(OCOR') \quad \ldots (2)$$

(R′ = CF_3, CCl_3, $CHCl_2$ and CH_2Cl)

The complexes had sharp melting points and were white to yellow solids, soluble in common organic solvents. In solution, $R_2Te(acac)_2$ was sen-

Table 1 – Analytical data for $R_2Te(acac)_2$ and its derivatives

Complex	m.p. (°C)	Found (%) (Calc.)		
		Te	C	H
$Ph_2Te(acac)_2$	132	26.3 (26.6)	55.3 (55.4)	4.6 (5.0)
$(CH_3)Te(acac)_2$	127	35.4 (35.8)	40.1 (40.5)	5.2 (5.6)
$(p\text{-}MeOC_6H_4)_2Te(acac)_2$	105	23.5 (23.6)	53.1 (53.4)	5.0 (5.2)
$Ph_2Te(dpm)_2$	166	19.5 (19.7)	62.8 (63.0)	7.3 (7.4)
$Ph_2Te(acac)(OCOCF_3)$	135	25.6 (25.8)	—	—
$Ph_2Te(acac)(OCOCCl_3)$	142	23.2 (23.5)	41.9 (42.1)	3.1 (3.1)
$Ph_2Te(acac)(OCOCHCl_2)$	117	24.8 (25.0)	44.6 (44.8)	3.4 (3.5)
$Ph_2Te(acac)(OCOCH_2Cl)$	109	26.8 (26.9)	47.9 (48.1)	3.9 (4.0)
$(p\text{-}MeOC_6H_4)_2Te(acac)(OCOCF_3)$	126	22.8 (23.1)	—	—
$(p\text{-}MeOC_6H_4)_2Te(acac)(OCOCCl_3)$	130	20.8 (21.1)	41.5 (41.8)	3.4 (3.5)
$(p\text{-}MeOC_6H_4)_2Te(acac)(OCOCHCl_2)$	142	22.1 (22.3)	44.1 (44.2)	3.6 (3.3)
$(p\text{-}MeOC_6H_4)_2Te(acac)(OCOCH_2Cl)$	131	23.7 (23.8)	47.0 (47.2)	4.3 (4.5)

sitive towards atmospheric oxygen and moisture, and turned brown on standing for 24 hr at room temperature. On being refluxed in non-aqueous solvents for 4-6 hr, the complexes decomposed giving unidentified products. The solid products isolated were, however, stable at room temperature. The molar conductances of the compounds (10^{-3} *M* soln.) in nitrobenzene/acetonitrile at 25°C were in the range 4.32-7.68 mhos cm^2 mol^{-1} indicating their non-electrolytic nature. Molecular weight determined cryoscopically in freezing nitrobenzene showed their monomeric nature.

In the formation of $R_2Te(acac)(OCOR')$, the replacement of the acac group is expected to be preceded by the protonation of the ligand. The vacant site is then filled by $-OCOR'$ with concomitant release of one of the -acac- group yielding mixed ligand complexes[15].

IR spectra

The IR spectra were recorded in KBr in the region 4000-400 cm^{-1} and in some cases also in $CHCl_3$ solution.

The free acacH showed split band with peaks at 1725 and 1700 cm^{-1} along with a slightly weak

band at 1620 cm^{-1} due to carbonyl stretching. The former two bands are due to $\nu_{as}COO$ and ν_{sy}-COO modes of the keto form while latter is due to νCO(enolic) coupled with the νC=C.

In the spectra of acetylacetonate complexes, the presence of two peaks in the region 1600-1500 cm^{-1} is characteristic of bidentate chelation[17,18] of the ligand and these bands are assigned to ν(C=O) and ν(C=C). The spectra of $R_2Te(acac)_2$ and $R_2Te(dpm)_2$ showed a coupled, broad and split band due to ν(C=O) and ν(C=C) at 1580 ± 10 cm^{-1}. The absence of a band at 1720 cm^{-1} ruled out the possibility of a Te−C bond involving the middle carbon atom of the acetylacetonate[5]. This suggests that the acac group in the compounds is bidentate[19].

In solution spectra (saturated solution of the compound in $CHCl_3$), bands observed at 1615 ± 5 cm^{-1} and 1580 ± 5 cm^{-1} are assigned to ν(C=O)+ν(C=C). This indicates that one of the acac ligand of $R_2Te(acac)_2$ is unidentate in nature while the other is bidentate.

In the spectra of $R_2Te(acac)(OCOR')$, vibrations associated with $\nu_{asy}COO$ and $\nu_{sy}COO$ of the halocarboxylate group appeared at 1700 ± 10 cm^{-1} and 1390 ± 10 cm^{-1}. Their difference ($-\Delta\nu COO = 310 \pm 10$ cm^{-1}), and occurrence of the combined band ν(C=O)+ν(C=C) at 1616 ± 5 cm^{-1} are characteristic of unidentate coordination of the acetylacetonate and halocarboxylate ligands[15,20].

^1H NMR spectra

The spectrum of $Ph_2Te(acac)_2$ showed two equally intense CH_3 resonances at δ 2.19. and 1.99 ppm, −CH resonances of appreciable intensity at δ 5.40 and 5.04 and two overlapping multiplets due to phenyl groups, centered in the region 8.0-7.0 ppm. Similarly, in the PMR spectrum of $Me_2Te(acac)_2$, the protons for acac group showed peaks due to $-CH_3-$ protons at δ 2.15 and 1.8, and peaks due to −CH− protons at δ 5.38 and 5.05. The methyl resonances (CH_3 attached to tellurium) occurred at δ 3.72 and 3.28. Each peak had a well resolved satellite band of NMR active isotope of ^{125}Te with coupling constant $^2J(^1H-^{125}Te) = 26 \pm 0.2$ Hz.

In the ^1H NMR spectrum of $Ph_2Te(dpm)_2$, the phenyl protons were observed at 7.96-7.26 ppm as multiplets. The −CH and CH_2 protons gave signals at 5.58 and 1.14 ppm respectively. The spectrum did not show multiplicity in contrast to that observed in the spectra of $Ph_2Te(acac)_2$ and $Me_2Te(acac)_2$. This shows that bulky dpm group forbids the isomeric equilibrium or exchange of ligands between unidentate and bidentate species in solution.

In the solid state, hexacoordination around tellurium may be suggested. This may be either a weak coordination (Te←0) from non-bonded oxygen of the -acac- group to tellurium atom or a weak secondary interaction between tellurium and non-bonded oxygen (Te→0) of the -acac- group. Similar results have been reported on the basis of X-ray data[21,22]. However, in solution state the IR spectra of $R_2Te(acac)_2$) revealed that one of the -acac- groups is unidentate while the other is bidentate in nature[6,7]. Absence of splitting in ν(C−O) absorptions in solution state spectra may be explained by the fact that interaction between non-bonded oxygen and tellurium observed in solid state[23], is absent in solution.

However, ^1H NMR spectra of $Ph_2Te(acac)_2$ and $Me_2Te(acac)_2$ showed two sets of peaks for all protons in contrast to the expectation of a single peak suggesting the presence of two geometrical isomers[24,25] in solution or unidentate-bidentate exchange of the ligand occurring in solution at NMR time scale[26]. The separation of two isomers by conventional techniques (such as TLC) was not possible. In the spectrum of $Me_2Te(acac)_2$ (each methyl peak attached to tellurium (CH_3-Te) had a well resolved satellite), the $^2J(^{125}Te-^1H)$ coupling constant being 26.0 Hz, which is almost of the same magnitude as reported for Me_2TeI_2 (26.0 Hz) in which a four coordinated tellurium atom has been reported[27]. It may be concluded that the compounds are four coordinated with basic pseudo-trigonal-bipyramidal geometry around central tellurium atom. In solid state an octahedral or a pseudo-pentagonal-bipyramidal geometry may be present.

Acknowledgement

Financial support from CSIR and UGC, New Delhi is gratefully acknowledged.

References

1 Irgolic K J & Zingaro R A, in *Reactions of organotellurium compounds "organometallic reactions"*, Vol. 2, Edited by I Becker & M Tsutsui, (Wiley-Interscience, New York) (1971) 117.
2 Raston C L, Secomls R J & White A H, *J chem Soc (Dalton)*, (1976) 2307.
3 Berly F J & Silver J, *J organomet Chem*, 188 (1980) 255.
4 Sadekov I D, Usachev A I, Bon V A, Korobor M S, Tseimakh I D & Minkin V I, *Zh obshch Chem*, 47 (1977) 2232.
5 Khandelwal B L, Singh A K, Singh H B, Prasad K M, Bhandari N S & McWhinnie W R, *J organomet Chem*, 291 (1985) 185.
6 Srivastava T N, Singh Jai Deo & Mehrotra Shashi, *Indian J Chem*, 24A (1985) 849.

7 Srivastava T N, Singh Jai Deo & Mehrotra Shashi, *Indian J Chem*, 25A (1986) 480.

8 Thayer J S & Smith K V, *Synth react inorg met org Chem*, 3 (1973) 101.

9 Paul R C, Bhasin K K & Chadha R K, *J inorg nucl Chem*, 37 (1975) 2339.

10 Bergman J, *Tetrahedron*, 28 (1972) 3323.

11 Alcock N W & Harrison D W, *J chem Soc (Dalton)*, (1982) 709.

12 Lederer K, *Ber dt Chem Ges*, 49 (1916) 1076.

13 Wieker M & Kaunzinger E, *J organomet Chem*, 129 (1977) 339.

14 Srivastava T N, Singh Jai Deo & Srivastava Sanjay Kumar, *Polyhedron*, 6 (1987) 219.

15 Aly M M & Elsaid A L, *J inorg nucl Chem*, 43 (1981) 45.

16 Cramer R E & Chudyk M A, *Inorg Chem*, 12 (1973) 1193.

17 Stults B P, Marianelli R S & Day V W, *Inorg Chem*, 14 (1975) 722.

18 Okeya S, Egawa F, Nakamura Y & Kawaguchi S, *Inorg chim Acta Lett*, 30 (1978) L319.

19 Thompson D W, *Inorg Chem*, 8 (1969) 2015.

20 Srivastava T N & Singh Jai Deo, *Indian J Chem*, 26A (1987) 260.

21 Alcock N W, Harrison W D & Howes C, *J chem Soc*, (Dalton), (1984) 1709.

22 Alcock N W, *Adv Inorg Chem & Radiochem*, 16 (1972) 1.

23 Pant B C, McWhinnie W R & Dance N S, *J organomet Chem*, 63 (1973) 305.

24 Hendrickson A R & Martin R L, *Inorg Chem*, 11 (1973) 2582.

25 Hendrickson A R & Martin R L, *Inorg Chem*, 12 (1974) 3021.

26 Dakternieks D, Giacomo R D, Gable R W & Hoskins B F, *J Am chem Soc*, 110 (1988) 6753

27 Smith K V & Thayer J S, *Inorg Chem*, 12 (1974) 3021.

Indian Journal of Chemistry
Vol. 29A, July 1990, pp. 707-709

Mixed ligand complexes of copper(II), nickel(II), cobalt(II) and zinc(II) with nitrilotriacetic acid and iminodiacetic acid as primary ligands and 2-aminophenol as a secondary ligand

Sunanda Das & M N Srivastava*
Department of Chemistry, University of Allahabad, Allahabad 211 002

Received 26 May 1989; revised 24 October 1989; accepted 18 December 1989

The stability constants of the title mixed ligand complexes determined potentiometrically in 50% aqueous dioxane medium, follow the order Cu > Co > Zn > Ni with NTA as the primary ligand and Cu > Zn > Co > Ni with IMDA as the primary ligand. At higher concentrations of 2-aminophenol, in Co(II)-IMDA-aminophenol system, both MLA and MLA_2 are formed but in other systems only MLA is formed. K_{MLA} values are in general less than K_1 (Amp) for simple 2-aminophenol complexes, and less or comparable to K_2 (Amp), but for Co(II)-IMDA-aminophenol complex, K_{MLA} is less than K_1 (Amp) but more than K_2 (Amp).

Mixed ligand complexes containing nitrilotriacetic acid (NTA) or iminodiacetic acid (IMDA) as a primary ligand have been investigated by many workers[1-6]. The stability constants of some metal complexes of *o*-aminophenol are also reported[7,8]. But a literature survey reveals that the solution studies of mixed ligand complexes containing *o*-aminophenol are not extensive. Only recently Venkatnarayan[9] has studied the ternary complex of Cu(II) with phthalic acid and *o*-aminophenol by *p*H titration technique. In this note, the stability constants of the title mixed ligand systems have been determined potentiometrically in 50% dioxane medium.

Experimental

A stock solution (0.1 *M*) of nitrilotriacetic acid (E. Merck) was prepared by dissolving the weighed amount in one equivalent of sodium hydroxide solution in doubly distilled water. A solution of iminodiacetic acid (Sigma) was also prepared in doubly distilled water and a solution of *o*-aminophenol (Fluka AG) was prepared in dioxane. All the metal salts used were of AR grade. Other reagents, apparatus and procedure were the same as described earlier[10]. The *p*H titrations were carried out at both 1:1:1 and 1:1:2 (metal:primary ligand:secondary ligand) molar ratios. All the titration mixtures were prepared in 50% dioxane containing a fixed amount (one equivalent) of perchloric acid and at ionic strength $\mu = 0.1$ *M* ($NaClO_4$).

Results and Discussion

Metal(II)-NTA-aminophenol systems

The titration curve for the binary 1:1 Cu(II)-NTA system (ML) showed a well marked inflexion at $a = 3$, indicating the formation of the stable $[Cu\text{-}NTA]^-$ chelate. It was of interest to note that another well marked inflexion appeared at $a \approx 3.5$. It thus showed the addition of extra OH, and possibly formation of a dimeric species $M_2L_2(OH)$. In 1:1 Cu(II)-aminophenol system (MA) the titration curve gave an inflexion at $a \approx 2$. In 1:1:1 Cu-NTA-aminophenol mixed ligand system (MLA), the first inflexion occurred at $a \approx 2$ ($p\text{H} \approx 4.0$) followed by a buffer region ($a = 2$-4) and then another inflexion occurred at $a \approx 4$. In 1:1:2 Cu(II)-NTA-aminophenol system, the first inflexion occurred at $a = 1$ ($p\text{H} \sim 4$), followed by a buffer region ($a = 1$-4), finally giving the inflexion at $a \approx 4$. Moreover, the experimental mixed ligand titration curves were well displaced from the theoretical composite curves[1,10,11]. These observations indicate the formation of the mixed ligand complex in the region $a = 3$-4.

The results thus show that in both 1:1:1 and 1:1:2 systems, the same mixed complex $[CuLA]^{2-}$ is formed. The calculations for the stability constants also support this contention. Both the systems lead to almost similar results giving stability constant values (K_{MLA} values), which agree well within experimental limits (± 0.1 log units).

Similar *p*H-titration curves were obtained with other metal ions, i.e., Ni(II), Co(II) and Zn(II). The composite curves were well separated from the experimental mixed ligand titration curves. Thus, all these results indicate the formation of the mixed complexes (M-NTA-aminophenol) in the buffer regions of $a = 3$-4.

Metal(II)-IMDA-aminophenol systems

The titration curve for the simple 1:1 Cu(II)-IMDA system (ML) showed a well marked inflexion at $a = 2$, indicating the formation of stable [Cu-IMDA] chelate. In 1:1:1 Cu-IMDA-aminophenol mixed ligand system (MLA curve), the first infle-

Table 1— Stability constants of mixed ligand complexes of Cu(II), Ni(II), Co(II) and Zn(II) with aminophenol

[Temp. = 30°C, μ = 0.1 *M* $NaClO_4$; medium = 50% dioxane]

Primary ligand	Stability constant	Metal ion			
		Cu(II)	Ni(II)	Co(II)	Zn(II)
1 NTA	log K_1	7.36±0.10	4.38±0.08	5.92±0.04	5.50±0.06
2 IMDA	log K_1	5.77±0.06	4.75±0.04	5.47±0.06	5.72±0.04
	log K_2	—	—	4.46±0.04	—

xion occurred at $a \approx 1$ (pH ≈ 4), followed by two more inflexions at $a \approx 2$ (pH ~ 6) and $a \approx 3$ (pH ~ 9) respectively.

In 1:1:2 Cu(II)-IMDA-aminophenol system the first inflexion occurred at $a \approx 0$ (pH ≈ 4) followed by a buffer region from $a = 0$ to $a = 2$. The second inflexion appeared at $a \approx 2$ (pH ~ 6.5), after which it showed another buffer region from $a = 2$ onwards.

The results show that in both 1:1:1 and 1:1:2 systems, the same mixed complex [CuL'A] is formed.

Similar pH-titration curves were obtained with Ni(II), Co(II) and Zn(II). In 1:1:2 Co(II)-IMDA-aminophenol system, the titration curve showed a well defined inflexion at $a \approx 2$, followed by a buffer region a = 2-3, finally giving another inflexion at $a \approx 3$. The analysis of this system yielded both log K_1 and log K_2 values but with other metal ions such as Ni(II) and Zn(II) only one constant log K_1 was obtained.

The protonation constants of 2-aminophenol determined by Irving and Rossotti's method[12] in 50% dioxane were found to be log $K_1^H = 11.28$ and log $K_2^H = 4.24$ at 30°C and an ionic strength of 0.1 *M* ($NaClO_4$). Charles and Freiser[7] have reported the corresponding values of 11.57 and 3.75 respectively.

The stability constants for the 1:1:1 mixed ligand systems were calculated in terms of the secondary ligand A as described earlier[10,11]. The 1:1:2 systems were analyzed by calculating $\bar{n}$ values at different pH values by Bjerrum's method[6,13].

Plots of $\bar{n}$ versus pA yielded the formation curves, from which the stepwise stability constants K_1 and K_2 for the mixed complexes MLA and MLA_2 were computed. In addition, the systems were also treated by a modified form of Irving and Rossotti's method[4,12]. The formation curves so obtained were analysed to get the stability constants which were refined by the method of successive approximation. The results, however, showed that even in 1:1:2 systems, only one mixed complex MLA was formed. But in Co(II)-IMDA-aminophenol system, both MLA and MLA_2 complexes were formed. The stability constants of the mixed ligand complexes are presented in Table 1.

The stability sequence with respect to metal ions is: Cu > Co > Zn > Ni with primary ligand NTA and Cu > Zn > Co > Ni with IMDA. Here it is interesting to observe that Ni(II) forms the least stable complexes and even the stability of Co(II) complexes is greater than that of Ni(II) complexes. Such observations have also been made earlier by Sigel[14] and others[7,15] in a number of systems, specially those in which ligands containing aromatic amino groups are involved.

A comparison of the stability of mixed NTA-aminophenol complexes and the IMDA-aminophenol complexes shows that with Cu(II) and Co(II) the mixed NTA complexes are more stable than the corresponding mixed IMDA complexes, but with Ni(II) and Zn(II), the order is reversed, i.e. IMDA > NTA.

Further, a comparison of the stability constants of the mixed ternary complexes (K_{MLA}) with K_1 and K_2 for the corresponding simple binary *o*-aminophenol complexes[7] shows that for Cu(II) complexes, K_{MLA} is less than K_1 and K_2 in both cases. In Ni(II) complexes, with NTA as primary ligand, K_{MLA} is less than K_1 and K_2, whereas with IMDA, K_{MLA} is less than K_1 but comparable to K_2. In Co(II) complexes, with NTA as primary ligand, K_{MLA} is comparable to K_1, but with IMDA, K_{MLA} is less than K_1 but more than K_2. In Zn(II) complexes, K_{MLA} values are less than K_1 but comparable to or slightly less than K_2.

References

1 Carey G H, Bogucki R F & Martell A E, *Inorg Chem*, 3 (1964) 1288.

2 Israeli J & Cecchetti M, *Talanta*, 15 (1968) 1031.

3 Sharma G & Tandon J P, *J inorg nucl Chem*, 32 (1970) 1273; *Z Naturforsch*, 25 (1970) 22.

4 Chidambaram M V & Bhattacharya P K, *J inorg nucl Chem*, 32 (1970) 3271.

5 Verma H S & Srivastava M N, *J inorg nucl Chem*, 37 (1975) 601.

6 Sinha P C, Saxena V K, Nigam N B & Srivastava M N, *Indian J Chem*, 28A (1989) 325.

7 Charles R G & Freiser H, *J Am chem Soc*, 74 (1952) 1385.

8 Bear J L & Clark E M,*J inorg nucl Chem*, 31 (1969) 1517.

9 Venkatnarayana G, Swamy S J & Lingaiah P, *Indian J Chem*, 23A (1984) 501.

10 Singh M K & Srivastava M N, *J inorg nucl Chem*, 35 (1973) 2433.

11 Ozer U Y, *J inorg nucl Chem*, 32 (1970) 1279.

12 Irving H & Rossotti H S, *J chem Soc*, (1953) 3397; (1954) 2904.

13 Bjerrum J, *Metal amine formation in aqueous solutions* (P Hasse, Copenhagen), 1941.

14 Sigel H, *Metal ions in biological systems*, Vol 2, *Mixed ligand complexes* (Marcel Dekker Inc, New York), 1973.

15 Lane T J, C S C & Sam A, *J Am chem Soc*, 82 (1960) 4462; 83 (1961) 2223.

Indian Journal of Chemistry
Vol. 29A, July 1990, pp. 710-712

Preparation and characterisation of diarylselenium (IV) trifluoroethoxides

Rajesh Khajuria, Sukhjinder Singh, K K Bhasin & R D Verma*

Department of Chemistry, Panjab University,
Chandigarh 160 014

Received 5 June 1989; revised and accepted 12 September 1989

A number of *p*-substituted diarylselenium (IV) trifluoroethoxides, $(RC_6H_4)_2Se(OCH_2CF_3)_2$, where R = H, *p*-$CH_3$, *p*-$CH_3O$, *p*-$C_2H_5O$, *p*-Br and *p*-Cl, have been prepared in excellent yields by metathesis between respective diarylselenium (IV) chloride and sodium trifluoroethoxide. These compounds are characterized by elemental analyses, IR, ^1H and ^{19}F NMR and mass spectral studies.

Alkoxides of selenium are much less studied as compared to other selenium compounds[1-3]. The chemistry of tetralkoxyselenuranes[5] (tetracoordinated selenium species) has received little attention because of their unstable nature. Some organylselenium (IV) alkoxides of the types $(C_6H_5)_2Se(OR')_2$, $C_6H_5Se(OR')_3$, $(CH_3)_2Se(OR')_2$, $Se(OR')_{4-n}X_n$, $C_6H_5Se(OR')_{3-n}X_n$ and $(C_6H_5)_2Se(OR')X$, where $R' = CH_3$, C_5H_5 and X = halide or nitrate are known[2-4]. It is only recently that a series of tetralkoxyselenuranes have been prepared and studied in detail[5]. To the best of our knowledge, no diarylselenium (IV) fluoroalkoxide is reported in the literature. In this note, we report the preparation and characterization of a number of *p*-substituted diarylselenium (IV) trifluoroethoxides in continuation of our work on fluorine containing diarylselenium (IV) derivatives[6].

Experimental

Diarylselenium (IV) chlorides were prepared by literature methods[2]. Sodium trifluoroethoxide was prepared by reacting sodium with excess trifluoroethanol. All the solvents were purified and dried by conventional methods. Trifluoroethanol (Fluka) was used as such.

The IR spectra of the compounds were recorded as solid smears/nujol mulls between AgCl plates on a Perkin Elmer-1430 spectrophotometer. ^1H and ^{19}F NMR spectra were obtained in CCl_4 on a Varian instrument model EM-390 using TMS and Freon-11 as internal and external references, respectively. Mass (EI) spectra were obtained on a micromass 7070 at 70eV. All the manipulations were carried out in dry N_2 atmosphere.

Selenium was determined volumetrically[7]. Fluorine was determined as described earlier[8] after fusing the compounds with sodium. Carbon and hydrogen were determined microanalytically.

General procedure for the preparation of diarylselenium (IV) trifluoroethoxides

Diarylselenium (IV) chloride (10 mmol) dissolved in ~40 ml of dichloromethane was added to sodium trifluoroethoxide (2.44g, 20 mmol) and the contents stirred magnetically at ambient temperature for 6 h under dry N_2 atmosphere. The insoluble materials were filtered off under positive pressure of N_2. Removal of solvent from the filtrate *in vacuo* yielded the desired diarylselenium (IV) trifluoroethoxide in > 96% yield.

Results and discussion

The reaction between sodium trifluoroethoxide and diarylselenium (IV) chloride in dichloromethane at ambient temperature yields the desired diarylselenium (IV) trifloroethoxide:

$$(RC_6H_4)_2SeCl_2 + 2CF_3CH_2ONa \xrightarrow{CH_2Cl_2} (RC_6H_4)_2Se(OCH_2CF_3)_2 + 2NaCl$$

R = H, *p*-CH_3, *p*-CH_3O, *p*-C_2H_5O, *p*-Br, *p*-Cl.

These compounds are faintly coloured, extremely moisture-sensitive low melting solids (45-55°C) and are soluble in common organic solvents. Their melting range is, however, comparable to the low melting points of $(C_6H_5)_2Se(OCH_3)_2$ and $(C_6H_5)_2Se(OCH_2CH_3)_2$ (36 and 53°C, respectively[9]). These trifluoroethoxides are hydrolysed by moisture instantaneously to the corresponding selenoxides as shown below:

$$(RC_6H_4)_2Se(OCH_2CF_3)_2 + H_2O \rightarrow (RC_6H_4)_2SeO + 2CF_3CH_2OH$$

Formation of diarylselenoxide was checked separately by reacting diarylselenium (IV) trifluoroethoxide with water in stoichiometric amounts. Volatile obtained was confirmed to be CF_3CH_2OH by ^1H an ^{19}F NMR. The elemental analysis and the appearance of a strong band at ~810 cm^{-1} (char-

acteristic of ν Se=O) in the infrared spectra of white solid obtained confirm the formation of the corresponding diaryl selenoxides (Table 2).

The IR bands at *ca.* 3030-3100 cm^{-1} in the spectra of trifluoroethoxides are assigned to the C−H stretching vibrations of the phenyl ring whilst bands at *ca.* 2770-3000 cm^{-1} may be attributed to the C−H stretching vibrations of $-OCH_2CF_3$ group and of *p*-substituents (CH_3, OCH_3, OCH_2CH_3) attached to the phenyl ring[7]. The C−F stretching vibrations generally appear in the region 1150-1300 cm^{-1} (ref. 10). The strong bands at *ca.* 1160-1280 cm^{-1} in the trifluoroethoxides are due to CF_3 stretching vibrations and may contain C−H vibrations as well. The bands at *ca.* 486-534 cm^{-1} have been assigned[7] to Se−O stretching vibrations in $(C_6H_5)_2Se(OR)_2$: R = CH_3, C_2H_5. The bands at *ca.* 500-560 cm^{-1} in the present compounds may be attributed to Se−O stretching vibrations. No other assignment are made for the rest of the IR bands because of overlapping of C−H vibrations of alkyl, alkoxy and phenyl groups and Se−C vibrations.

^1H NMR data of the trifluoroethoxides are given in Table 2 along with assignments. Interesting features of data are chemical shifts for the phenyl protons. A perusal of Table 2 clearly reveals the inductive effect of *p*-substituent on phenyl ring protons. The separation between the peaks observed for phenyl protons changes drastically when the nature of the *p*-substituent is electron releasing, whereas it is minimum for electron withdrawing *p*-substituent. The phenyl protons nearer to $-Se(OCH_2CF_3)_2$ group are more deshielded and appear at lower fields in comparison to the phenyl protons nearer to the electron releasing *p*-substituents. The minimum separation observed for C_6H_4 protons in $(p\text{-}BrC_6H_4)_2Se(OCH_2CF_3)_2$, probably reveals the comparable electron withdrawing abilities of −Br and $-Se(OCH_2CF_3)_2$ groups. Similar observations have recently been made in the case of diarylselenium (IV) trifluoroacetates[6].

^{19}F NMR spectra of these compounds exhibit a single peak (as a triplet) at *ca.* δ −74 to −78 ppm (Table 2) as expected for $-OCH_2CF_3$ group.

Table 1—Analytical data, important IR bands and mass spectral peaks

Compound*	Found (Calc), %				IR† (cm^{-1})	Mass (EI)
	C	H	F	Se		
$(C_6H_5)_2SeX_2$	44.3 (44.5)	3.18 (3.2)	25.8 (26.4)	17.95 (18.3)	3080m, 2920m, 2875m, 2780m, 1285vs b, 1160vs b, 560m, 540m.	234 ($(C_6H_5)_2Se^+$,vs), 157 ($C_6H_5Se^+$, s), 154 ($(C_6H_5)_2^+$, s), 77 ($C_6H_5^+$, m).
$(CH_3C_6H_4)_2SeX_2$	46.8 (47.0)	3.8 (3.9)	24.9 (24.8)	17.1 (17.2)	3071m, 3030m, 2930m, 2870m, 1285vs b, 1160vs b, 590w, 560w.	262 ($(CH_3C_6H_4)_2Se^+$, vs), 232 ($(C_6H_4)_2Se^+$m), 182 ($(CH_3C_6H_4)_2$, s), 171 ($CH_3C_6H_4Se^+$, m), 99 ($CF_3CH_2O^+$, w), 91 ($CH_3C_6H_4^+$, s), 76 $C_6H_4^+$, s).
$(CH_3OC_6H_4)_2SeX_2$	43.8 (44.0)	3.5 (3.6)	23.4 (23.2)	15.7 (16.1)	3087w, 3025m, 2963m, 2928m, 2867m, 1266vs, 1164vs, 610m, 557sh	294 ($(CH_3OC_6H_4)_2Se^+$, vs), 214 ($(CH_3OC_6H_4)_2^+$, s), 187 ($CH_3OC_6H_4Se^+$, s), 107 ($CH_3OC_6H_4^+$, m), 99 ($CF_3CH_2O^+$, w), 76 ($C_6H_4^+$, w).
$(C_2H_5OC_6H_4)_2SeX_2$	45.9 (46.2)	4.1 (4.2)	21.6 (22.0)	15.1 (15.2)	3080m, 2950ms, 2915w, 1275vs b, 1164vs b, 610w, 520s.	322 ($(C_2H_5OC_6H_4)_2Se^+$, vs), 242 ($(C_2H_5OC_6H_4)_2^+$, s), 99 ($CF_3CH_2O^+$, m), 76 ($C_6H_4^+$, m).
$(ClC_6H_4)_2SeX_2$	38.2 (38.4)	2.3 (2.4)	22.4 (22.8)	15.3 (15.8)	3100ms, 3010mw, 2935ms, 2875ms, 1280s, 1165vs b, 562 m.	302 ($(ClC_6H_4)_2Se^+$, vs), 222 ($(ClC_6H_4)_2^+$, m) 191 ($ClC_6H_4Se^+$, s), 156 ($C_6H_4Se^+$, s), 152 ($(C_6H_4)_2^+$, s), 111 ($ClC_6H_4^+$, m), 99 ($CF_3CH_2O^+$, m), 76 ($C_6H_4^+$, m).
$(BrC_6H_4)_2SeX_2$	32.5 (32.6)	1.9 (2.0)	19.5 (19.3)	12.9 (13.4)	3080w, 3047m, 3000mw, 2930m, 2868mw, 1280s, 1170s b, 560m.	392 ($Br^{80}C_6H_4)_2Se^+$, vs), 312 ($(Br^{80}C_6H_4)_2^+$, s), 236 ($Br^{80}C_6H_4Se^+$, s), 156 ($C_6H_4Se^+$, s), 152 ($(C_6H_4)_2^+$, s), 99 ($CF_3CH_2O^+$, m), 76 ($C_6H_4^+$, m).

*X = OCH_2CF_3

†s = strong; b = broad; m = medium; w = weak; sh = shoulder

Table 2 – ^1H and ^{19}F NMR chemical shifts (δ, ppm)

Compound	δH					δF
	C_6H_5/C_6H_4	CH_3	OCH_3	$\underline{OCH_2}CH_3$	$\underline{OCH_2}CF_3$	$OCH_2\underline{CF_3}$
$(C_6H_5)_2Se(OCH_2CF_3)_2$	7.39-8.00	—	—	—	2.86q	−77.8
$(CH_3C_6H_4)_2Se(OCH_2CF_3)_2$	7.29-7.92	2.36s	—	—	3.86q	−77.9
$(CH_3OC_6H_4)_2Se(OCH_2CF_3)_2$	6.92-7.86	—	3.82*	—	3.82*	−75.7
$(C_2H_5OC_6H_4)_2Se(OCH_2CF_3)_2$	6.86-7.82	1.36t	—	4.00*	4.00*	−74.8
$(BrC_6H_4)_2Se(OCH_2CF_3)_2$	7.63-7.79	—	—	—	3.92q	−74.4
$(ClC_6H_4)_2Se(OCH_2CF_3)_2$	7.50-7.96	—	—	—	3.89q	−73.9

s, singlet; t, triplet, q, quartet

*Nearly superimposed signals (centred at the mentioned values) were observed for two different sets of protons due to (i) $\underline{CH_3}O$ and $\underline{OCH_2}CF_3$ protons and (ii) $CH_3\underline{CH_2}O$ and $\underline{OCH_2}CF_3$ protons.

A single peak (triplet) has been observed at δ −80.6 ppm in the ^{19}F NMR spectrum of $Se(OCH_2CF_3)_4$ at ambient temperature[5].

Six naturally occurring isotopes of selenium produce a highly characteristic mass spectral pattern for selenium containing fragment ions in these compounds. The mass spectral data of compounds containing peaks corresponding to isotopes ^{80}Se and ^{35}Cl along with relative intensities are given in Table 1. Molecular ion peak is not observed in the present compounds. The common intense peak cluster in the spectra of the present compounds corresponds to the ion $(RC_6H_4)_2Se^+$. The ion CF_3CH_2O was also observed in most of the compounds with varying intensities. The general characteristic pattern for some of the common ion peaks in most of these compounds may be represented by Scheme 1.

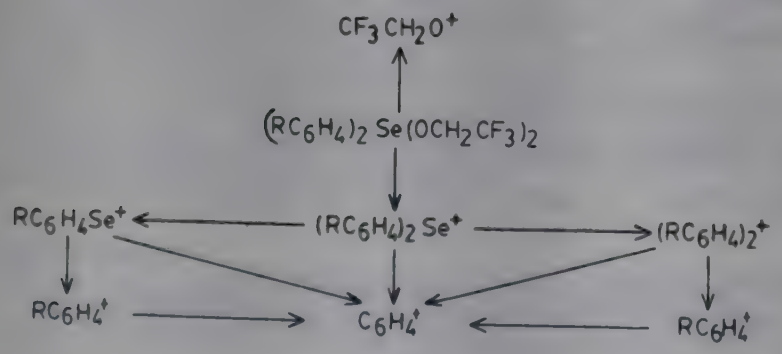

SCHEME 1

Acknowledgement

R Khajuria is grateful to the CSIR, New Delhi, for financial assistance.

References

1 *The chemistry of organic selenium and tellurium compounds*, Edited by S Patai & Z Rappoport (John Wiley & Sons), Vol I (1986) and Vol II (1987).

2 *Selenium*, Edited by R A Zingaro & W C Cooper (Van Nostrand, Reinhold, New York), 1984, and references therein.

3 *Organic selenium compounds: Their chemistry and biology*, Edited by D L Klayman & W H H Günther (Wiley Interscience, New York), 1973.

4 Paetzold R & Horn V, *Z anorg allg Chem*, 395 (1973) 186.

5 Denney D B, Denney D Z, Hammond P J & Hsu Y F, *J Am chem Soc*, 103 (1981) 2340.

6 Khajuria R, Singh S, Bhasin K K & Verma R D, *Synth react inorg metal-org Chem*, 19(5) (1989) 519.

7 Gould E S, *Anal Chem*, 23 (1951) 1502.

8 Singh S, Amita, Gill M S & Verma R D, *J fluorine Chem*, 27 (1985) 133.

9 Paetzold R & Linder U, *Z anorg allg Chem*, 350 (1967) 295.

10 *Fluorine chemistry*, Edited by J H Simons, (Academic Press, New York) 1954.

Indian Journal of Chemistry
Vol. 29A, July 1990, pp. 713-715

Dioxouranium(VI) complexes of tetradentate schiff base ligands

S Singh, V Chakravortty & K C Dash*

Department of Chemistry,
Utkal University, Vani Vihar, Bhubaneswar 751 004

Received 27 September 1989;
revised and accepted 26 December 1989

Twelve neutral dioxouranium(VI) complexes of tetradentate schiff bases obtained by the condensation of pyridine-2-carboxaldehyde or 2-acetylpyridine with ethylenediamine and propylenediamine are reported. The complexes have the general formula $UO_2(L)X_2$, where L = neutral tetradentate ligand and $X = Cl^-$, NCS^-, NO_3^-. The complexes are characterised by analytical, electrical conductivity and infrared spectral studies. The thiocyanate ions are N-bonded and the nitrate ions are bonded in a bidentate manner.

Schiff bases obtained from the interaction of pyridine-2-carboxaldehyde with diamines[1], triamines[2] and other amino compounds[3] are an interesting class of ligands. As a part of our studies on the coordination chemistry of actinides involving multidentate schiff base ligands, we report here twelve mononuclear dioxouranium(VI) complexes with neutral tetradentate schiff base ligands derived from the condensation of pyridine-2-carboxaldehyde or 2-acetylpyridine with ethylenediamine and propylenediamine (see structure I). One of the aims of the present study was to obtain complexes with higher coordination numbers[4-7], which are rather unusual for transition metals.

Experimental

Hydrated dioxouranium(VI) chloride and dioxouranium(VI) nitrate were BDH reagents and used as supplied. Ethanolic solution of $UO_2(NCS)_2$ was obtained as reported[8]. Pyridine-2-carboxaldehyde and 2-acetylpyridine were Fluka reagents.

C, H and N microanalyses, determination of U and S and all the physicochemical measurements were carried out as reported[7].

All the complexes were synthesised according to a common procedure. In a typical preparation, 0.21 ml (2mmol) pyridine-2-carboxaldehyde and 0.07 ml (1 mmol) ethylenediamine were made to react with continuous stirring under reflux in EtOH (5 ml) for 30 min when the colour changed

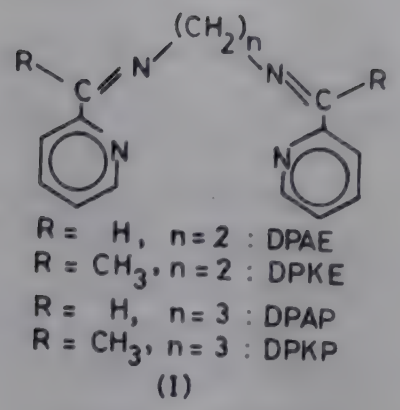

(I)

to deep brown. The solution was cooled to room temperature and to this deep brown ligand solution, a solution of $UO_2Cl_2.nH_2O$ (0.341 g, 1 mmol) in EtOH (5 ml) was added with continuous vigorous stirring. Immediately, an yellow precipitate appeared. It was further stirred for 4h, then collected on a glass frit, washed successively four times with 5 ml portions of EtOH, followed by Et_2O and finally dried *in vacuo* (yield 45%). In other complexes, the yield varied from 50 to 60%.

Results and discussion

The compounds synthesized are presented in Table 1 with their analytical and other characterisation data. They all conform to the formula $UO_2(L)X_2$. The poor solubility of these complexes in suitable organic solvents precluded determination of their molecular weights by cryoscopic method[3] and preparation of crystals for structural studies. Determination of relative molecular masses of the synthesised coordination complexes was attempted by Rast method but inhomogeneity of complexes with known solid solvents of high cryoscopic constants at higher temperatures did not permit measurements of melting points of solutions. The conductances of a few complexes could be measured in dilute solutions ($\sim 10^{-3}$ *M*) of $MeNO_2$, DMF or DMSO and they were found to be non-ionic. Higher conductance values observed for some thiocyanato and nitrato complexes may be attributed to the replacement of coordinated anions by DMF or DMSO molecules due to solvolysis. But in $MeNO_2$ all the complexes were found to be non-electrolytes.

The infrared spectra provide information regarding the nature of the bonding in the UO_2^{2+} ion, the NCS^- and NO_3^- anions and the coordination mode of the ligands. A fairly sharp band in the complexes observed at 1594-1648 cm^{-1} sug-

Table 1 – Analytical and other characterisation data of dioxouranium(VI) complexes[a]

Sl. No.	Complex (Empirical formula)	M.P. (°C)	Found (Calc.) %				
			U	C	H	N	Cl/S
1	$UO_2(DPAE)Cl_2$	278	41.00	29.00	2.50	9.50	12.40
	$(UC_{14}H_{14}N_4O_2Cl_2)$		(41.11)	(29.02)	(2.42)	(9.67)	(12.26)
2	$UO_2(DPAE)(NCS)_2$	185	38.00	30.50	2.30	13.60	10.10
	$(UC_{16}H_{14}N_6O_2S_2)$		(38.14)	(30.77)	(2.24)	(13.46)	(10.26)
3	$UO_2(DPAE)(NO_3)_2$	165	37.40	26.30	2.00	13.10	
	$(UC_{14}H_{14}N_6O_8)$		(37.66)	(26.58)	(2.22)	(13.29)	
4	$UO_2(DPKE)Cl_2$	100	39.00	31.30	2.60	9.00	11.50
	$(UC_{16}H_{18}N_4O_2Cl_2)$		(39.21)	(31.63)	(2.97)	(9.23)	(11.70)
5	$UO_2(DPKE)(NCS)_2$	110	36.40	33.00	2.80	12.90	9.70
	$(UC_{18}H_{18}N_6O_2S_2)$		(36.50)	(33.13)	(2.76)	(12.88)	(9.82)
6	$UO_2(DPKE)(NO_3)_2$	185	36.10	29.10	2.50	12.80	
	$(UC_{16}H_{18}N_6O_8)$		(36.06)	(29.02)	(2.73)	(12.73)	
7	$UO_2(DPAP)Cl_2$[b]	> 310	40.10	30.20	2.50	9.10	11.80
	$(UC_{15}H_{16}N_4O_2Cl_2)$		(40.13)	(30.35)	(2.70)	(9.44)	(11.97)
8	$UO_2(DPAP)(NCS)_2$[c]	> 330	37.00	31.80	2.40	13.20	10.20
	$(UC_{17}H_{16}N_6O_2S_2)$		(37.30)	(31.97)	(2.50)	(13.10)	(10.03)
9	$UO_2(DPAP)(NO_3)_2$[d]	> 336	36.90	27.60	2.30	13.2	
	$(UC_{15}H_{16}N_6O_8)$		(36.84)	(27.86)	(2.48)	(13.0)	
10	$UO_2(DPKP)Cl_2$	> 310	38.10	32.70	3.10	9.20	11.50
	$(UC_{17}H_{20}N_4O_2Cl_2)$		(38.33)	(32.85)	(3.22)	(9.02)	(11.43)
11	$UO_2(DPKP)(NCS)_2$	> 330	35.80	34.00	3.10	12.50	9.50
	$(UC_{19}H_{20}N_6O_2S_2)$		(35.73)	(34.23)	(3.00)	(12.61)	(9.60)
12	$UO_2(DPKP)(NO_3)_2$	> 310	35.10	30.00	2.80	12.30	
	$(UC_{17}H_{20}N_6O_8)$		(35.31)	(30.27)	(2.97)	(12.46)	

[a] All the complexes, except 7, 8 and 9, are yellow in colour; [b] grey; [c] light yellow; [d] green.

Abbreviations:

DPAE = 1,2-di(pyridine-2-aldimino)ethane; DPKE = 1,2-di(pyridine-2-ketimino)ethane;

DPAP = 1,2-di(pyridine-2-aldimino)propane; DPKP = 1,2-di(pyridine-2-ketimino)propane.

gested the coordination of the ligands through the nitrogen of the azomethine group[9]. Pyridine ring vibrations observed at 1590 and 1570 cm^{-1} in the ligands shifted to higher frequencies on complexation indicating coordination of the pyridine nitrogen in all cases[10]. The ligands thus behave as N_4-tetradentate ligands. The thiocyanato complexes showed bands in the regions 2040-2052 cm^{-1} and 776-841 cm^{-1} corresponding to $\nu(C\equiv N)$ and $\nu(C-S)$ vibrations, respectively, of the $-NCS$ group suggesting N-coordination of this ambidentate anion[11,12], in agreement with the 'hard' character of the UO_2^{2+} ion[13]. All nitrato complexes exhibited bands at 1509, 1305, 1055, 856, 776 cm^{-1} corresponding to the bidentate mode of coordination[14-16]. The magnitude of splitting of ν_4-ν_1 was found to be ~200-240 cm^{-1} suggesting the bidentate coordination of the NO_3^- ion to the UO_2^{2+} group[15]. Bands appearing at 895-920 cm^{-1} and 780-810 cm^{-1} in all these complexes are attributed to the asymmetric and symmetric stretching vibrations of the O=U=O group. This indicates that the linearity of the UO_2^{2+} species is maintained in the complexes[17,18].

The electronic spectral bands of the complexes in DMF solution below 300 nm and at 360 nm correspond to those of the complexing ligands (the same values are obtained for the free ligands). The third band expected around 400 nm due to the UO_2^{2+} group is absent in the complexes where a continuous structureless band is observed. The low solubility of the complexes

prevented the exact location of these bands of very low molar extinction coefficients. The electronic spectra, therefore, do not provide much assistance in determining the environment of the metal atom in these complexes[19,20].

On the basis of these results, the formula suggested for all the complexes is $UO_2(L)X_2$. A coordination number of 8 is suggested for chloride and thiocyanato complexes. The coordination number is increased to 10 in the case of nitrato complexes due to the small bite of the bidentate nitrate group.

Acknowledgement

The authors thank the CSIR, New Delhi for a generous grant.

References

1 Masaaki H & Kyoko K, *Inorg chim Acta*, 104 (1985) 47.
2 Spencer C T & Taylor L T, *Inorg Chem*, 12 (1973) 644.
3 Kuncheria B, Devi G & Indrasenan P, *Inorg chim Acta*, 155 (1989) 255.
4 Mohanta H N & Dash K C, *J inorg nucl Chem*, 39 (1977) 1345, *J Indian chem Soc*, 57 (1980) 26.
5 Mohanta H N & Dash K C, *Indian J Chem*, 15A (1977) 657; *Synth React inorg met-org Chem*, 8 (1978) 43; 9 (1979) 325; *Russ J inorg Chem*, 25 (1980) 586.
6 Panda C R, Chakravortty V & Dash K C, *J less-common Metals*, 135 (1987) 77.
7 Singh S, Chakravortty V & Dash K C, *Indian J Chem*, 28A (1989) 255.
8 Isapkina I S & Ellert G V, *Russ J inorg Chem*, 13 (1968) 730.
9 Burger K, Ruff F, Ruff I & Egyed I, *Acta chim hung*, 46 (1965) 1.
10 Bell C F, Lott K A K & Hearn N, *Polyhedron*, 6 (1987) 39.
11 Bailey R A, Kozak S L, Michelsen T W & Mills W N, *Coord Chem Rev*, 6 (1971) 407.
12 Burmeister J L, in *Chemistry and biochemistry of thiocyanic acid and its derivatives*, edited by A A Newmann (Academic Press, London) 1975, p. 68.
13 Majumdar A K & Bhattacharya R G, *J Indian chem Soc*, 51 (1974) 235.
14 Addison C C, Logan N, Wallwork S C & Garner C D, *Quart Rev*, 25 (1971) 289.
15 Curtis N F & Curtis Y M, *Inorg Chem*, 4 (1965) 804.
16 Hester R W & Grossman E L, *Inorg Chem*, 5 (1966) 1308.
17 Chacko J, *Synth React inorg met-org Chem*, 12 (1982) 361.
18 Fankuchen I, *Z Kristallogr*, 91 (1935) 473.
19 Graziani R, Marangoni G, Paolucci G & Forsellini E, *J chem Soc Dalton Trans*, (1978) 818.
20 Dash K C & Mohanta H N, *J inorg nucl Chem*, 40 (1978) 400.

Indian Journal of Chemistry
Vol. 29A, July 1990, pp. 716-720

Synthesis and structural characterization of the lanthanide(III) complexes of 2-acetylpyridine isonicotinoyl hydrazone

T R Rao* & Genda Singh

Department of Chemistry, Faculty of Science,
Banaras Hindu University, Varanasi-221 005, India

Received 1 September 1989; revised 28 December 1989;
accepted 22 January 1990

2-Acetylpyridine isonicotinoyl hydrazone (2-ApINH) forms complexes of the types $[M(2\text{-ApINH})_2Cl_3]$ [M = La, Ce, Pr, Nd, Sm and Eu], $[M'(2\text{-ApINH-H})_3]$ [M' = La, Ce, Pr, Nd and Sm] and $[Eu(2\text{-ApINH-H})_2(OH)]$, which are characterized by elemental analysis, molar conductance, magnetic susceptibility, electronic, IR and ^1H and ^{13}C NMR spectral techniques. The spectral parameters, $\bar{\beta}$, $b^{1/2}$, δ (%) and η calculated from the absorption spectra of Nd(III) complexes, suggest a weak covalent metal-ligand bond formation. Infrared and NMR spectral data suggest a neutral tridentate nature of 2-ApINH in the addition complexes and uninegative tridentate behaviour in the deprotonated complexes. The absorption spectral profiles suggest a coordination number of nine around Nd(III) ion in the complexes.

As a part of our systematic investigation on the lanthanide complexes of various hydrazides and their schiff bases[1-5], we describe here, the results of our studies on the synthesis and structural characterization of La(III), Ce(III), Pr(III), Nd(III), Sm(III) and Eu(III) complexes of 2-acetylpyridine isonicotinoyl hydrazone (2-ApINH) (I).

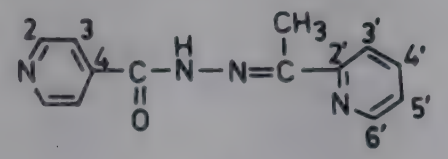

(I)

Experimental

Hydrated lanthanide chlorides (99.99% purity) obtained from M/s Indian Rare Earths Ltd, Kerala (India) were used as such. All the other chemicals used were BDH or S. Merck reagents. 2-Acetylpyridine isonicotinoyl hydrazone was prepared by refluxing isonicotinic acid hydrazide (25 mmol in 40 ml of absolute ethanol) and 2-acetylpyridine (30 mmol in 20 ml of absolute ethanol) for ~4 h. The colourless precipitate obtained on slow cooling of the reaction mixture was filtered off and washed repeatedly with cold ethanol. The crude product was recrystallized from ethanol; m.p. 164°C. [Anal. Found: C, 65.15; H, 5.00; N, 23.30; N_2H_4, 13.35%. Calcd. for $C_{13}H_{12}N_4O$: C, 65.00; H, 5.00; N, 23.33; N_2H_4, 13.33%].

Trichloro-bis(2-acetylpyridine isonicotinoyl hydrazone)lanthanide (III) complexes, $[Ln(2\text{-}ApINH)_2Cl_3]$, [*Ln = La, Ce, Pr, Nd, Sm and Eu*]

These were prepared by mixing together solutions of 2-ApINH (4.0 mmol in 20 ml ethanol) and the appropriate lanthanide chloride (2.0 mmol in 15 ml of ethanol-THF) and digesting the reaction mixture on a water bath for 1/2 hr. The precipitated complexes were filtered off, washed several times with ethanol and dried *in vacuo.*

Tris-(2-acetylpyridine isonicotinoylhydrazonato)lanthanide(III) complexes, $[Ln(2\text{-}ApINH\text{-}H)_3]$ [*Ln = La, Ce, Pr, Nd and Sm*] *and hydroxobis(2-acetylpyridine isonicotinoylhydrazonato)europium (III),* $[Eu(2\text{-}ApINH\text{-}H)_2(OH)]$

These were prepared by mixing together aqueous solutions of the appropriate metal chloride (2.0 mmol in 20 ml), 2-ApINH and KOH (6.0 mmol each in 20 ml) and adjusting the *p*H of the solution to ~7.5. The precipitated complexes were digested on a water bath for 1 h, filtered off, washed successively with water, aqueous-ethanol and ethanol and dried at room temperature.

The metal ions, after destroying the organic matter with aqua regia followed by treatment with sulphuric acid, were estimated volumetrically by EDTA titration[6]. Chloride was estimated gravimetrically as AgCl. Hydrazine was determined volumetrically after subjecting the complexes to acid hydrolysis. C, H and N were microanalysed on a Perkin-Elmer Analyser, model 240C. The details of equipment used for various physical measurements were reported earlier[3]. The mass spectrum was recorded on a Varian Mat CH-7 mass spectrometer.

Results and discussion

Characterization of 2-ApINH

The nujol mull infrared spectrum of 2-ApINH showed bands at 1670, 1620, 1550, 1300 and 1040 cm^{-1} which may be assigned to the amide I, $\nu(C=N)$, amide II, amide III and $\nu(N-N)$

Table 1 – Analytical data and general behaviour of Ln(III) complexes of 2-ApINH

Complex	m.p. (°C)	Found (Calc.) %				μ_{eff} (B.M.)
		N	Cl	M	N_2H_4	
$[La(2\text{-}ApINH)_2Cl_3]$	258[d]	15.49	14.50	19.40	8.90	diamag.
		(15.44)	(14.68)	(19.15)	(8.82)	
$[Ce(2\text{-}ApINH)_2Cl_3]$	221[d]	15.40	14.58	19.31	—	2.61
		(15.41)	(14.66)	(19.28)		
$[Pr(2\text{-}ApINH)_2Cl_3]$	264[d]	15.40	14.63	19.35	8.80	3.93
		(15.40)	(14.64)	(19.37)	(8.80)	
$[Nd(2\text{-}ApINH)_2Cl_3]$	249[d]	15.30	14.55	19.70	8.75	4.37
		(15.33)	(14.57)	(19.74)	(8.76)	
$[Sm(2\text{-}ApINH)_2Cl_3]$	236[d]	15.20	14.40	19.98	8.70	2.24
		(15.20)	(14.45)	(20.41)	(8.69)	
$[Eu(2\text{-}ApINH)_2Cl_3]$	252[d]	15.20	14.40	20.56	8.65	3.39
		(15.17)	(14.42)	(20.58)	(8.67)	
$[La(2\text{-}ApINH\text{-}H)_3]$	> 300	19.61	—	16.25	11.20	diamag.
		(19.62)		(16.32)	(11.22)	
$[Ce(2\text{-}ApINH\text{-}H)_3]$	> 300	19.58	—	16.30	—	2.13
		(19.60)		(16.35)		
$[Pr(2\text{-}ApINH\text{-}H)_3]$	> 300	19.55	—	16.42	11.21	4.12
		(19.58)		(16.42)	(11.19)	
$[Nd(2\text{-}ApINH\text{-}H)_3]$	> 300	19.52	—	16.75	11.14	4.73
		(19.51)		(16.75)	(11.15)	
$[Sm(2\text{-}ApINH\text{-}H)_3]$	> 300	19.41	—	17.39	11.00	2.34
		(19.37)		(17.33)	(11.07)	
$[Eu(2\text{-}ApINH\text{-}H)_2OH]$	> 300	17.35	—	23.55	9.91	3.27
		(17.31)		(23.48)	(9.89)	

d – decomposition temperature.

modes[7,8]. A band observed at 3180 cm^{-1} is characteristic of the $\nu(-NH-)$ mode. The ^1H NMR spectrum of 2-ApINH showed $-C(O)NH-$ and the $-CH_3$ signals at δ 11.14 and 2.52 while all the aromatic protons were observed as multiplets in the range δ 8.76-7.38. The ^{13}C NMR spectrum showed ten signals corresponding to thirteen carbon atoms of the molecule. All the ^{13}C signals have been approximated applying the principle of substituent additivity[9]. The $>C=O$ and $N=C(CH_3)$ groups showed the signals at 163.11 and 150.78 ppm respectively. In the mass spectrum of 2-ApINH the base peak observed at $m/z = 106$ corresponds to the fragment $NC_5H_4CO^+$. The molecular ion peak (M^+) appears with 15% intensity at $m/z = 240$.

Characterization of complexes

The analytical data of the complexes (Table 1) indicate formation of 1:2 and 1:3 (metal:ligand) types of complexes corresponding to the general formulae $Ln(2\text{-}ApINH)_2Cl_3$ and $Ln(2\text{-}ApINH-H)_3$. Thus, 2-ApINH reacts with the hydrated metal chlorides as a neutral ligand in ethanolic solution and as a uninegative species in basic medium.

All the complexes were found to be yellow or orange-red in colour, stable at room temperature and soluble only in coordinating solvents like pyridine, DMF and DMSO. Some neutral (1:3) complexes were only partially soluble even in DMSO. All the 1:2 complexes decomposed below 300°C while the 1:3 (neutral) complexes did not melt upto 300°C. The molar conductances of 0.001 *M* DMF solutions showed 1:1 electrolytic nature of the 1:2 complexes (38.0-44.9 $ohm^{-1}\ cm^2\ mol^{-1}$) and non-electrolytic behaviour of the 1:3 complexes[10] (2.4-5.7 $ohm^{-1}\ cm^2\ mol^{-1}$).

The room temperature magnetic moments of the complexes, which were corrected for diamagnetism, showed very little deviation from the Van

Table 2 – Electronic spectral data of Nd(III) complexes of 2-ApINH

Complex	Band max. (cm^{-1}) in nujol (in DMF)	Transitions	Calc. parameters* (spectrum in DMF)
$[Nd(2\text{-ApINH})_2Cl_3]$	11430	$^4I_{9/2} \rightarrow {}^4F_{3/2}$	
	(11560)		
	12500	$\rightarrow {}^4F_{5/2}$	$\bar{\beta} = 0.9863$
	(12485)		$b^{1/2} = 0.0828$
	13550	$\rightarrow {}^4F_{7/2}$	$\eta = 0.0069$
	(13570)		
	14770	$\rightarrow {}^4F_{9/2}$	$\delta(\%) = 1.3800$
	(—)		
	17035	$\rightarrow {}^4G_{5/2}, {}^2G_{7/2}$	
	(17095)		
	19050	$\rightarrow {}^4G_{7/2}$	
	(19065)		
	—	$\rightarrow {}^4G_{9/2}$	
	(19495)		
$[Nd(2\text{-ApINH-H})_3]$	11415	$^4I_{9/2} \rightarrow {}^4F_{3/2}$	
	(11560)		
	12425	$\rightarrow {}^4F_{5/2}$	
	(12395)		
	13425	$\rightarrow {}^4F_{7/2}$	$\bar{\beta} = 0.9828$
	(13570)		$b^{1/2} = 0.0927$
	14705	$\rightarrow {}^4F_{9/2}$	$\eta = 0.0087$
	(—)		
	17065	$\rightarrow {}^4G_{5/2}, {}^2G_{7/2}$	$\delta(\%) = 1.7500$
	17035	$\rightarrow {}^4G_{7/2}$	
	18870		
	(18795)	$\rightarrow {}^4G_{9/2}$	
	19495		
	(19495)		

*Parameters are calculated from the hypersensitive bands.

Vleck values[11], indicating little participation of 4*f*-electrons in bond formation.

In the spectra of the 1:2 complexes, $Ln(2\text{-ApINH})_2Cl_3$, the amide I and amide II bands were found to undergo bathochromic shifts (1650-1645 cm^{-1}) and the amide III a hypsochromic shift (1315-1310 cm^{-1}) suggesting coordination of the carbonyl oxygen. However, the amide I, II, III bands totally disappeared from the spectra of the 1:3 complexes, $Ln(2\text{-ApINH}-H)_3$, and a sharp band diagnostic of $>C=N-N=C<$ group[12] appeared at 1600 cm^{-1} which indicated the transformation of the carbonyl group to C–OH through amide $\rightleftharpoons$ imidol tautomerism and subsequent coordination of the imidol oxygen. Appearance of new peaks characteristic of $\nu(NCO^-)$ (1515-1510 and 1365-1360 cm^{-1} regions) further supported imidol oxygen coordination[13]. The $\nu(N-N)$ mode underwent a hypsochromic shift of 20-30 cm^{-1} in the spectra of all the complexes indicating azomethine nitrogen coordination[14]. The ring skeletal and the in-plane and out-of-plane ring deformation modes of the ligand (990, 590 and 405 cm^{-1} respectively) underwent hypsochromic shifts (10-20 cm^{-1}, 30-35 cm^{-1} and 35-45 cm^{-1}) suggesting coordination of 2-acetylpyridyl ring nitrogen[15].

The absorption spectra of the Nd(III) complexes were recorded in nujol as well as in 0.002 *M* DMF solution. The spectral data along with various calculated bonding parameters are given in Table 2. The $^4I_{9/2} \rightarrow {}^4G_{5/2}, {}^2G_{7/2}$ band is commonly used in determining coordination environment, composition and stability constants of Nd(III) complexes. The spectral features in the hypersensitive band region were found to differ

Table 3 – ^1H and ^{13}C NMR Spectral data* of 2-ApINH and the La(III) complexes

Proton/carbon atom	2-ApINH	$[La(2\text{-}ApINH)_2Cl_3]$	$[La(2\text{-}ApINH\text{-}H)_3]$
H_3C-	2.52s	2.53s	2.70
$-NH-$	11.14s	11.34s	–
HC_2	8.76d	8.77d	8.67d
$HC_3 + HC_{5'}$	7.81d	7.87s	7.79s, 7.73s
$HC_{3'}$	7.38d	7.43d	7.46s
$HC_{4'}$	8.01m	8.03m	8.13s
$HC_{6'}$	8.62d	8.70d	8.67d
$>CO$	163.11	164.15	170.08
$NC(CH_3)$	150.78	154.46	154.87
H_3C-	12.74	13.60	13.77
C_2	149.96	150.20	149.95
C_3	122.06	122.60	122.18
C_4	–	–	144.09
$C_{2'}$	154.84	157.28	156.77
$C_{3'}$	120.38	121.57	123.58
$C_{4'}$	136.58	139.07	139.51
$C_{5'}$	124.22	125.10	125.15
$C_{6'}$	148.61	149.31	149.37

*^{13}C NMR data measured in ppm w.r.t. DMSO-d_6 (39.50 ppm).
s – singlet; d – doublet; m – multiplet.

markedly in the solid and solution spectra of the $[Nd(2\text{-}ApINH)_2Cl_3]$ complex. The nujol mull spectral profile resembled that of nine-coordinated $Nd_2(SO_4)_3.8H_2O$ (solid) reported by Karraker[16] while the DMF solution spectrum had a close similarity with that of the eight-coordinated complex $(CH_3)_3NHNd(hfaa)_4$ [hfaa = $CF_3COCH\text{-}COCF_3$] in ethanol reported by Karraker[17] (Fig. 1). Thus, the change in coordination number from 9 to 8 in going from the solid to the DMF solution spectrum may be due to elimination of one of the chlorides from the coordination sphere in the solution state.

However, the spectral features in the hypersensitive region of the $[Nd(2\text{-}ApINH-H)_3]$ are similar in the solid and DMF solution states suggesting nine coordination[16] around the metal ion and a similar environment in both the phases. All the bands show significant red shifts compared to their positions in the aquo-neodymium ion[18]. Such shifts have been attributed by Jørgensen[19] to the effect of crystal field upon the interelectronic repulsion among the 4*f*-electrons. The various bonding parameters calculated[20,21] from the solid and solution state spectral suggest a weak covalent bond between the metal ion and 2-ApINH.

The ^1H and the ^{13}C NMR spectra of 2-ApINH and the La(III) complexes were recorded in DMSO-d_6 solution and the spectral data along with the assignments are given in Table 3. The numbering scheme of the carbon atoms is the same as shown in (I). The spectrum of $[La(2\text{-}ApINH)_2Cl_3]$ shows a down-field shift of $-NH-$ signal suggesting coordination of the carbonyl oxygen and/or azomethine nitrogen[22]. The slight downfield shift of the $-CH_3$ signal supports coordination of the azomethine nitrogen. The spectrum of $[La(2\text{-}ApINH-H)_3]$, however, does not exhibit the signal corresponding to the $-NH-$ group, and this can be explained by the enolisation of the carbonyl group through amide ⇌ imidol tautomerism. Coordination of the ring nitrogen of 2-acetylpyridyl group is suggested in both the complexes, on the basis of downfield shifts of the HC_4, and HC_6, signals. The unaltered positions of the isonicotinoyl ring protons rule out the coordination of the ring nitrogen of the moiety in both the complexes.

The metal ion in $[La(2\text{-}ApINH)_2Cl_3]$ induced a downfield shift in the $>C=O$ and $N=C(CH_3)$ resonances by ~1 and ~4 ppm respectively suggesting coordination of the carbonyl oxygen and azomethine nitrogen[23]. Coordination of the azomethine nitrogen was also suggested by the down-field shift of the $-CH_3$ signal. In the case of $[La(2\text{-}ApINH-H)_3]$, coordination of the carbo-

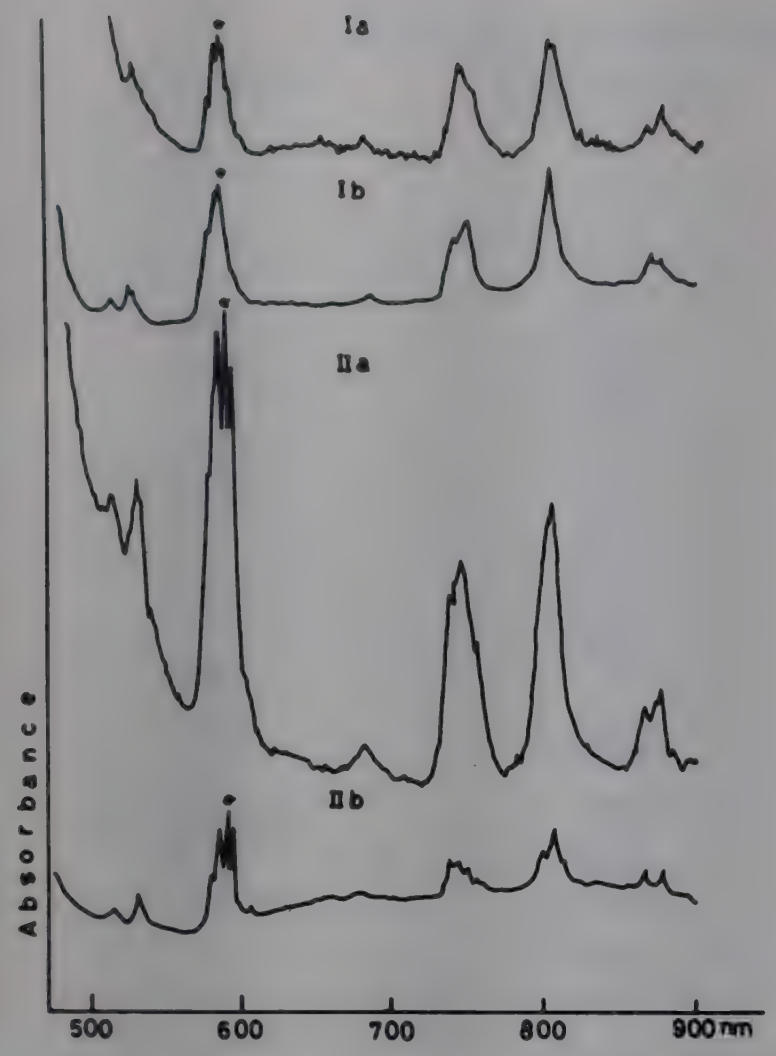

Fig. 1 – Electronic spectra of (I) $Nd(2\text{-}ApINH)_2Cl_3$ and (II) $Nd(2\text{-}ApINH\text{-}H)_3$ [a : in nujol; b : in DMF. Representative bands are shown by asterisk

nyl oxygen and azomethine nitrogen was likewise suggested on the basis of relatively large downfield shifts of $>C=O$ and $N=C(CH_3)$ signals. Further, the observed downfield shifts of the $C_{2'}$, $C_{3'}$, $C_{4'}$, $C_{5'}$, and $C_{6'}$ signals indicated coordination of the 2-acetylpyridyl ring nitrogen[24], in both the complexes. All the signals relating to the isonicotinoyl ring remained almost unaltered. Thus, the ^1H and ^{13}C NMR spectral data support the conclusion drawn on the basis of the IR spectra about the coordination of the carbonyl oxygen, azomethine nitrogen and the ring nitrogen of the 2-acetylpyridyl moiety and non-involvement of the isonicotinoyl ring nitrogen.

Based on the elemental analyses and various physicochemical studies, the empirical formulae $[M(2\text{-}ApINH)_2Cl_3]$ (M = La, Ce, Pr, Nd, Sm and Eu), $[M'(2\text{-}ApINH-H_3]$, (M' = La, Ce, Pr, Nd and Sm) and $[Eu(2\text{-}ApINH-H)_2OH]$ may be tentatively proposed for the present complexes involving non-deprotonated tridentate ligand in the 1:2 and uninegative tridentate species in the 1:3 complexes. The metal is nine-coordinated in both the adducts and deprotonated complexes except in $[Eu(2\text{-}ApINH)_2OH)]$ which involves seven-coordination.

Acknowledgement

Thanks are due to the Head, Department of Chemistry, Banaras Hindu University, for providing laboratory facilities. The recording of the mass spectrum at RSIC, IIT, Madras is gratefully acknowledged. One of us (G.S.) thanks the CSIR, New Delhi, for the award of a fellowship.

References

1 Rao T R, Khan I A & Aggarwal R C, *Proc Indian Acad Sci (Chem Sci)*, 97 (1986) 13.
2 Rao T R, Khan I A & Aggarwal R C, *J less-common Met*, 115 (1986) 325.
3 Rao T R, Singh G & Khan I A, *Trans Met Chem*, 14 (1989) 15.
4 Rao T R, Khan I A & Aggarwal R C, *J Indian chem Soc*, 63 (1986) 380.
5 Rao T R & Singh G, *Synth react inorg met-org Chem*, 19 (1989) 263.
6 Lyle S S & Rahaman M M, *Talanta*, 10 (1963) 1177.
7 Figgins P E & Busch D H, *J phys Chem*, 65 (1961) 2236.
8 Rana V B, Sahni S K, Gupta S P & Sangal S K, *J inorg nucl Chem*, 69 (1977) 1098.
9 Silverstein R M, Bassler G C & Morrill T C, *Spectroscopic identification of organic compounds*, 4th edn. (John Wiley, New York) 1981, 264.
10 Geary W J, *Coord Chem Rev*, 7 (1971) 81.
11 Van Vleck J H & Frank A, *Phys Rev*, 34 (1929) 1494.
12 El-Gayel E & Iskander M F, *J inorg nucl Chem*, 33 (1971) 107.
13 Rao C N R, *Chemical application of infrared spectroscopy* (Academic Press, New York), 1963, 265.
14 Braibanti A, Dallavale F & Pellingheli M A, *Inorg Chem*, 7 (1968) 1430.
15 Nagano K, Kinoshita H & Hirakawa A, *Chem Pharm Bull*, 12 (1964) 1198, 1207.
16 Karraker D G, *Inorg Chem*, 7 (1968) 473.
17 Karraker D G, *Inorg Chem*, 6 (1967) 1863.
18 Carnal W T, Fields P R & Rajnak K, *J chem Phys*, 49 (1968) 4412.
19 Jørgensen C K, *Acta chem scand*, 11 (1957) 1981.
20 Henrie D E & Choppin G R, *J chem Phys*, 49 (1968) 477.
21 Sinha S P, *Spectrochim Acta*, 22 (1966) 57.
22 Patil S A & Kulkarni V H, *Inorg chim Acta*, 95 (1984) 195.
23 Domiano P, Pelizzi C, Predieri G, Viglani C & Palla G, *Polyhedron*, 3 (1984) 281.
24 Jones A J, Grant D M, Russell J G & Froenkel G, *J phys Chem*, 73 (1969) 713.

Indian Journal of Chemistry
Vol. 29A, July 1990, p. 721

ANNOUNCEMENTS

The 42nd Pittsburgh Conference & Exposition on Analytical Chemistry and Applied Spectroscopy

The 42nd Pittsburgh Conference & Exposition on Analytical Chemistry and Applied Spectroscopy will be held during March 4-8, 1991 at McCormick Place-on-the Lake, Chicago, Illinois, USA. Papers are invited for oral or poster presentation in the following areas: Atomic, vibrational and mass spectroscopy; liquid, gas and supercritical fluid chromatography; electrochemistry; thermal analysis etc., and application in biomedicine, forensic science, material characterisation etc.

Abstracts of the papers should be sent before 3 August 1990 to Mrs Alma Johnson, Program Secretary of the Conference. Further information may be obtained from Victor C. Zadnik, Exposition Chairman, Pittsburgh Conference, 300 Penn Center Blvd., Suite 332, Pittsburgh, PA 15235 USA.

Tenth National Symposium on Catalysis and Fourth Indo-Soviet Seminar on Catalysis

The Tenth National Symposium on Catalysis and the Fourth Indo-Soviet Seminar on Catalysis will be held on 18-20 December 1990 and 21 December 1990 respectively at the Indian Institute of Technology, Madras. All areas of catalysis will be covered and communications will be presented in the form of plenary lectures, contributed papers and poster presentations.

Further details may be obtained from Prof. C N Pillai, Convener Catalysis Symposium, Department of Chemistry, Indian Institute of Technology, Madras-600 036.

Indian Journal of Chemistry
Vol. 29A, July 1990, p. 722

Erratum

Paper entitled "Synthesis and characterisation of dimethyltellurium dicarboxylates" by P.C. Srivastava and A. Trivedi, *Indian J. Chem.*, 29A (1990) 489-490:

Structure (I) on p. 490 has been printed wrongly in the reversed form. The correct structure is shown below.

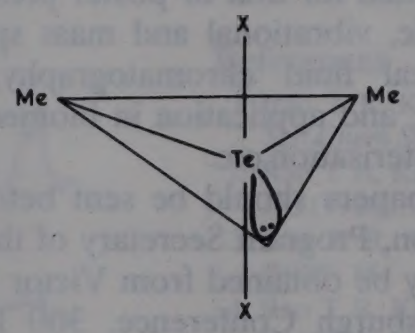

(I)

वैज्ञानिक तथा अनुसंधान पुस्तकालय
SCIENTIFIC & RESEARCH LIBRARY
Accession No. .....
17 JUL 1990
सी.एफ.टी.आर.आई. क्षेत्रीय केन्द्र
C.F.T.R.I. REGIONAL CENTRE, LUDHIANA

ADVERTISEMENT TARIFF

(effective from 1-7-90)

For all monthly RESEARCH PERIODICALS

(IJPAP, IJC(A), IJC(B), IJEB, IJT, JSIR)

	Print-Area M.M.	I-Insertion Rs.	6-Insertions Rs.	12-Insertion Rs.
Full Page	230 × 170	1500.00	7500.00	15000.00
Half Page (Upright)	230 × 80	800.00	4000.00	8000.00
(Across)	110 × 170			
Quarter Page	110 × 80	500.00	2500.00	5000.00
II & III Cover Page	230 × 170	1600.00	8000.00	16000.00
IV Cover Page	230 × 170	1800.00	9000.00	18000.00

For all Bimonthly & Quarterlies RESEARCH PERIODICALS

(IJRSP, IJBB, MAPA, IJMS, IJFTR, R&I)

	Print-Area	I-Insertion	6-Insertions	12-Insertions
Full Page	230 × 170	1000.00	5000.00	10000.00
Half Page (Upright)	230 × 80	600.00	3000.00	6000.00
(Across)	110 × 170			
Quarter Page	110 × 80	400.00	2000.00	4000.00
II & III Cover Page	230 × 170	1100.00	5500.00	11000.00
IV Cover Page	230 × 170	1200.00	6000.00	12000.00

FOR COMBINED ADVERTISEMENT:

The rates for advertisements in 2 to 4 periodicals 10% extra and 5 to 6 periodicals 15% extra.

Matter for advertisement in the camera ready form for black & white reproduction should reach one month in advance.

Advertisement charges (by Demand Draft/Cheque) payable to "PUBLICATIONS & INFORMATION DIRECTORATE, NEW DELHI" should be sent in advance.

All correspondence should be addressed to the Senior Sales & Distribution Office, Publications & Information Directorate, Hill Side Road, New Delhi-110012.

RN 7090/63

Valuable CSIR Periodicals

LAST CHANCE

Offered at 50%
On First Come First Served Basis

A few of the Old issues of the following Scientific/Technical Journals for the years upto 1985 are available for sale.

1 Indian Journal of Pure & Applied Physics (Monthly)
2 Indian Journal of Radio & Space Physics (Bimonthly)
3 Indian Journal of Chemistry-A (Monthly)
4 Indian Journal of Chemistry-B (Monthly)
5 Indian Journal of Experimental Biology (Monthly)
6 Indian Journal of Biochemistry & Biophysics (Bimonthly)
7 Indian Journal of Marine Sciences (Quarterly)
8 Indian Journal of Technology (Monthly)
9 Indian Journal of Fibre & Textile Research (Quarterly)
10 Journal of Scientific & Industrial Research (Monthly)
11 Research & Industry (Quarterly)
12 Medicinal & Aromatic Plants Abstracts (Bimonthly)
13 Current Literature on Science of Science (Monthly)

Kindly rush your enquiries & for details, write to:

The Senior Sales & Distribution Officer
Publications & Information Directorate (CSIR)
Hillside Road, New Delhi 110012

Printed & Published by Dr. G. P. Phondke, Director, Publications & Information Directorate (PID)
Hillside Road, New Delhi 110 012, at PID Photocomposition Unit

Regd No. D(C)-1018